

Biphasic Continuous Synthesis of Furfural: Insights into Reactor and Process Optimization

Citation for published version (APA):

Papaioannou, M. (2023). *Biphasic Continuous Synthesis of Furfural: Insights into Reactor and Process Optimization*. [Phd Thesis 1 (Research TU/e / Graduation TU/e), Chemical Engineering and Chemistry]. Eindhoven University of Technology.

Document status and date:

Published: 11/05/2023

Document Version:

Publisher's PDF, also known as Version of Record (includes final page, issue and volume numbers)

Please check the document version of this publication:

- A submitted manuscript is the version of the article upon submission and before peer-review. There can be important differences between the submitted version and the official published version of record. People interested in the research are advised to contact the author for the final version of the publication, or visit the DOI to the publisher's website.
- The final author version and the galley proof are versions of the publication after peer review.
- The final published version features the final layout of the paper including the volume, issue and page numbers.

[Link to publication](#)

General rights

Copyright and moral rights for the publications made accessible in the public portal are retained by the authors and/or other copyright owners and it is a condition of accessing publications that users recognise and abide by the legal requirements associated with these rights.

- Users may download and print one copy of any publication from the public portal for the purpose of private study or research.
- You may not further distribute the material or use it for any profit-making activity or commercial gain
- You may freely distribute the URL identifying the publication in the public portal.

If the publication is distributed under the terms of Article 25fa of the Dutch Copyright Act, indicated by the "Taverne" license above, please follow below link for the End User Agreement:

www.tue.nl/taverne

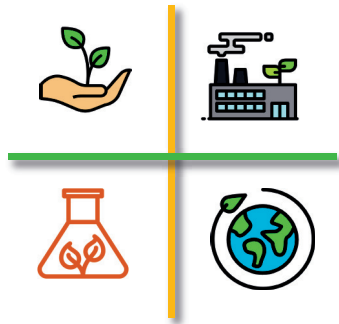
Take down policy

If you believe that this document breaches copyright please contact us at:

openaccess@tue.nl

providing details and we will investigate your claim.

Biphasic Synthesis of Furfural: Reactor Insights and Process Optimization



Myrto Papaioannou

Biphasic Continuous Synthesis of Furfural: Insights into Reactor and Process Optimization

PROEFSCHRIFT

ter verkrijging van de graad van doctor aan de Technische Universiteit Eindhoven,
op gezag van de rector magnificus prof.dr. S.K. Lenaerts, voor een commissie
aangewezen door het College voor Promoties, in het openbaar te verdedigen op
donderdag 11 mei 2023 om 16:00 uur

door

Myrto Papaioannou

geboren te Athene, Griekenland

Dit proefschrift is goedgekeurd door de promotoren en de samenstelling van de promotiecommissie is als volgt:

Voorzitter: prof. dr. ir. F. Gallucci
Promotor: prof.dr.ir. J. van der Schaaf
Co-promotor: dr. M.F. Neira d'Angelo
Leden: prof.dr.ir. J. van der Schaaf
dr. M.F. Neira d'Angelo
prof.dr.ir. B. Schuur (Universiteit Twente)
prof.dr.ir. W. de Jong (Technische Universiteit Delft)
prof.dr. E. Rebrov
prof.dr.ir. M. van Sint Annaland

Het onderzoek of ontwerp dat in dit proefschrift wordt beschreven is uitgevoerd in overeenstemming met de TU/e Gedragscode Wetenschapsbeoefening.

This research was performed under the framework of Chemelot InSciTe and is supported by contributions from the European Regional Development Fund (ERDF) within the framework of OP-Zuid and with contributions from the province of Brabant and Limburg and the Dutch Ministry of Economy.

Biphasic Continuous Synthesis of Furfural: Insights into Reactor and Process Optimization
Myrto Papaioannou

Eindhoven University of Technology, 2023

A catalogue record is available from the Eindhoven University of Technology Library
ISBN 978-90-386-5729-5

Printed by ProefschriftMaken

To my parents Arsinoi and Xenofon,

To Vassilis,

Στους γονείς μου Αρσινόη και Ξενοφών,

Στο Βασίλη,

Table of Contents

Summary	9
Nomenclature	13
Biomass Conversion and Furfural Synthesis using Intensified Reactor Technology	17
1.1. Biomass to bio-based chemicals.....	19
1.2. Furfural as a promising bio-based platform chemical.....	23
1.3. Process intensification for biomass valorization	30
1.4. Aim & outline of the thesis	36
Furfural Production by Continuous Reactive Extraction in a Millireactor under Taylor Flow	
Regime	39
Abstract	40
2.1. Introduction	41
2.2. Experimental Section	43
2.3. Results and Discussion.....	46
2.4. Practical Considerations	57
2.5. Conclusions	58
Kinetic Models of Furfural Synthesis from C5 Sugar Streams	59
Abstract	60
3.1. Introduction	61
3.2. Experimental section	65
3.3. Results and discussion	66
3.4. Conclusions	79

Effect of Feed Composition on the Continuous Synthesis of Furfural in a Biphasic Millireactor	81
Abstract	82
4.1. Introduction	83
4.2. Experimental section	85
4.3. Results and discussion	87
4.4. Conclusions	102
Conceptual Process Design of Scaled-up Furfural Biphasic Production & Techno-Economic Evaluation	105
Abstract	106
5.1. Introduction	107
5.2. Methodology & Approach	109
5.3. Results and discussion	118
5.4. Conclusions	136
Conclusions & Outlook.....	139
6.1. Conclusions	141
6.2. Recommendations	143
Appendices	147
Appendix A	148
Appendix B	154
Appendix C	160
Appendix D	163
References	177
Research output.....	201
Acknowledgements.....	203
About the author	207

Summary

The fast depletion of fossil resources and the tightening of environmental regulations has drawn the attention to lignocellulosic biomass (2nd generation) as an alternative carbon source for the production of chemicals and fuels. Under the right process conditions, lignocellulosic biomass can be selectively converted to platform chemicals. Among the possible routes of lignocellulosic biomass valorization, furfural production has attracted great industrial interest. Commercialized for decades and not yet well understood, this reaction proceeds via acid-catalysed dehydration of C5 sugars and includes several undesired furfural degradation reactions that lead to insoluble humins. Thus, the process presents selectivity limitations and has proved challenging to translate to continuous operation. Recently, an alternative process that has received significant research attention is the biphasic synthesis of furfural, where the synthesis and in-situ furfural extraction into an organic solvent is presented as a strategy to prevent furfural degradation. While the literature presents very promising furfural yields during the conversion step, the relevance of this process concept and its prospects of industrial implementation depend on issues such as, among others, the overall yield gains, the nature of the feedstock, and the overall energy efficiency of the process (including solvent recovery).

The main goal of the present dissertation is the assessment of the biphasic continuous synthesis of furfural focusing on the effects of reactor and process conditions on the process performance. **Chapter 1** provides an overview of the two main aspects related to intensified furfural production. In the first section of this chapter, the valorization routes of lignocellulosic biomass in industrial and smaller scale are discussed showing the importance and the potential of the renewable feedstocks. The literature review focuses on the synthesis of furfural, presenting the mechanistic aspects of its production from C5 sugars as well as relevant process considerations. The second section of this chapter presents the main principles of process intensification focusing on the concept of micro/millireactor and on the application of process intensification on furfural synthesis targeting at overcoming the selectivity barriers. The main body of the thesis contains three stages. The first stage (Chapter 2) is a proof of concept for the continuous synthesis of furfural from xylose (as model feed) in biphasic conditions. The second stage (Chapters 3 and 4) explores the feedstock type and its impact on furfural production. Finally, the third stage (Chapter 5) contains a techno-economic evaluation of the proposed design of furfural production process.

In **Chapter 2**, the use of a biphasic millireactor for the production of furfural via acid dehydration of xylose is demonstrated resulting to increased furfural selectivity (ca. 70%) and reduced humins formation, with minimal use of chemicals at almost complete xylose conversion and short residence time. Under these conditions, negligible formation of humins (<2% at 190°C) is achieved showing the stable continuous operation. Even though the millireactor was chosen as an ideal lab-scale reactor for research purposes, it also served as an example of intensified reactor technology identified as key to the success of this process concept. Finally, the assessment of the mass transfer performance of furfural in-situ extraction concludes that the mass transfer coefficient of the biphasic reactor and the selection of the solvent (expressed as furfural partition coefficient in the biphasic system) are the main parameters affecting furfural yield.

The second stage of this dissertation investigates the effect of feedstock type on furfural production. After demonstrating the proof of concept of the biphasic continuous synthesis of furfural from xylose (as model feed), **Chapter 3** explores the mechanism of furfural formation from C5 sugars (i.e., xylose and arabinose) in temperature range up to 190°C by aiming at shedding light in several aspects of the complex reaction scheme (usually studied for a narrow set of experimental conditions) that remain under debate. The concluded mechanism of xylose conversion path describes the participation of reaction intermediates during furfural degradation reactions. Unlike xylose, the reaction of arabinose dehydration to furfural can be modelled accurately as a one-step dehydration with a parallel arabinose degradation scheme. For both C5 sugars, the developed kinetic models (and the set of fitted parameters) are used for process and reactor optimization purposes showing that high reaction temperatures (> 200°C) and short residence time render the highest furfural yield (>70%). After establishing the C5 sugars conversion mechanisms to furfural, the research scope is extended to the investigation of feedstocks composition. Therefore, in **Chapter 4**, several feedstock types are experimentally tested including different xylose concentrations and mixtures of C5/C6 sugars with model compounds. The experimental findings show that there is no impact on the rate of xylose conversion when increasing initial xylose concentration, but furfural selectivity is negatively affected for more concentrated feeds (>6wt% xylose) concluding that diluted feeds favour furfural selectivity. The comparison between the two C5 sugars (i.e., xylose and arabinose) reveals that arabinose is less reactive than xylose upon dehydration under the same reaction conditions, hence requiring greater reaction temperatures to achieve significant yields. Furthermore, the experiments with C5/C6 sugars mixtures demonstrated that the co-production of HMF does not affect furfural selectivity. Finally, real feedstocks (i.e., side-stream from food industry and herbaceous hydrolysate) are successfully assessed demonstrating the versatility of the biphasic

continuous reactor. The experimental trends are well predicted by the developed kinetic model using model feeds supporting the validity of the kinetic model.

The third stage of this thesis includes a techno-economic evaluation of a biphasic continuous process of furfural production. In **Chapter 5**, the design of scaled-up furfural production in a biphasic continuous system is proposed by studying three main process parameters: organic solvent, feedstock type and feedstock concentration. The case studies are simulated and evaluated mainly in terms of reaction performance, energy demands and economic potential. Regarding the first parameter (i.e., solvent selection), the 2-sec-butylphenol is selected as a better solvent than MIBK in terms of furfural selectivity and process economics as a result of higher furfural partition coefficient in 2-sec-butylphenol and their difference in boiling point resulting to different downstream separation train. After gathering the main observations from Chapters 3 and 4, various promising feedstock-candidates for furfural production are evaluated. The assessment of various C5-rich industrial feedstocks indicates that the process with softwood-based hemicellulosic stream has high furfural selectivity (87%) and better process economics. Through this study, we find that the cost of the reactors and the use of steam for heat supply are the main contributors to the CAPEX and OPEX, respectively, resulting in furfural minimum selling price (MSP) higher than the market price. Therefore, more concentrated feedstock streams requiring smaller reactor volume and lower energy demands are investigated. Given that furfural production is an energy-intensive process and high reaction temperature is required dictated by the kinetics, a high-level heat integration is performed resulting to further reduction of OPEX and carbon footprint.

The conclusions of the research work presented in the aforementioned chapters are summarized in **Chapter 6**. In the same chapter, an outlook on the areas that could be considered for future research is also provided. The proposed recommendations are likely to enhance the robustness of the suggested process design and its applicability in industrial level.

Nomenclature

Abbreviations

LCM	Lignocellulosic material
PI	Process Intensification
MMR	Micro/Milli Reactor
RT	Room temperature
BPR	Back pressure regulator
HPLC	High Performance Liquid Chromatography
GC	Gas Chromatography
ODEs	Ordinary Differential Equations
NMR	Nuclear Magnetic Resonance
LC-MS	Liquid Chromatography-Mass Spectroscopy
MALDI-TOF	Matrix-assisted laser desorption/ionization-time of flight
MW	Molecular Weight
ID	Internal Diameter
DES	Deep Eutectic Solvent
HYD	Hydrolysate
MF	Model Feed
CAPEX	Capital expenditure
OPEX	Operating expenditure
NRTL	Non-random tow liquids
SR-POLAR	Schwarzentruber and Renon equation-based polar method
CSTR	Continuous Stirred Tank Reactor
KPI	Key Performance Indicator

Abbreviations

TCI	Total Capital Investment
FCI	Fixed Capital Investment
WC	Working Capital
SU	Start-up costs
MSP	Minimum Selling Price
MP	Medium Pressure Steam
HP	High Pressure Steam
DP _{<i>i</i>}	Degradation product from compound <i>i</i>
PDMS	Polydimethylsiloxane
PTFE	Polytetrafluoroethylene

Chemicals

GVL	γ -Valerolactone
THF	Tetrahydrofuran
DMSO	Dimethyl sulfoxide
HMF	5-Hydroxymethylfurfural
MIBK	Methyl isobutyl ketone
FA	Formic acid
LA	Levulinic acid
PLA	Polylactic acid
PEF	Polyethylene Furanoate

Symbols

$k_{L,a}$	Mass transfer coefficient [1/s]
m	Partition coefficient [$M_{furf}^{org}/M_{furf}^{norg}$]
X	Conversion [%]
Y_i	Yield of compound i [%]
S_i	Selectivity of compound i [%]
B	Mole balance [%]
Fv^k	Volumetric flow in phase k [mL/min]
C_i^0	Initial concentration of compound i [wt%]
$[i]$	Molar concentration of compound i [M]
MT	Mass transfer rate [M^{org}/s]
L_{uc}	Length of caps of slugs in Taylor flow [m]
L_{film}	Length of film of slugs in Taylor flow [m]
k_i	Reaction rate constant of compound i (including catalyst dependency) [$M_{catalyst}/s$]
k_i'	Reaction rate constant of compound i [1/s]
n_i	Number of moles of compound i [mol]
n_i^0	Initial number of moles of compound i [mol]
STY	Space Time Yield [$Y_{furf}/min/M_{CSsugar}^{in}$]
$V_{reaction}$	Reaction volume [m ³]
T	Temperature [°C]
H/C	Ratio of heating to cooling duty [kW/kW]

Greek Symbols

τ	Residence time [s]
δ	Film thickness [m]
λ	Wavelength [nm]

Superscripts

org	Organic phase
inorg	Inorganic/aqueous phase
Tot	total

Subscripts

V	volume
X (or xyl)	Xylose
Furf	Furfural
I	Intermediate of xylose dehydration
FI	Degradation product of furfural with intermediate
Arab	Arabinose
ADP	Degradation products from arabinose

CHAPTER 1

Biomass Conversion and Furfural Synthesis
using Intensified Reactor Technology

1.1. Biomass to bio-based chemicals

1.1.1. Lignocellulosic material and 2G feedstocks

In the past years, depletion of world resources, increasing environmental pollution and climate change have led us to seek a transition to renewable resources, for example by replacing the fossil-based resources with biomass. Biomass has always been a source of energy in society and industry. Initially, wood was used as burning material for heating purposes and, later, it was used as raw material for transportation systems during Industrial Revolution in limited extend [1]. Biomass is considered a renewable and carbon-neutral resource because it can be easily regrown by capturing through photosynthesis *nearly* the same amount of CO₂ that is released when burnt [2]. Therefore, the need for switching from the current crude oil refinery to carbon-neutral biomass refinery is imperative. Despite the historical broad use of biomass, there was not a distinct definition and classification of biomass until the 1970s [3] where environmental concerns associated with the chemical industry were on the rise. More recently in 1999, the biomass addressed for the production of bio-products and bio-fuels was coined as “Industrial Biomass” [4,5], which is defined as:

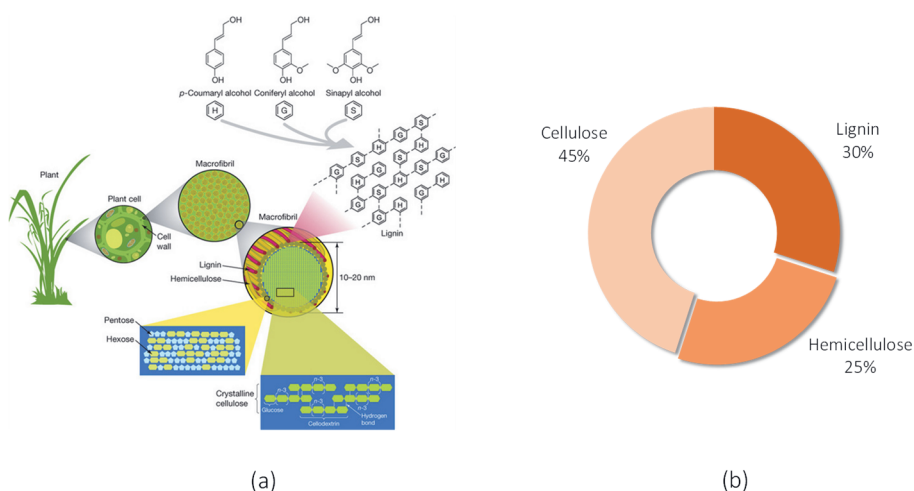
“Any organic matter that is available on a renewable recurring basis (excluding old-growth timber), including dedicated energy crops and trees, agricultural food and feed crop residues, aquatic plants, wood and wood residues, animal wastes, and other waste materials usable for industrial purposes (energy, fuels, chemicals, materials) and include wastes and co-wastes of food and feed processing.”

The first attempts of valorizing industrial biomass towards the production of biofuels include the use of edible resources [6,7]. This is the “1st Generation Biomass”. Due to ethical considerations, further biorefinery technology developments shifted to non-edible feedstocks (“2nd Generation Biomass”) [7]. Finally, the “3rd Generation Biomass” is based on algae, and is mainly considered for bio-fuels production [6,8]. Although recent research works have reported possible valorization routes of algae sugar-rich hydrolysates [9,10], mostly for bioethanol production from the C6 fraction, the pre-treatment processes of 3G biomass feedstocks are not fully developed yet.

While 2G biomass feedstocks hold the promise of CO₂ neutrality, it is widely available and it does not interfere with the food value chain, other aspects of feedstock sustainability are addressed in European directives and guidelines aiming at protecting and preserving the natural environment [11,12]. Protecting biodiversity of the environment and minimizing waste generation [11] (e.g., through recyclability of waste streams or residues in biomass

handling processes) are among the most important criteria that biomass feedstocks *should* fulfil in order to be considered sustainable [13]. While these aspects are not addressed in detail in this work, recent literature and research reports project sufficient 2G biomass feedstocks for the sustainable production of bio-based chemicals [14–16]. To that extent, some types of “2nd Generation” feedstocks are considered in the present work as appropriate feedstocks for bio-based chemicals such as furfural.

2G biomass groups include all the plant based biomass material (lignocellulosic material [LCM]) such as wheat straw, agricultural waste, plant and forest residues [17–20]. Increased quantities of wood-based biomass are available in Northern Europe, more specifically in Scandinavia (e.g., Finland and Sweden), where significant R&D efforts on biomass processing have been conducted. [21]. The most common biomass types in this area are pine, birch and spruce [22]. On the other hand, other European countries (such as Germany and Netherlands) have also high potential for the development of biorefinery industry because of their central location, which facilitates feedstock distribution [21].



Scheme 1.1. (a) LCM [23] and (b) Typical composition of lignocellulosic material [24]

Generally, LCM contains three types of bio-polymers: (1) cellulose, (2) hemicellulose and (3) lignin as depicted in Scheme 1.1. Ash, salts and lipids are also found in LCM, but in smaller amounts [20]. On average, cellulose comprises ca. 45% of the biomass, hemicellulose 25% and lignin 30%, as depicted in Scheme 1.1 [24]. Nevertheless, the composition in LCM varies depends on the nature of biomass. For example, sugar beets and rice straw contain 55% and

24% hemicellulose, respectively. Hence, the target product of biomass processing will define which feedstock type is more suitable [17].

1.1.2. Biomass valorization processes

The processing of biomass has limitless opportunities for the production of biobased chemicals, fuels, and polymers. Multiple process steps are usually required. In Table 1.1., a summary of the main methods of biomass–conversion is listed. First, thermochemical processes are some of the most studied and applied methods of biomass valorization. The main processes in this category are combustion, gasification, and pyrolysis. Combustion is widely used in industry for steam and/or electricity generation. Thus, (partially) replacing fossil feeds by bio-based waste residues is seen as a simple and viable way to reduce CO₂ and NO_x emissions [25], while the energy sector gradually transitions to “greener” energy sources [26,27]. In addition, by exposing biomass to high temperatures but a relatively less oxidizing atmosphere, gasification processes target biomass upgrade to valuable gases (e.g., syngas) [28]. The gaseous mixture can be directly used for power or energy production. Otherwise, it can be used as intermediate for the production of biobased liquid fuels (e.g., biodiesel) or biomethane [29,30]. Finally, biomass pyrolysis also takes place at high temperatures but in the complete absence of oxygen and typically short residence times (ca. 1s). This process renders bio-oil (i.e., a mixture of bio-oxygenates) as main product, and char and gases as by-products [31,32]. Even though thermochemical processes are more mature compared to other bio-based technologies, they are still not widely commercialised, although some examples of industrial applications exist (e.g., by BTG [33]). The high energy consumption (to reach high process temperatures), the low process selectivity and low-value products make these processes not economically feasible and less favored [34,35].

In recent years, a shift in the field of biomass valorization has triggered research into processes that seek a more selective conversion of biomass into added value chemicals and fuels. This type of processes typically take place at lower temperatures in aqueous media (vs. the earlier gas phase thermochemical processes) and make use of several types of (bio or chemo)catalysts. In such a way, biomass preserves most of its chemical functionality. According to this valorization strategy, biomass usually undergoes an initial fractionation step, where its main constituents (i.e., cellulose, hemicellulose, and lignin) are isolated into separate streams that may be upgraded via biochemical or chemocatalytic pathways (Table 1.1). There are various LCM fractionation processes, but the most common ones are Organosolv, Kraft pulping and steam explosion [36]. Organosolv and Kraft processes use solvents (organic or inorganic acid and bases, respectively) and steam explosion uses high-pressure steam to isolate cellulose [37–39].

With respect to further valorization of biomass fractions, biochemical processes use various microorganisms that decompose the LCM constituents to more valuable chemicals. Sugar fermentation is the most widely investigated and developed biochemical process. Sugar fractions of biomass are converted to alcohols (e.g., bio-ethanol) in the presence of yeast [40]. Bio-ethanol production from biomass has been extensively reported because of its use in gasoline as fuel blend under the legal framework imposed by European Union [13]. In order to successfully perform sugar fermentation, biomass fractions should first undergo enzymatic hydrolysis, another biochemical treatment that allows breaking of sugar polymeric chains to monomers [41] at low temperature and in the presence of enzymes. To reduce plant footprint, cost and energy input, these two biochemical processes can be combined in a one-step process that makes this route more attractive and feasible [42,43]. The main challenge in the biochemical processes is that LCM pre-treatment step should be selected carefully in order to minimize the presence of inhibitors in the reaction medium and decrease the efficiency of the process [41].

Table 1.1. Methods of biomass processing

Process Type	Method	Main products	Reference
Thermochemical	Combustion	Heat	[25–27]
	Pyrolysis	Char, Gas, Oil	[32,44,45]
	Gasification	Char, gas, syngas (CO/H ₂)	[29,30,46,47]
	Hydrothermal Upgrade (Liquefaction)	Oil, Char, Gas, aqueous phase organics	[48,49]
Biochemical	Fermentation	Alcohol, Chemicals	[40,50–52]
	Anaerobic digestion	Biogas	[53,54]
	Enzymatic hydrolysis	Chemicals	[41,55]
Chemocatalytic	Hydrogenation	Chemicals	[56–58]
	Oxidation	Chemicals/fuels	[59,60]
	Transesterification	Biodiesel	[61,62]
	Acid/Base Dehydration	Chemicals	[63–65]

Alternatively, numerous chemocatalytic processes (using both homogenous and heterogenous catalysts) have been developed to upgrade biomass fractions into valuable chemicals. Here, a short overview of the main chemocatalytic valorization pathways of the main LCM components is provided. First, within the sugar fraction of LCM, *cellulose* is one of the most valuable products that can be valorized as such (e.g., for the production of fibers [66]), or as a source of C₆ monomeric sugars (e.g., glucose) via hydrolysis of the sugar polysaccharides [20,28]. One of the most attractive platform chemicals from the C₆ sugars is 5-hydroxymethylfurfural (HMF), which is an intermediate for the production of biobased chemicals and bio-polymers (e.g. Levulinic acid, PEF) [20,67]. Cellulose can also undergo

catalytic oxidation forming products that are used in pharmaceuticals, medicine and cosmetics [59]. Similarly to cellulose, *hemicellulose* contains polymeric chains of C5 sugars (i.e., xylan and arabinan). By hydrolysis, hemicellulose can be converted into its respective building blocks (mostly xylose and arabinose) [17,20,28,68]. The main valorization pathway of C5 sugars is via the acid-catalyzed dehydration to furfural, an important platform chemical [20,67]. This conversion is precisely the focus of this thesis, so a more detailed discussion on the furfural synthesis and applications is covered in Section 1.2. At last, *lignin* is an amorphous biopolymer consisting of cross-linked aromatic units [20,69,70]. Until recently, lignin was merely discarded or burnt for providing on-site heat in the biorefineries [69,71]. However, the interest in lignin valorization has drastically increased in the past few years for both biobased chemicals and biofuels [71,72]. Lignin can be converted to biobased intermediates such as phenolic aldehydes or aliphatic carboxylic acids, biofuels and biobased alcohols [73–76].

Thus, considering the technological developments in the field of biomass valorization and possible line of products derived from it, it is plausible to envision future bio-refinery concept(s) that cover the future needs of chemical and fuels. Nevertheless, it is also evident that multiple reactor and/or process engineering solutions need to be in place to realize a complete biorefinery scheme and effectively valorise all biomass fractions.

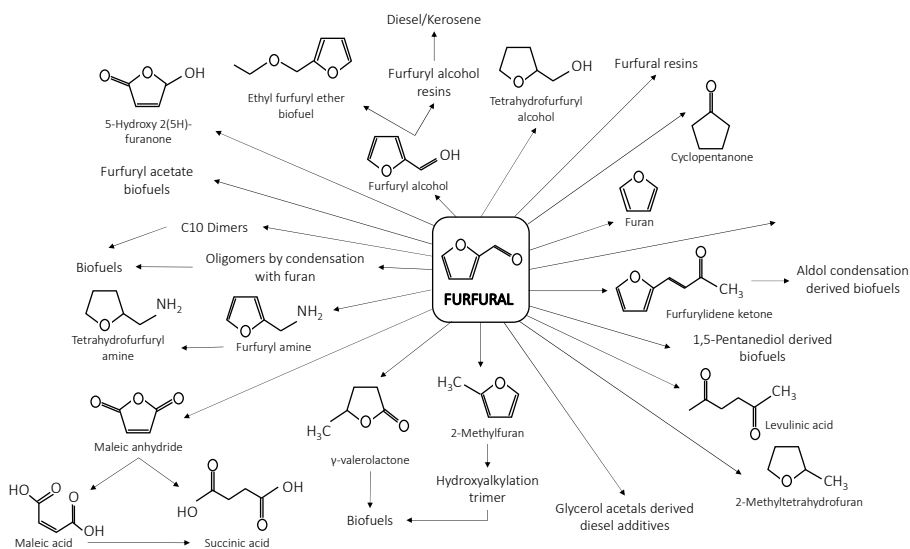
1.2. Furfural as a promising bio-based platform chemical

1.2.1. Furfural applications

Furfural is the main building block produced from the hemicellulosic fraction of biomass, it has a wide range of applications, and it is therefore considered as one of the most promising commodity biobased chemical [20,77–81]. It is widely used *as is* in different sectors. It is used in oil refining (as extraction solvent to remove chemicals of low lubricating quality from crude oil) [82], in the paper making industry (as decolorizing agent for crude wood resin) [78,83], in the agriculture sector (as fungicide and nematicide) [78,84], and in the food and drinks sector (as flavor enhancer, for example in cocoa, coffee, alcoholic beverages) [84,85]. Apart from the direct application of furfural in several industries, furfural is also an excellent intermediate in the synthesis of important biobased chemicals and polymers. The opportunities of furfural valorization are numerous (Scheme 1.2.), conferring furfural a significant role in the biobased chemical industry.

Depending on the reaction conditions and selected catalyst, furfural may undergo a different conversion pathway, leading to the synthesis of distinct furfural derivatives. Furfural hydrogenation is the most prevalent valorization pathway, which renders furfuryl alcohol,

cyclopentanone, or tetrahydrofurfuryl alcohol, again widening the range of applications. Among these, γ -valerolactone (GVL) has received great interest, as it has low toxicity, it is biodegradable, and presents excellent properties as solvent for pharmaceutical industry, as well as in various steps of biomass valorization processes [86,87]. Furans and tetrahydrofurans can also be used as fuel blend in gasoline and diesel [81,88]. In addition, furfural and furfuryl alcohol could be combined with phenols, acetone or urea for the formation of resins [89–93]. The furfural hydrogenated products could be further converted to 2-methylfuran, levulinic acid, or 1,5-pentanediol in a secondary step, usually via hydrogenolysis, hydrolysis or hydration reactions. These can be used as fuel additives and precursors of chemicals used in pharmaceutical industry and polymers synthesis. [94–98].

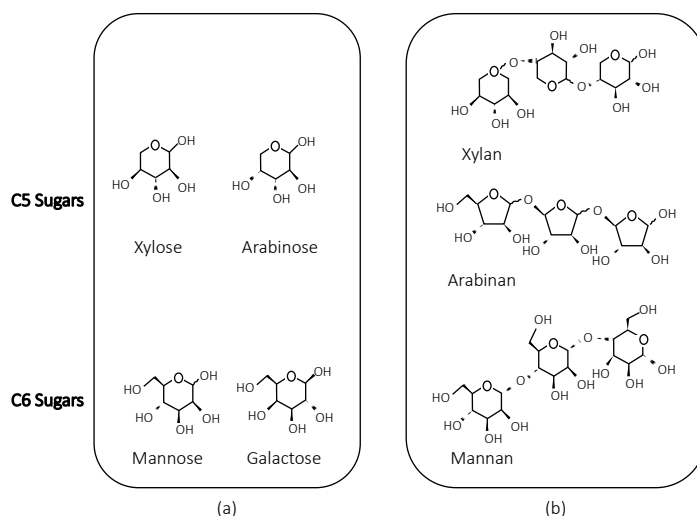


Scheme 1.2. Furfural as platform chemical

Alternatively, other conversion paths include furfural decarbonylation and oxidation, producing furfurylidene ketone and maleic anhydride or furoic acid, respectively. Several of these have important applications in the pharmaceutical industry. For example, furoic acid is further converted to furoyl chloride, which is an important chemical intermediate for the synthesis of various pharmaceuticals such as mometasone [99]. Finally, furfural derivatives can also be used as soil enhancers and organic fertilizers via the amination of furfural and the synthesis of furfuryl amine [100].

1.2.2. Furfural synthesis: mechanistic insights

Lignocellulosic material contains ca. 24% of hemicellulose depending on the biomass type [20,101]. Hemicellulose is consisted of polysaccharides and mainly contains C5 sugars (mainly xylan and arabinan), and C6 sugars in lower concentrations (typically mannan and galactan) [102]. The monomeric building units of these polysaccharides are xylose, arabinose, mannose, and galactose, respectively (Scheme 1.3a.). The abovementioned monomeric units in C5 polysaccharides are linked through glycosidic bonds in the α or β orientation¹. More specifically, xylose and mannose units are linked via β -1,4 bonds and arabinose monomers are linked via α -(1,5) linkages, as depicted in Scheme 1.3b [103]. Galactose monomers are linked via β -(1,4) and α -(1,3) bonds [104]. Hydrolysis of these polysaccharides in aqueous medium and in the presence of an acid catalyst breaks these glycosidic bonds, thereby freeing the monomeric units [105]. Once released from the polymeric chain, xylose and arabinose (i.e., the C5 monomeric sugars) can be converted to furfural via a sequence of dehydration reactions.

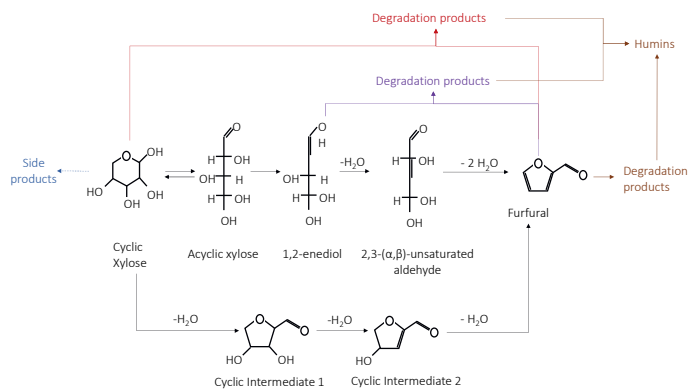


Scheme 1.3. (a) C5 and C6 monomer sugars in hemicellulosic fraction of LCM; (b) Sugars linkages in polymeric chains

¹ The difference between the two orientation lies in the stereochemistry of the two carbon atoms linked. In the case of α orientation, the linked carbon atoms have the same stereochemistry, whereas in the β orientation the two carbon atoms have the opposite stereochemistry [106].

Extensive research has tried to shed light into the complex mechanism of the acid-catalyzed dehydration of xylose to furfural. Most of mechanistic paths, reported in literature, mention that relatively high temperatures (>120°C) and inorganic Brönsted acid catalyst such as H₂SO₄

or HCl are required [107–110]. Organic Brønsted acids such as formic and acetic acid in various concentrations have also been studied as catalysts for furfural production [111,112]. The two most accepted mechanisms to describe this Brønsted acid-catalyzed conversion propose the ring opening of cyclic xylose as a first step, as depicted in Scheme 1.4. The first mechanism (i.e., the 1,2-enolization) further proposes the formation of 1,2-enediol as the subsequent step, followed by dehydration to furfural. The second mechanism (i.e., β -elimination) considers that xylose is directly converted to the first dehydrated intermediate (2,3-(α,β)-unsaturated aldehyde). This intermediate further dehydrates to furfural [113,114]. With relatively less supporting evidence, a third theory suggests the conversion of cyclic xylose to furfural, with intermediate dehydration products in cyclic form [107,115–117]. Moreover, studies have demonstrated that tandem catalysis, including Brønsted and Lewis acid catalysts (in homogeneous or heterogeneous form), promotes furfural selectivity. In this case, it has been suggested that xylose isomerizes into xylulose in the presence of both Brønsted and Lewis acid catalysts [118]. Then, xylulose is further dehydrated into furfural, presumably following a similar mechanism but more selectively than xylose. The use of heterogeneous catalysts (e.g., zeolites, ion-exchange resins) for furfural production has also been widely investigated [119–121]. In these cases, mechanistic studies are lacking due to the complexity and diversity of active sites. Therefore, relatively simplistic approaches (e.g., one-step xylose dehydration to furfural) have been adopted to interpret and model the reaction mechanism on solid catalysts. In addition to the reactions leading to furfural, its subsequent acid-catalyzed degradation has been widely reported in literature [108,110,118,122,123]. Other parallel and sequential reactions (i.e., involving the feed, reaction intermediates and/or furfural) have been postulated to explain furfural selectivity losses (Scheme 1.4). Nevertheless, due to limited consensus, this topic remains an important subject of research [108,123–125].



Scheme 1.4. Overview of reaction mechanisms proposed for furfural formation from xylose using Brønsted acid catalyst

Similarly to xylose, arabinose (i.e., another important C5 sugar present in hemicellulose streams) dehydration to furfural has also been studied using inorganic and organic acids as catalysts (e.g., sulfuric acid and concentrated formic acid) [112,126,127]. Nevertheless, much lesser insights into the reaction mechanism starting with arabinose have been published in the literature [126]. Thus, the topic remains an important subject of research, as a proper kinetics analysis in wide range of reaction temperature and catalyst is key to the proper design of reactors and processes despite the extensive discussion on the mechanistic aspects of xylose and arabinose dehydration reactions.

Table 1.2. Main studies of mechanisms of furfural formation from arabinose and xylose for various conditions in homogeneous systems

#	Substrate	Catalyst	Reaction temperature	Mechanism	Reference
1	Xylose	H ₂ SO ₄ (0.1-2M)	120-160°C	1,2-enolization	[114,123]
2	Xylose	HCl (0.05M)	160-210°C	1,2-enolization	[124]
3	Xylose	HCl (0.1M)	130-170°C	β -elimination	[108]
4	Xylose	H ₂ SO ₄ (0.001-0.04M)	250°C	β -elimination	[107]
3	Xylose	H ₂ SO ₄ (16-52wt%) HCl (0.1M)-CrCl ₃ ·6H ₂ O (0.02-0.135M)	67-127°C 105-145°C	Via xylulose formation	[113] [118]
4	Xylose	CH ₂ O ₂ (30-64wt%)	130-170°C	1,2-enolization	[112]
5	Xylose	HCl (0.05-0.15M)- mineral salts	170-210°C	1,2-enolization, β - elimination	[125] [112]
6	Arabinose	H ₂ SO ₄ (0.05-0.1M)	140-200°C	1,2-enolization	[126]
7	Arabinose	CH ₂ O ₂ (10-62wt%)	130-170°C	1,2-enolization	[112]

1.2.3. Furfural synthesis: process considerations

The first industrial furfural production process was developed by the company Quaker Oats in 1921 [84], and to-date it remains nearly unchanged. Here, biomass, water, and sulfuric acid are fed to the batch-operated reactor vessels at ca. 150°C. After a relatively long reaction time, the liquid phase is collected and fed to the downstream section for furfural purification. Most of furfural production is currently located in China (with 74% of the furfural market share in 2020 [128]), Dominican Republic (host of the largest furfural production unit, with

an average production of ca. 35 kton/year from sugar cane bagasse [129]), and South Africa. Other countries with industrial furfural production units are USA, Austria, Italy and Belgium [128,130]. The production plants in China mainly operate in batch mode following the (original or slightly modified) Quaker Oats process [131]. In general, it is a process with relatively low CAPEX but poor furfural yields (max.50%). In Dominican Republic and South Africa, the industrial production of furfural is also partly based on the batch Quaker Oats process, and partly on the more recent and sophisticated Rosenlew continuous process [131]. The latter is an autocatalytic process in which the organic acids released from the lignocellulosic material act as catalysts [84]. The reactor is a stripping column where LCM and steam are fed counter-currently. During operation, furfural is stripped into the gas phase with the rest of volatile compounds [84]. While the Rosenlew process concept promises better yields and a continuous (economically advantageous) operation, the process efficiency is limited by the mass transfer between the different phases. Other process innovations attempting continuous and effective furfural production have also been operated in industry. Among them, the continuous version of Quaker Oats process was developed in Florida and contemplated a horizontal continuous reactor where pre-treated biomass was fed continuously. The reactor had intermediate nozzles for superheated steam and catalyst (dilute sulfuric acid) injections [84]. At the reactor exit, a cyclone was placed to separate the solid residue from the vapor phase. Nevertheless, the plant ceased operation due to high maintenance costs amidst other reasons [84]. Moreover, the SUPRAYIELD process has been developed in pilot-scale as a promising furfural production process [132]. Once furfural is formed at high temperatures (180-240°C), it is instantly removed from the reaction medium, which is kept under boiling conditions. Then, the stripping steam is condensed, and furfural is obtained [84,133]. However, the use of large amounts of steam to keep the high temperature in the reactor and the delicate control of pressure to maintain it under boiling conditions make this process energy demanding and less viable. Additionally, Vedernikov et. al introduced a process of furfural formation from bagasse using concentrated sulfuric acid. It is described that furfural yield is enhanced by coupling biomass hydrolysis and sugars dehydration in one step [133,134]. The process performance is remarkable and competitive, but the very high acid concentrations caused severe issues related to the equipment corrosion. Finally, other plants in pilot scale activities have targeted the production of furfural. Lignol Energy Corporation developed an Organosolv-based technology for the fractionation of wheat straw addressed for cellulose enzymatic hydrolysis followed by sugars fermentation for ethanol production. According to reports, producing only ethanol via this process was not financially feasible, but the co-production of xylose, furfural, acetic acid and lignin makes this process more attractive [135]. Similarly, a biomass refining unit in pilot scale was developed by CIMV (Compagnie Industrielle de la Matière Végétale). Their fractionation process results in paper pulp (i.e., the cellulose fraction),

hemicellulosic syrup and sulphur-free lignin [133,136]. Currently, the plant in Lenzing (Austria) is a large biorefinery facility that focuses on the production of cellulosic fibers from wood for pulp and other applications (e.g., textile). During the wood processing (cooking), furfural is formed and it is isolated from a multi-step separation process including condensation, extraction and distillation [137,138].

More recent R&D efforts at lab and pilot scales aim at overcoming the selectivity barrier of this process described in Section 1.2.2. Examples include the use of additives with catalytic effects in the desired/undesired reactions. One of the most widely reported strategies is the addition of metal halides and Lewis acid catalysts (e.g., FeCl_3 , CrCl_3), which have proved to promote the furfural synthesis pathway over the undesired degradation reactions [118,125]. Similarly, it is also reported that the addition of salts (e.g., NaCl) might have catalytic effects that promote furfural selectivity [125,139]. Salts can also be used in the reaction when coupled with in-situ furfural removal via extraction or stripping. In this respect, the use of salts is known to promote furfural separation via the so called “salting-out effect” or minimizing water evaporation, respectively (i.e., a thermodynamic effect). Moreover, the use of (water-miscible) ionic liquids as additives or co-solvents has also been evaluated as strategy to boost furfural selectivity due to solvation effects, although its effect seem to be limited to lower reaction temperature (up to 160°C) [140,141]. Even though they seem a promising addition to the optimization of furfural production, they are still not applied on industrial scale due to limited knowledge of their physico-chemical and equilibrium properties, and lack of an efficient recovery processes [140]. Another type of (water-miscible) co-solvents with positive effect on furfural selectivity are organic solvents such as γ -valerolactone (GVL), THF or DMSO. They have been reported to stabilize the intermediates state and promote the reaction towards furfural synthesis (i.e., solvation effect). In these cases, furfural selectivity can be improved up to ca. 80-90% [142,143]. Finally, the use of water-immiscible solvents (biphasic system) has also been investigated with positive effects on furfural yield. The solvent does not (necessarily) interfere with the kinetics, but it acts as extracting agent for furfural in-situ removal preventing it from further degradation reactions [110,139,144,145]. Several organic solvents have been reported useful for this application, with the most popular being toluene, MIBK and 2-sec-butylphenol [108,110,145,146]. Important properties of these solvents are their stability under reaction conditions and the furfural partition coefficients in the water/solvent mixture. Other aspects such as the ease of separation of the furfural/solvent mixture, the solvent toxicity and its environmental impact are also gaining recognition among the scientific community. For example, throughout the duration of this PhD thesis, the use of “green” water-immiscible Deep Eutectic Solvents (DES) for this application has been investigated leading to very promising results (due to their greenness, their high partition coefficients and ease of separation [147,148]). The biphasic

synthesis of furfural is the main focus of this thesis, so a more detailed discussion on this subject is provided in Section 1.3.3.

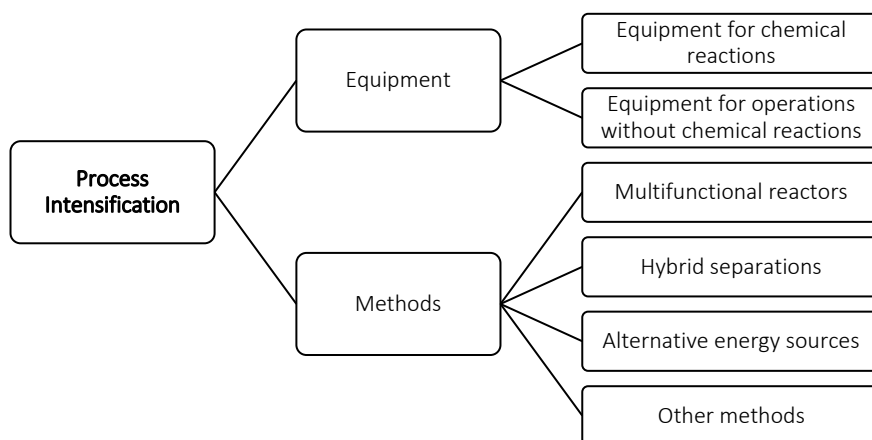
1.3. Process intensification for biomass valorization

1.3.1. Main principles and applications of Process Intensification (PI)

The interest of scientific and industrial community towards process intensification has risen over the years, and multiple of its advantages have been widely reported. The concept of process intensification has been defined by Reay et. al. as [149]:

“Process development involving dramatically smaller equipment which leads to improved control of reaction kinetics giving higher selectivity/reduced waste products, higher energy efficiency, reduced capital costs and reduced inventory/improved intrinsic safety/fast response times. ”

To that end, PI strategies (Scheme 1.5) mainly consist of developments of novel equipment (e.g., reactors or other contactors) and/or methods (e.g., combining reactions and separations) that, in a general sense, aim at: (1) maximizing the intra and intermolecular events ensuring higher conversion and selectivity, (2) ensuring that all molecules experience the same process conditions, (3) optimizing driving forces and maximizing the surface areas, and (4) maximizing the synergy between different operating units and processes [150,151].



Scheme 1.5. Principles of Process Intensification for technology development [151]

While the possibilities are endless, examples of innovative equipment that align with the principles of PI are multiphase contactors. They allow for exceptionally fast heat and mass transfer of species across interphases, such as structured (micro)reactors (see details in Section 1.3.2) and high gravity reactors (e.g., spinning disc reactor or rotating packed beds) [150,152–154]. In this thesis, they are often referred as intensified reactor technologies. This type of devices has been proved highly efficient to perform multiphase (gas-liquid, liquid-liquid, and even gas-liquid-solid and liquid-liquid-solid) reactions or separations, where minimizing un-wanted concentration and/or temperature gradients was key to maximize yields or minimize energy demands [155–157].

Another important strategy to achieve PI is the combination of several reactions and/or reaction and separation, in a so-called *multifunctional* reactor. This strategy is only advantageous when the combination of processes in a single unit has a synergistic result (e.g., it helps overcome a thermodynamic barrier or it prevents a desired species from degrading). Characteristic examples are reactive membranes operations, reactive stripping, and reactive extraction. For example, reactive membranes are applied during the detoxification process to eliminate process inhibitors (e.g., HMF, furfural, inorganic and organic acids) during biofuels production via fermentation. This approach allows for a reduction of processes steps, as well as a significant reduction in the energy consumption for separation step. Otherwise the separation process would be conducted via the highly energy consuming processes of evaporation or extraction [158,159]. Reactive stripping is another example where a reaction (usually in the liquid phase) is combined with in-situ separation (usually of the product) via stripping to a gas phase (e.g., steam or an inert gas) in order to overcome selectivity losses or thermodynamic limitations. In fact, reactive stripping has been successfully applied to the furfural production processes, by feeding C5 sugar-rich stream and the acid catalyst solutions to the reactor along with steam. The formed furfural is stripped out of the liquid to the steam phase, and eventually removed from the reactor in vapor phase. This configuration leads to improved furfural yield (increase by ca. 50%) [121,160] with respect to the case that reaction and separation take place in two subsequent steps [84]. Similarly, reactive extractions combine a reaction with an extraction process (sometimes of a reactant or a product) to boost process performance. It has been applied in the selective production of bio-based carboxylic acids, furfural and their recovery [161]. In order to maximize the performance of these multifunctional reactors, it is important to ensure high mass transfer rates and large interfacial areas to ensure fast extraction. Thus, the successful implementation of these PI strategies is to some extent reliant on the use of intensified reactor technologies.

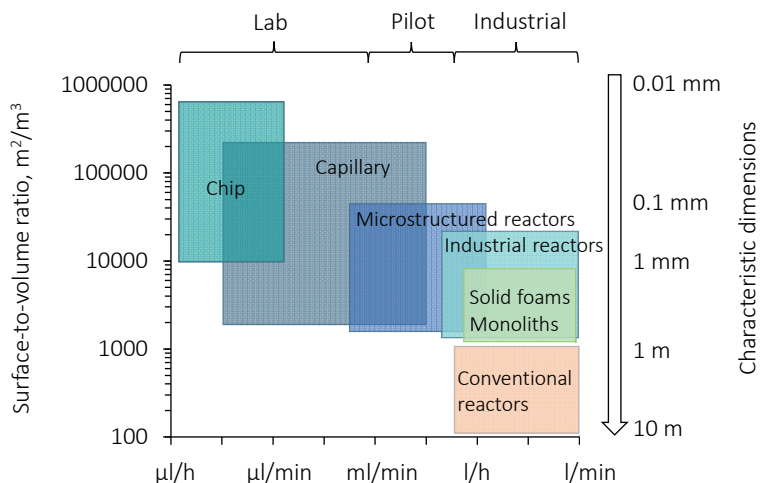
In addition, it is also common among intensified technologies to operate in continuous mode. Continuous processes have lower material requirements, and their operation time is shorter

compared to batch systems. Furthermore, the operating conditions can be easily monitored and adjusted to process demands. Even then, a full transition from batch to continuous operation is often hindered by limited knowledge of the process (e.g., limited understanding on kinetics and effect of transport mechanisms), or other process hurdles (e.g., formation of solid by-products that may cause blockages).

Thus, while it is evident that process intensification strategies offer great potential to develop sustainable and cost-competitive bio-refinery processes, the eventual deployment of such strategies in industry will rely on the development of the necessary first-principles knowledge of the underlying chemical and physical phenomena (e.g., reaction kinetics and mass transfer rates). Besides, it is important to *properly* assess the overall impact of implementing PI strategies from a holistic perspective.

1.3.2. Micro/Milli-Reactors (MMR)

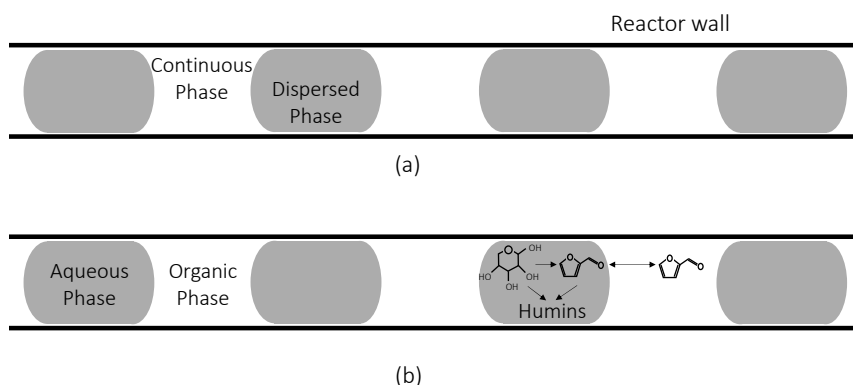
Flow micro- and milli-reactors are continuously operated devices with an inner diameter varying from 0.1 up to 3 mm [65,162]. MMRs are usually made of hydrophilic or hydrophobic material depending on the application. The most common materials for capillaries and chip microreactors are glass, silica or PDMS. MMRs are usually made of stainless steel, glass, or other alloys such as Hastelloy.



Scheme 1.6. Comparison and scalability of flow reactors [163]

As depicted in Scheme 1.6., due to the increase of reactor inner diameter to achieve greater throughputs, the surface-to-volume ratio typically decreases when scaling-up flow reactors

[163]. Due to their small inner diameter (or high surface-to-volume ratio), MMRs benefit from enhanced mass and heat transfer performance. This advantage is more relevant in the case of multiphase systems where the small reactor diameter facilitates the creation of high interfacial areas (up to $13000 \text{ m}^2/\text{m}^3$ [163] against $100\text{--}2500 \text{ m}^2/\text{m}^3$ for conventional reactor [164,165]) and, hence, increased mass transfer coefficient (e.g., $k_{\text{La}} = 10^{-2}$ up to 10 s^{-1} [162,163] against $10^{-4}\text{--}10^{-2} \text{ s}^{-1}$ for conventional reactor [166–168]). For gas-liquid or liquid-liquid systems, Taylor flow (Scheme 1.7a) is one of the most stable flow regimes in microchannel flow reactors in a wide range of flow rates. The Taylor flow development is generally described as a flow pattern of a biphasic fluid system consisting of elongated bubbles of dispersed phase separated by slugs of continuous phase [169]. In the case of liquid-liquid systems, the nature of continuous phase (e.g., aqueous, or organic) depends on the nature of the MMR wall material (e.g., hydrophilic, or hydrophobic, respectively). The development of Taylor flow has been thoroughly studied and published correlations allowing for accurate prediction of mass transfer properties based on flow properties (i.e., slug length and velocity) [170,171]. In addition to enhanced mass transfer properties, the Taylor flow regimes in MMRs promote the heat transfer properties of the system. It has been reported that liquid-liquid Taylor flow can significantly promote the heat transfer in MMR when compared to a single-phase system. [172,173]. The effects of enhanced heat and mass transfer performance of MMRs is demonstrated for various biomass conversion processes, including the selective synthesis of furanics and valorization of (e.g., HMF and furfural) in biphasic systems [65,155,174].



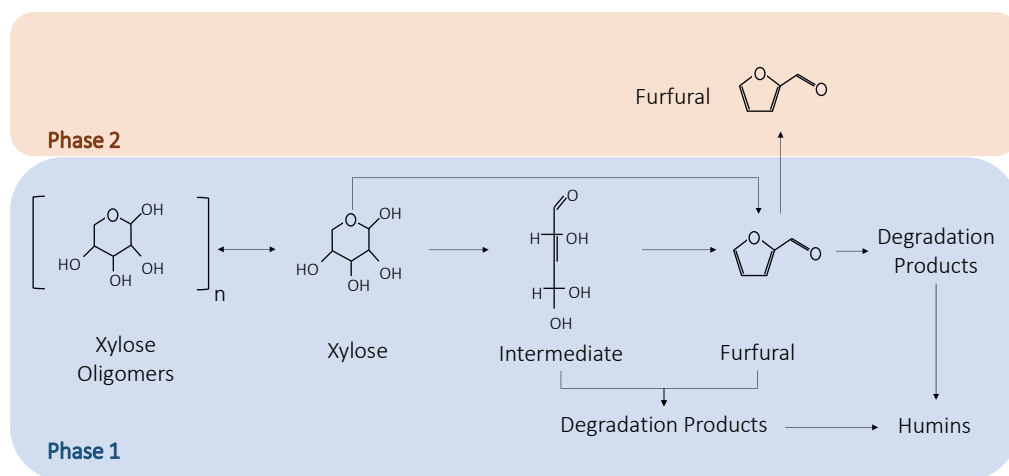
Scheme 1.7. Taylor flows development in millireactor (a) and Taylor flow development in biphasic furfural production with hydrophobic reactor wall (b)

MMRs are usually employed for research purposes at laboratory scale, since they allow for a high throughput scanning of different reaction conditions while using small quantities of

reagents and solvents [163]. Another advantage of using MMR is the good control of reaction parameters (e.g., residence time, temperatures), which allows for reliable and faster testing, decreased use of materials and precise kinetic studies. Owing to their benefits for laboratory testing, MMRs have been used for more complex systems including heterogeneously-catalyzed reactions [175–177]. In this respect, the solid catalysts are loaded as beds or coated on the inner reactor walls. The main challenge of the MMRs is their limited scalability, which usually comprises a trade-off between costs and performance (if scaling-up is achieved via numbering-up or sizing-up, respectively). In this case, understanding reaction kinetics and mass transfer rates is key to address such a trade-off and propose optimal scale-up strategies accordingly [178].

1.3.3. Process intensification for furfural production: state-of-the art and future challenges

To date, the main challenges in the synthesis of furfural continue to revolve around furfural selectivity and the consequent formation of (solid) humins, which would cause pressure build-up and clogging threatening the prospects of any continuous operation. Various technologies based on process intensification can contribute to address these challenges. For example, the combination of furfural synthesis with its in-situ removal (Scheme 1.8.) is an effective measure to minimize the extent of furfural degradation, and therefore that of humins formation.



Scheme 1.8. Concept of process intensification application on furfural production

Among the possible ways to combine reaction with in-situ furfural removal, reactive stripping has received most of the industrial attention to-date [84,179]. Examples of this concept used

at industrial scale are the Rosenlew and SUPRAYIELD processes, as discussed in Section 1.2.3. More recently, it has been demonstrated that steam can be replaced by an inert “non-condensable” gas (e.g., H_2 , if a subsequent furfural hydrogenation step is envisioned in the same plant [180,181]), leading to a less energy consuming separation and less furfural dilution [121,160]. Nevertheless, co-evaporation of water cannot be entirely prevented in this process, leading to a trade-off between energy demands and furfural yields.

On the other hand, furfural synthesis via reactive extraction has received (mostly) academic interest in the last 10 years, and few patents based on this concept reveal industrial attention too [182–184]. In this process, the aqueous sugar stream is mixed with a water-immiscible organic solvent that extracts furfural from the reaction medium as soon as it is produced. In this way, it is possible to increase furfural yields (i.e., up to 70%, depending on process conditions [108,118,185,186]), as well as to reduce the number of unit operations (i.e., reaction and extraction in the same unit). This concept has been demonstrated with various mineral acids (mostly H_2SO_4 and HCl) and heterogeneous catalysts [120,187,188] along with several organic solvents by the most popular being toluene, MIBK and 2-sec-butylphenol [108,185,189]. Despite the promises of the biphasic synthesis of furfural, its full optimization potential and industrial competitiveness remain subject of research. In this context, several research gaps are identified and summarized below.

First, the effect of reactor technology on the success of the biphasic synthesis of furfural remains relatively unexplored. The initial studies reported on this process prior to the start of this PhD thesis made use of autoclave-type batch reactors for screening purposes (e.g., testing effects of solvents and reactivity for pure model compounds, also in combination with solid catalysis [108,185,189]). Most of these works were conducted at mild reaction temperatures (up to $170^\circ C$), and the effects of mass transfer rates were left unexplored or deemed irrelevant under these conditions. Nevertheless, it is conceivable that more extreme operating conditions (e.g., higher temperatures) would also require faster mass transfer rates, thus making the choice of reactor technology of greater relevance. In addition, it is also expected that the poor control of reaction time in batch reactors (due to extended heating and cooling times) will play a role in the overall yield gains. In this line, the present thesis and other studies reported in the last few years address the benefits of mass transfer rates and continuous operations for this reaction [110,139,176,190].

While any attempts of process intensification should be based on a reliable characterization of kinetic scheme as function of process parameters (such as temperatures, type and concentration of acid catalysts, or presence of additives in the reaction medium), a solid understanding of kinetic mechanisms and predictive kinetic modelling for the synthesis of

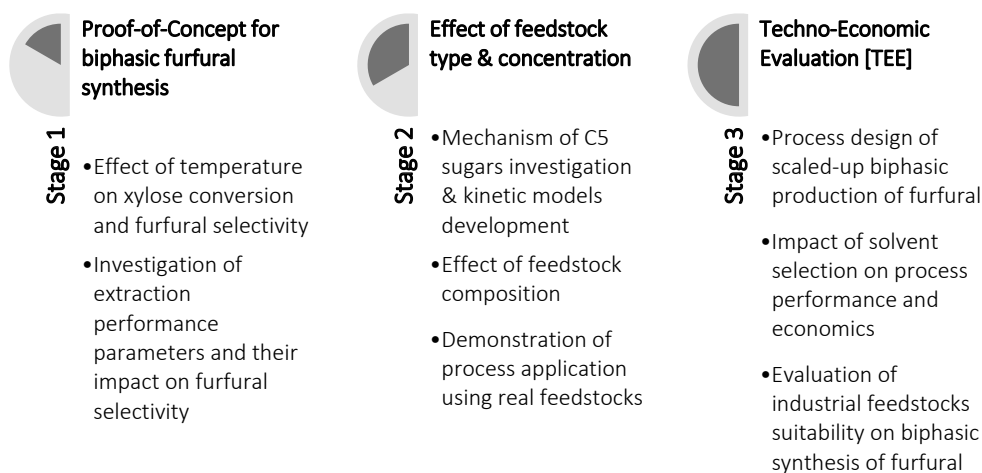
furfural is lacking. Literature and industrial experience point at H_2SO_4 as one of the most attractive catalysts for this reaction, featuring good activity, industrial experience (also for biomass processing), and less corrosivity than other counterparts (e.g., HCl). Nevertheless, even for H_2SO_4 , a reliable kinetic model able to predict the reaction performance in a wide range of temperature and acid concentrations does not exist.

In addition, recent trends in the field of biomass valorization look at the prospects of biomass fractionation prior to (chemo-/bio-)catalytic upgrade of all individual biomass constituents. Thus, the future synthesis of furfural may have to contemplate the waste biorefinery streams as primary feedstock in contrast to the current industrial experience where furfural is produced from raw lignocellulosic feedstocks (e.g., corn-cobs, rice husks). In this context, fundamental aspects of the effect of feed type and composition (incl. impurities) on furfural production need to be investigated.

Finally, while the effect of introducing organic solvents in the reactor performance alone seems to be promising, the impact on process techno-economic and environmental performance (e.g., accounting for energy for separation etc.) remains a subject of industrial interest.

1.4. Aim & outline of the thesis

The present thesis is part of the HORIZONTAL Project supported by Chemelot InSciTe (Institute of Science and Technology). The overall aim of the project is the valorization of hemicellulosic streams towards various building blocks, making use of the improved performance of technologies based on process intensification. Ultimately, the HORIZONTAL project aims at identifying processes with financial potential suitable for scale-up and piloting towards economically viable applications.



Scheme 1.9. Three-stage approach of the continuous biphasic furfural production research

Within the HORIZONTAL project, this PhD thesis focuses on the biphasic synthesis of furfural from hemicellulosic streams. The work follows a three-stage approach, as depicted in Scheme 1.9:

The first stage consists of a proof of concept for the continuous synthesis of furfural from xylose (as model feed) in biphasic conditions. To this end, Chapter 2 showcases the advantages of using a millireactor (hereby considered as model example of intensified reactor technology) for the biphasic synthesis of furfural in continuous operation. This chapter investigates the effect of temperature on furfural yields and carbon balance (incl. humins), and dives into the relevance of mass transfer rates on furfural production.

The second stage zooms into the effect of feedstock (type and composition) on furfural synthesis. First, Chapter 3 explores the mechanism of furfural formation from xylose and arabinose (i.e., the most representative C5 sugars in hemicellulose streams). For these two sugars, a kinetic model valid in a wide temperature range (up to 190°C) is developed and used to identify the optimum reaction conditions to maximize furfural yields. Next, Chapter 4 presents an experimental investigation on the influence of feed type and composition on furfural production employing a biphasic millireactor. The work uses pure xylose, arabinose, and mixtures of C5 sugars with glucose-fructose in order to investigate their impact on the mechanism of furfural formation. Moreover, two real feedstocks (i.e., biomass hydrolysate and food waste streams) are used in the experiments to compare the reaction performance against that of the model feeds.

Finally, the last stage consists of an economic evaluation for the biphasic production of furfural from realistic feedstocks. To this end, Chapter 5 presents a detailed techno-economic assessment (including estimations of CAPEX/OPEX) of this process. The study considers two different solvents (i.e., MIBK and 2sec-butylphenol) with distinct boiling points and furfural partition coefficient, as well as a sensitivity analysis of feedstock types. Various hemicellulosic feedstocks available in industry are evaluated in terms of furfural production and financial feasibility. Furthermore, the sugars concentration and its impact on furfural minimum selling price is investigated. At last, a high-level energy integration is performed and the main opportunities for savings are identified.

CHAPTER 2

Furfural Production by Continuous Reactive Extraction in a Millireactor under Taylor Flow Regime

Based on:

*M. Papaioannou, M.F. Neira d'Angelo, R.J.T. Kleijwegt, J. C. Schouten, J. van der Schaaf,
Furfural Production by Continuous reactive extraction in a millireactor under Taylor Flow
Regime, Ind. Eng. Chem. Res. 2019, 58, 35, 16106-16115*

Abstract

This study demonstrates the use of a millireactor as intensified technology for the continuous production of furfural via acid dehydration of xylose in a biphasic media. Very rapid extraction of furfural, aided by fast mass transfer rates, is key to preventing furfural subsequent degradation. Thus, by operating at elevated temperatures (i.e., 150–190°C), it is possible to maintain high furfural selectivity (ca. 70%) at high xylose conversion (ca. 80%) and very short residence times (up to 2.5 min). A reaction mechanism is proposed based on the observed conversion-selectivity trends, and on the analysis of product distribution. The contribution of humins to the carbon balance is remarkably low due to the high furfural extraction rates achieved in the millireactor. Through first-principle reactor modelling, we further demonstrate the potential of combining intensified reactor technologies with the extractive synthesis of furfural and show that solvent optimization will be crucial to boost furfural selectivity above 80%.

2.1. Introduction

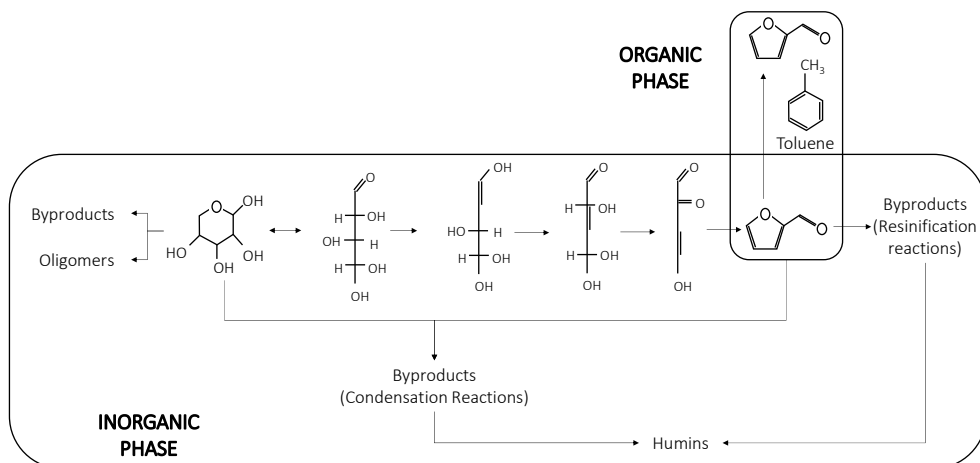
Recently, the conversion of biomass into chemicals and fuels has attracted increasing attention [191,192] because of the fast depletion of fossil resources and the environmental impact associated with their use. Among the existing biomass feedstocks, nonedible and abundant lignocellulose (which consists of lignin, cellulose, and hemicellulose) is one of the most attractive. One of the most important derivatives of lignocellulose is xylose, a pentose largely abundant in the hemicellulose fraction, which accounts for 25–30% of the total biomass. In an acidic environment, xylose readily dehydrates to furfural, an important building block for the production of furfuryl alcohol [24] and other polymer precursors [81,193].

The production of furfural at industrial scale was first realized in 1921 with the Quaker Oats process, in which the dehydration of xylose was conducted batch wise in the presence of diluted sulfuric acid (ca. 2wt %) at low temperatures (ca.153 °C) and long residence time (ca. 5 h). Severe furfural degradation under these reaction conditions resulted in low furfural yields, which triggered further attempts of process optimization in the following years. In the 1960s, Quaker Oats introduced a continuous process in which furfural is stripped using steam in order to decrease its subsequent degradation into humins. Later in 1991, the SUPRAYIELD process [80,84] made use of a two-reactor approach (one operating at 240°C, and the other at 180°C) to reduce the residence time to 1h, and increase product selectivity [84].

The renewed interest in this conversion during the past decade has given rise to significant research which aims at a more fundamental understanding of the reaction mechanism (especially that of humins formation) as a means to propose further optimization strategies. Various studies suggest possible mechanisms for the production of furfural from xylose [84,107,112,122,194]. The most accepted mechanism (Scheme 1) [107] suggests an initial isomerization reaction, followed by three subsequent dehydration reactions leading to furfural. Further, furfural in the acidic aqueous solution undergoes a series of undesired degradation reactions (resinification reactions) that result in humins formation. Additionally, parallel reactions of xylose (e.g. condensation reactions) [107,109,118,121,125,195–198] have also been suggested in the literature as plausible routes to humins formation. Nevertheless, due to the difficulties to follow all reaction intermediates and degradation products, the true mechanism of this reaction remains under debate. As for the catalyst choice for xylose dehydration, Brönsted acid catalyst is the most common type. Extensive research has also been performed in the use of heterogeneous catalysts for furfural production [121,198] it has been reported that the combination of Brönsted and Lewis acid catalyst consists one of the solutions toward the optimization of furfural production [118]. Moreover, the use of CO₂ has been reported as an alternative catalyst choice [199]. Finally

the addition of ionic liquids has been reported to be beneficial for the furfural formation [140,200].

On the basis of the premise that an important route to humins formation starts from furfural, Weingarten et al. proposed the in-situ removal of furfural from the aqueous solution by extraction to an organic solvent (e.g., methyl- isobutyl-ketone or MIBK) [108] to increase the selectivity of furfural. In such way, the reaction can successfully be conducted at higher reaction temperatures (150–170°C), which allow for faster reaction rates with no significant drop in selectivity of furfural due to its direct extraction to the organic solvent. To that extent, it is expected that the benefits of furfural selectivity compensate the disadvantages of cofeeding a solvent (e.g., separation costs). Still, the required residence times to achieve significant yields under these conditions remain relatively long (e.g., 50 min). Besides, from an industrial point of view, a continuous process would be in fact more advantageous. For such system, the use of micro/milli scale reactors would be advantageous as they offer enhanced mass and heat transfer rates, as well as excellent control of residence time and reaction conditions, especially if operated in the Taylor flow regime. These characteristics are important to tune product distribution and maximize the extraction efficiency, which in turn will increase furfural selectivity. Moreover, millireactor can be used for high throughput experimentation, allowing fast and safe screening of different process conditions (e.g., temperature, residence time).



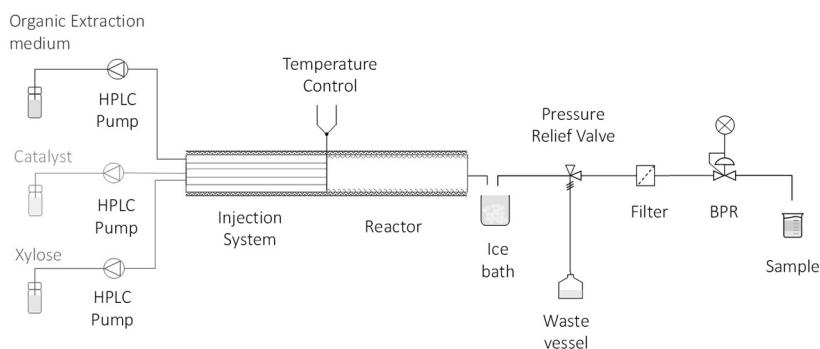
Scheme 2.1. General mechanism of furfural production in a biphasic system

In this work, a tubular millireactor was used for the continuous conversion of xylose to furfural using sulfuric acid as catalyst and toluene as extracting medium. In the present study, xylose is used as a model compound, representative of a sugar-rich hydrolysate stream, or even other hemicellulosic waste stream like corncobs [201]. An innovative injection system has been designed for the present study to effectively control the reaction temperature and the residence time. This work focuses on the use of very short residence times ($\tau = 80\text{-}396$ s), which have been largely unexplored in the open literature, and yet highly beneficial to minimize degradation reactions. Moreover, the influence of several parameters (e.g., temperature) on the furfural yield has been assessed to shed light on the reaction mechanism. Finally, as the extraction performance has significant impact on furfural selectivity, a sensitivity analysis is performed in order to investigate the optimum operating conditions and ultimately propose approaches of process optimization.

2.2. Experimental Section

2.2.1. Experimental set-up and procedure

The biphasic dehydration of xylose is conducted in the continuous experimental set-up sketched in Scheme 2.2. The set-up includes three pumps for xylose solution, acid solution and toluene, respectively. The injection system consists of three concentric tubes 1.5 m long with inner diameter of $6.25 \cdot 10^{-5}$ m, $1.7 \cdot 10^{-3}$ m and $3.86 \cdot 10^{-3}$ m for feed, sulfuric acid, and toluene solutions respectively to allow parallel pre-heating of the three separate streams up to reaction temperature. Right after that, mixing of the three streams takes place at the entrance of the reactor, which consists of 1.9 m in length with an inner diameter of $4.1 \cdot 10^{-3}$ m inner diameter tube with PTFE inner walls and a stainless-steel mesh around it to provide the necessary structural integrity, as depicted in Scheme 2.2. According to this configuration, the reaction volume (and thus the residence time) is very well defined. Both the injection system and reactor are heated up to the desired reaction temperature via heat tracing around them. At the reactor inlet of toluene and xylose streams, a thermocouple is placed in order to record the temperature. The biphasic mixture is quenched in an ice bath followed by a pressure safety relief and a filter (20 μm) pores that protects the subsequent back-pressure regulator (BPR) from any solids formed during the reaction. Samples are taken after the BPR at atmospheric pressure and room temperature. The reported results are reproducible within 9% experimental error.



Scheme 2.2. Set-up configuration of continuous reactive extraction of furfural

For the furfural degradation reactions in monophasic conditions, a series of small glass vials (1.5 mL) are used as batch reactors, since severe degradation reactions and reactor blocking were evidenced under these conditions in the flow reactor. Nevertheless, the millireactor (with a nearly ideal plug-flow behaviour) and the batch reactor are expected to have similar performance when operating in monophasic conditions. The glass vials are heated in an oil bath at the desired reaction temperature. At different residence times, the glass vials are taken from the oil bath and immediately cooled in an ice bath. The collected samples were filtered using filters of 1.2 μ m. The analytics procedure is identical to the one described above using HPLC instrumentation.

The partition coefficient experiments were performed in an autoclave batch reactor from titanium. The aqueous phase (1wt% furfural) and the organic phase were inserted in a volumetric ratio of 1:2. The reactor was pressurized with nitrogen. The temperature was set using a heating jacket. The stirring rate was 700 rpm for 30 min. The settling time was 1 h and samples were taken every 15 min from both phases. The presented distribution coefficient is the average of the four samples per temperature.

2.2.2. Materials and Analysis

The materials used for the experiment and for the calibration of the instrumentation were 98+% D-xylose from Alfa Aesar, furfural of 99% purity obtained by Sigma Aldrich, 98% pure H₂SO₄ by Sigma Aldrich and 99.7% toluene purchased from Biosolve. Finally, Pelikan Blue Ink was used for the slug flow development. All chemicals were used without any further treatment. Prior to analysis, the samples were filtered using syringe filters from glass fiber and with 1.2 μ m porous size obtained from ThermoScientific. The inorganic phase was analyzed with HPLC instrumentation (Shimadzu SIL-20A High-Pressure Liquid Chromatograph). Xylose and sulfuric acid were detected with a RI detector (Waters 2414).

Furfural was detected with UV-VIS detector (SPD-M20A) at the wavelength $\lambda=254$ nm. The column for the HPLC was Agilent Metacarb 67C and water as mobile phase at the rate of 0.5 mL min⁻¹. The oven temperature was set at 85°C. The organic phase was analyzed by GC instrumentation (Varian CP-3800). Toluene and furfural were detected with build-in FID detector. The column was Varian capillary FactorFour CB Sil 5 CP. Helium was used as carrier gas at the constant flow of 1.5 mL min⁻¹. The temperature ramp starts at 120°C for 20 min and then to 250°C for 5 min.

2.2.3. Modelling approach

The reactor model consists of a set of nonlinear ordinary differential equations (i.e., ODEs) that describe the mole balances of the main components (i.e., xylose and furfural) in the two phases (i.e., water and toluene) present in the reactor. This model assumed an ideal plug flow behaviour, which is reasonable when operating under Taylor flow regime, and that only furfural is exchanged via mass transfer between the aqueous and the organic phases. Further, the model considers the kinetics proposed by Weingarten et al., [108] as they are, among all the kinetics reported in the literature, the best to describe our experimental trends. This kinetic model includes three reactions: direct xylose dehydration to furfural (R1), xylose and furfural condensation (R2), and furfural resinification (R3). Different values of mass transfer coefficient (k_{La}) and partition coefficient (m) are considered in a sensitivity analysis. k_{La} ranges from 1×10^{-4} s⁻¹, a value representative of a reactor with poor mixing, to 1 s⁻¹, a value representative of an intensified reactor with enhanced mass properties like the spinning disc reactor [202]. The values of m were 2 and 20 $M_{furf}^{org} (M_{furf}^{inorg})^{-1}$, representing solvents with poor and high affinity to furfural, respectively. The lowest value is close to those of furfural in the mixture toluene-water, whereas the highest value is closer to recently investigated solvents [203]. The complete set of ODEs (Appendix A.1.) were solved numerically using MATLAB® software.

2.2.4. Definitions

After collecting the data from the analysis, the following equations (2.1.)-(2.5.) were used for data evaluation.

$$\text{Xylose Conversion: } X = \frac{n_x^0 - n_x}{n_x^0} \quad (2.1.)$$

$$\text{Furfural yield (total): } Y_f = \frac{n_f}{n_x^0} \quad (2.2.)$$

$$\text{Furfural selectivity: } S_f = \frac{n_f}{n_x^0 - n_x} \quad (2.3.)$$

$$\text{Mole Balance: } B = \frac{n_x + n_f^{org} + n_f^{inorg}}{n_x^0} \quad (2.4.)$$

$$\text{Partition Coefficient: } m = \frac{C_f^{org}}{C_f^{inorg}} \quad (2.5.)$$

2.3. Results and Discussion

2.3.1. Biphasic Production of Furfural

Effect of temperature and residence time on Biphasic production of furfural

Figure 2.1a. presents the effect of temperature on the xylose conversion and the furfural selectivity at $\tau=396$ s. As expected, temperature has a positive effect on xylose conversion, which increases significantly above 160°C. Simultaneously, furfural selectivity increases with temperature until it reaches a maximum of ca 70% at 170°C. At temperatures higher than 170°C, furfural selectivity drops along with a visible darkening of the reaction medium, indicating that degradation reactions are enhanced under these conditions. This maximum in the selectivity to furfural with increasing conversion suggests furfural formation is a two-step reaction: initially intermediates are formed from xylose, and they subsequently are converted to furfural. Once furfural is formed in quantitative amounts, degradation reactions become more significant, especially at higher temperatures. The importance of the in-situ extraction becomes evident from Figure 2.1b., where the furfural yield in the inorganic phase (i.e., the reaction medium) and in the organic phase (i.e., the extracting medium) are presented. The yield of furfural in the inorganic phase remains relatively low, whereas that in the organic phase increases rapidly after 160°C, when the xylose conversion begins to take off. The significant decrease of the furfural concentration in inorganic phase demonstrates the effect of extraction on selectivity.

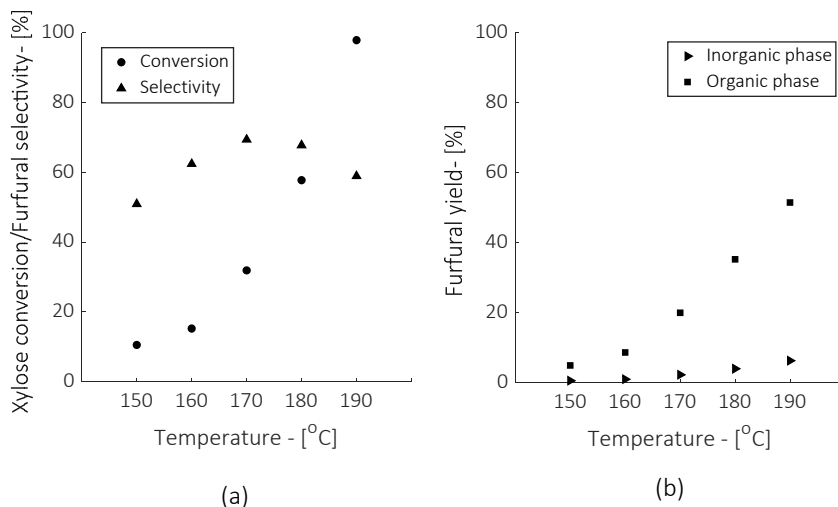


Figure 2.1. Xylose conversion and furfural selectivity [a] and Furfural yield in inorganic and in organic phases [b] with temperature for $\tau=396$ s; 0.1M H_2SO_4 , $F_v^{\text{org}}/F_v^{\text{inorg}}=2:1$, toluene, $C_x^0=4\text{wt}\%$

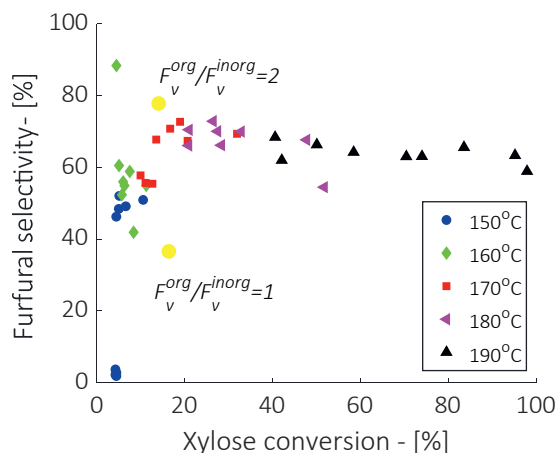


Figure 2.2. Furfural selectivity with xylose conversion at 150°- 190°C; $\tau=80\text{--}396\text{s}$ (left to right); 0.1M H_2SO_4 , $F_v^{org}/F_v^{inorg}=2:1 \text{ mL}^{org} (\text{mL}^{inorg})^{-1}$, toluene, $C_x^0=4\text{wt}\%$
**The two yellow points correspond to $\tau=132 \text{ s}$*

Figure 2.2. describes the relation between xylose conversion and furfural selectivity at various reaction temperatures and residence times. As expected, xylose conversion increases with temperature and residence time. The formation of furfural however only becomes significant at around 10% xylose conversion, when furfural selectivity reaches a maximum of ca. 70–80%. This trend further supports the mechanism assumption that furfural is not the direct dehydration product of xylose, but instead, xylose is initially converted into intermediate products, which seem to require moderate temperatures and residence times to be subsequently converted into furfural. Thus, the activation energy of the conversion of the intermediates to furfural is higher than that of their formation. Further increasing xylose conversion (up to 40%) does not have a major impact on furfural selectivity, which remains nearly constant at ca. 70%. When xylose conversion is further increased, furfural selectivity decreases slightly, but later it reaches a plateau at ca.65%. This can be explained by the fact that the activation energies of furfural formation from intermediates and its subsequent degradation are comparable.

The mild decrease in furfural selectivity reflects the undesired formation of by-products. In other words, the degradation of furfural into humins is not accelerated more than that of furfural production at higher temperatures. This observation is of high relevance as it indicates that high reaction temperatures would allow us to speed the reaction rate

sufficiently enough to minimize the residence times required to achieve relevant yields. In this study, the increased reaction temperatures, and the use of an intensified reactor lead to a synergistic effect of accelerated kinetics of furfural formation and the high mass transfer rates, resulting to high yield. Furthermore, operating at relatively higher temperatures allows for better opportunities for heat integration in a complete process scheme. Finally, it is also attractive to operate at high xylose conversion because high raw material conversion and high furfural selectivity decrease essentially the recycle costs in a complete process scheme. Similar behaviour in terms of xylose conversion and furfural selectivity has been reported in literature [108,118,140,199,200]. More specifically, 30% of xylose conversion and 60% furfural selectivity at 160°C have been presented [108]. However, these results were obtained in 20 min residence time, which is remarkably longer than the residence time in the present work. Hence, the use of the proposed system indicates that efficient production of furfural can be achieved at short residence time and, thus, smaller reactor volume. Overall, it is observed that the in-situ extraction prevents further decrease of furfural selectivity, which would be the case in a monophasic system. As depicted in Figure 2.2., when lower O/I is used, furfural selectivity is remarkably lower compared to the base case ($F_v^{org}/F_v^{inorg} = 2:1$), whereas xylose conversion is in the same range, showing the advantage of in-situ extraction in furfural production. However, furfural selectivity is limited to max. 70%. There are two main reasons for this. First, the furfural extraction is limited by high temperatures through the partition coefficient of furfural between toluene and water, as will be further discussed later. Second, it is possible that the intermediate compounds can also degrade under the reaction conditions and, as a result, furfural selectivity cannot further increase.

Carbon balance and reaction mechanism

The carbon balance is investigated in an attempt to observe the conditions of humins formation during the reaction. Besides increasing furfural selectivity, preventing humins formation is important to ensure long term stable operations. Figure 2.3. shows the carbon balance as a function of conversion, temperature, and residence time. Since the main components detected and quantified are xylose and furfural, the unbalance accounts for (1) soluble intermediates (i.e., furfural precursors), (2) soluble humins (precursors), and (3) non-soluble humins. The carbon balance remains above 90% up to ca. 40% conversion and 170°C, indicating that up to 10% intermediate products form at the very initial phase of the reaction (i.e., at low xylose conversions), which are quickly converted to furfural consecutively. Above 40% conversion and 180°C, the carbon balance rapidly decreases until ca. 60%, likely due to very fast degradation reactions under these conditions. This is in line with a visible darkening of the reaction mixture at elevated temperatures and residence times. More specifically, as shown Figure 2.3., the mole balance remains almost constant at 95% up to 25% xylose

conversion. A further increase in xylose conversion shows a linear decrease in the carbon balance.

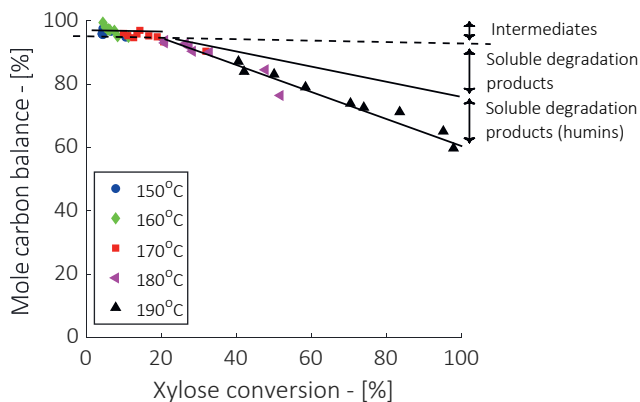


Figure 2.3. Mole balance with xylose conversion for 150°C-190°C; 0.1M H₂SO₄, $F_v^{org}/F_v^{inorg}=2:1$ mL^{org} (mL^{inorg})⁻¹, toluene as solvent, $C_{xy}^0=4$ wt%

Quantification of the solid formation was performed by a gravimetric analysis of the humins deposited during ca. 80 min of operation in the filter located at the reactor outlet. As shown in Table 2.1., the contribution of the solids to the carbon balance is not significant.

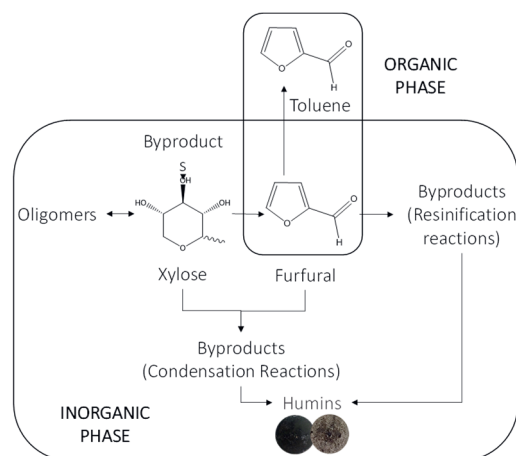
Table 2.1. Solids Formation and Carbon balance*

Time on stream [min]	Mole Carbon Balance w/o solids [%]	Total mass of solids [mg]	Mole Carbon balance w. solids [%]
81	84.2%	56	85.9%

*Total flow=7.5 mL/min, T=190°C, $C_x^0=4$ wt%, Organic phase: Toluene, $F_v^{org}/F_v^{inorg}=2:1$ mL^{org} (mL^{inorg})⁻¹

Considering that solids contribution in the carbon balance is minimized by in-situ furfural extraction, the remaining unbalance consists of dissolved degradation products. Additional peaks were observed in the HPLC chromatograms of the experiments. According to the observed trends in the areas of these peaks with respect to residence time, it can be speculated that they correspond either to intermediate products prior to furfural formation or to soluble degradation products, precursors of insoluble humins. However, the identification of all these compounds was not possible. One intermediate that is frequently

mentioned in the literature is xylulose [118]. However, in the present work, the results of HPLC and NMR (Appendix A.2.) do not suggest the presence of xylulose in the reaction mixtures. Moreover, it was found that xylobiose (i.e., xylose dimer) has similar retention time as one of the unknown peaks in the HPLC chromatogram. Its contribution to the mole balance is minor (even at lower temperatures) and negligible at higher temperatures ($T > 180^\circ\text{C}$). Nonetheless, quantification of the remaining unknown compounds is not possible without their prior identification. Therefore, LC-MS and MALDI TOF analyses (Appendix A.3.) were conducted on the reaction solutions to get further insight into the nature of the soluble reaction products, and possibly the reaction mechanism. The LC-MS analysis indicates the presence of xylose degradation reactions that render soluble high molecular weight compounds ($\text{MW} \gtrsim 550$), as well as reactions between xylose and furfural. Additionally, the last dehydration intermediate before furfural formation ($\text{MW}=114$) was detected. According to the MALDI TOF analysis, xylose oligomers are present already in the stock solution, as well as in the reaction mixture. This suggests that traces of xylose oligomers might be present in the original xylose purchase mixture. Additionally, it is plausible that xylose oligomers may be formed under reaction conditions in the inorganic phase and in the presence of Brønsted catalyst. Xylose oligomers are converted rapidly to xylose in acidic environment (Appendix A.4.). Similar behaviour has also been reported for the glucose system [204]. On the basis of the general kinetic model of cellulose hydrolysis, glucose reacts to several products. Among them, fructose and HMF are the most significant. However, the production of disaccharides is one reaction path present in acid hydrolysis. Hence, it could be expected that comparable reaction network might be present in this system as well.



Scheme 2.3. Plausible mechanism of furfural production

All the possible mechanisms leading to furfural production including its extraction are summarized in Scheme 2.3. On the basis of the analysis above, it can be concluded that apart from furfural formation, there are many other parallel reactions affecting furfural selectivity; directly via condensation reactions and indirectly through altering xylose concentration (xylose oligomerization).

2.3.2. Furfural degradation in monophasic system

Individual batch experiments of furfural degradation with the same sulfuric acid concentration (0.1M H₂SO₄) have been executed. The goal of these experiments is to observe the behaviour of furfural degradation reactions without the presence of xylose. So far, there is no clear conclusion in the literature regarding the reaction order of furfural degradation. However, most studies assume that it is first order reaction [205] and the same assumption is considered in this study (Appendix A.5.).

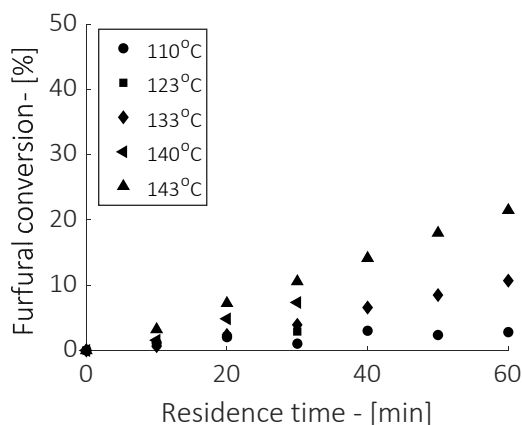


Figure 2.4. Furfural conversion at 0.1M H₂SO₄ and C_{furf}⁰=1wt%

From Figure 2.4., it can be observed that furfural conversion increases linearly with residence time. Hence, the experimental data and the plot of $\ln(1-X_F)$ against residence time (as presented in Appendix A.5.) fit the assumption of the first-order kinetics and they are in agreement with the majority of literature [195]. The comparison of furfural resinification rate with furfural extraction rate is of significant importance in order to investigate whether extraction is fast enough to prevent furfural degradation.

2.3.3. Effect of mass transfer rates on furfural selectivity

In essence, the benefits of the biphasic production of furfural lay in the effective extraction of furfural via mass transfer from the aqueous solution to an organic phase, where

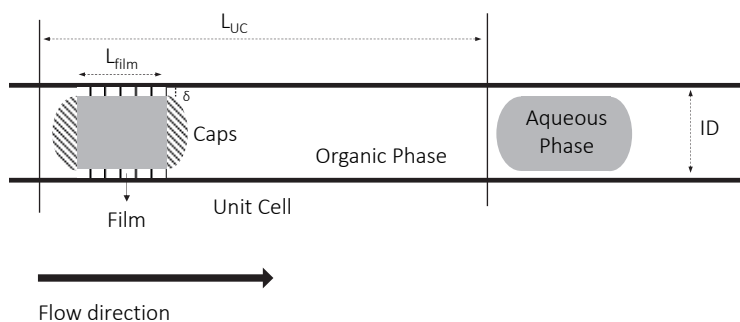
degradation reactions do no longer take place. In turn, this results in an increase of furfural selectivity. The efficiency of this approach is determined by the relation between the mass transfer rates of furfural (2.6.) and the furfural degradation rates.

$$MT = k_L a * (m * C_{\text{furf}}^{\text{inorg}} - C_{\text{furf}}^{\text{org}}) \quad (2.6.)$$

The extraction rate is affected by (a) the ratio of organic-to-inorganic volumetric flows affecting the interfacial areas and the driving force of furfural extraction, (b) the configuration of the reactor influencing the mass transfer coefficient and (c) the temperature defining the partition coefficient. These parameters are investigated separately.

Estimation of mass transfer coefficient

The millireactor used in this study was operated in the Taylor flow regime, which may be described as an alternating sequence of slugs and bubbles that flow through the channel with a nearly ideal plug flow behaviour (Scheme 2.4.). In the current system, toluene is in the slugs and the aqueous solution is in the bubbles. Thus, furfural is transferred from bubbles to the slugs through (1) the bubble caps, and (2) the toluene film formed between the slug and the reactor wall. The size and shape of the bubbles determine the mass transfer coefficient.



Scheme 2.4. Description of unit cell in Taylor flow for $F_v^{\text{org}}/F_v^{\text{inorg}}=2:1 \text{ mL}^{\text{org}} (\text{mL}^{\text{inorg}})^{-1}$

The Taylor flow development has been verified visually using ink and water to represent the aqueous phase and toluene for the organic phase (Appendix A.6.). To calculate the mass transfer coefficient, it is crucial to define the extraction mechanisms and their significance. Based on the shape and the size of the slugs, and the properties of the two immiscible phases, it was found that the dominant mechanism for furfural mass transfer is through the caps of the slug (Appendix A.7.). The calculation of the mass transfer coefficient ($k_L a$) was based on the equations presented in literature [206] and the detailed calculations of mass transfer

coefficient are presented in Appendix A.7. An interesting analysis is the comparison of the degradation reaction rate constant with the mass transfer rate as depicted in Figure 2.5. The degradation reaction rate is calculated at 190°C and it remains constant as it is not affected by the volumetric flow.

As explained before, the volumetric flow defines the length and the shape of slugs (as presented in Appendix A.7.), which affects the extraction performance for both mechanisms (i.e., through film and the caps). As presented in Figure 2.5. the degradation reaction rate constant is on overall comparable with the mass transfer rate. More specifically, the mass transfer rate is lower than furfural degradation reaction rate for volumetric flows less than 0.07 mL s⁻¹. In this region, the extraction performance is expected to be limited affecting furfural selectivity. For higher volumetric flows, the mass transfer rate is higher than furfural degradation rate and the degradation reactions involving furfural are expected to be limited. On the basis of the aforementioned observations, it is expected that the mass transfer properties of the selected reaction system have significant impact on furfural selectivity.

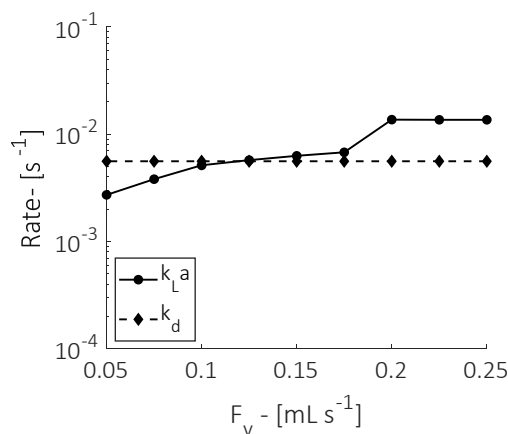


Figure 2.5. Comparison of mass transfer coefficient $k_L a$ (straight line) and furfural degradation reaction rate constant k_d (dashed line) with the volumetric flow (F_v) at 190°C

Effect of temperature on the water-toluene partition coefficient of furfural

Separate experiments for the determination of furfural partition coefficient (m) at reaction temperatures were performed in an autoclave reactor. An experiment at RT was performed and used as the base case. In Figure 2.6., the partition coefficient at this temperature is ca. 4 $M_{\text{furf}}^{\text{org}} (M_{\text{furf}}^{\text{inorg}})^{-1}$, as presented in literature [146]. The furfural partition coefficient

decreases with temperature, as expected, because mutual solubility between toluene and water increases with temperature.

For temperatures from 170 and 180°C, the partition coefficient decreases to a value of ca. $2.2 M_{\text{furf}}^{\text{org}} (M_{\text{furf}}^{\text{inorg}})^{-1}$. At 190°C, the partition coefficient decreases even further to 1.4, implying that the use of toluene even at this extreme condition is still beneficial for the present process, although not ideal. However, the extraction performance is clearly diminished from elevated temperatures, which leads to a selectivity decrease.

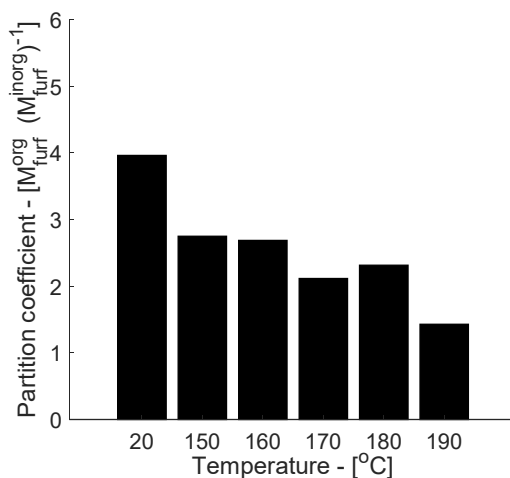


Figure 2.6. Furfural Partition Coefficient in toluene with temperature; $F_v^{\text{org}}/F_v^{\text{inorg}}=2:1 \text{ mL}^{\text{org}} (\text{mL}^{\text{inorg}})^{-1}$, toluene, $C_{\text{furf}}=1\text{wt}\%$

Sensitivity Analysis of Extraction Performance on Furfural Production

As previously discussed, the extraction performance has a significant impact on furfural selectivity. The present sensitivity analysis aims to define the optimum conditions of the biphasic furfural production with respect to product yield. The main variables influencing the extraction performance, and thus the selectivity, are (1) the mass transfer coefficient ($k_L a$), (2) the partition coefficient (m) and (3) the volumetric ratio between the organic to aqueous phase (O/I). Thus, these are the three process parameters that were investigated in this section. Figure 8 shows the results of this evaluation at 170°C. Similar analysis is performed at 190°C (Appendix A.8.). It should be noted that the model is based on the kinetics by Weingarten et. al, [23] which consider two main degradation routes (i.e., xylose and furfural condensation reactions, and furfural resinification), but do not account for xylose oligomerization reactions. Nevertheless, based on experimental observations, the latter

seem to have limited extent under the reaction conditions of this study. Besides, this model does not consider the formation of any intermediate species prior to furfural, which appears to be of relevance at low xylose conversions (i.e., below 10–20%). This means that the furfural yields predicted by this model at low conversions lack accuracy. Thus, the sensitivity analysis will be mostly focused on the predictions at higher conversions.

As shown in Figure 2.7a., the reference monophasic reaction of xylose in acidic medium leads to complete conversion in about 100 min residence time under the reaction conditions considered, while the yield does not increase beyond 45% due to significant degradation reactions. With respect to the reference case, introducing in-situ product extraction to a solvent with a relatively low affinity to furfural results in a very minor effect on xylose conversion, attributed to a decrease in the extent of xylose-furfural condensation reactions, and a visible yield increase (Figure 2.7b.). However, such increase in yield is only significant (i.e., from 45% to 75% at full conversion) when relatively fast mass transfer rates apply (i.e., $k_L a$ above 0.01 s^{-1}). When this condition is satisfied, it is remarkable to notice that the effect of further increasing the mass transfer coefficient does not play a significant role on furfural yield, as the organic phase quickly saturates. On the other hand, when very low mass transfer coefficients apply, the rate of furfural degradation compete with that of its extraction, and the overall effect of performing the reaction in a biphasic media is limited. Figure 2.7c. displays the model predictions using a solvent with greater affinity toward furfural (i.e., greater m). For example, greater m values may be realized when using salty aqueous solution [125] and/or organic solvents like MIBK or 2-sec-butylphenol [203]. It is evident that the beneficial effects of furfural extraction on the final yield are more significant than in the previous scenario with a lower m (i.e., 90 vs 75% yield at full conversion). There is now a larger “storage” capacity of furfural in the organic solvent and a greater driving force for its extraction. Regardless the type of solvent, we observe that the rise in furfural yield increases with the mass transfer coefficients, and it levels off for mass transfer coefficient greater than 10^{-3} s^{-1} . Although increasing the mass transfer coefficient enhances only the rate of the extraction, coupling large mass transfer coefficients with high partition coefficients (e.g., by suitable solvent selection/design) promotes both the rate and the final extent of furfural extracted, showing an even greater impact on the final yield.

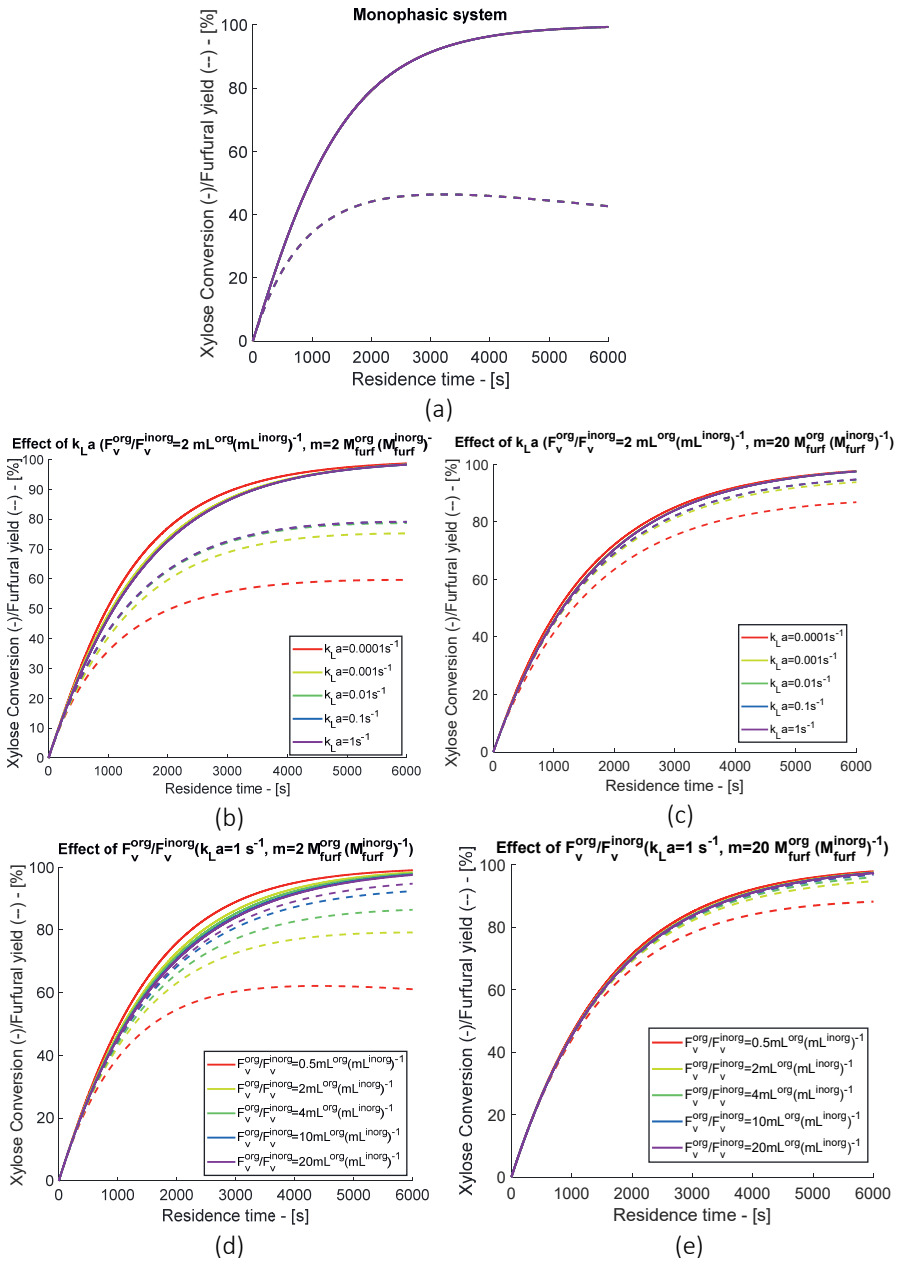


Figure 2.7. Xylose conversion and furfural yield with residence time at 170°C

(a) Monophasic reaction; (b) effect of $k_L a$ with $F_v^{org}/F_v^{inorg} = 2 \text{ mL}^{org}/(\text{mL}^{inorg})^{-1}$ and $m = 2 M_{furf}^{org}/(M_{furf}^{inorg})^{-1}$; (c) effect of $k_L a$ with $F_v^{org}/F_v^{inorg} = 2 \text{ mL}^{org}/(\text{mL}^{inorg})^{-1}$ and $m = 20 M_{furf}^{org}/(M_{furf}^{inorg})^{-1}$; (d) effect of F_v^{org}/F_v^{inorg} with $k_L a = 1 \text{ s}^{-1}$ and $m = 2 M_{furf}^{org}/(M_{furf}^{inorg})^{-1}$; (e) effect of F_v^{org}/F_v^{inorg} with $k_L a = 1 \text{ s}^{-1}$, $m = 20 M_{furf}^{org}/(M_{furf}^{inorg})^{-1}$

Another strategy to maximize the effect of performing the reaction in a biphasic media consists of increasing the organic- to-inorganic ($F_v^{\text{org}}/F_v^{\text{inorg}}$) ratio, although this is of course not the preferred option as it will result in greater reactor volumes, downstream separation costs and overall energy demand. Still, it may be considered as an optimization value to compensate for limitations of the solvent. The predicted performance using various O/I ratios of a poor solvent (i.e., $m=2 M_{\text{furf}}^{\text{org}} (M_{\text{furf}}^{\text{inorg}})^{-1}$) and a better solvent (i.e., $m=20 M_{\text{furf}}^{\text{org}} (M_{\text{furf}}^{\text{inorg}})^{-1}$) are displayed in Figure 2.8b, e, respectively. In this analysis, an intensified reactor system (i.e., $k_L a = 1 \text{ s}^{-1}$) is considered. Similarly, to the observed effect of m , increasing the $F_v^{\text{org}}/F_v^{\text{inorg}}$ ratio speeds the extraction rate (i.e., by increasing the driving force for mass transfer), and enlarges the “storage” capacity of furfural in the organic phase. Thus, it is possible to exceed 90% yield at full conversion when using $F_v^{\text{org}}/F_v^{\text{inorg}} = 10 \text{ mL}^{\text{org}} (\text{mL}^{\text{inorg}})^{-1}$ for a poor solvent (i.e., $m=2 M_{\text{furf}}^{\text{org}} (M_{\text{furf}}^{\text{inorg}})^{-1}$), and only $F_v^{\text{org}}/F_v^{\text{inorg}} = 1 \text{ mL}^{\text{org}} (\text{mL}^{\text{inorg}})^{-1}$ for a better solvent (i.e., $m= 20 M_{\text{furf}}^{\text{org}} (M_{\text{furf}}^{\text{inorg}})^{-1}$). Logically, the former scenario would result in severe product dilution and increase in processing and energy costs. This further emphasizes the relevance of combining solvent selection and reactor design. A further increase in the reaction temperature to 190°C (Appendix A.8.), it is observed a 3-fold reduction in residence time (i.e., a 3-fold reduction of reactor volume) to achieve full conversion, and a sharper decrease in furfural yield after the maximum value is achieved because of the greater activation energies for the furfural synthesis reaction with respect to those of the furfural degradation reactions. Overall, special attention should be paid to the temperature dependence of the partition coefficients, as it may not be negligible, as observed experimentally for toluene (Figure 2.6.). Pending the design of optimized solvents [148], increasing the $F_v^{\text{org}}/F_v^{\text{inorg}}$ ratio could be considered as a valid strategy to optimize furfural yields.

2.4. Practical Considerations

As shown in this work, the principles of process intensification (e.g., in-situ extraction and increased mass transfer rates) are very attractive for the synthesis of furfural and will be key in the transition from the traditional batch to a stable flow process. Further, we have demonstrated that through a combination of solvent and reactor selection, it is possible to run the reaction continuously, extend the stable operation window for this reaction, increase furfural yields, and reduce reactor size significantly. Nevertheless, in view of the practical implementation of this process, several considerations need to be considered in a broader perspective, for example, considering costs and environmental impact. While the benefits of millireactor technology (e.g., fast mass transfer rates, well-defined flow distribution, small inventory) have been instrumental in our laboratory study, it is an expensive technology and not yet scalable for multiphase bulk processes. Here, other scalable intensified reactor technologies (e.g., the spinning disc reactor [207], oscillatory baffled flow reactors or scalable

agitated baffled reactor [208,209] will become of relevance. Concerning the solvent, we have used toluene in this study to demonstrate the concept of furfural in-situ extraction. However, the partition coefficient proved to be poor, leading to substantial amounts of solvent to reach a significant boost in selectivity. Further, toluene is not a “green” solvent and the downstream process of furfural purification is very energy demanding. Thus, other solvents should be considered for the practical implementation of this process [148]. In terms of feed, we believe that this process and intensification strategies will be particularly important in the valorization of sugar-rich hydrolysate streams, which will become of relevance in the future biorefinery where biomass is first separated into its fractions prior to valorization into high-value chemicals. Our initial results with this type of feeds have shown very promising results and will be reported soon.

2.5. Conclusions

In the present study, a millireactor operating under the Taylor flow regime was used for the production and in-situ extraction of furfural using diluted sulfuric acid as catalyst and toluene as extracting medium. Because of the enhanced mass transfer properties of the millireactor and its ease of control of the residence time, we were able to maintain high furfural selectivity (ca. 70%) at high xylose conversion (ca. 80%) and extremely short residence times (less than 2.5 min). Remarkably, this process configuration rendered minimal humins formation (<2% at 190°C), thus allowing uninterrupted continuous operation. Yet, an important knowledge gap concerning the reaction mechanism and the intermediate and degradation products remain as important bottleneck to further understand and intensify this reaction. On the basis of the observed conversion-selectivity trends, and on the analysis of the liquid samples (where various xylose-oligomers and products from condensation reaction between xylose and furfural were observed), we were able to throw some light into the reaction mechanism. Further, through an in-depth analysis of the mass transfer effects on the process performance and a modelling-aided sensitivity analysis, we have concluded that optimizing the solvent selection and/or F_v^{org}/F_v^{inorg} ratio can lead to nearly 100% yield if the reactor performance guarantees a sufficiently high mass transfer coefficient. The model predictions consistently reveal that mass transfer coefficient (i.e., and thus the reactor design and the operating flow regime) is an important parameter to achieve optimal results, especially under highly reactive conditions (e.g., elevated temperatures) which increase reaction rates but are prone to rapid product degradation. Thus, based on these results we can envision that further enhancing the mass transfer properties (e.g., in a spinning disc reactor) would allow for further extending the operation windows of this reaction. Hence, the results of this study are conducive toward the development of a robust and compact continuous reactor for the selective production of furfural in biphasic media.

CHAPTER 3

Kinetic Models of Furfural Synthesis from C5
Sugar Streams

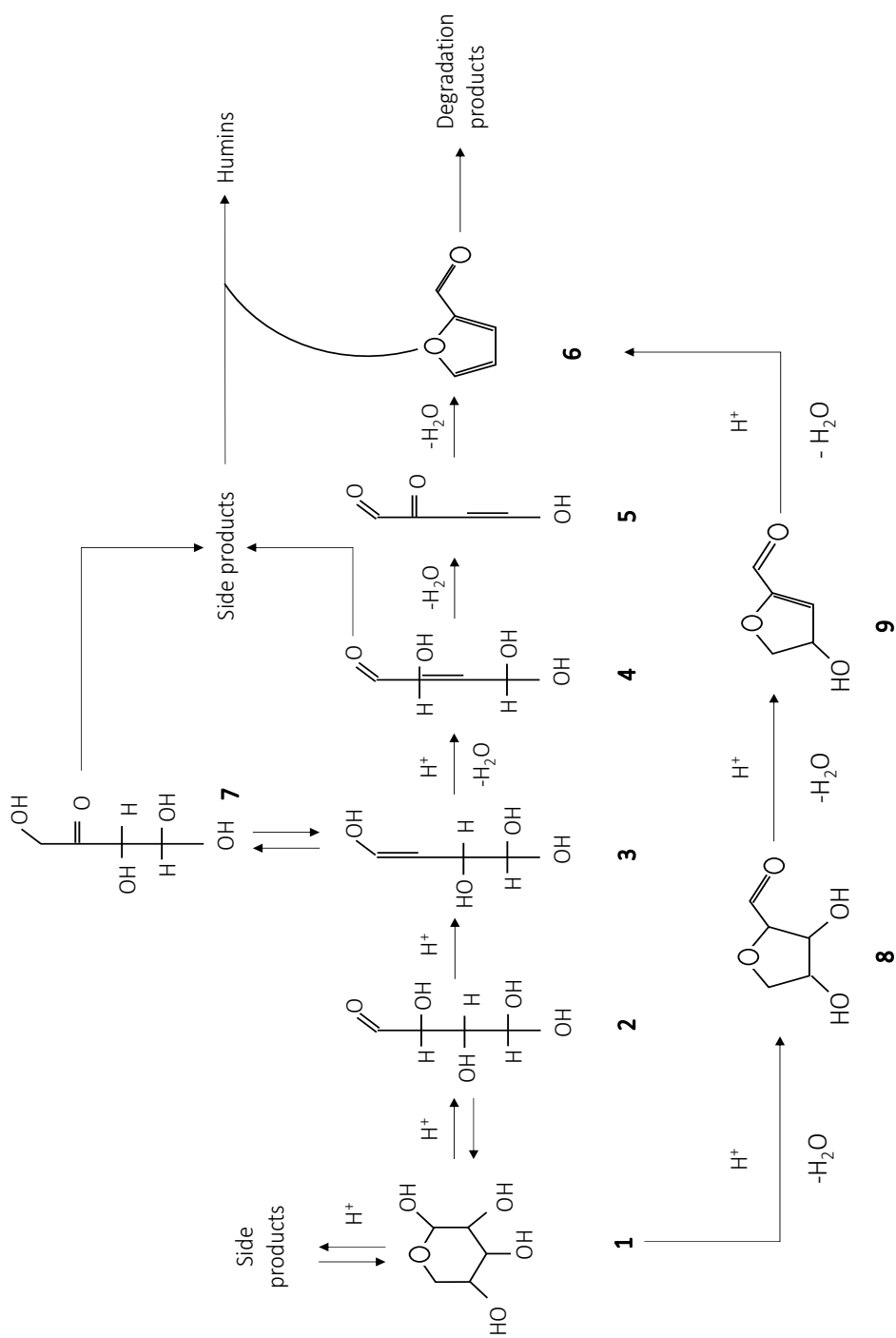
Abstract

The mechanism of furfural formation has been studied for years as part of the hemicellulose valorization network, but several aspects of the complex reaction scheme (usually studied for a narrow set of experimental conditions), remain under debate. This work sheds light into the H₂SO₄-catalyzed C5 sugar-to-furfural reaction mechanism in a wide temperature range of 120-190°C. The work is based on the mechanism reported by Krzelj et. al. [123], which was developed for temperatures from 120-160°C, and is hereby revisited and extended until 190°C. Comparison of the conversion-selectivity trends observed experimentally against Krzelj's model predictions in the entire temperature range (120-190 °C) confirms the validity of the reaction mechanism proposed by Krzelj et. al. [1] and suggests that no additional degradation pathways need to be taken into account for an accurate description of the system. However, both xylose conversion and furfural yield are underestimated when Krzelj's kinetic model is extrapolated beyond the temperature range for which it was developed. Thus, an updated set of kinetic parameters for the temperature range 120-190°C is presented. Following a similar methodology, the work extends to the investigation of arabinose dehydration mechanism. Ultimately, the developed kinetic models are used for the determination of optimized conditions for selective furfural production. The sensitivity analysis shows that the optimum temperature range is ca. 190-200°C.

3.1. Introduction

The valorization of lignocellulosic material (LCM) is very attractive for the production of biobased chemicals and bio-fuels. Among all the types of LCM, hardwood [210], hemicellulose waste stream (e.g., from pulp and paper, and cellulosic ethanol plants) [211], corn stover and switchgrass [212,213] are, based on their high C5 sugars content, promising feedstocks for furfural synthesis. The depolymerization of xylan and other C5 sugar results in xylose monomers, which convert under acidic conditions to furfural. Furfural is one of the main precursors of biobased chemicals, and it is mostly valorized via hydrogenation processes [214] for the production of furfuryl alcohol, which is then used for biobased resins, fuels additives and soil enhancers [78,215,216]. Because of the high potential of furfural as platform chemical, its synthesis has received great interest in industry and academia. Several works look at the optimization of reaction conditions [211], use of novel (solid) acid catalysts, or even novel process concepts (e.g., addition of co-solvents) [187,217] or to maximize yields. To that extent, kinetic modelling of this reaction is key to assess and develop innovative concepts.

The elucidation of the reaction mechanism of xylose conversion in the presence of Brönsted acid catalysts has been investigated for years. An in-depth understanding of the mechanism is important at academic level as well as for the design and optimization of industrial scale reactors and processes. It is established that furfural is formed from C5 sugars (typically xylose and arabinose) in the presence of Brönsted acid catalyst and high temperature. However, its production suffers from poor selectivity due to the presence of multiple degradation reactions [108,133,214].



Scheme 3.1. Mechanisms overview of xylose dehydration using Brønsted acid catalyst [107,109,218]

Various mechanistic paths are reported in literature, but three are the most accepted theories (Scheme 3.1). According to two of these mechanisms, the cyclic form of xylose (i.e., xylopyranose, hereby labelled as species **1**) undergoes a ring opening reaction as the first step, leading to aldopentose (**2**). The first theory considers the formation 1,2-enediol (**3**) from the aldopentose (**2**), and the subsequent rapid isomerization to ketopentose (**7**). The latter is believed to be an equilibrium reaction. In parallel, the dehydration of 1,2 enediol takes place at slower rate, leading to an aldehyde (**4**), which is further dehydrated in two steps in the C-4 and C-5 positions to form furfural (**6**). Based on the difference of the rates of 1,2 enediol conversion paths, it can be speculated that the formation of intermediate **4** is the rate limiting step of the mechanism of furfural formation. The fact that there is no proton transfer to aldopentose (**2**) shows the irreversible 1,2 enediol formation [219]. According to the second theory that still relies on the initial ring-opening of xylopyranose (**1**), furfural formation proceeds via β -elimination to form 2,3-(α,β)-unsaturated aldehyde intermediate (**4**). In this case, the acyclic form of xylose is directly dehydrated to **4**. Furfural is then formed by two dehydration steps of the unsaturated aldehyde [113,114] similar to previous mechanism. However, this mechanism cannot explain the intramolecular proton transfer. Finally, a third theory that appears weaker than the previous two, considers the direct conversion of cyclic xylopyranose (**1**) to furfural in three dehydration steps with intermediate products in cyclic form (compounds **8** and **9**). This theory cannot explain the intramolecular proton transfer neither the protonation of intermediates during dehydration. Based on literature findings, it can be concluded that xylose conversion mechanism is better explained using the mechanistic paths of acyclic xylose conversion i.e., 1,2 enediol formation and β -elimination. It is plausible that these two mechanisms coexist [107,109]. The dominant mechanism depends on the reaction conditions such as temperature, catalyst, and catalyst concentration. Finally, it can be speculated that the rate limiting step is the formation of intermediate **4**. The most common catalysts that promote furfural formation are Brønsted acid catalysts such as H_2SO_4 or HCl [107–110]. The use of tandem Brønsted and Lewis acid catalysis has also been reported as a means to promote furfural yield. The most prevailing understanding is that xylose selectively isomerizes into xylulose and lyxose in the presence of Lewis acid catalysts, and that xylulose then dehydrates in three steps to furfural in the presence of Brønsted catalyst via a reaction mechanism that has not been studied in detail [118].

Apart from the main route of xylose dehydration to furfural, many parallel and subsequent reactions leading to furfural selectivity loss have been reported. It is well-established that furfural resinification (self-condensation) in acidic conditions is a significant source of furfural yield loss [108,110,122,123,195]. On the other hand, evidences of parallel degradation routes involving condensation of furfural with other reaction intermediates and/or sugars

have been reported too [108,123,124,220]. Analysis of product mixtures with LC-MS and MALDI-TOF support this hypothesis [110]. The condensation reaction of xylose has also been reported as another parallel degradation reaction leading to yield loss [221,222]. While the existence of these condensation reactions between furanics and sugar (derivatives) in acidic media is not itself under debate, the question about the extent that each of them contributes to the yield losses during the furfural synthesis process typically arises when attempting to model the kinetics of this reaction. Our recent work on the kinetics of xylose dehydration in a temperature range of 120-160°C and a wide range of sulfuric acid concentration supports that furfural is formed via 1,2-enolization, and that the role of intermediates in the degradation pathways is significant [123]. Similar findings were reported by Dussan et. al with formic acid as catalyst [112]. They also conclude that the reactions that lead to loss of furfural are the degradation of xylose with one of the intermediate products, as well as furfural resinification. Dunlop et al. suggest that the degradation reactions occur via a parallel reaction of furfural with xylose, with an intermediate, and the consecutive reaction of furfural destruction [124]. Other kinetic models propose an additional degradation reaction of furfural with xylose [108] or direct xylose degradation to undesired products [125,222].

Being less abundant within the hemicellulose fraction of LCM, arabinose as furfural precursor has also received less research attention, with only a few studies dedicated to elucidating the mechanism and derive kinetics models for this reaction. Yasuda et. al are among the first to investigate the mechanism of furfural formation from arabinose using H₂SO₄ at high reaction temperature (up to 200°C) [126]. The work of Yasuda proposes a rather elaborated mechanism for this reaction, in which the reaction intermediates react in parallel with furfural, similarly as earlier discussed with xylose. However, for the sake of kinetic modelling, the authors reduce the scheme to a direct one-step arabinose to furfural conversion, and a parallel arabinose-furfural degradation pathway. Similarly, Dussan et. al studied this reaction [112] with concentrated formic acid at lower reaction temperatures (130-170°C), concluding that direct single-step furfural formation from arabinose and the condensation of the latter describes adequately the conversion and the selectivity trends. Nevertheless, the mechanism through reaction intermediate and parallel degradation of arabinose and furfural also describe the experimental data with sufficient accuracy.

The aim of this work is two-fold. First, the study aims to investigate the C5 sugars (i.e., xylose and arabinose) dehydration routes to furfural and develop kinetic models that are able to predict conversion and selectivity data in a temperature range up to 190°C. Recent literature points at higher temperatures as the optimum conditions to maximize furfural yields [145,211,223]. For the kinetic modeling, the experimental data presented in Chapter 2 on xylose dehydration is used in the present study. These and additional kinetic data are

collected in a millireactor operated in a continuous biphasic mode (under the Taylor flow regime) using diluted sulfuric acid (0.1M) as catalyst, toluene as extractant, and up to 400s of residence time. As demonstrated in Chapter 2 and in agreement with literature [139,185], the presence of extraction medium (i.e., toluene) does not affect the xylose dehydration kinetics in dilute aqueous solutions (i.e., up to ca. 6wt% xylose), and it allows the in-situ extraction of furfural, therefore delaying the rate of degradation reactions. From a kinetic modeling perspective, this is also advantageous since it allows the investigation of a wider range of residence times and temperatures without excessive carbon-losses that would otherwise obscure the development of potential reaction intermediates. The second goal of the work is to use the developed kinetic models as a tool to identify the optimum operating conditions for selective furfural production from a hemicellulosic C5-rich stream.

3.2. Experimental section

3.2.1. Experimental Set-up and procedure

The experiments of biphasic continuous furfural production from xylose used for the kinetics analysis were performed in a continuous experimental set up as reported in Chapter 2. In the same literature, the materials and the analytic methods performed are described in detail. The same experimental configuration and analysis protocols are used for the experiments using arabinose.

3.2.2. Definitions

The equations (1) – (5) show the definitions of conversion, yield and selectivity used in the present work accordingly.

$$\text{Xylose Conversion:} \quad X = \frac{n_x^0 - n_x}{n_x^0} \quad (3.1.)$$

$$\text{Furfural yield (total):} \quad Y_f = \frac{n_f}{n_x^0} \quad (3.2.)$$

$$\text{Furfural selectivity:} \quad S_f = \frac{n_f}{n_x^0 - n_x} \quad (3.3.)$$

$$\text{Reaction rate constant:} \quad k_i' = \frac{k_i}{[H]^+} \quad (3.4.)$$

$$\text{Residence time:} \quad \tau = \frac{V_R \epsilon_{aq}}{F_V} = \frac{V_R \epsilon_{org}}{F_V} \quad (3.5.)$$

3.2.3. Modelling approach

A set of ordinary differential equations (ODEs) that describe the mole balances of all species in the aqueous and organic phases in the reactor are derived according to the following assumptions:

- The reactor behaves as 1D plug flow reactor, with co-current biphasic Taylor flow regime.

- There is transfer of furfural (and not of any other species) from the aqueous phase to the organic phase, according to the mass transfer correlations for Taylor flow regime [179]. The mass transfer coefficient is calculated based on the properties of the Taylor flow regime, in which it has been proved that furfural transfer through the slug caps is the most dominant mechanism of mass transfer (Appendix A.7).
- Furfural partition coefficient between toluene and water was determined according to procedure presented in Chapter 2, Section 2.3.3, *Effect of temperature on the water-toluene partition coefficient of furfural*.
- Two reaction mechanisms are considered for the kinetics of arabinose conversion, as reported in Scheme 3.4.

The resulting set of ODEs (Appendix B.1) is implemented and solved in MATLAB® using ode15s solver. The data fit of the kinetic parameters was performed using the *lsqnonlin* solver. This solver minimizes the sum of squares of the functions and it is based on Levenberg-Marquardt method. The objective function uses the concentration of sugars and furfural from the experiments and the respective calculated concentrations in each iteration based on the mole balances. After determination of the kinetic parameters, the same set of equations is used for the sensitivity analysis of reaction and extraction parameters i.e., optimum reaction temperature and residence time, and furfural partition coefficient and minimum organic-to-inorganic ratio.

3.3. Results and discussion

3.3.1. Mechanism insights and modelling of xylose dehydration at higher reaction temperatures (160-190°C)

According to our previous study, the reaction intermediates following the first xylose dehydration (compounds **3**, **4** and **5** from Scheme 3.1.) play a significant role in the mechanism of furfural formation and degradation [123]. This analysis is reported for a wide range of sulfuric acid concentration (0.1-2M), but reaction temperature is limited to 150°C. Figures 3.1a, 1b and 1c show the model predictions against the experimental observations during biphasic synthesis of furfural in the range of 150-190°C. It is evident that the model predicts the conversion/selectivity data rather accurately up to 150-160°C, but it vastly underpredicts the performance (both conversions and yields) at higher temperatures.

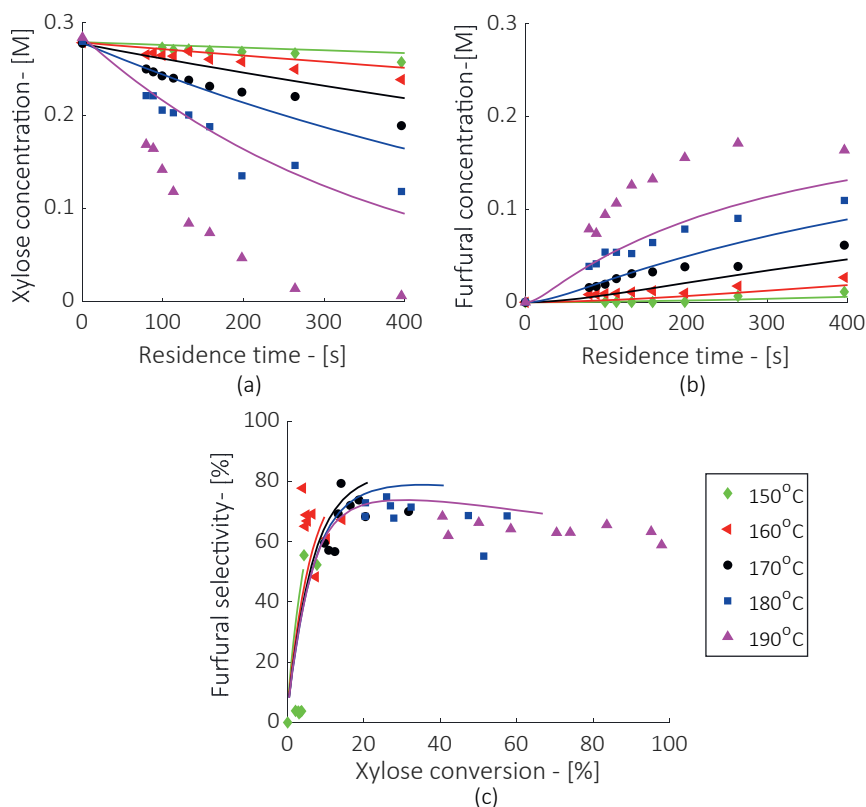
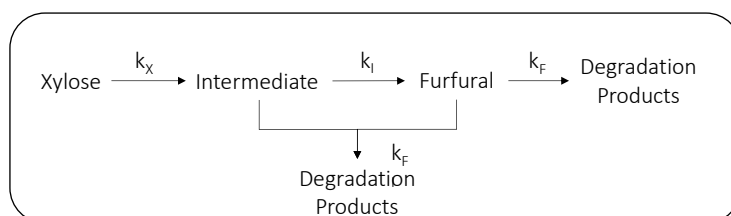


Figure 3.1. Experimental data collected at 150-190 °C against extrapolated model predictions based on kinetics by Krzelj et al. [123], developed until 150°C. (a) Xylose concentration, (b) furfural concentration with residence time, and (c) furfural selectivity vs. xylose conversion for $\tau=400$ s. Other reaction conditions: toluene as extraction medium, $F_v^{org}/F_v^{inorg}=2:1$ mL^{org} (mL^{inorg})⁻¹, $[H_2SO_4]=0.1M$, $C_{xyl}^0=4wt\%$.

Remarkably, the selectivity-conversion trends reported in Figure 3.1c show a rather good alignment between model predictions and experiments for all temperatures tested, even when the model was built only up to 150°C. This suggests that the overall reaction scheme proposed by Krzelj et. al. [123] until 150°C remains valid at higher temperatures, particularly with respect to degradation pathway, while the formation of furfural from xylose seem inadequate at higher temperatures. It can be speculated that the agreement of the experimental data with the trend of xylose conversion and furfural selectivity (Figure 3.1c) confirms that intermediate compounds play a key role on furfural synthesis even at higher reaction temperatures. On the other hand, other studies propose (in some cases with supporting evidences when using HCl as catalyst [65,108,109]) that xylose degrades in parallel [65,125]. This route was proved insignificant by Krzelj et. al [98] when using H₂SO₄ as

catalyst, and it is thus considered unlikely in the present work as well. Still, the likelihood of such mechanism was evaluated in this work and again deemed unlikely under the current set of conditions (see Appendix B.2.). Therefore, for kinetic modelling purposes, the present work considers the mechanism depicted in Scheme 3.2, in which one of the dehydration steps is assumed to be significantly faster than the other and, hence, the intermediate species are lumped in order to facilitate the model development.



Scheme 3.2. Proposed mechanism for Brønsted-acid catalysed xylose dehydration

Despite the agreement in the correlation between xylose conversion and furfural selectivity, both xylose conversion and furfural yield are underestimated individually, as shown in Figures 3.1a. and 3.1b. Thus, this work reports a more accurate determination of the kinetic parameters at higher temperatures for both xylose and arabinose conversion.

First, we strive for a reduction of the number of unknown parameters in the model. To that end, the intrinsic reaction rate constant of the first dehydration step (k_x from Scheme 3.2.) is first determined individually following an integral method approach and a first order assumption: see Figure 3.3a. with the plotted $\ln\left(\frac{C_x}{C_x^0}\right)$ versus residence time data, and the slope of the fitted line representing the magnitude of k_x for each temperature; and see Figure 3.3b with the corresponding Arrhenius plots to calculate pre-exponential factors and activation energies. Next, since the selectivity-conversion relationship (Figure 3.1c) appears to be independent of temperature and properly described by Krzjelj's model [123], we speculate that kinetic parameters for the condensation of furfural with intermediates (i.e., k_{FI}) reported in that work for temperatures below 160 °C, remain valid for the temperature range 160-190°C. Finally, the reaction rate of furfural resinification reaction (k_F) is introduced in the model based on Krzjelj et. al. [123]. All equations incorporated in the model are presented in Appendix B.1., and the fitted kinetic parameters are shown in Table 3.1. As shown in Figures 3.2., the adjusted kinetic model fits the experimental data satisfactorily, and represents a remarkable improvement with respect to the earlier model's predictions shown in Figure 3.1.

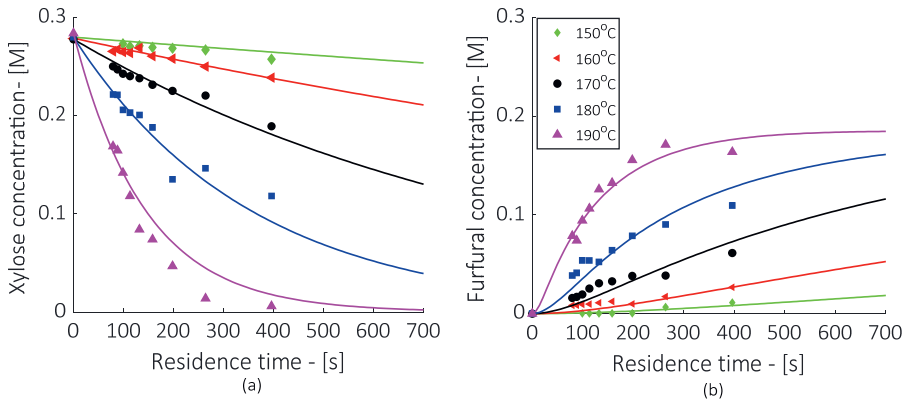


Figure 3.2. Data fit for xylose (a) and furfural (b) concentrations for mechanism B for 150-190°C, extraction medium: toluene, $F_v^{org}/F_v^{inorg}=2:1 \text{ mL}^{org} (\text{mL}^{inorg})^{-1}$, $[\text{H}_2\text{SO}_4]=0.1\text{M}$, $C_{\text{xy}}^0=4\text{wt}\%$

Next, to ensure the robustness of the kinetic model and corresponding values of kinetic parameters, the independency of the fitted values (k_{Fi}) with respect to the initial guesses was confirmed for initial values in the range of 10^{-6} s^{-1} to 10^{-2} s^{-1} (Appendix B.3.). Initial guesses greater than 10^{-2} s^{-1} lead to minor deviations in the final fitted value, further reassuring the robustness of the model. It is demonstrated in Figure 3.3. that model prediction and experimental data are in a very good agreement (within 10%). Moreover, the xylose conversion and furfural yield profiles have a very good fit with the proposed kinetics ($R^2=97.97\%$ and 97.59% for xylose and furfural concentrations, respectively) (Appendix B.4.).

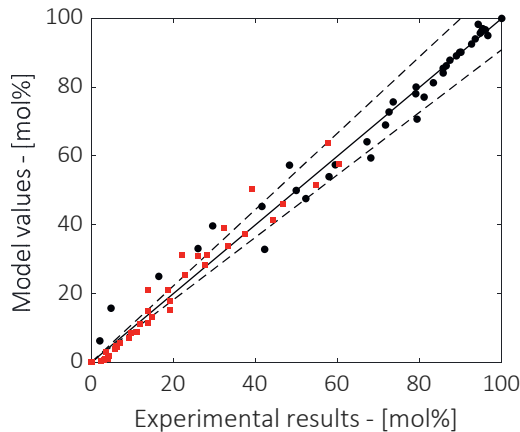


Figure 3.3. Parity plot for the model prediction and experimental data for xylose normalized concentration (round symbols) and furfural normalized concentration (square symbols) within 10%

As shown in Figure 3.4b. and Table 3.1., xylose dehydration is the slowest reaction step (i.e., lowest k_x) and has the greatest activation energy in the entire xylose-to-furfural scheme, which indicates that this is the rate limiting step in the synthesis of furfural. The calculated activation energy (159 kJ/mol) is also in line with other reported values in literature using organic and inorganic Brönsted acid catalysts [108,112,123,125,222] and it is comparable with reported activation energies of glucose dehydration in inorganic Brönsted catalyst [224].

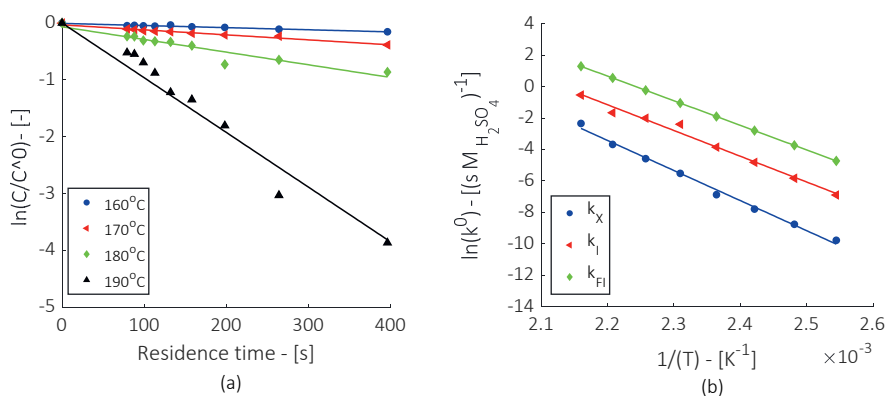


Figure 3.4. Determination of reaction rate constant of xylose dehydration (a), Arrhenius plot for reaction rate constants for 120-190°C (b), extraction medium: toluene, $F_v^{org}/F_v^{inorg}=2:1$ mL^{org} (mL^{inorg})⁻¹, $[H_2SO_4]=0.1$ M, $C_{xyI}^0=4$ wt%

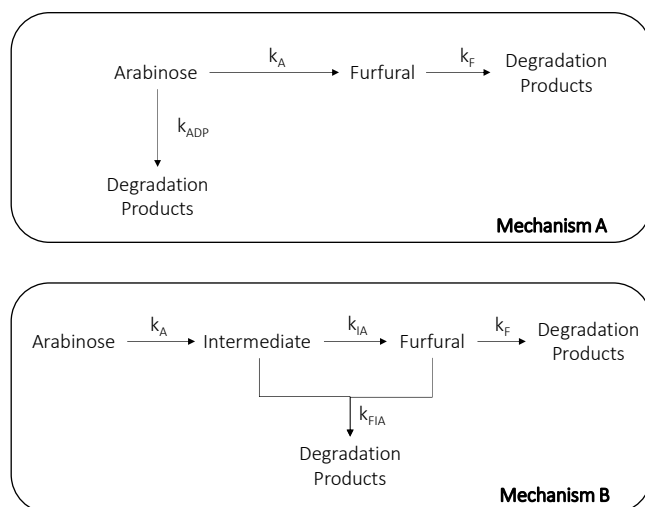
On the other hand, the second dehydration step has a lower activation energy, but still greater than that of the parallel degradation of that same intermediate with furfural. This indicates a (positive) dependency of selectivity on temperature. However, the rate of degradation reactions is not negligible, setting a mechanistic barrier to the maximum furfural formation. Thus, alternative process approaches should be considered to further promote furfural selectivity and decrease the impact of degradation reactions leading to loss of selectivity.

Table 3.1. Xylose conversion to furfural: kinetic parameters.

Reaction Rate Coefficient	Pre-exponential factor [s^{-1}]	Activation Energy [kJ/mol]	R ² [%]	Reference
k_X'	38.68	159.11	99.4%	This work
k_I'	34.89	136.20	98.6%	This work
k_{FI}'	35.12	130.20	99.81%	[123]
k_F'	8.57	62.00	99.15%	[123]

3.3.2. Mechanism investigation and model validation of arabinose dehydration at higher reaction temperatures (160-190°C)

To complete the kinetic analysis of the C5 sugars conversion to furfural, this work looks at the mechanism of arabinose dehydration and corresponding kinetic fitting, which is a topic under-represented in the current literature. Two mechanisms are considered in the current work (Scheme 3.3.). They both propose a parallel degradation pathway. Mechanism A involves a direct conversion of arabinose to degradation products, whereas Mechanism B considers the formation of an intermediate compound and its parallel condensation with furfural, similarly as described for the case of xylose.

**Scheme 3.3.** Mechanisms for Brønsted acid-catalysed arabinose dehydration to furfural

Following the rationale previously discussed for xylose, Mechanism B was deemed at first as the most plausible mechanism for arabinose as well. Nevertheless, as shown in Appendix B.6., the fittings between experimental data and model predictions according to Mechanism B did not lead to satisfactory results, and the fitted kinetic constants against temperature (i.e., Arrhenius plots) did not follow the expected (linear) trends. This suggests that Mechanism B does not accurately describe the arabinose-to-furfural conversion mechanistic pathway, and Mechanism A is considered for further analysis.

As depicted in Figure 3.5., the predicted concentration profiles of both arabinose and furfural according to Mechanism A fit accurately the experimental data. In order to improve the accuracy of the fitted kinetic parameters, the reaction rate of furfural resinification reaction (k_F) reported by Krzelj et. Al. [123] (Table 3.1.) is considered valid, similarly as previously done in the case of xylose.

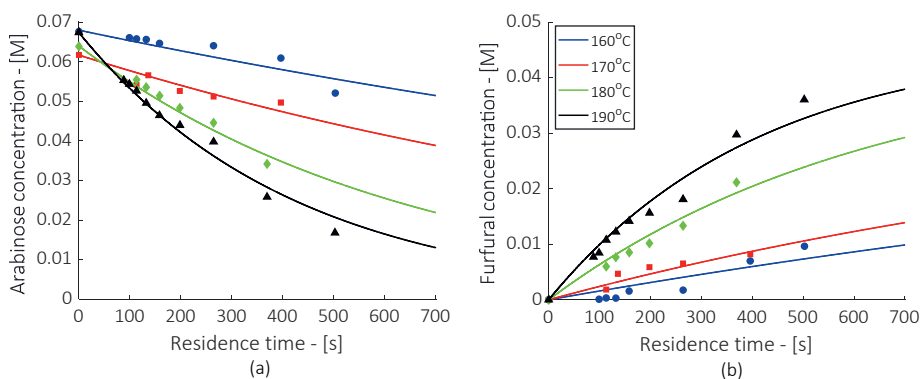


Figure 3.5. Data fit for arabinose (a) and furfural (b) concentration for mechanism A at 160-190°C, extraction medium: toluene, $F_v^{org}/F_v^{inorg}=2:1$ mL^{org} (mL^{inorg})⁻¹, $[H_2SO_4]=0.1M$, $C_{arab}^0=1wt\%$

Then, the independence on the fitted values of the initial guess was confirmed, denoting the robustness of the model. Finally, the correlation matrix of reaction rate constants was evaluated to assess possible interdependence of the kinetic parameters. This analysis showed a strong interdependence between k_A and k_{ADP} (i.e., diagonal in correlation matrix of 0.9971), which is expected as they both add to arabinose conversion.

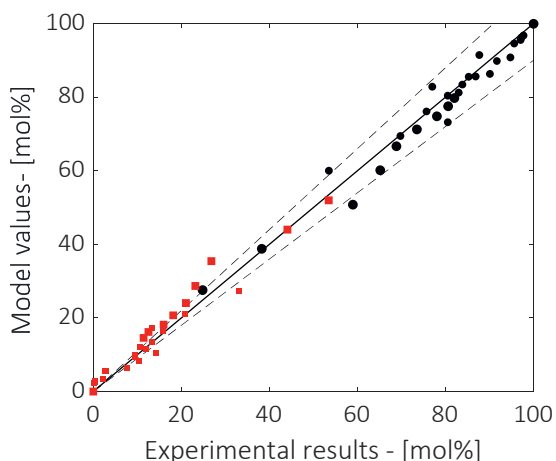


Figure 3.6. Parity plot for the model prediction and experimental data for arabinose normalized concentration (round symbols) and furfural normalized concentration (square symbols) within 10%

As depicted in Figure 3.6., both arabinose conversion and furfural yield fit well the model prediction for both models, and they show very good fit ($R^2=97.06\%$ and $R^2=95.80\%$ for arabinose and furfural concentrations respectively) (Appendix B.8).

Finally, Figure 3.7. shows the Arrhenius plots for the fitted kinetic parameters against temperature, and Table 3.2. summarizes pre-exponential factors and activation energies for all relevant reaction steps in the arabinose-to-furfural conversion. The values of activation energy are mostly in line with the reported values using organic and inorganic acid catalysts [109,220,225,226]. Nevertheless, the activation energy of arabinose degradation reaction determined in this work is relatively lower than others in the literature for concentrated (30wt%) formic acid (i.e., 80.99 kJ/mol) against 125.80 kJ/mol).

Table 3.2. Arabinose conversion to furfural: kinetic data

Reaction Rate Coefficient	Pre exponential factor [s^{-1}]	Activation Energy [kJ/mol]	R^2 [%]	Reference
k_A'	26.38	116.96	97.95%	This work
k_{ADP}'	16.08	80.99	99.65%	This work

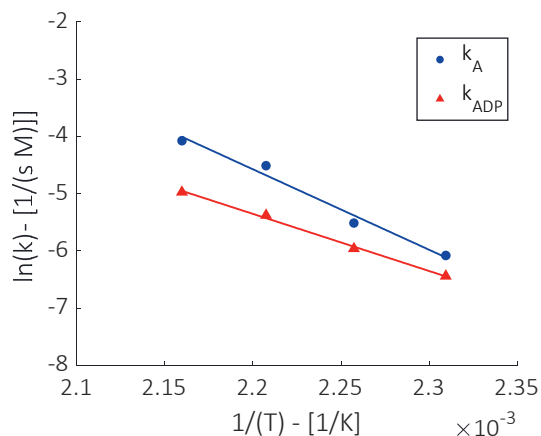


Figure 3.7. Arrhenius Plot for reaction rate constants of arabinose dehydration to furfural formation, 160-190°C, extraction medium: toluene, $F_v^{org}/F_v^{inorg}=2:1 \text{ mL}^{org} (\text{mL}^{inorg})^{-1}$, $[\text{H}_2\text{SO}_4]=0.1\text{M}$, $C_{arab}^0=1\text{wt}\%$

Looking at the values obtained for the kinetic constants (Figure 3.7 and Table 3.2), it is observed that the parallel degradation of arabinose is the slowest step, while it has a much lower activation energy than the desired route to furfural. Thus, likewise in the case of xylose, high reaction temperatures also favour selective furfural formation from arabinose. However, when comparing the kinetics of dehydration of these two C5 sugars (i.e., xylose and arabinose), it is evident that xylose requires a greater activation energy, but it reacts much faster than arabinose under the explored temperature range. This observation is in line with literature [109,127].

3.3.3. Assessment of optimum conditions for biphasic furfural synthesis

Evaluation of optimum reaction conditions

Once established the accuracy of the developed kinetic model for xylose and arabinose dehydration, this section builds upon that knowledge to identify the optimum window of operating conditions to maximize furfural yield from xylose and arabinose. To that end, we developed a 1D plug flow reactor model to describe the H_2SO_4 -catalyzed dehydration of C5 sugars (i.e., xylose and arabinose) according to the kinetics described previously considering the initial concentrations of C5 sugars used in the experiments and the development of the kinetic models. The effect of initial sugars concentration is further examined in Chapter 4. Based on the findings of Chapter 4, we conclude that the observations of the present section are considered valid given that further increase of initial sugar concentration negatively affects furfural yields. This study assumes biphasic conditions (i.e., furfural production in aqueous media and in-situ extraction to an organic solvent). Figure 3.8. shows a contour plot to describe the combined effect of residence time and temperature on the xylose (a)

and arabinose (c) conversion, and on the furfural yield from these sugars (b and d, respectively), for a given set of reaction conditions and extraction performance. It is evident that, for both sugars, the highest furfural yields (ca. 70-80%) is achieved in the region of ca. 200-220 °C and around 400-500 s of residence time. Combinations of lower temperatures and longer residence times are also effective to achieve full sugar conversions, but furfural selectivity (and thus yield) reaches a maximum in that temperature region. This is partly explained by kinetic reasons (i.e., in the parallel sugar/intermediate conversion scheme to furfural, greater temperatures favour the desired pathway, $E_{a,desired} > E_{a,undersired}$); and partly due to the temperature-dependent effect of in-situ extraction, already explained in Chapter 2 (i.e., at greater temperatures $k_F > k_A$). When comparing the performance of the two C5 sugars, it is obvious that they have different reactivity. With respect to xylose, arabinose requires an additional 10 or 20°C in the reaction temperature to reach the same sugar conversion or furfural yield, respectively. Nevertheless, the maximum achievable yield is highest for arabinose feeds within the conditions explored in this study.

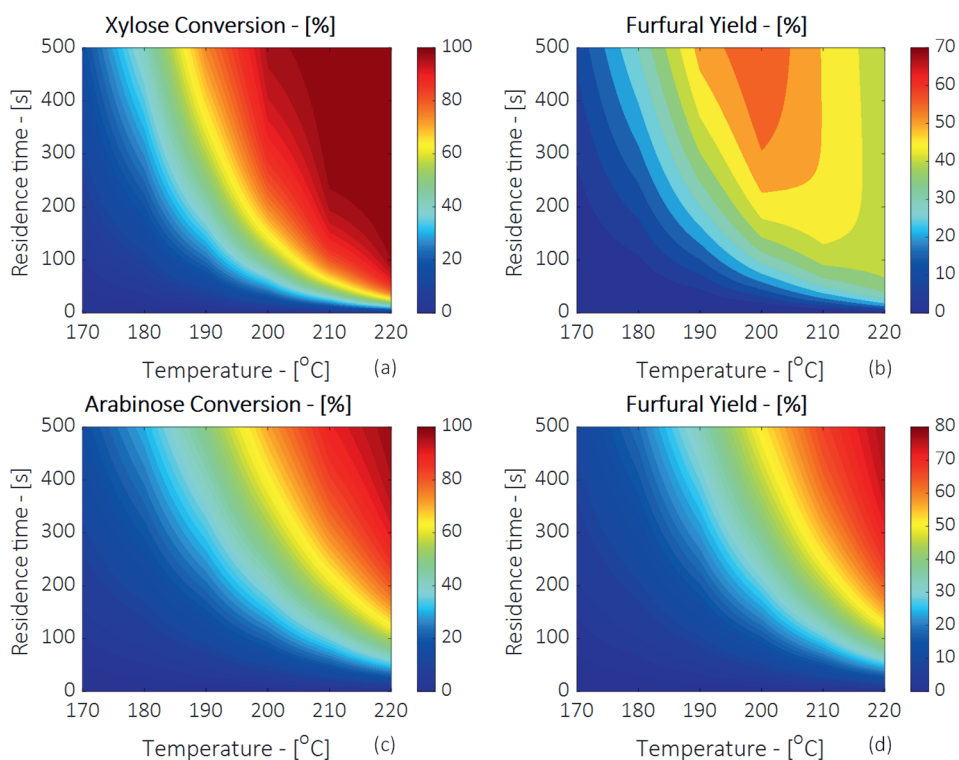


Figure 3.8. Plots for determination of optimum operating conditions for biphasic furfural production for xylose dehydration (a, b) and arabinose dehydration (c, d), extraction medium: toluene, $F_V^{org}/F_V^{inorg}=2:1 \text{ mL}^{org} (\text{mL}^{inorg})^{-1}$, $[\text{H}_2\text{SO}_4]=0.1\text{M}$, $C_{xy}^0=4\text{wt}\%$, $C_{arab}^0=1\text{wt}\%$

Next, Figure 3.9. provides an insight into the yield distribution to degradation products for a temperature range of 170-220°C, 500s of residence time, and starting from xylose (a) and arabinose (b). The two types of degradation products considered are those originated from consecutive furfural resinification (i.e., DP_F , shown by black bars) and those from the parallel degradation pathway from xylose intermediates or from arabinose (i.e., DP_{F+I} or DP_A , shown by blue and orange bars, respectively). For both sugars, the parallel degradation pathway is by far the most predominant, and the main responsible for furfural yield losses. Thus, operating conditions that keep minimum concentrations of xylose intermediates (for the case of xylose) and arabinose (for the case of arabinose) seem an important strategy to maximize furfural yields.

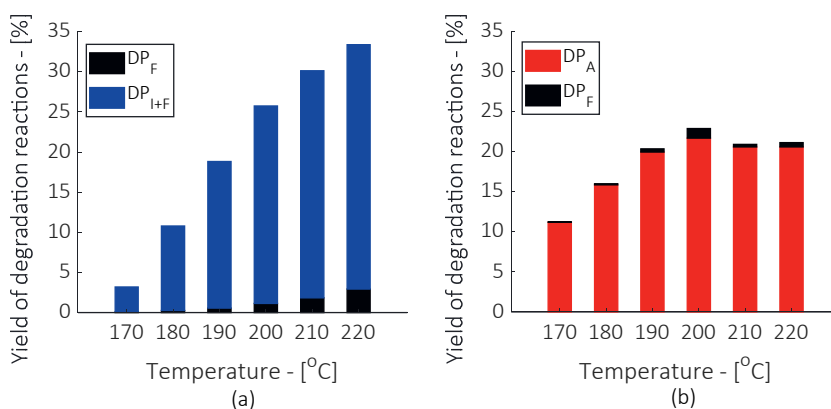


Figure 3.9. Yield of degradation products for 170-220°C at 500s for xylose (a) and arabinose (b), extraction medium: toluene, $F_v^{org}/F_v^{inorg}=2:1 \text{ mL}^{org} (\text{mL}^{inorg})^{-1}$, $[\text{H}_2\text{SO}_4]=0.1\text{M}$, $C_{xylose}^0=4\text{wt}\%$, $C_{arab}^0=1\text{wt}\%$

Finally, it is important to note that the validity of the developed kinetic model beyond 190 °C has not been confirmed in this study, so this analysis should be only considered qualitatively. The exact optimum (i.e., the highest yield and corresponding temperature) may slightly differ in reality, although literature reports are in line with these predictions above 190°C [211,220].

Evaluation of optimum extraction conditions

So far, this chapter has investigated the reaction mechanism and kinetic modelling of the furfural synthesis from C5 sugars, as well as its impact of on the temperature-selectivity relationship. In short, we have seen that a maximum of 70-80% furfural yield can be achieved when operating in a biphasic reactor at an optimum temperature of ca. 200-220°C, depending on the C5 sugar. In addition, furfural yields can be further enhanced by improving

the extraction performance, thereby overcoming the mechanistic selectivity challenge. Thus, similarly as discussed in Chapter 2 with a kinetic model from the literature [10], this section includes an (updated) sensitivity analysis of the impact of extraction performance on the furfural synthesis process, this time with the kinetic models developed for xylose and arabinose in this Chapter. It should be noted that the initial C5 sugars concentrations used here are the same as in the previous section *Evaluation of optimum reaction conditions*.

As a reminder, the performance of the furfural in-situ extraction depends on (a) the furfural partition coefficient in the organic solvent, (b) the volumetric feed ratio of organic to aqueous flow rate, and (c) the mass transfer properties of the reactor. Based on the degradation reaction rate constants discussed in the previous sections, it may be inferred that the minimum mass transfer coefficient of $k_{La} = 10^{-2} \text{ s}^{-1}$ would be required for a sufficiently fast furfural extraction in the examined temperature (Appendix B.9.). This mass transfer properties can be achieved in a millireactor or other intensified reactor type. Thus, for a given reactor that satisfies such criteria, two sensitivity analyses for the parameters (a) and (b) are discussed below.

First, the impact of furfural partition coefficient m , i.e., a thermodynamic proxy for the suitability of solvent of choice, is assessed. Figure 3.10b shows that the presence of an organic solvent for furfural extraction is essential to improve furfural yield when compared to the monophasic reference case for xylose. Solvents with low m lead to furfural yield gains of ca. 20%. Figures 3.10a and b show that, a minimum furfural partition coefficient of $5 M_{\text{furf}}^{\text{org}}(M_{\text{furf}}^{\text{inorg}})^{-1}$ is required to reach furfural selectivity $>75\%$ at almost complete xylose conversion ($\tau > 850\text{s}$). Further increase of furfural partition coefficient ($m > 10 M_{\text{furf}}^{\text{org}}(M_{\text{furf}}^{\text{inorg}})^{-1}$) renders furfural selectivity of 80%-90%. It is observed that an increase of m from 10 to 15 $M_{\text{furf}}^{\text{org}}(M_{\text{furf}}^{\text{inorg}})^{-1}$ leads to a marginal increase of furfural selectivity, given the limited concentrations of furfural in aqueous phase under these conditions. The diminished effect of m on furfural yield for higher furfural partition coefficients is also attributed to the fact that at this range of furfural partition coefficient (i.e., $m > 10 M_{\text{furf}}^{\text{org}}(M_{\text{furf}}^{\text{inorg}})^{-1}$) furfural production is limited by the kinetics (i.e., reaction rates) and the mass transfer properties have reached their optimum. Examples of suitable solvents with high furfural partition coefficient are MIBK and 2-sec-butylphenol. In addition, use of salts in the aqueous medium also has a positive effect on m [108,139,221,227]. Another category of solvents recently identified for their high potential as furfural extraction medium are Deep Eutectic Solvents (DESes). They are considered non-toxic, biodegradable non-flammable and water-immiscible solvents, and some of them present furfural partition coefficient of ca. $40 M_{\text{furf}}^{\text{org}}(M_{\text{furf}}^{\text{inorg}})^{-1}$ [228,229].

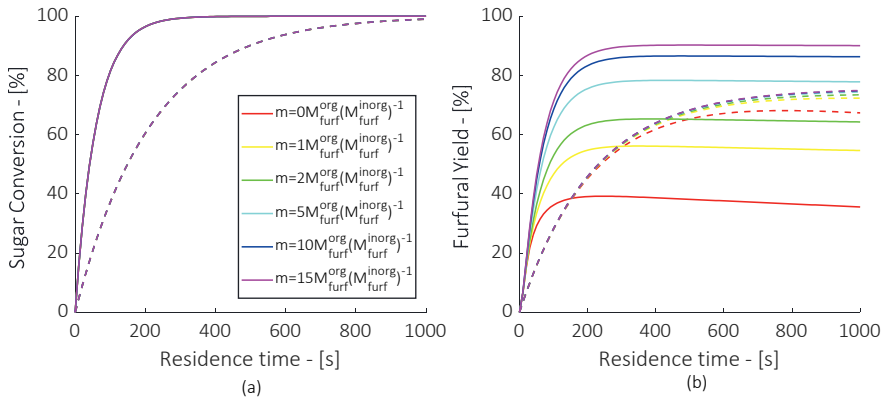


Figure 3.10. Sensitivity analysis of m and its effect on xylose (-) and arabinose (--) conversion (a) and furfural yield (b) at 200°C for extraction medium, $F_v^{org}/F_v^{inorg} = 2:1 \text{ mL}^{org}(\text{mL}^{inorg})^{-1}$, $k_L a = 10^{-2} \text{ s}^{-1}$, $[\text{H}_2\text{SO}_4] = 0.1 \text{ M}$, $C_{\text{xy}}^0 = 4 \text{ wt\%}$, $C_{\text{arab}}^0 = 1 \text{ wt\%}$

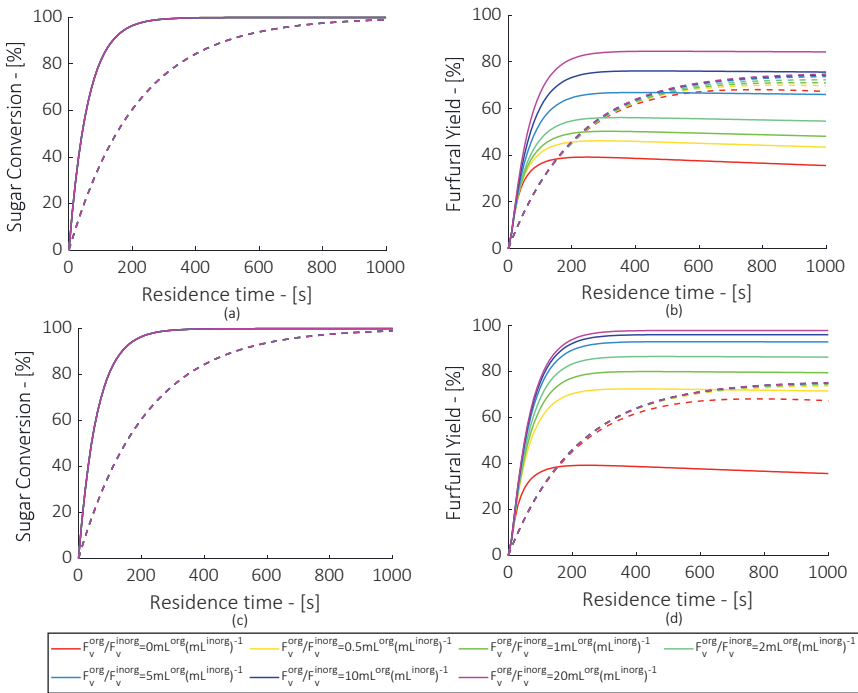


Figure 3.11. Sensitivity analysis of F_v^{org}/F_v^{inorg} and its effect on xylose (-) and arabinose (--) conversion and furfural yield at 200°C for $m=1 \text{ M}_{\text{furf}}^{org}(\text{M}_{\text{furf}}^{inorg})^{-1}$ (a, b) and $m=10 \text{ M}_{\text{furf}}^{org}(\text{M}_{\text{furf}}^{inorg})^{-1}$ (c, d), $k_L a = 10^{-2} \text{ s}^{-1}$, $[\text{H}_2\text{SO}_4] = 0.1 \text{ M}$, $C_{\text{xy}}^0 = 4 \text{ wt\%}$, $C_{\text{arab}}^0 = 1 \text{ wt\%}$

Several solvents that satisfy the m criteria exist and have been tested. However, oftentimes solvent selection is a more complex task that need to consider aspects like energy requirements for solvent purification, as well as safety and toxicity aspects. So even when maximizing m is a clear strategy to increase furfural yields, sometimes a solvent with a relatively low m may be considered for this process. In those cases, a compensation strategy may be to increase the volumetric ratio of organic to aqueous feed rate. In the case of biphasic operations with an organic solvent with a minimum furfural partition coefficient (i.e., $m=1 M_{\text{furf}}^{\text{org}}(M_{\text{furf}}^{\text{inorg}})^{-1}$ as depicted in Figures 3.11a. and 3.11b.), the minimum ratio of $F_{\text{v}}^{\text{org}}/F_{\text{v}}^{\text{inorg}}$ of $10 \text{ mL}^{\text{org}}(\text{mL}^{\text{inorg}})^{-1}$ would be required for a furfural yield of >70% for xylose. In this case, the furfural partition coefficient is still very low to reach equilibrium between the organic and inorganic phase and further increase of $F_{\text{v}}^{\text{org}}/F_{\text{v}}^{\text{inorg}}$ is required to dilute furfural in the organic phase and increase the “storage” capacity in the organic phase. On the contrary, when a solvent with high furfural partition coefficient is used for furfural extraction (e.g., $m=10 M_{\text{furf}}^{\text{org}}(M_{\text{furf}}^{\text{inorg}})^{-1}$, Figures 3.11c and 3.11d.), the minimum ratio of $F_{\text{v}}^{\text{org}}/F_{\text{v}}^{\text{inorg}}$ drops to $2 \text{ mL}^{\text{org}}(\text{mL}^{\text{inorg}})^{-1}$, which will clearly benefit process economics (i.e., smaller process equipment, less energy input in separation train, etc). Here, the effect of $F_{\text{v}}^{\text{org}}/F_{\text{v}}^{\text{inorg}}$ is lower on furfural yield because the mass transfer performance is already close to optimum conditions. As for arabinose case, it is observed in both analyses (as depicted in Figures 3.10. and 3.11.) that the overall effect of extraction is limited. In the reaction scheme of arabinose dehydration (Scheme 3.3-Mechanism A), furfural participates in one degradation reaction (resinification reaction) and, hence, the opportunity of furfural selectivity improvement is limited. Finally, the limited extraction performance can be explained by the fact that furfural concentration under the examined conditions is very low and the aqueous is very dilute.

3.4. Conclusions

The present work presents insights on the reaction mechanism and a kinetic model for the C5sugar-to-furfural conversion starting from xylose and arabinose. It is concluded that the mechanism of furfural formation from xylose includes the formation of intermediates, and a significant participation of those in a parallel degradation reaction with furfural. On the other hand, arabinose conversion can be accurately modelled according to a parallel scheme including a one-step arabinose-to-furfural reaction followed by sequential furfural resinification, and the direct degradation of arabinose. A set of kinetic parameters (i.e., kinetic constants and activation energies) for the established mechanism of C5 sugar dehydration is calculated for a wide reaction temperature (120-190°C) using a biphasic continuous experimental configuration. Based on the determined kinetics, optimum temperatures of ca. 190-200oC and residence time of ca. 3min, lead to maximum ca.80% furfural selectivity under the given assumptions on extraction performance. Finally, a sensitivity analysis of the furfural extraction parameters based on the developed kinetic

models indicates that the furfural partition coefficient of extraction medium should be minimum 5 and the minimum ratio of F_v^{org}/F_v^{inorg} should be 10 and 2 for solvents with low and high furfural partition coefficient respectively in order to enhance the mass transfer properties of the biphasic reactor.

CHAPTER 4

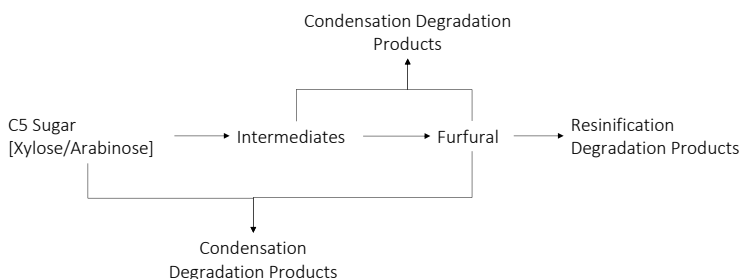
Effect of Feed Composition on the
Continuous Synthesis of Furfural in a Biphasic
Millireactor

Abstract

This research assesses the effect of feed composition on biphasic continuous furfural synthesis, including synthesized feeds of model compounds and two examples of real streams (i.e., C5 sugar-rich food waste stream and herbaceous hydrolysate). We demonstrate a stable continuous operation up to 170°C without any severe solid formation or reactor clogging thanks to rapid in-situ furfural extraction. From the model feed experiments, we conclude that diluted feeds favour furfural selectivity (up to 85%), even at high conversions. Selectivity drops with xylose concentration suggest the presence of unwanted parallel reactions of intermediates and furfural or parallel reactions of higher order with respect to xylose. The presence of C6 sugars in the feed leads to the co-production of HMF without affecting furfural selectivity, when compared to the case with pure xylose. This indicates that sugars dehydrate in parallel without interfering with each other, despite the formation of organic acids. The results with model feeds are representative of those with the real feeds. Ultimately, the use of intensified reactors coupled with biphasic extraction, previously demonstrated with diluted xylose streams, is proved appropriate to withstand the challenges of real feeds.

4.1. Introduction

Lignocellulosic material (LCM) is an excellent candidate as a renewable resource to replace fossil based raw materials for chemicals production [20,191]. Focusing on the hemicellulosic sugars, their main valorization route is the synthesis of furfural, which is the dehydration product of C5 sugars (e.g., xylose and arabinose), and an excellent polymer precursor [230]. Currently, furfural is synthesized industrially using entire biomass as a feed (i.e., without prior fractionation of all biomass constituents), thus wasting ca. 75 wt% of the biomass (i.e., the cellulose and lignin content). An attractive and more sustainable valorisation route of these type of feeds goes via biomass fractionation, subsequent depolymerization to C5 and C6 sugars (e.g., xylose and glucose), and further dehydration to furanics (e.g., furfural and 5-Hydroxymethylfurfural, also known as HMF), which are excellent candidates for biobased polymers and plastics [81,108,160,179,204,231,232]. In the past years, new interesting concepts (e.g., using ionic liquids [200] or in-situ product separation [160]) have been proposed as means to overcome the selectivity limitations that these processes entail, mainly attributed to the degradation of the products and part of the feed in acidic medium. Taking the Brönsted acid catalysed dehydration of xylose as an example (Scheme 4.1.), evidences show that both xylose and furfural undergo various degradation reactions that lead to remarkable product loss and solid formation. This challenges the desired shift from batch to continuous processing [84,107,108,123,233,234]. The work of Huber's and Dumesic's groups demonstrated that introducing water-miscible organic solvents such as GVL and THF into the reaction medium can significantly increase furfural yields due to solvation effects [142,211]. Their most recent work successfully demonstrates yields up to around 80% using GLV/H₂O mixtures during the HCl catalysed xylose dehydration. Yet, the gains in product yields are shaded by the increase in downstream solvent purification costs and energy demands. In addition, the yields to (in)soluble humins and their effect on time-on-stream stability in these kind of systems remains elusive.



Scheme 4.1. Overview of proposed mechanisms of furfural formation from C5 sugars in the presence of Brönsted catalyst

Another attractive approach that has gained increasing attention over the last years is the combined dehydration and in-situ extraction of furfural to a water-immiscible organic solvent [110,148,235] (i.e., in biphasic conditions). In this way, subsequent degradation reactions and thus humin formation can be significantly reduced, while the solvent recovery is less energy intensive. Multiple organic solvents have been proposed for this purpose such as toluene, MIBK and 2-secbutylphenol [108,118,203], as well as other more sustainable options such as deep-eutectic solvents [148]. Indeed, the attractiveness of the process largely depends on the choice of solvent, as it influences the partition coefficient of furfural and the downstream purification train. In addition, the success of the biphasic synthesis depends on the interfacial areas and mass transfer rates of the reactor system. We have previously demonstrated [110] that the use of intensified reactor technologies (i.e., reactors that promote interfacial areas between phases and/or mass transfer rates like microreactors or spinning disc reactors [202,207]) are key to widen the operation conditions, shorten residence times (i.e., from hours to 500 s), minimize humin formation (i.e., from 39wt% to < 2wt% solid formation [234]), and thus prevent reactor fouling during the continuous dehydration of xylose to furfural. Using a millireactor under the Taylor flow regime (i.e., an example of such intensified reactor technology), xylose as a model feed and toluene as extracting solvent, we showed that the conversion can successfully achieve high furfural selectivity (nearly 80%) and a minor amount of insoluble humins (<1 wt%), thus allowing for continuous and stable continuous operation. Comparable results could be expected using other reactor technologies with similar mass transfer properties. Nevertheless, while the process configuration proved attractive to process xylose as model feed, its suitability to process realistic feeds remains an open question. Variations in sugar type and concentrations, as well as the presence of impurities inherent to biomass feedstocks or generated during biomass pre-treatment may pose a threat to the performance and stability of the continuous biphasic synthesis of furfural.

Among all the available LCM, wheat straw, seaweed, corn cobs and sugarcane bagasse may be attractive feedstocks for the synthesis of furfural due to their high sugar content, particularly from its hemicellulose fraction, compared to other biomass feedstocks [81]. After biomass fractionation and hydrolysis, the hemicellulosic hydrolysate stream usually consists of a lignin-free acidic solution of ca. 20wt% C5 sugars in water [236–238]. Acid neutralization is required for stability purposes, and typically leads to sugar dilution down to ca. 5-10 wt.%. Low amounts of C6 sugars are also present in hemicellulosic hydrolysates [239,240], yielding HMF after dehydration. HMF is rather unstable [233,241], forming humin-like degradation products and organic acids [146,234,242]. These may interfere during the synthesis of furfural (e.g., as a catalyst of dehydration and/or degradation reactions), thus affecting the furfural yield [222]. Another promising feedstock for a second generation biorefinery is a side

stream from food industry. For example, industries that process sugar products from natural resources (e.g., sugar cane) or starch (e.g., corn cobs) produce substantial amounts of streams that are rich in carbohydrates. These streams can be further valorised into furfural, also contributing to a sustainable waste management in an integrated biorefinery concept.

In this work, we assess the biphase continuous synthesis of furfural in a millireactor as technology to valorise hemicellulose-derived streams. The work initially examines the process time-on-stream stability, and evaluates the effects of xylose concentration (1, 4, 6 and 8wt%), sugar type (xylose, arabinose, glucose, and fructose) and solvent (i.e., toluene and MIBK) on furfural yield. Finally, the study is extended to two examples of real feeds, including a wheat straw hydrolysate stream and a side stream food industry.

4.2. Experimental section

4.2.1. Set-up Configuration

The experiments of biphase continuous furfural production reported in this section were performed in the continuous experimental configuration described in *Section 2.2. Experimental section* of Chapter 2. After some experimental runs of this chapter, the solids trapped in the filter (corresponding to several measurements at different residence times) are collected and weighted as indication of the yield to insoluble humins.

4.2.2. Materials & Analysis

The materials used for the experiment and the calibration of the instrumentation were 98+% D-xylose from Alfa Aesar, furfural of 99% purity and 98% pure H₂SO₄ by Sigma Aldrich, 99.7% toluene purchased from Biosolve, high purity grade D-Fructose by Amresco, 98% purity 5-HMF obtained by Acros organics, levulinic acid 98% from Sigma Aldrich, 98% Formic acid by VWR chemicals and MIBK 99% pure by Alfa Aesar and DL-Arabinose from Alfa Aesar. The hemicellulosic hydrolysate was provided by the Netherlands Organisation for Applied Scientific Research TNO[®] (Feed 1) and it was produced from wheat straw following an Acetone Organosolv process [243]. Subsequently, the liquor combined with pulp washings was processed using a 20 L rotary evaporator at 60°C to remove acetone from the sample. The obtained Organosolv hydrolysate and the precipitated lignin were kept at room temperature overnight to allow for additional lignin precipitate formation. The liquid was then decanted and centrifuged. Wet lignin precipitate was redissolved in 60% w/w aqueous acetone and processed again in the rotary evaporator. After overnight settling the wash liquid was decanted and centrifuged. Hydrolysate and wash liquid were combined and stored at 4°C. The food side stream was obtained from COSUN[®] (Feed 2) and it is produced from spent sugar beet pulp treatment. Several additives (e.g., mineral acids) were used in the

process of arabinose extraction. The final steps of arabinose purification consist of nanofiltration and crystallization providing a rather pure hemicellulosic stream. Food side stream was diluted with water in order to reach the desired arabinose concentration. More information on the background of the process are available on the patent filed by COSUN® [244]. All the remaining chemicals were used without any additional treatment. Prior to analysis, the samples were filtered using syringe filters from glass fiber and with $1.2 \cdot 10^{-6}$ m porous size obtained from ThermoScientific. The inorganic phase was analyzed with HPLC instrumentation (Shimadzu SIL-20A High-Pressure Liquid Chromatograph). Xylose, glucose, HMF and sulfuric acid were detected with a RI detector (Waters 2414). Furfural was detected with UV-Vis detector (SPD-M20A) at wavelength $\lambda=254$ nm. The column for the HPLC was Agilent Metacarb 67C and water as mobile phase at the rate of $0.0083 \cdot 10^{-6} \text{ m}^3 \text{ s}^{-1}$. The oven temperature was set at 85°C . The organic phase was analyzed by GC instrumentation (Varian CP-3800). Levulinic acid, formic acid and fructose were detected with a RI detector. The column used was Biorad 87H. Sulfuric acid 0.004M was used as eluent at $0.01 \cdot 10^{-6} \text{ m}^3 \text{ s}^{-1}$ and the temperature was set at 30°C . Toluene, MIBK and furfural were detected with build-in FID detector. The column was Varian capillary FactorFour CB Sil 5 CP. Helium was used as carrier gas at the constant flow of $0.025 \cdot 10^{-6} \text{ m}^3 \text{ s}^{-1}$. The temperature ramp for the toluene solutions starts at 250°C for 1200s and then to 250°C for 5 min., whereas for MIBK the temperature ramp starts at 120°C for 4 min, then temperature increases by 20°C K/min for 600s and finally it reaches 400°C for 600 min.

4.2.3. Definitions

The equations (4.1.) – (4.4.) show the definitions of sugar conversion, furfural yield and other mathematical expressions used in the research.

$$\text{Sugar Conversion:} \quad X = \frac{n_s^0 - n_s}{n_s^0} \quad (4.1.)$$

$$\text{Furfural yield (total):} \quad Y = \frac{n_f}{n_s^0} \quad (4.2.)$$

$$\text{Furfural selectivity:} \quad S = \frac{n_f}{n_s^0 - n_s} \quad (4.3.)$$

$$\text{Mole Carbon Balance:} \quad B = \frac{n_s + n_f}{n_s^0} * 100 \quad (4.4.)$$

$$\text{Space Time Yield:} \quad \text{STY} = \frac{n_f}{n_s^0 * t} \quad (4.5.)$$

Where n are the number of moles, n^0 are the number of moles at $t=0$ s and t is the residence time. In terms of reproducibility, the experiment with 1wt% initial xylose concentration was performed twice and all results are within 9% experimental error.

4.3. Results and discussion

4.3.1. Time on stream performance and solid formation during the biphasic synthesis of furfural

The formation of insoluble humins during xylose dehydration is one of the main challenges to guarantee stable continuous operation. Hence, the time-on-stream performance is investigated in Figure 4.1., using xylose as model feed and a temperature of 190°C (i.e., the highest within this research work) to enhance humins formation. The results show stable performance in terms of conversion and selectivity for at least 80 min. During this continuous operation, we did not observe blockages or significant pressure build-up (Appendix C.1.). This is in agreement with the limited amount of solids recovered in the filter at the end of the process, which corresponds to a yield of ca. 0.01% (measured by gravimetric analysis), i.e., much lower than reported in literature for similar conditions (i.e., 10-15wt% [145,211]). Similar time-on-stream trends are found for all experimental conditions explored in this study, although greater yields to humins were found in some cases (more details will be reported in the corresponding section). In the case of real feedstocks, the amount of solid degradation products (humin) is expected to be higher when compared to model feeds due to the presence of C6 sugars (which also leads to humins formation through HMF degradation reaction path) and organic acids, which contribute to degradation reactions [245].

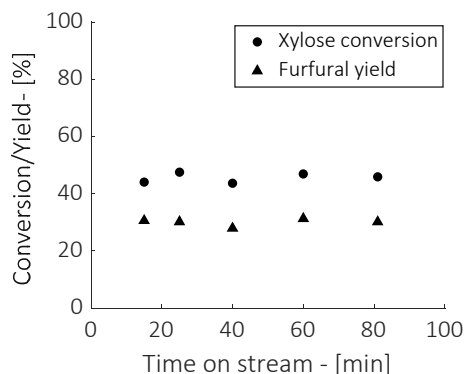


Figure 4.1. Xylose Conversion (●) and Furfural Yield (▲) with time on stream at 190°C, $C_{xy1}^0 = 4\text{wt}\%$, toluene, $[\text{H}_2\text{SO}_4] = 0.1\text{M}$, $F_v^{\text{org}} = 3.75 \text{ mL min}^{-1}$, $F_v^{\text{inorg}} = 1.875 \text{ mL min}^{-1}$

4.3.2. Experiments with model compounds

Effect of initial xylose concentration

The effect of initial xylose concentration on the xylose consumption and furfural production against residence time is shown in Figures 4.2a. and 4.2b., respectively. The initial xylose concentration does not significantly affect the conversion (Figure 4.2a.), inferring to a first-order reaction as most kinetic studies suggest [108,123,133,246]. This observation is validated by the agreement between the data and the model prediction (using kinetic model from Chapter 3, Section 3.3.1. *Mechanism Insights & modelling for xylose dehydration at higher reaction temperatures*), also presented by the solid lines in Figure 4.2a. The calculated values of xylose conversion (Appendix C.2) are also in agreement with literature under similar conditions (ca. 20% conversion at 160 s in this study vs. 10% conversion reported by Dumesic et. al [142] at same temperature and residence time, 5wt% xylose, 0.05M H₂SO₄). On the other hand, the initial xylose concentration does impact furfural synthesis (Figure 4.2b), particularly at initial stages of the reaction. In general, we see that under dilute conditions, furfural is selectively formed and (furfural selectivity remains nearly constant at ca. 80%) at residence time $t > 200$ s over the entire range of conversions and does not decrease at longer residence times (Appendix C.2.), unlike one may expect from the reaction mechanism shown in Scheme 4.1. It should be noted that the extraction of furfural to the organic phase minimizes the extent of consecutive reactions, which would become unavoidable at even longer times. Under more concentrated conditions, and most notably in the case of 8wt% xylose, furfural formation appears hampered, leading to slower increase of furfural selectivity with the residence time. In this case, maximum furfural selectivity is decreased with respect to more dilute experiments. As discussed in this work and more extensively by Krzelj et al. [123], this trend is explained by the increase in concentration of reaction intermediates (i.e., furfural precursors) that are prone to irreversible degradation reactions, thus leading to an overall decrease in selectivity and yield. A plausible explanation for the slower increase of furfural concentration in the case of $C_{xyI}^0=8\text{wt}\%$ could involve the parallel and irreversible reaction of furfural with intermediates of higher order, although no considerable evidence is collected in this work. It is plausible that second order degradation reactions of same intermediates or condensation reactions between different intermediates (as presented in LC/MS chromatogram in Appendix A.3.) might take place decreasing the concentration of intermediates available for furfural production and leading to reduced yields. Thus, the selectivity drop at greater xylose concentrations counter-balances the benefits commonly associated with the use of concentrated feedstock solutions (i.e., more compact equipment, greater throughput, and lower purification costs). Process optimization should be carefully assessed as a compromise between furfural selectivity, reactor volume and energy/costs of the downstream purification steps.

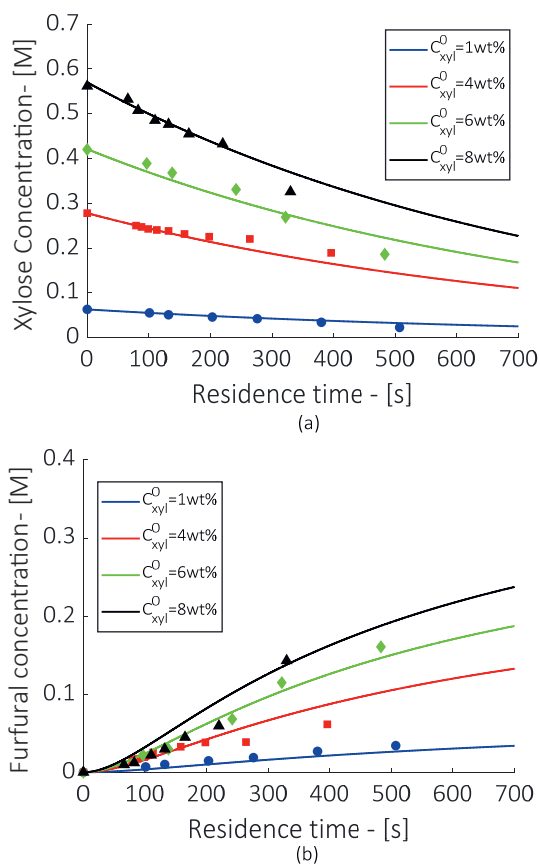


Figure 4.2. Profiles of xylose (a) and furfural concentration (b) at 170°C, toluene, $F_v^{org}/F_v^{inorg}=2:1$, $[H_2SO_4]=0.1M$ with model prediction (-). The model predicts experimental data satisfactorily.

Effect of C5 and C6 sugars

First, we evaluate the differences of various C5 sugars as feed for the synthesis of furfural. We focus on xylose and arabinose, which are the most important C5 sugars that are present in hemicellulosic streams and yield furfural upon dehydration. Figure 4.3. shows the evolution of C5 sugar and furfural concentrations as a function of residence time using xylose and arabinose as feed. When the two C5 sugars are compared under the same conditions, xylose converts faster and more selectively to furfural than arabinose, in line with previous reports [33], [34]. This trend is also in line with kinetic analysis presented in Chapter 3 (see model predictions as lines in Figure 4.3.). Considering the arabinose kinetics, selective conversion of arabinose would require greater reaction temperatures and likely shorter

residence times to maximize yields. Next, we evaluate the effect of glucose and fructose (i.e., an important intermediate in the C6 dehydration pathway to HMF) in the feed stream during the synthesis of furfural using toluene as extracting solvent. This choice of solvent allowed us to evaluate the possible effect of (toluene insoluble) C6 derivatives (e.g., HMF) on the C5 dehydration route in the water phase.

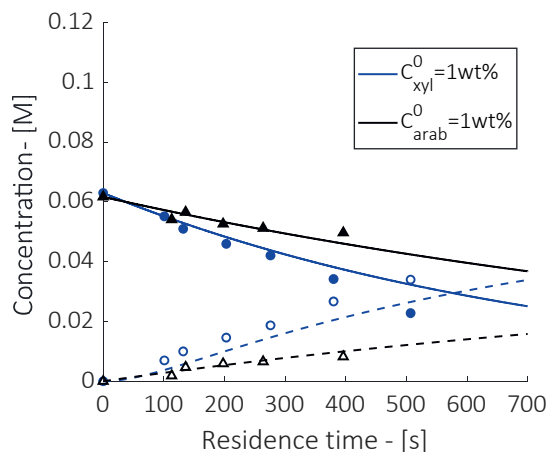


Figure 4.3. Xylose (a) and Furfural (b) concentration profiles with residence time for xylose (1wt%) and arabinose (1wt%), 170°C, toluene, $F_v^{org}/F_v^{inorg}=2:1$, $[H_2SO_4]=0.1M$ with model prediction for C5 sugar (-) and furfural (--). Closed symbols are for xylose (●) and arabinose (▲). Open symbols are for furfural respectively. The model predicts experimental data satisfactorily.

Figure 4.4. shows that xylose and furfural concentrations are not affected by the presence of fructose, glucose, or their dehydration derivatives. Note that this experiment is performed under unusually high concentration of C6 sugars, which are typically present in low amounts in hemicellulose hydrolysate streams. This further reassures the previous conclusion. Likewise, additional monophasic experiments (Appendix C.3) further demonstrate that C6 dehydration does not yield furfural and that the C5 dehydration product mixture does not affect the C6 dehydration route. This suggests that all sugar dehydration routes proceed independently. It may be also inferred that the HMF degradation products such as formic acid (FA) and levulinic acid (LA) [213], which are also overly represented in this experiment (Figures 4.5.) do not interfere in the dehydration of xylose in the range of concentrations explored in this study. The hydronium ion concentration is increased by 0.2% because of the formation of LA and FA, which is likely too low to affect the pH of the reaction solution. Thus, the yield to furanics as a function of residence time remain unaffected when performing the

dehydration of all sugars simultaneously with respect to single-sugar experiments. Consequently, expensive pre-purification steps could be eliminated from the process.

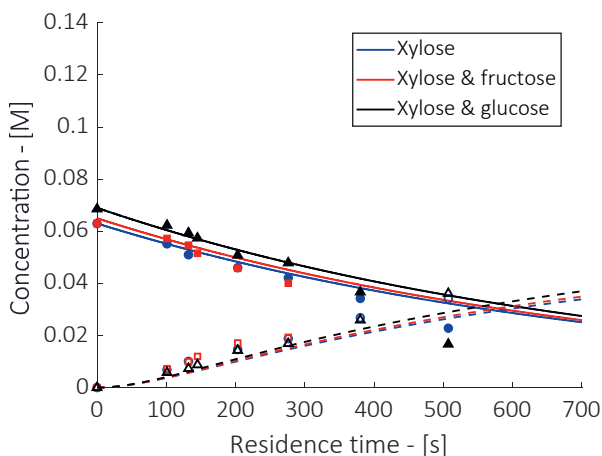


Figure 4.4. Xylose (closed symbols) and furfural (open symbols) concentration profiles with residence time^{*1} for xylose (1wt%), xylose/fructose (1wt%/1wt%) and xylose/glucose (1wt%/1wt%), 170°C, toluene, $F_v^{org}/F_v^{inorg}=2:1$, $[H_2SO_4]=0.1M$ with model prediction^{*2} for xylose (-) and furfural (--). The model predicts experimental data satisfactorily.

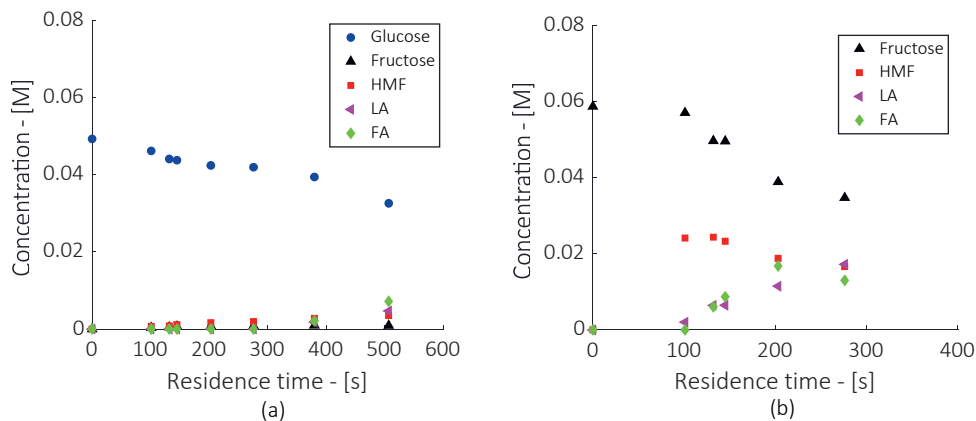
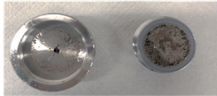




Figure 4.5. C6 sugars conversion and products yields with residence time^{*1} for xylose/glucose (1wt%/1wt%) (a), xylose/fructose (1wt%/1wt%) (b), 170°C, toluene, $F_v^{org}/F_v^{inorg}=2:1$, $[H_2SO_4]=0.1M$

^{*1}Note that the experiments with fructose and residence times greater than 300s yielded to excessive solid formation and could not be measured accurately.

Figures 4.5a. and 4.5b. show the concentration profiles of C6 sugars (glucose and fructose accordingly) and their dehydration products (i.e., HMF, levulinic and formic acids) when co-feeding fructose and glucose, respectively, together with xylose in the feed stream. Expectedly, the yield to HMF directly from fructose is greater than that from glucose, since the latter requires an additional reaction step (i.e., the initial isomerization of glucose to fructose) that is not favoured in the presence of Brønsted acids [242]. Thus, the synthesis of HMF and its subsequent degradation products is limited when co-feeding glucose to xylose. It is also observed that for both substrates, i.e., xylose-fructose and xylose-glucose, the selectivity to weak acids LA and FA (total concentration of 0.02 and 0.01M, respectively) increases as that of HMF decreases, together with a visible formation of black humins (Scheme 4.3.).

Substrate	Solids Formation
1wt% Xylose	
1wt% Xylose and 1wt% Fructose	
1wt% Xylose and 1wt% Glucose	

Scheme 4.3. Solids formation on the filter, run time=4 hours, 170°C, toluene, $F_V^{org}/F_V^{inorg}=2:1$, $[H_2SO_4]=0.1M$

Besides maximizing product yield, minimizing humin formation is another crucial point of attention for the desired shift to a continuous process (even more if solid catalysts are used). We have previously shown that the combination of fast mass transfer rates and very short residence times was key to maintain minimal formation of solids during the synthesis of furfural from model C5 sugars [110]. Under such conditions, the limited amount of degradation products was mostly soluble. Nevertheless, when C6 sugars are present in the reaction mixture, the extent of HMF degradation and solid formation under dehydration conditions is visibly greater. Scheme 4.3. shows the solids retained on the filter during the run of one complete experiment (4 hours of total run) for the different substrates. It is evident that using only xylose as reactant yields the least amount of solids (i.e., 0.4 mg), followed by the experiment with xylose and glucose (i.e., 0.8 mg), and finally by that with

xylose and fructose (i.e., 10.7 mg). Since the furfural selectivity is independent of the substrate, it may be safely inferred that the difference between the solids formed during the xylose-only experiment and the rest is the result of HMF degradation reactions. Notice that toluene selectively extracts furfural while HMF and its derivatives remain in the reaction medium, subjected to further degradation reactions. The reported amount of solid humins formed when feeding mixed sugars poses a severe challenge for a long-term and stable continuous process. Thus, the choice of solvent will play a key role.

Solvent Consideration

In this section, the use of toluene and MIBK during the continuous biphasic synthesis of furfural is examined. Both organic solvents are inexpensive, commercially available, widely used in industry, and are well-established for furfural purification processes [247,248]. Furfural has higher partition coefficient in MIBK than in toluene ($m_{\text{MIBK}}=7 M_{\text{furf}}^{\text{org}}/ M_{\text{furf}}^{\text{inorg}}$, $m_{\text{toluene}}=2.2 M_{\text{furf}}^{\text{org}}/ M_{\text{furf}}^{\text{inorg}}$ at 170°C) [108,110,118] (Appendix C.4), and in both cases it decreases at higher temperatures [110] (Appendix C.5.). Thus, greater selectivity to furfural may be expected when using MIBK with respect to those with toluene. Nevertheless, Figure 4.6. shows that both xylose and furfural concentrations against residence time are nearly independent of solvent type. Greater benefits on furfural selectivity would be expected when using solvents with furfural partition coefficient of around one order of magnitude higher such as 2-sec-butyphenol or deep eutectic solvents [145,148], as predicted by our previous modelling work [110].

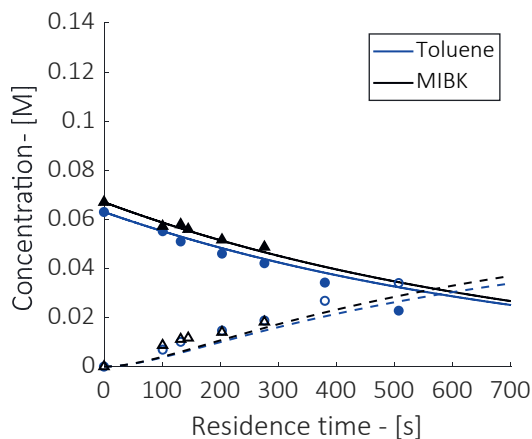


Figure 4.6. Xylose (closed symbols) and furfural (open symbols) concentration profiles with residence time using toluene (blue) and MIBK (black), 170°C, $C_{\text{xy}}^0 = 1\text{wt}\%$, $F_{\text{V}}^{\text{org}}/F_{\text{V}}^{\text{inorg}}=2:1$, $[\text{H}_2\text{SO}_4]=0.1\text{M}$ with model prediction* for C5 sugar (-) and furfural (-). The model predicts experimental data satisfactorily.

Unlike toluene, MIBK is able to co-extract furfural and HMF from the reaction mixture. Figures 4.7a. and 4.7b. show the effect of extracting solvent on the C6 conversion and reaction products. Here, the use of MIBK has a positive impact on the yield of HMF with respect to toluene. The co-extraction of furfural as well as HMF preserves higher selectivity of both furanics and prevents their subsequent degradation. This is evidenced by the lower concentrations of LA and FA, as well as by a significant (i.e., above 58-fold) decrease in solid formation when using MIBK, as illustrated in Scheme 4.4.

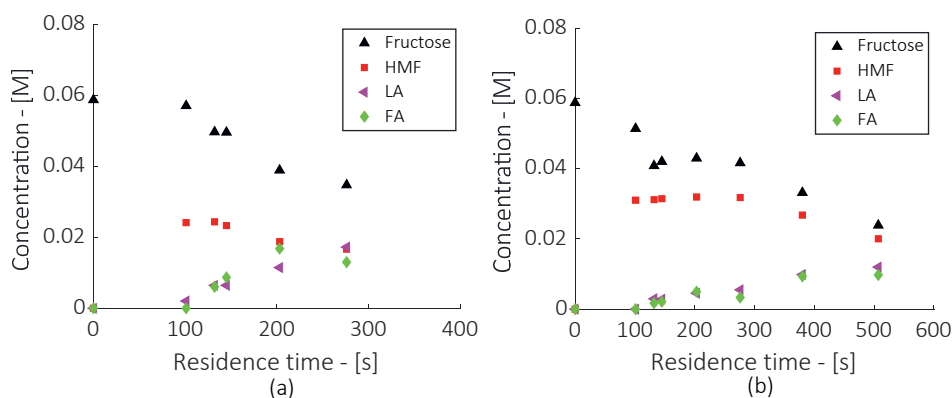




Figure 4.7. C6 sugars (closed symbols) and products (open symbols) concentration profiles with residence time using toluene (a) and MIBK (b), 170°C, $F_v^{org}/F_v^{inorg}=2:1$, $[H_2SO_4]=0.1M$

Extraction Medium	Solids Formation
Toluene	
MIBK	

Scheme 4.4. Solids formation on the filter for toluene (a) and MIBK (b), run time=4 hours, 170°C, $F_v^{org}/F_v^{inorg}=2:1$, $[H_2SO_4]=0.1M$

4.3.3. Experiments with real feedstocks

Wheat straw hydrolysate (TNO[®])

A wheat straw hydrolysate sample with the composition reported in Table 4.5. was evaluated in the process under consideration. The sample has less than 5wt% of sugars, it is already acidic (pH=1.2) (Appendix C.7.), and it contains a mix of C5 and C6 sugars (i.e., xylose, arabinose, and glucose). After mixing with the catalyst stream, the final pH drops to 0.78. A limited amount of furfural and HMF, possibly produced during acid hydrolysis, are also present in the sample.

Table 4.5. Composition of sugars and main furanics in real feeds

Feedstock	Compound	Composition (wt%)
Wheat Straw Hydrolysate (TNO [®])	Xylose	2.402
	Arabinose	0.002
	Glucose	0.232
	Furfural	0.09
	HMF	0.681
Side Stream from food industry (Cosun [®])	Xylose	0.02
	Arabinose	40.9
	Glucose	<0.01
	Fructose	<0.01
	Mannose	0.08
	Fucose	0.03
	Rhamnose	0.17
	Galactose	0.06
Sucrose	<0.01	

Based on the experimental procedure of the hydrolysate production, minor amounts of (monomeric) phenolics are present in ppm level. Acetic acid is expected to be present in the hydrolysate, but during HPLC analysis prior to experiments, no acetic acid was detected. Presumably, acetic acid concentration is below detection limit. Moreover, a small amount of oligomers (e.g., 5.7 mM xylobiose) is present in the solution. Finally, while traces of low molecular weight lignin fragments could be expected, these were not detected according to the current analytical procedure.

Figure 4.8. presents the conversion of xylose and arabinose when feeding the hydrolysate stream. With respect to the model feed, the conversion of both sugars in the real and model feed are comparable for short residence times, whereas some differences start to arise at longer reaction times ($\tau > 200$ s). This is attributed to the additional conversion of sugars that

already starts in the pre-heating section of the reactor when feeding the (already acidic) real feed. As indicated in the experimental section, in a standard experiment with model feeds, the sugar and the acid streams are fed and pre-heated to reaction temperature separately in order to have a good control of the residence time. However, this was not possible when starting with an acidic feed. Therefore, the real feed is in this case exposed to two consecutive reaction zones: (1) the pre-heating zone, where sugars dehydration takes place with a temperature gradient in monophasic conditions; and (2) the reactor zone, where sugars dehydration takes place at constant reaction temperature and in biphasic conditions (i.e., with in-situ furfural removal). Thus, one-to-one comparison between the two types of experiments is not possible. In practice, to minimize the extent of the reaction in the pre-heating zone, the hydrolysate feed can be neutralized prior to injection, or injected cold directly to the reactor. However, both approaches may bring undesired consequences like excessive waste of acids and oversized reactors, respectively. Thus, to assess the validity of this concept to treat real feeds, we have chosen to run our experiments according to the most plausible industrial operation: by feeding the already acidic hydrolysate stream to an on-purpose pre-heat section.

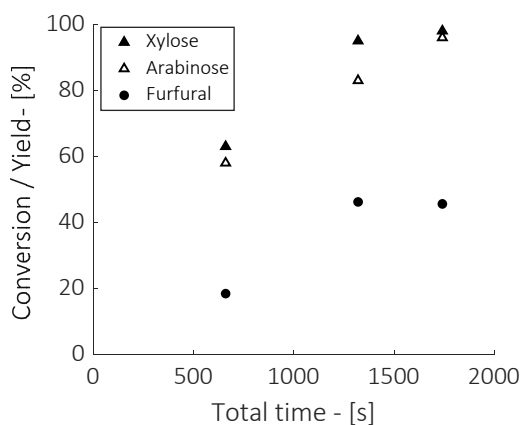


Figure 4.8. C5 Sugars Conversion and Furfural Yield with residence time in reactor for wheat straw hydrolysate (HYD), 170°C, toluene, $F_v^{org}/F_v^{inorg}=2:1$, $[H_2SO_4]=0.1M$

To estimate the extent of the additional xylose conversion in the pre-heating zone, a 1D plug flow model (which includes mole and heat balances over the pre-heat and reactor zones and considers the actual acid concentration in both zones as well as furfural extraction only in the latter) is developed using the fitted kinetic parameters presented in Chapter 3 for xylose and arabinose conversion, respectively. The temperature profile for the pre-heating section

is available in Appendix C.6. The enhanced heat transfer properties of the millireactor and the carefully designed pre-heating section allow for stable reactor inlet temperatures of all three streams (i.e., extraction solvent, wheat straw hydrolysate and catalyst). The results of the model prediction, as presented in Figures 4.9a., 4.9b. and 4.9c., demonstrate that the trends observed with model feeds (MF) and those predicted by the 1D plug-flow model are good descriptors of the real feeds behaviour (HYD). This supports the validity of previous conclusions derived from model feeds experiments and suggests that the presence of impurities in real feeds (such as C6 sugars and their products) do not interfere significantly during the synthesis of furfural. The developed kinetic model accurately predicts both xylose and arabinose conversion, as well as the yields of furfural obtained with feedstocks using model compounds (MF) and real feeds (HYD). At low residence times, the reactions proceed quite selectively towards furfural. In line with our previous observations with model feeds, operating with dilute feeds and short residence time ($\tau < 300\text{s}$) results in excellent selectivity and very limited degradation. It is interesting to notice that no significant degradation reactions took place up to 300s during the monophasic conversion in the pre-heat section. For longer residence time, however, a slight drop in furfural yield is observed in the real feed with respect to the model feed. Here, the non-negligible conversion xylose in the pre-heating section in monophasic conditions (i.e., without in-situ extraction) led to significant degradation. This emphasizes the effectiveness of in-situ furfural extraction.

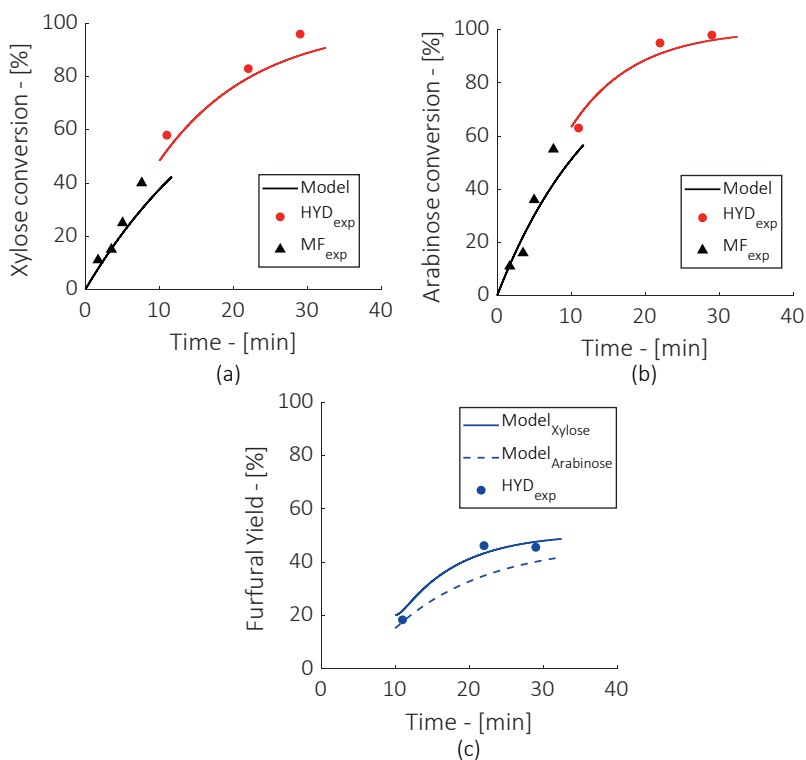


Figure 4.9. Comparison of experimental data for hydrolysate (HYD) and feedstock with model compound (MF) with model prediction for (a) xylose, (b) arabinose and (c) furfural, 170°C, toluene, $F_v^{org}/F_v^{inorg}=2:1$, $[H_2SO_4]=0.1M$ with model prediction* for C5 sugar (-) and furfural (-/-). The model predicts experimental data satisfactorily.

Hemicellulosic stream from food processing (Cosun®)

A hemicellulosic side stream of food processing with the composition detailed in Table 4.5. is used for the continuous synthesis of furfural in a biphasic media. This sample contains more than 40wt% of a mix of sugars, being arabinose the most abundant. Unlike the previous hydrolysate stream, this stream does not contain any acid. Thus, it is a very attractive feed for the synthesis of furfural.

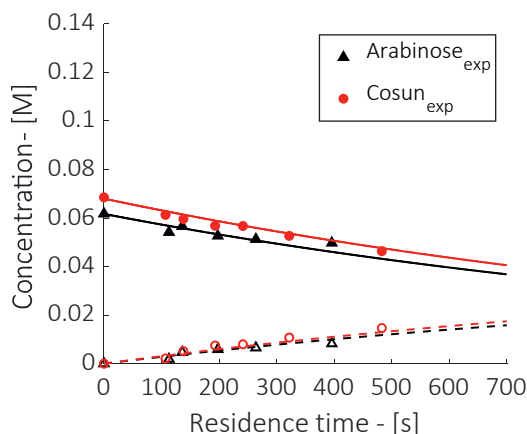


Figure 4.10. Arabinose (- and closed symbols) and Furfural (-- and open symbols) concentration profiles with residence time for arabinose [model compounds] and Cosun® food side stream, 170°C, toluene, $F_v^{org}/F_v^{inorg}=2:1$, $[H_2SO_4]=0.1M$ with model prediction for arabinose (-) and furfural (--). The model predicts experimental data satisfactorily.

According to Figure 4.10., it is evident that the conversion of arabinose and corresponding synthesis of furfural follow the exact same trends in the model feed and the real feed. Once again, the experiments with model feeds (and kinetic model derived from them) are good predictors of the behaviour of this real feed. In addition, it can be inferred that the presence of impurities of this stream (perhaps in concentrations below detection limits) does not significantly affect the continuous synthesis of furfural. With respect to the process performance, this real food waste stream led to a promising 70% selectivity and a negligible amount of solid formation, but a relatively low ca. 40% conversion under this reaction conditions. As discussed in Chapter 3, xylose converts faster to furfural compared to arabinose.

4.3.4. Comparison with literature and other process considerations

Due to the increasing interest in the production of furfural from hemicellulose, various reactors and processes have been proposed in recent years for this application. In this work, we assess the continuous synthesis in biphasic (extractive) media using a millireactor under Taylor flow, which was chosen as a model system representative of other intensified reactors (i.e., reactors with relatively fast mass transfer rates). To assess the attractiveness of this concept, in this section we compare the performance of this technology with respect to that of other furfural synthesis processes described in the literature. Table 4.6. summarizes the most relevant literature data based on the use of mineral acids as catalyst. This table includes

process descriptors (e.g., reactor type, feed type, reaction conditions, solvent type, etc.) as well as performance indicators (i.e., sugar conversion and furfural production). For comparison purposes, the furfural production rate is expressed as space time yield, normalized per initial sugar concentration.

When only looking at the sugar conversion, we compare our results with others obtained with similar temperature, acid type and concentration, since no effects of mass transfer (and thus reactor type) are expected in this homogeneously catalysed conversion. Here, we see that the current technology shows a relatively higher conversion vs. low residence times when compared to batch reactors (entry 3 and 4) under same conditions. Possibly, these batch reactors were operated for longer time than strictly needed to achieve full conversion. Extending the comparison to other flow reactors, our conversion vs. residence time performance seems to be on par when accounting for a linear effect of acid concentration (i.e., entry 1), and regardless of the solvent. On the other hand, this technology significantly outperforms others based on HCl in a batch reactor (entries 9 and 10), likely due to a different intrinsic activity of this catalyst. With respect to furfural productivity, on the other hand, we find greater differences among the different technologies. Here, our technology is among the best performant, only preceded by our previous work (entry 13), and the work by Dumesic et. al (entry 2), both at higher temperatures. In line with our previous findings, it appears that higher temperatures are advantageous for the synthesis of furfural due high activation energies. This and the use of miscible solvents can partly explain the attractive results by Dumesic et. al [18]. Among the results obtained at the same temperature (170°C), the performance reported in this study both with model and real feeds are by far the highest, even when compared to other biphasic systems [12], [24]. This is attributed to an effective extraction of furfural (i.e., higher mass transfer rates), which allows to operate at greater conversions with minimum degradation. Better results can be still achieved after solvent optimization, since furfural partitioning in the toluene/water system is rather low. Finally, when compared to other experiments with real feeds (entry 5, 8 and 11), the proposed technology shows the most promising performance.

Table 4.6. Literature Overview of Furfural Production

#	Reactor ^a	Feed type ^b	T [°C]	C _{HF} ⁰ [M]	C _{sug} ⁰ [M]	Catalyst	Residence time [min] ^d	System ^c	Reaction Mixture	Extraction medium	F _{org} /F _{inorg}	C5 Sugar conversion	ST ^e	Ref.
1	CF	MF	170	0.133	N/A	0.05M H ₂ SO ₄	2	M	H ₂ O/GVL	N/A	N/A	20%	4 · 10 ⁻³	[142]
2	CF	MF	190	0.27	N/A	0.05M HCl	1	M	H ₂ O/GVL	N/A	N/A	30%	2.7 · 10 ⁻¹	[142]
3	Batch	MF	170	0.67	N/A	0.1M H ₂ SO ₄	30	B	H ₂ O	toluene	2:1	100%	7 · 10 ⁻³	[185]
4	Batch	MF	170	0.33	N/A	0.1M H ₂ SO ₄	30	B	H ₂ O	toluene	2:1	100%	6.4 · 10 ⁻³	[185]
5	CF	RF	170	0.71	N/A	0.44M H ₂ SO ₄	42	M	H ₂ O/THF	N/A	N/A	70%	1.6 · 10 ⁻²	[211]
6	CF	MF	170	0.067	N/A	0.1M H ₂ SO ₄	9	B	H ₂ O	toluene	2:1	61%	6.2 · 10 ⁻²	This work
7	CF	MF	170	0.07	N/A	0.1M H ₂ SO ₄	9	B	H ₂ O	MIBK	2:1	60%	6.3 · 10 ⁻²	This work
8	CF	RF	170	0.09	0.016	0.16M H ₂ SO ₄	5	B	H ₂ O	toluene	2:1	92%/70%	9.3 · 10 ⁻²	This work
9	Batch	MF	170	0.67	N/A	0.1M HCl	15	B	H ₂ O	MIBK	1:1	25%	1.3 · 10 ⁻²	[108]
10	Batch	MF	170	0.067	N/A	0.1M HCl	120	B	H ₂ O	toluene	1:1	31%	3.4 · 10 ⁻²	[118]
11	Batch	RF	170	0.186	N/A	N/A	60	B	H ₂ O	2-sec-butylphenol	1:1	30%	3.2 · 10 ⁻²	[145]
12	CF	MF	170	0.333	N/A	0.15M HCl	8	M	H ₂ O	N/A	N/A	45%	4.8 · 10 ⁻²	[249]
13	CF	MF	190	0.28	N/A	0.1M H ₂ SO ₄	4.5	B	H ₂ O	toluene	2:1	93%	1.4 · 10 ⁻¹	[110]
14	CF	MF	210	0.21	N/A	0.44M H ₂ SO ₄	11	M	H ₂ O/THF	N/A	N/A	100%	2.12 · 10 ⁻²	[211]
15	CF	MF	163	0.13	N/A	0.44M H ₂ SO ₄	44	M	H ₂ O/THF	N/A	N/A	25%	1.58 · 10 ⁻²	[211]

^a CF: Continuous Flow, ^b MF: Model Feed, RF: real feed, ^c M: monophasic, B: biphasic, ^d Residence time for flow reactors: $t_{CF} = V_R/F_v$, ^e Space Time Yield unit: [Y_{furf}/min]/M_{(C_{sugar})ⁱⁿ}

Based on these findings, we conclude that continuous flow reactors with enhanced mass transfer rates are promising for the valorisation of hemicellulose streams, also when processing real feeds, as they allow for a reduction of the residence time and humins formation, and thus render high furfural yields and time-on-stream stability [110,142,249,250]. Thus, it seems plausible to envision a continuous process where the relatively small amounts of humins formed are collected downstream in a set of parallel filters with intermittent cleaning. Nevertheless, other important considerations should be considered to further assess the scalability prospects of this process. First, dedicated stability studies (i.e., longer times on stream) should be conducted to assess its feasibility under a wider range of feeds and process conditions. With respect to the choice reactor technology, scaling up millireactor technology is challenging, but comparable mass transfer rates may be achieved in more scalable reactors such as packed bed columns with high surface area packings [251,252], or more innovative reactors like the spinning disc reactor [207,253]. Finally, solvent selection is of utmost importance for the overall sustainability and cost-efficiency of the process [254]. Although toluene and MIBK are adequate choices for the current investigation, as they are readily available and allow for comparison with literature data, the use of renewable, biomass-based, and non-toxic solvents is preferred from a sustainable point of view. Among of them, deep-eutectic solvents (DES) have demonstrated very good performance improving furfural yield up to 50% in lab scale [148]. Thus, there is significant room for sustainable process intensification in the synthesis of furfural by coupling reactor intensification and solvent optimization strategies.

4.4. Conclusions

This work focuses on the effect of feed composition during the continuous biphasic synthesis of furfural using a millireactor, as an example of intensified reactor technology (i.e., a reactor with high mass transfer rates). To that end, we examine both model and real biomass feeds. Using model feeds, we have shown that increasing xylose concentration in the feed does not significantly affect the rate of sugar conversion but compromises the final furfural selectivity to some extent. The decrease of furfural selectivity at greater xylose concentrations may counterbalance the advantages usually related with the use of concentrated feedstock solutions. With respect to xylose, arabinose is less reactive upon dehydration and less selective towards furfural. The addition of glucose and/or fructose to the xylose feed stream leads to a parallel C6 dehydration route (yielding HMF and derivatives) but does not alter xylose conversions and furfural selectivity with respect to the case with pure xylose feeds. This suggests no significant interaction among the C5 and C6 dehydration routes and encourages the use of realistic feeds for the continuous synthesis of furfural using biphasic medium. However, rapid humins formation from HMF threatens the stability of the continuous operation when co-feeding fructose to the feed stream and using toluene as

extracting solvent. On the contrary, using MIBK to co-extract furfural and HMF leads to minimal humins formation and thus stable performance. Finally, the continuous synthesis of furfural using biphasic media has been extended to real feeds (i.e., a wheat straw hydrolysate provided by TNO[®] and an arabinose-rich food side stream provided by COSUN[®]). The results with real feeds were well represented by our previous studies with model feeds. The tested samples yielded 50% and 30% furfural yield, respectively under non-optimized conditions, and led to a stable continuous operation. Here, the combination of short residence time and rapid extraction of the furanic products to the organic phase was key to achieve high yields and stable operations. The kinetic model developed in Chapter 3 for xylose and arabinose dehydration were used to predict the performance of all tested feed types (including real feeds). The model predictions are in good agreement with the experimental results, supporting the validity of the model and the underlying assumptions on the mechanisms of C5 sugars conversion paths. Finally, the performance of the proposed technology is critically compared with other furfural synthesis processes described in literature, showing the attractiveness of the proposed approach.

CHAPTER 5

Conceptual Process Design of Scaled-up
Furfural Biphasic Production & Techno-
Economic Evaluation

Abstract

In the pursuit of alternative resources for the production of chemicals and fuels, lignocellulosic biomass has tremendous potential for the production of biobased platform chemicals such as furfural. The viability of the biphasic continuous production of 5 kton/yr furfural is evaluated by simulating three case studies. MIBK and 2-sec-butylphenol are evaluated as solvent, and the latter has been identified as the most suitable for in-situ furfural removal mainly due to its high furfural partition coefficient and boiling point. In the second study, the comparison of several C5-rich industrial feedstocks is assessed. The result indicates that the process with softwood-based hemicellulosic stream has high furfural selectivity (87%) and better process economics. The third case study shows that an increase of C5 sugar concentration in the feedstock results in remarkable decrease of reactor size, hence CAPEX, and OPEX due to smaller process flows making these processes financially competitive. Finally, a high-level heat integration result in a further reduction of OPEX and carbon footprint up to ca. 24% and 85%, respectively.

5.1. Introduction

The reduction of fossil resources for the production of chemicals and energy has been the focus of the world's research agenda and policies for many years [11,255]. In this light, it is crucial to translate advanced technologies from research to industrial level as well as to promote the adaptation and update of existing units of biomass processing [256,257]. In order to comply with the current and upcoming regulations and ethics, second generation feedstocks (e.g., non-food, low-cost and abundant lignocellulosic biomass [36,192]) should be considered for the production of bio-chemicals and bio-fuels [11,258,259]. Among the vast portfolio of bio-based chemicals, furfural, obtained from the C5 sugar fraction of biomass, is one of the most attractive platform chemical. Its subsequent processes (e.g., hydrogenation) can lead to the production of valuable bio-based chemicals (e.g., furfuryl alcohol, cyclopentanone) and polymers (e.g., PLA, PEF) [230,260].

The synthesis of furfural takes place by acid dehydration of C5 sugars (i.e., xylose and arabinose) in aqueous media. Under the same reaction conditions, furfural formation is seriously challenged by parallel and subsequent degradation reactions that consume furfural and parts of the feed [84,108,123,124]. This affects the overall selectivity of the furfural production process. Thus, synthesizing furfural with high yields has been a long-term challenge. Three main processes set the ground for industrial production of furfural [84,179,261]. Firstly, the Quaker Oats batch process developed in USA in 1921 used dilute sulfuric acid and relatively high temperatures (ca. 150°C) to convert sugarcane bagasse (i.e., a hemicellulose rich feedstock) to low yields of furfural (i.e., 50% based on C5 fraction). Next, SUPRAYIELD is a modification of the Quaker Oats process, in which furfural is formed at high temperatures (close to its boiling point), and instantly removed to the vapor phase [84,214]. Although energy intensive, this process achieves relatively higher (i.e., 50-70%) furfural yields. Finally, the Vedernikov's continuous process uses concentrated acid catalyst for the one-step hydrolysis of hardwood and in-situ C5 sugar dehydration, leading to increased furfural yields (ca. 70%) and decreased cellulose destruction during biomass pretreatment. Then, cellulose can be further converted to bioethanol [134]. However, this technology is tailored to hardwood as feedstock. Other reported processes of furfural production are included as part of a complete biorefinery scheme that aims at valorizing almost all lignocellulose compounds (i.e., cellulose, hemicellulose, and lignin). For example, Biofine is a commercial process in Italy for the continuous production of furfural and levulinic acid. Here, furfural is removed via stripping, reaching furfural yields of 50-70% using sulfuric acid [20]. Another example is the Lignol process in Canada, which uses the Organosolv fractionation technology and produces ethanol and furfural. However, the reported yields are low and further investigation is required [135]. Currently, the main furfural production sites are

located in China, South Africa and Dominican Republic [262], and most of them produce furfural in monophasic conditions and still operate at low furfural yields [261,263].

More recent developments on furfural synthesis include the contribution of Marcotullio et al. [125], who report high furfural yields (70-80%) from xylose using HCl and halides. A scaled-up conceptual design includes furfural production from straw and the downstream recovery of furfural by extraction with toluene and subsequent distillation. In their work, Marcotullio et al. [125] demonstrate the advantages of adding metal halides on furfural yields, and provide significant insight on the mechanistic aspects of furfural formation from xylose with the combination of mineral Brønsted acids with salts and metal halides. Similar approaches to promote sugars dehydration and furfural selectivity via tandem catalysis using Brønsted and Lewis acid catalysts (e.g., HCl with $\text{CrCl}_3 \cdot 6\text{H}_2\text{O}$) has been proposed by other research groups [118,264]. Besides, replacing mineral acids by solid acid catalysts is very promising, since issues such as catalyst recovery and stability of the feed and product streams during transport, storage and downstream purification can be largely simplified. However, problems such as humins deposition on the solid catalyst and consequent loss of catalyst efficiency should be considered. Other ways of coping with the challenge of furfural selectivity include the addition of salts, water miscible organic solvents and ionic liquids [120,142,148,187,188].

One of latest research directions in the field takes advantage of the benefits of coupling the synthesis of furfural with its in-situ extraction in a biphasic (i.e., aqueous-organic) media. Similar to the synthesis of furfural coupled with in situ stripping, this biphasic process combines reaction and separation as key strategy for process intensification [110,160]. Furfural removal allows for minimum furfural degradation in parallel undesired reactions [108,110,160], broadening the operating window for stable operation. Nevertheless, the success of these strategies requires an appropriate reactor technology with enhanced mass transfer properties [110]. More specifically, the mass transfer rates should exceed the furfural degradation rates in order to preserve high selectivity, as discussed previously in Chapters 2 and 3. Examples of promising reactor technologies with enhanced mass transfer properties and high interfacial area between the two phases are microreactors [265], static mixer reactor [266] and the spinning disc reactors [207,253]. In general, process intensification strategies are key for the successful transition from batch to continuous production of furfural. Despite the established advantages of the biphasic synthesis of furfural on yield per pass, its implications on the overall process (e.g., including cost and energy of the downstream separation track) have not been fully addressed yet. It is expected that these will depend on the solvents and the feedstock of choice considering the multiple feedstocks available in the current and prospect biorefinery scenes, as well as their composition of C5 sugars and other impurities. Considering the current direction of the

chemical industry towards the valorization of side streams and the reduction of waste, it is critical to have a comparative study evaluating the opportunities of furfural production as part of an integrated biorefinery plant.

In this work, the design of several scaled-up (i.e., 5 kton/yr product) processes of biphasic synthesis of furfural are simulated and thoroughly evaluated in terms of their techno-economic performance. The principles of process intensification are followed by combining the synthesis and in-situ extraction of furfural in a single step, as well as proposing high-level opportunities for heat integration for the most relevant scenarios. In this way, the process designs always seek maximum performance as well as minimum costs and environmental impact (i.e., maximum yields, energy efficiency, minimum waste generation and CO₂ footprint, and minimum plant size). Initially, two organic solvents (i.e., 2-sec-butylphenol and MIBK, as representative examples of high and low boiling point solvents) are examined in order to assess the net impact on furfural yields and energy demands of the overall process. Furthermore, the present work elaborates on the effect of feedstock types (including xylose as model compound and other hemicellulose-rich streams from various biorefinery sectors) and zooms into the impact of sugar concentration on the design, furfural yield, energy demands and ultimately on the overall process economics (i.e., the furfural selling price). Finally, the environmental impact of the processes using various feedstock types is reviewed based on the generated waste and the energy requirements of the process scheme, and the process areas with the highest carbon footprint are identified.

5.2. Methodology & Approach

5.2.1. Process Design

General scope and assumptions

In the present study, the furfural plant capacity is considered constant at 5 kton/yr, which is within the range of typical product capacities in biomass processing plants and similar studies [125,145,267,268]. The study assumes that this plant is integrated within an existing biorefinery where the feedstock is readily available (more details on the feeds are given in section *Case studies*). In order to make a comparative assessment of all case studies, the conditions at the reactor inlet (i.e., sugar concentration, temperatures and pressures of the feedstock, catalyst, and solvent streams) are set at comparable values and the reactor volume is considered constant (Table 5.1.). The reaction performance is calculated based on experimental observations and previously validated modelling studies (Chapters 3 and 4, [112,123,224,264]). The main process specifications and characteristics are presented in Table 5.1. More diluted products (with water) are less desired because this will affect both subsequent furfural treatment (e.g., furfural hydrogenation) and logistic costs. For the sake

of clarity, this work reports the non-detailed conceptual designs of the various process configurations considered.

Table 5.1. Specifications of furfural production process

Process Specification	Value
Furfural production rate	5 kton/year
Reactor volume (for 1 CSTR)	1m ³
Reaction temperature	200°C
Reactor pressure	50 bar
Reactor residence time (in minutes)	$\tau = V_{\text{reaction}}/F_V^{\text{tot}}$
Catalyst	H ₂ SO ₄ (0.1M)
C5 Sugars concentration (at reactor inlet)	1-4.5wt%
Sugars conversion	100%
$F_{V,\text{org}}/F_{V,\text{inorg}}$	2:1
Furfural purity (target)	>95%

Technology selection and simulation approach

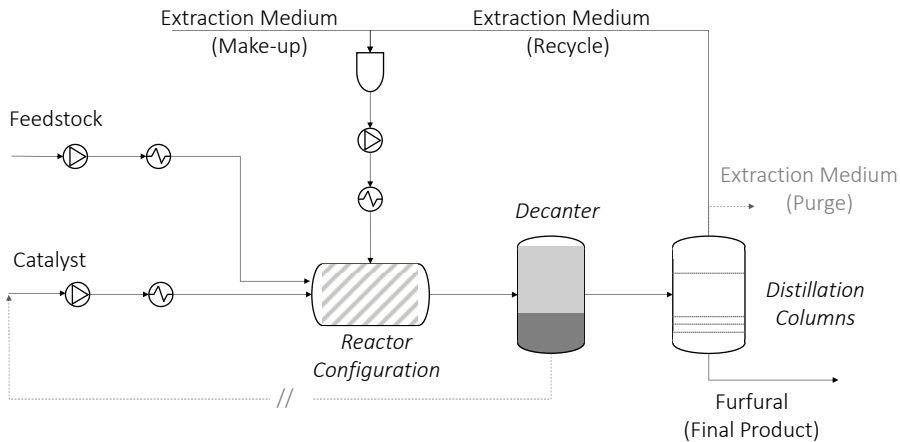
The process design is performed using APSEN Plus[®] software according to the following general assumptions:

1. The process operates at steady state.
2. The liquid in all equipment is perfectly mixed, and the heat of mixing is negligible.
3. There are no heat losses from the simulation blocks
4. The reactor is modelled isothermally.
5. The aqueous and organic phases are described with NRTL and SR-POLAR thermodynamic models, respectively [269].

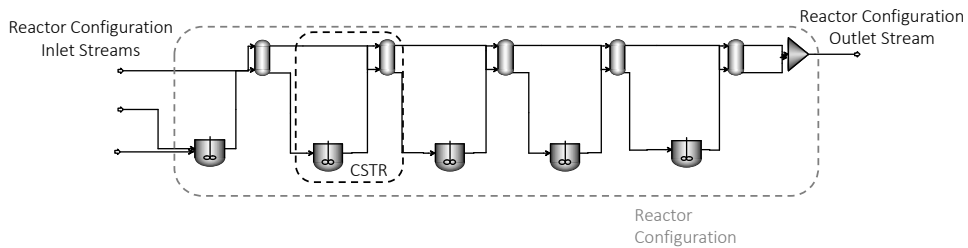
Scheme 5.1. shows the general process flowsheet for the synthesis of furfural. Three major sub-sections may be identified: 1) Injection, 2) Furfural production and 3) Downstream purification.

The injection section comprises three inlet streams to feed the extraction medium, the feedstock, and the catalyst to the reactor. Prior to reactor inlet, heat exchangers and pumps are used to bring inlet streams to desired temperature and pressure, as presented in Table 5.1. Note that in case of (already acidic) hemicellulosic feedstocks, a lower reactor inlet

temperature is set in order to avoid possible undesired reactions that may take place before the reactor inlet. An inlet temperature at 120°C and short time ensure that there is no xylose conversion prior to reactor inlet [123].



Scheme 5.1. General Process Flowsheet of Furfural formation in biphasic system



Scheme 5.2. Modelling approach of reactor configuration for biphasic furfural production

Based on our previous work, a biphasic flow reactor that operates close to plug flow behaviour is preferred to maximize the yield to furfural ([110], Chapters 2-4). In practice, this may be achieved in a tubular reactor (e.g., microreactors under the Taylor flow regime or packed-bed columns) or in a sequence of stirred tanks. The latter shows technological maturity, potential for scalability and temperature control [270,271]. Thus, in this work, the reactor is modelled by 5 CSTRs in series (Scheme 5.2.). To account for the effect of in-situ extraction, each CSTR is followed by an extraction column operated under the same reaction conditions (Scheme 5.2.). The reactor model includes all reactions presented in Tables 5.2.-5.3., which contain xylose, arabinose, mannose, and glucose dehydration reactions, as well

as all parallel reactions in the respective reaction schemes in the presence of inorganic homogeneous catalysts. This design uses well-established kinetic models (experimentally validated in a wide range of reaction conditions) and thermodynamic data from ASPEN Plus® database to predict product yields and phase distribution (i.e., partition coefficients) as function of reaction conditions. Based on our previous experimental work, the yield to insoluble degradation products (i.e., solid humins) is limited even at higher temperatures (Chapter 4). Thus, in addition to furfural as main product, the carbon balance is closed with the formation of water-soluble degradation products that result from furfural resinification and from the condensation of furfural and other xylose dehydration intermediates. A similar approach is considered for the C6 dehydration pathway.

Table 5.2. C5 sugars reactions

Reaction	Range of reaction conditions	Reference
Xylose Path		
$C_5H_{10}O_5 \rightarrow C_5H_8O_4 + H_2O$	$T=100-190^\circ C, [H^+]=0.1\text{ M},$	([123], Chapter 3)
$C_5H_8O_4 \rightarrow C_5H_4O_2 + 2H_2O$	$C_{xyf}^0 = 4\text{wt}\%$	
$C_5H_8O_4 + C_5H_4O_2 \rightarrow DP1$	$T=100-190^\circ C, [H^+]=0.1-2\text{ M},$ $C_{xyf}^0 = 1-4\text{wt}\%$	
Reaction	Range of reaction conditions	Reference
Arabinose Path		
$C_5H_{10}O_5 \rightarrow C_5H_8O_2 + 3H_2O$	$T=160-190^\circ C, [H^+]=0.1\text{ M},$	(Chapter 3)
$C_5H_{10}O_5 \rightarrow DP1$	$C_{ar}^0 = 1\text{wt}\%$	
Furfural Degradation		
$C_5H_4O_2 \rightarrow DP3$	$T=120-140^\circ C, [H^+]=0.1-2\text{ M},$ $C_{furf}^0 = 0.023\text{ M}$	[123]

Table 5.3. C6 sugars reactions

Reaction	Range of reaction conditions	Reference
Glucose Path		
$C_6H_{12}O_6 \rightarrow C_6H_6O_3 + 3H_2O$	$T=140-180^\circ C, [H^+] = 0-1\text{M},$	[233]
$C_6H_{12}O_6 \rightarrow DP5$	$C_g^0 = 2-20\text{wt}\%$	

Reaction	Range of reaction conditions	Reference
Mannose Path		
$C_6H_{12}O_6 \rightarrow C_6H_6O_3 + 3H_2O$	T=110-130°C, $[H^+] = 0.045 M$, $C_{man}^0=5wt\%$	[264]
$C_6H_{12}O_6 \rightarrow DP6$		
HMF Degradation		
$C_6H_6O_3 \rightarrow C_5H_8O_3 + CO_2H_2$	T=140-180°C, $[H^+] = 0-1M$, $C_{HMF}^0=4-16wt\%$	[233]
$C_6H_6O_3 \rightarrow DP7$		

As for the downstream separation process, the first step includes a filter at the reactor outlet to prevent any solid humins from entering the downstream section, and to ensure stable continuous operation. Then, a decanter is placed in order to separate the two (i.e., aqueous, and organic) phases at low temperature and atmospheric pressure. This will prevent subsequent furfural degradation (and selectivity loss) in the decanter. Under these conditions, the furfural partition coefficient is higher than that at reaction conditions, so more furfural is extracted to the organic phase. The organic phase is sent to a separation section that targets the recovery of the extraction medium and the purification of the furfural product stream. Since distillation is a very well-known industrial technology for solvent recovery and furfural purification [146,254,272], this separation track consists of one or more distillation columns depending on the solvent of choice and feedstock type. All distillation columns operate under vacuum and low temperature ($T < 100^\circ C$) in order to prevent in-line furfural degradation. Details on the process and technology selection will be discussed in the Case Studies section. The aqueous phase from the decanter mainly contains sulfuric acid and soluble organic products from the degradation reactions. This stream is not directly recirculated to the reactor inlet because impurities will build up and negatively affect the process performance. Thus, it is assumed that the aqueous acidic stream from the reactor outlet is diverted to the wastewater treatment facility, where the organic compounds are removed. Several processes are applicable for the purification of these streams in the wastewater treatment facilities for organics removal such as the adsorption using activated carbon is a very common practice [273]. From this process, a “cleaner” stream of aqueous sulfuric acid is recycled back to the reactor.

Case studies

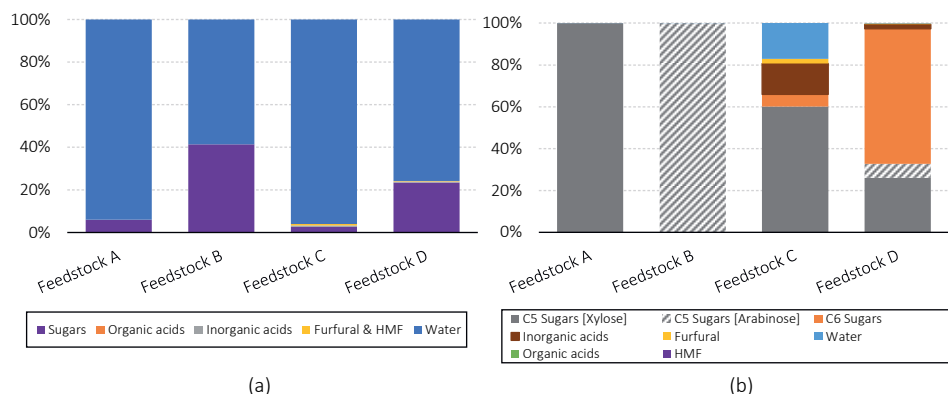
Case study 1: This case study focuses on the evaluation of extraction medium for in-situ furfural removal. A wide range of water-immiscible organic solvents has been reported for this application [108,110,118]. Although not the most effective, toluene and MIBK are the

most common, since they are relatively well-established industrial solvents, with an adequate affinity towards furfural and low boiling points (110°C and 116°C at 1 bar for toluene and MIBK, respectively). According to previous findings, both toluene and MIBK lead to similar furfural yields (Chapter 4, [108,185]), while the latter is also effective in the extraction of HMF (i.e., a component that may be present in hemicellulose hydrolysate streams and is also prone to degradation reactions). Thus, MIBK is one of the solvents of choice in this study. On the other hand, high boiling solvents offer attractive opportunities for energy savings in the downstream separation section, as will be further elaborated in this study. Among them, 2-sec-butylphenol (boiling point 230°C at 1 bar) is a promising candidate with a high furfural extraction capacity [144]. Its suitability as furfural extraction medium has been demonstrated with model compounds (i.e., xylose) and real lignocellulosic feedstocks (biomass hydrolysates) [145,203]. Thus, 2-sec-butylphenol is chosen in this study as a representative example of high boiling solvent due to the implications from the process design point of view. Nevertheless, the study of solvents for this application is an active field of research, where not only the extracting capacity (i.e., partition coefficients) but also sustainability and toxicity issues are taken into account [148,274].

Case study 2: In this case study, several types of feedstocks are evaluated, with a focus on hemicellulose-rich streams found in various sectors of industry, including well-established industries like food and pulping, as well as less conventional yet promising biorefinery processes based on Organosolv biomass fractionation. The nature of the original biomass feedstock and the subsequent refining process define the composition of the hemicellulosic stream that enters the furfural production plant. Accordingly, five feedstock types (i.e., feedstocks A to D), with the compositions described in Scheme 5.3., are considered in this study. Feedstock A consists of pure xylose in aqueous solution. Although it is not a typical feedstock that will be found in industry, it is still included in the present study as benchmark to evaluate the effect of impurities on the overall process. Feedstock B is a representative side-stream from food-processing industry. Although this is a very wide sector and the available hemicellulosic streams vary depending on the food processing and feedstock type, this study focuses on a hemicellulose-rich stream from sugar beets processing which has high C5 sugar content and no acid, making this stream very attractive for furfural production (Chapter 4). Feedstock B has originally higher arabinose concentration (ca.40wt%). However, dilution of this feedstock prior to reactor inlet is considered in order to be within the range of model accuracy (as developed in Chapter 3) and have comparable initial C5 sugar concentrations for all feedstocks. Feedstock C is a representative example of agricultural waste processed via Organosolv fractionation process. This is an attractive approach for the fractionation of herbaceous lignocellulosic material (LCM) and hardwoods. In particular, we consider wheat straw (i.e., a herbaceous material with the highest hemicellulosic content) as

a relevant agricultural waste, and a typical composition of an Organosolv processed hemicellulosic stream [243]. Although these works report high concentrations of C5 sugars, it is expected that post fractionation process will lead to further dilution to remove any lignin left in the hydrolysate [275,276]. Note that similar streams have been successfully processed experimentally in our previous work (Chapter 4). Finally, feedstock D is a hydrolysate from softwood processing. It originates from a modification of the previous fractionation method, this time applied to softwood, followed by a selective and optimized hydrolysis step using sulfuric and/or formic acid, which yields a hydrolysate rich in C5 sugars [277]. This hydrolysate also contains high concentration of mannose (i.e., a C6 sugar), which is typical for softwood hydrolysates [278–280]. While Organosolv-based biorefineries target, in principle, maximum valorization potential of all sugars by prior fractionation of biomass into its constituents, the present work addresses the valorization of C5 sugars, whereas the C6 sugar and their derivatives remaining in the hemicellulose hydrolysate stream are treated as impurities. For further valorization of the C6 sugars, a modification of the process should be considered, and its economic feasibility critically analyzed, accordingly. Another interesting feedstock candidate is a side stream from the pulp and paper industry. Some pulping process concepts propose isolation of the hemicellulose stream prior to the main pulping step via hot water extraction [145,211]. Such stream would be an interesting candidate for furfural production. However, due to the limited information found on the composition of this type of hemicellulosic streams, this feed was not included in the main study. Instead, and only as a reference, the corresponding analysis is provided in Appendix D.12., and no definite conclusions are drawn from it.

Case study 3: The third case study focuses on the effect of sugar concentration on the equipment size and energy requirements of the process. This study is applied to feedstock A, again chosen as benchmark, as well as feedstocks B and C as representative examples where sugar concentration may be subject to further optimization.



Scheme 5.3. Feedstock compositions (a) and insight into carbon distribution (b)

5.2.2. Process Evaluation

Mass and energy balance

Mass and energy balances obtained from ASPEN Plus[®] simulations are used to compute key performance indicators (KPI's). Important KPI's are sugars conversion and furfural selectivity in the reactor section, feedstock inflow required to meet target production (i.e., an indicator of the total mass-yield achieved by the process) as well as total energy demand. The estimation of energy requirements includes three major contributors: 1) heating duty based on steam consumption to heat up reactor inlet streams and reboilers in distillation columns; 2) cooling energy at the reactor outlets, storage tanks and distillation column condensers using water; and 3) electricity requirements, which are calculated based on the power demand of the pumps.

Techno-economic evaluation (TEE) & economic viability analysis

A preliminary techno-economic evaluation (TEE) is performed in order to get insight on the relative profitability of the processes with different extraction media and feedstock types. This TEE includes CAPEX and OPEX calculations, according to the general assumptions summarized in Table 5.6. The purchased equipment cost is estimated using ASPEN Process Economics Analyzer[®]. In this cost estimation, Netherlands is selected as plant location. For comparison purposes, the main indicator to assess the profitability of the process is the furfural minimum selling price (MSP). The main assumptions of the economic viability analysis are the payback time (depreciation time) at 20 years, the furfural production rate (Table 5.1.), taxation (35%), annual depreciation [281] and the calculated IRR that should exceed the discount rate (8%) in order to have a profitable case.

Table 5.6. Parameters for Techno-Economic Evaluation [281]

Parameter	Calculation
Fixed Capital Investment (FCI)	Direct +indirect costs
Direct Cost	Equipment installation, insulation, paint, building, service facilities, land adjustments
Indirect Cost	Construction expenses, contractor fee, contingency
Working Capital (WC)	15% TCI
Start-up Costs (SU)	20% TCI
Total Capital investment (TCI)	FCI + WC
Manufacturing Costs	Direct production costs + Fixed charges
Direct Production costs	Raw materials + chemicals + utilities+ operating labour + maintenance +laboratory + patenting
Maintenance	2% FCI
Laboratory	10% Operating labour
Fixed costs	Depreciation, taxes, insurance, rent
Plant Overhead	60% Operating labour

In Table 5.7., the costs of main materials and energy costs are presented. The price of feedstock A as pure compound is presented, but the price of the remaining hemicellulosic feedstocks is not considered. In this, it is assumed that the present process is developed within an existing biorefinery, and the feedstock stream is available as is.

Table 5.7: Prices and costs of raw materials, solvents and utilities

Item	Cost	Reference
Xylose	5 €/kg	[282]
Sulfuric acid	0.3 €/kg	[282]
2-sec-butylphenol	45 €/t	[145,283]
MIBK	2 €/kg	[282]
Low pressure steam	10 €/ton	<i>Assumption</i>
Medium pressure steam	20 €/ton	<i>Assumption</i>
High pressure steam	40 €/ton	[145]
Cooling water	0.25 €/ton	[145]
Electricity	96.6 €/MWh	[255]

Energy integration

Overall, the process operates at elevated temperatures indicated by the kinetics of sugars dehydration. Thus, increased utilities requirements are anticipated for both cooling and

heating, providing opportunities for energy integration. In this section, an investigation of heat integration potential is performed at a conceptual level for the most promising feedstock types. Then, the economic viability of the optimized design is estimated.

Environmental considerations

A high-level assessment of the environmental impact of the process is addressed in the study by evaluating the following main categories: CO₂ emissions associated with the production process (i.e., including direct emissions during process and indirect by generation of utilities, but excluding post-generation steps such as transportation and usage), waste generation during the process, and particularly that of water hazardous substances. In addition, all process concepts discussed in this work are equally committed to the concept of circular economy, so this criteria, although highly relevant, is not considered as a distinguishing factor among process scenarios.

5.3. Results and discussion

5.3.1. Case study 1: Solvent selection

Two solvents (i.e., MIBK and 2-sec-butylphenol) are investigated for the in-situ extraction of furfural. Figures 5.1a illustrates the dependency of furfural partition coefficient between the organic solvents and water (i.e., m defined as $m = C_{\text{furf}}^{\text{org}} / C_{\text{furf}}^{\text{inorg}} [(M_{\text{furf}}^{\text{org}}) / (M_{\text{furf}}^{\text{inorg}})]$) as a function of temperature and furfural concentration. Figures 5.1b shows the same data, but this time represented as furfural concentration in the organic phase vs. that in the water phase at equilibrium. In general, greater temperatures favor the solubility of furfural in water (Figure 5.1b). Therefore, for both solvents, it is observed that furfural partition coefficient decreases (i.e., lesser affinity to the organic phase and more to water) as temperature increases. Whereas the total concentration of furfural in the system has limited impact on furfural partitioning between MIBK and water, that is not the case for 2-sec-butylphenol. With that solvent and at lower temperature (20°C), increasing concentrations of furfural to the system tend to partition preferentially towards 2-sec-butylphenol (i.e., increasing m). On the contrary, m at 200°C slightly decreases with increasing furfural concentration. These values of furfural partition coefficient in 2-sec-butylphenol (as depicted in Figures 5.1.) are comparable to the values measured at high temperatures, as reported in literature [145]. Appendix D.1. contains the ternary plots of both organic solvents at low and high temperature.

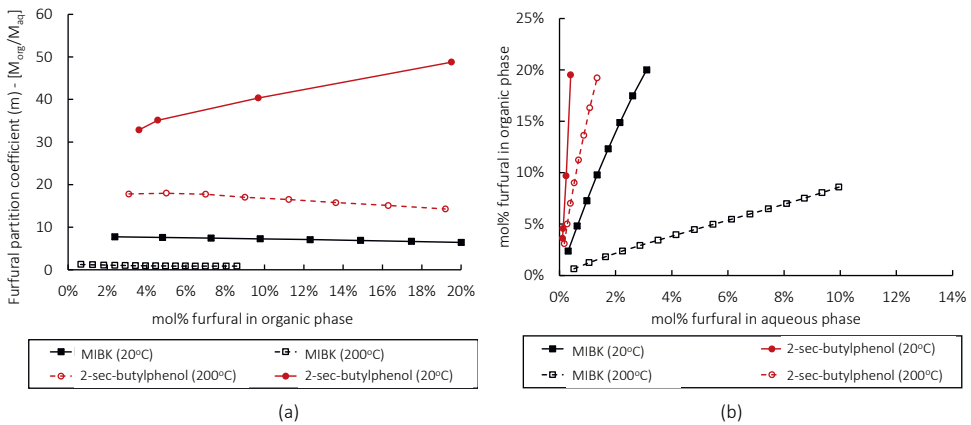


Figure 5.1. Furfural molar composition in aqueous phase against furfural molar composition in organic phase for MIBK and 2-sec-butylphenol at 20°C and 200°C (a) and furfural partition coefficient $[m]$ with furfural molar composition in organic phase for MIBK and 2-sec-butylphenol at 20°C and 200°C (b)

Table 5.8. presents the performance of the two processes based on these two solvents. The ASPEN Plus® model flowcharts are available in Appendix D.3. While both processes achieve almost complete xylose conversion, furfural selectivity is remarkably higher in the case of 2-sec-butylphenol under the same reaction conditions. Both processes operate at the same reaction temperature (thus operate under the same kinetic conditions), but 2-sec-butylphenol leads to a higher furfural yield than MIBK (i.e., 86 vs. 78%, respectively) due to the higher partition coefficient and the improved efficiency of in-situ extraction, as explained earlier (Chapters 2 and 3). With respect to the downstream separation section, the two cases under consideration present two distinct scenarios due to the differences in boiling points of the two solvents (i.e., 116°C and 227°C for MIBK and 2-sec-butylphenol, respectively) with respect to that of furfural (i.e., 162°C) and water (i.e., 100°C), and due to their relative miscibility with the furfural/water mixtures. First, the MIBK rich phase exits the decanter with most of the furfural and some water. As a low boiling solvent, MIBK is recovered from the top of the so-called “solvent recovery column”, still containing a considerable amount of furfural that needs a subsequent furfural purification step. Then, the remaining furfural and water that is collected from the bottom of the solvent recovery column is mixed with the aqueous furfural stream exiting the reactor, which also contains some MIBK. This ternary (i.e., furfural, water, MIBK) mixture requires again two consecutive separation steps to recover the three fractions of interest: furfural as the desired product, as well as the MIBK and the aqueous streams that are recycled back to the reactor. Note that the binary mixtures of MIBK-water, and furfural-water form azeotropes at 65°C (0.5 bar) and 78°C (0.5 bar), respectively. In total, the MIBK case requires three distillation columns to achieve a

satisfactory separation. The case of 2-sec-butylphenol, a higher boiling point solvent, allows the full recovery of the solvent in a single distillation column (i.e., the solvent recovery column), while the water/furfural mixture experiences phase separation and is therefore pre-fractionated in a decanter into a furfural rich phase, and a furfural poor phase (Appendix D.1.). The decanter operates under the same conditions as the inlet stream to avoid additional utility input. The furfural rich phase has sufficient grade as final product while the remaining furfural in the dilute phase is recovered in a second distillation column (i.e., the furfural purification column). Thus, for an adequate separation, the 2-sec-butylphenol case results in significantly lower separation requirements (equipment and energy) than the MIBK case. However, while the case of MIBK renders 100% pure furfural as final product, a slightly more dilute product stream (95%) is obtained in the case of 2-sec-butylphenol. Although the difference in purity is not too substantial, producing a more dilute product stream is not desired from an economic point of view (i.e., due to larger equipment and more storage and transportation needs), and it may also affect the product value, as well as the efficiency of the subsequent applications. Yet, this might not be an issue in the case of in-site subsequent reactions (e.g., furfural hydrogenation to cyclopentanone [180,181,260,284]). Alternatively, furfural purity can be further increased by adding furfural-selective membrane to the separation track. Although still under development phase, recent works report successful results during the purification of furfural and HMF from aqueous solutions with low energy consumption using liquid supported membranes [148]. Finally, although both solvents are completely recycled to the reactor inlet, MIBK has a lower purity (88.7% solvent), which may have a negative effect in the reactive extraction process.

Table 5.8. Process performance for 5 kton/year furfural production for feedstock A

Process indicator	MIBK	2-sec-butylphenol
Feedstock per product flows [kton feedstock/kton furfural]	33.4 (2kton xylose/kton furfural)	30.4 (1.84kton xylose/kton furfural)
Reactor residence time	2.6'	2.9'
Xylose conversion	93%	92%
Furfural Selectivity	84%	93%
Furfural purity	100%	95% furfural/5% water
# of distillation columns	3	2
Solvent recovery	100%	100%
Solvent purity	88.7% MIBK, 11.3% water	100%

Energy indicator	MIBK	2-sec-butylphenol
Heating Duty (kW)	77906	22318
Cooling Energy (kW)	68700	15964
Electricity (kW)	270	235

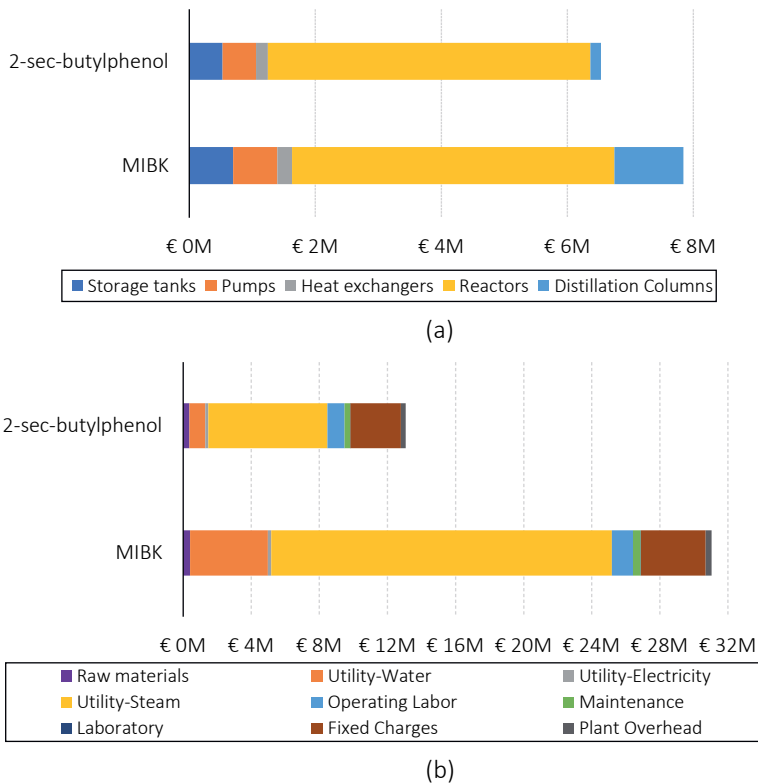


Figure 5.2. CAPEX (a) and OPEX (b) for MIBK and 2-sec-butylphenol for feedstock A

Figures 5.2a. and 5.2b. show the CAPEX and OPEX for the two selected solvents (details on equipment cost, material and utilities, and financial calculations can be found in Appendix D.4). For both solvents, the main contributors to the CAPEX are the reactors and the distillation columns. Thus, mostly attributed to the intensive separation requirements, the MIBK case leads to greater CAPEX. Likewise, the OPEX (Figure 5.2b), is largely determined by the utilities, specifically steam to fulfil heating duties, and it is therefore significantly greater

for the MIBK process than for the 2-sec-butylphenol counterpart. Therefore, as depicted in Figures 5.2a. and 5.2b., it can be concluded that the process with 2-sec-butylphenol is more economically attractive than with MIBK. This is a result of a higher furfural partition coefficient, poor water miscibility, and high boiling point (i.e., significantly higher than that of furfural). Nevertheless, other solvents with similar thermodynamic properties may be more attractive when aspects such as environmentally friendliness and toxicity are considered. In this work, 2-sec-butylphenol is chosen for further evaluation.

5.3.2. Case study 2: Feedstock composition

The effect of different feedstock types (i.e., feedstocks A to D as described in *Process Design, Case Studies* section) on the furfural production process using 2-sec-butylphenol as extraction solvent is assessed according to the KPIs reported in Table 5.9. Note that our study sets the furfural production rate (i.e., 5 kton/year for all cases) as basis for comparison, precisely to accommodate the differences in feed properties. It is shown that feedstocks with lowest sugar concentration (i.e., C, with about 2.5wt% sugar in the fresh feed) require a higher feed inflow than the more concentrated feeds (i.e., A and D) to meet the target annual production of furfural. These C5 sugar concentrations are within the typical range reported in the literature, and in most kinetic models [108,110,112,123,125,222]. It is also within the range of sugars concentration in hydrolysate streams (2-10wt%) [145,211,275].

Despite the differences in sugar concentration, all processes based on feeds with xylose as main C5 sugar (i.e., feeds A and C) achieve furfural selectivities in the range 85-90%. The isolated effect of sugar concentration in the overall process is further evaluated in *Case study 3*. When comparing the process performance of feedstocks A (i.e., pure xylose) and C (i.e., hemicellulosic herbaceous hydrolysate with xylose and other C6 sugar derivatives and organic acids), the latter reaches a slightly lower xylose conversion (i.e., 92 vs. 85%), attributed to the slightly shorter residence time (i.e., 2.9' vs. 2'), and comparable selectivities (i.e., 93 vs. 91%, respectively). It should be noted that feedstock C has already furfural in its composition (as depicted in Scheme 5.3b.) and, thus, less amount of xylose is required when compared with the other feedstocks (5.73 kton/yr for feedstock A vs ca. 9 kton/yr for feedstocks A and D). Thus, it is possible to conclude that the content of C6 sugars and (C6-derived) HMF in feed C does not affect the process performance significantly. However, more significant differences between these two feeds lie on their distinct downstream separation track, and the corresponding energy requirements and final product composition. Unlike in case of feedstock A, the reactor outlet stream in case of feedstock C contains formic acid. Therefore, in case of feedstock C (see process flowchart in Appendix D.3.), the formic acid together with furfural and water leaves from the top of the first distillation column, and is subsequently fed to decanter where formic acid and water are separated from furfural [285].

The ternary plot for this three-component mixture (furfural-water-formic acid) extracted from ASPEN Plus® is provided in Appendix D.2.). Owing to this extra decanting step, the energy requirement of the subsequent distillation column (furfural purification) is reduced when compared to case A. In addition, 100% pure furfural is achieved when using feedstock C, whereas feedstock A lead to 95% furfural. More significant differences are found when comparing feedstocks A and B (i.e., pure xylose and arabinose in water, respectively). Even though they both contain pure compounds, feedstock B reaches only ca. 50% furfural yield, and therefore requires a much greater inlet flow to reach the desired furfural production. This is the result of the different kinetics of the two C5 monomeric sugars (thoroughly discussed in Chapter 3 and 4), as well as the difference in their respective inlet concentrations. As already discussed in Chapters 3 and 4, greater reaction temperatures would be required to maximize the arabinose-to-furfural yield. A further optimization of the process design for feedstock B at 200°C was examined by increasing the reactor volume (and, hence, the residence time) in order to increase furfural yield. It was observed that the effect of PFR by having 5 CSTRs in series was decreased leading to lower selectivity than predicted from the kinetic models developed in Chapter 3. One approach to maintain the plug flow behaviour in this process with feedstock B is to increase the number of CSTRs and each CSTR will have smaller volume. However, this approach will lead to significantly increased CAPEX due to increased number of reactors affecting the financial viability of the process.

Table 5.9. Process performance for 5 kton/year furfural production using 2-sec-butylphenol

KPI	Feedstock A	Feedstock B	Feedstock C	Feedstock D
Feedstock per product flows [kton feedstock/kton furfural]	30.4	46.8	47.6	23.2
C5 Sugar per product flows [kton C5 sugar/kton furfural]	1.84 (Xylose)	4.22 (Arabinose)	1.15 (Xylose)	1.52 (Xylose) 0.38 (Arabinose)
C5 Sugar concentration [wt%]	6%	9%	2.4%	6.6% (Xylose) 1.67% (Arabinose)
Residence time	2.9'	2'	2'	4'
Xylose Conversion	92%	-	85%	94%
Arabinose Conversion	-	51%	-	82%
Furfural Selectivity	93%	73%	91%	87%
Furfural purity (Furfural/Water)	95%/5%	93%/7%	100%	100%
# Distillation columns	2	2	2	2
Solvent recovery	100%	100%	100%	100%
Solvent purity	100%	100%	100%	99.8% 2-sec-butylphenol, 0.2% HMF
Energy Indicator	Feedstock A	Feedstock B	Feedstock C	Feedstock D
Heating Duty (kW)	22318	33538	37018	17263
Cooling Energy (kW)	15964	26155	24102	11666
Electricity (kW)	235	334	340	185

The presence of C6 sugars (and their derivatives) in the feed is evaluated with feedstocks C and D. Note that this model does not include any cross condensation between furfural and HMF, in line with our previous experimental observations (Chapter 4). Nevertheless, the effect of C6-derived organic acids on pH and thus on furfural yield is indeed accounted for. Likewise, the furfural yield obtained from feedstock D (i.e., 80%) responds to the expectations for the conversion of xylose and arabinose mixtures. As previously discussed, the conversion of arabinose takes longer and leads to lower furfural yield than that of xylose. As depicted in Figure 5.3b., a similar carbon distribution is observed for both furfural and levulinic acid for feeds C and D. Levulinic acid is an excellent precursor for the production of γ -valerolactone and it is also produced from the cellulose valorization route [224,286]. Additionally, it is demonstrated that γ -valerolactone enhances furfural formation from xylose when added in the reaction medium [287,288], although this effect has not been accounted for in the model. It appears that there is an opportunity of integrating the proposed process with the production of γ -valerolactone and further optimize furfural production by adjusting the downstream process accordingly.

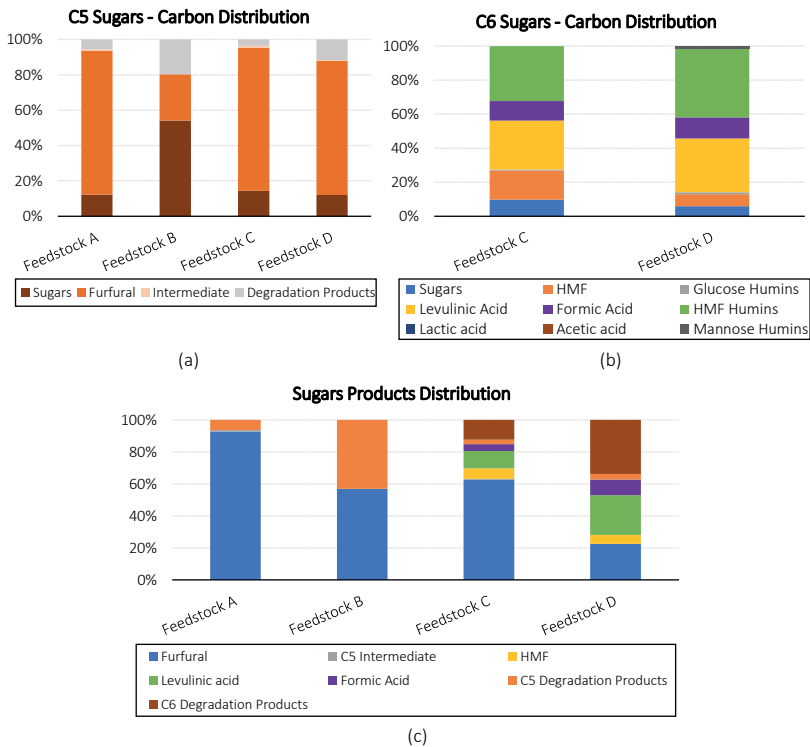


Figure 5.3. Carbon Distribution at the Reactor outlet for C5 Sugars (a) and C6 Sugars (b) after Sugars Dehydration and Sugars dehydration product distribution (c)

The second part of Table 5.9 summarizes the energy requirements for the conversion of each feedstock type. In general, the energy requirements (e.g., in utilities in heat exchangers to warm up organic and inorganic streams) are expectedly proportional to the feed inflows. Therefore, more dilute feedstock C requires more energy than concentrated feeds (e.g., D). Arabinose-rich feeds (e.g., feedstock B) also require overly large inflows to compensate for low yields, so their energy requirements are also significant. Slight deviations from this rationale are found in the cooling duties for feedstock B (cooling duty B > cooling duty C). As presented in the process flow diagrams (Appendix D.3.), four out of five CSTRs require utilities for cooling for feedstocks C and D. These feedstocks are already acidic, so they are fed to the first CSTR at relatively lower temperature when compared to feedstock A (i.e., pure compound). This explains the relatively disproportional cooling demands of these feeds as depicted in Figure 5.4.

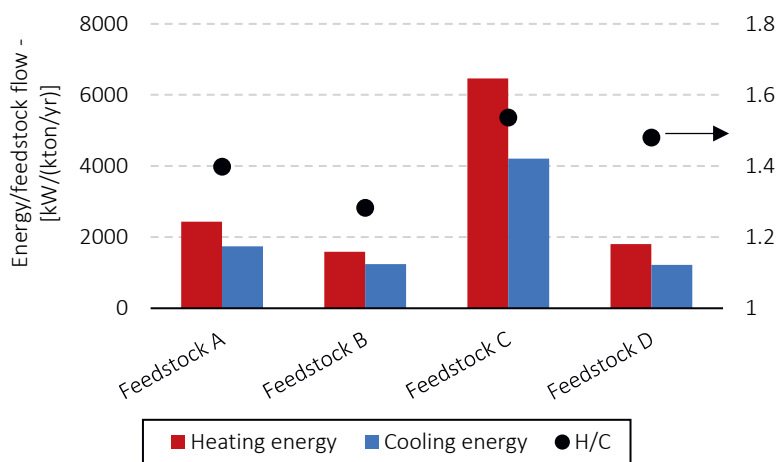


Figure 5.4. Energy requirements per inlet feedstock flow

In conclusion, the process performance of feedstock C is comparable to feedstock A (base case) in terms of xylose conversion and furfural selectivity. Nevertheless, a more dilute product stream is obtained in feedstock A, which might be undesirable for storing, distribution and perhaps applications of final product. On the other hand, the product stream is 100% pure for feedstocks C and D, which widens its market options and makes these processes very attractive.

Finally, an economic evaluation is performed for these processes. Figures 5.5a. and 5.5b. show the CAPEX and the OPEX calculations per feedstock type, respectively. It is obvious that

the CAPEX, largely influenced by the cost of the reactors, does not vary significantly among the feedstock types. This is because the reactor technology and size were the same for all cases (note that variations in residence time were met by adjusting flow rates). Among all cases, a slightly higher CAPEX is calculated for feedstock C (a highly dilute feed), due to increased volumetric flows and resulting in bigger equipment (e.g., tanks, heat exchangers).

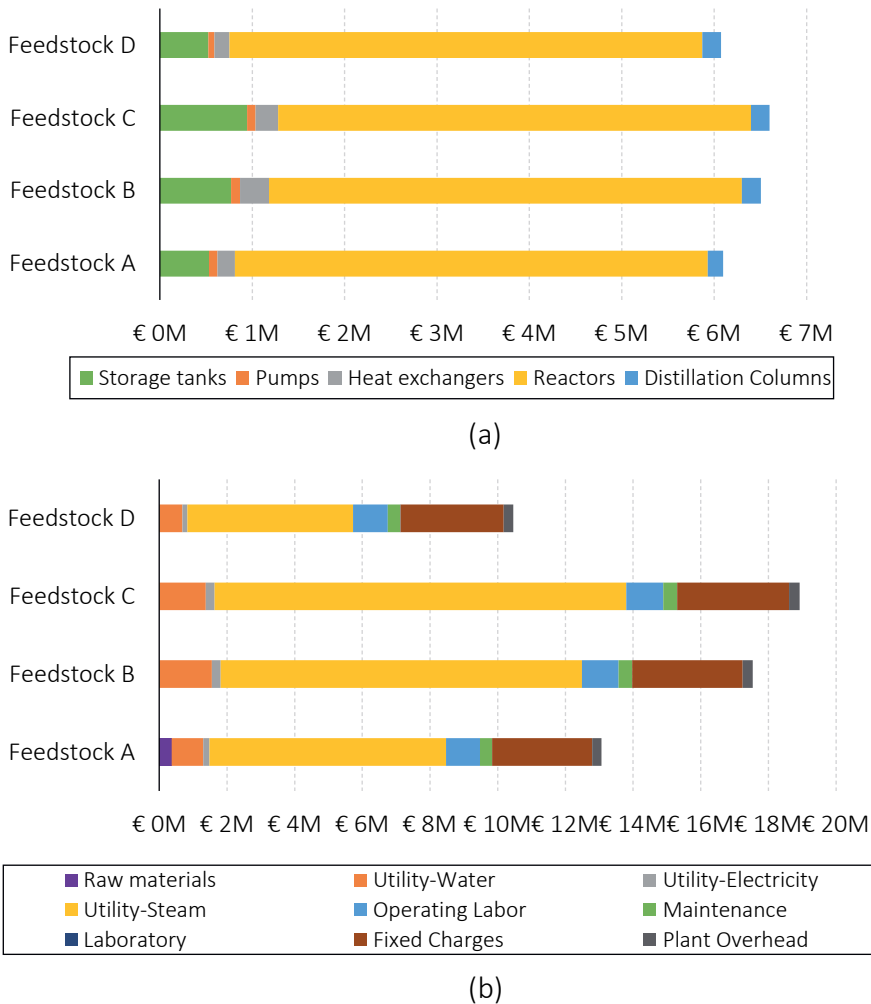


Figure 5.5. CAPEX (a) and OPEX (b) calculations for various feedstock types

Regarding the operating expenses, largely determined by the steam consumption, feedstocks B and C have the greatest OPEX due to the low initial sugar concentration or poor

yields (i.e., greater flow rates to reach target production). Another important contributor to the OPEX is the feedstock price (Appendix D.5.). Here, pure xylose (i.e., feedstock A) is likely not a realistic feedstock and it is also more expensive when compared to hydrolysate streams in similar concentration ranges (i.e., feedstock D). Thus, the lowest operational expenses are found for feed D, which is hereby considered the most attractive type of hemicellulosic feedstock for biphasic furfural production.

The financial viability of the process is estimated using the furfural MSP as assessment criterion. Here the furfural market price is estimated at 1-2 €/kg depending on the vendor, the quantity and production process [145,282,289,290], and it is used as a comparison indicator to assess the financial viability of the process. Hence, the uncertainty due to large market price variation is not included in the calculation. Figure 5.6. shows that, for all processes considered, furfural MSP is higher than the current furfural market price. The main contributor to the MSP is the large use of steam for the pre-heating of reactor inlet streams as described above. Thus, it is important to assess alternatives to reduce the energy consumption to further improve the financial viability of the process (see following sections). Note that no heat integration has been applied so far to any of these process concepts, so the comparison of the MSP with the furfural market price (determined by an industrially optimized process) is not entirely fair. Nevertheless, this analysis already points at feedstock D as a very attractive feedstock for this process.

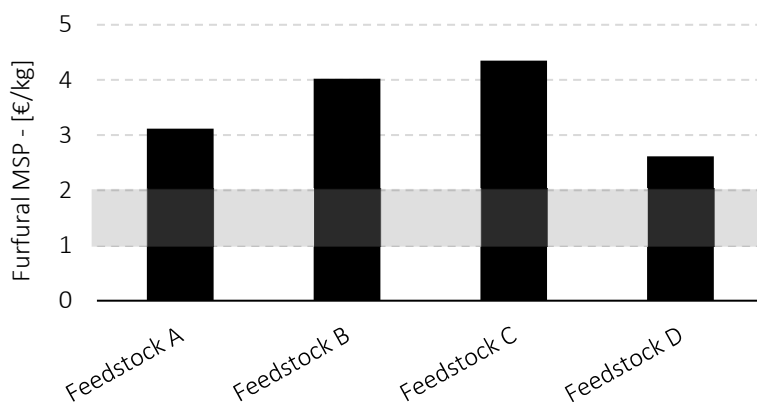


Figure 5.6. Furfural MSP for feedstocks of Case study 2

5.3.3. Case study 3: Feedstock concentration

Based on the conclusions of previous section, the heating requirements and the reactor costs are the main contributors to the process economics. Thus, an important parameters to

assess is the sugar concentration in the feedstock, which in turn affects volumetric flow rates of the process. Therefore, this case study compares the performance of a new set of processes at various sugar concentrations. To that end, this new case study is based on feedstock A (i.e., pure xylose, chosen as reference), and the two worst performing feedstocks B (i.e., highly concentrated arabinose waste stream that was originally diluted to meet the typical concentrations of a hydrolysate stream), and feedstock C (i.e., a hydrolysate stream, which previously led to the highest furfural selectivity and yet performed poorly due to its very high dilution). Furfural production is still set at 5 kton/yr (like in previous cases), and furfural selectivity is also maintained comparable to the corresponding base case. The process flowcharts of this study are shown in Appendix D.6. For feedstocks A and C, the study considers an increase of initial xylose concentration up to 6wt%, under the assumption that the prior biomass pre-treatment step can provide such a stream, likely by decreasing the washing cycles or evaporation. The calculations for the additional steam demands in the case of evaporation are presented in Appendix D.7. The impact on OPEX and furfural MSP are very small (i.e., increase by 0.1% and 0.2% respectively), so the analysis below is considered representative. As for feedstock B, the previously considered pre-feed dilution step (as described in section *Case study 2: Feedstock composition*) is no longer applicable, and therefore the feed is directly fed to the reactor. Upon mixing with the catalyst solution, the stream is diluted to 20wt% arabinose concentration.

Figures 5.7. show the impact of increasing the C5 sugar concentration for all examined feedstock types on the reactor volume while keeping furfural yields nearly constant. According to the model predictions and the reaction kinetics considered in this work, it is possible to reduce the reactor volume by increasing the C5 sugar concentration, with almost no sacrifice in furfural yields, as expected from the kinetics (Figure 5.7.). At the same time, this increase in concentrations also results in a significant reduction of energy requirements (Table 5.10.), as well as other equipment costs.

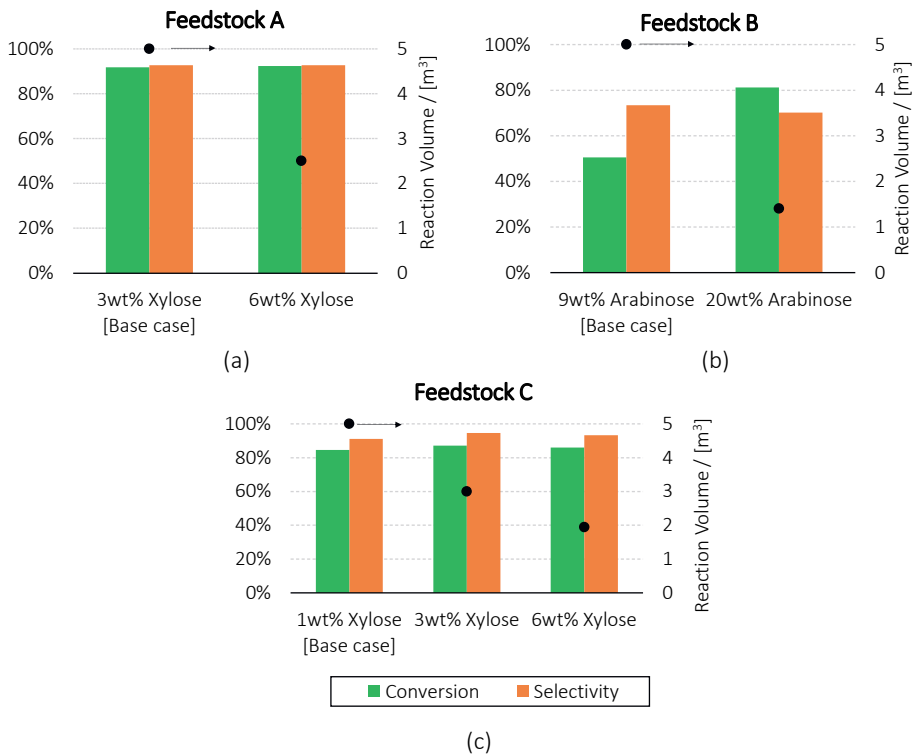


Figure 5.7. Comparison of process performance of concentrated feedstocks A (a), feedstock B (b) and feedstock C (c)

Table 5.10. Energy Requirements of processes in Case study 3

Energy indicator (kW)	Feedstock A 6wt% Xylose	Feedstock B 20wt%arabinose	Feedstock C 3wt% Xylose	Feedstock C 6wt% Xylose
Heating demands	10748	4853	18851	10725
Cooling demands	8356	4481	12824	7591
Electricity	136	75	197	125

Figures 5.8. shows the impact of increasing sugar concentrations on the calculated CAPEX and OPEX for all the feeds studied. It is evident in all cases that the reduction of water content in the feedstock significantly improves process economics by reducing both CAPEX (through reactor volume reduction) and OPEX (via decreasing heating demands of the inlet feedstock

flows). For feedstock A, doubling the xylose concentration from 3 to 6wt% leads to a 14% CAPEX reduction, and a major 36% saving in OPEX. Similarly, concentrating feedstock C from 1 to 3wt%, leads to 15% and ca.40% savings in CAPEX and OPEX, respectively. Further feed concentration to 6wt%, leads to a total CAPEX and OPEX reduction of 47% and ca.70%, respectively. As for feedstock B, the increase of 55% in initial arabinose concentration results in 50% reduction in CAPEX and almost 74% in OPEX.

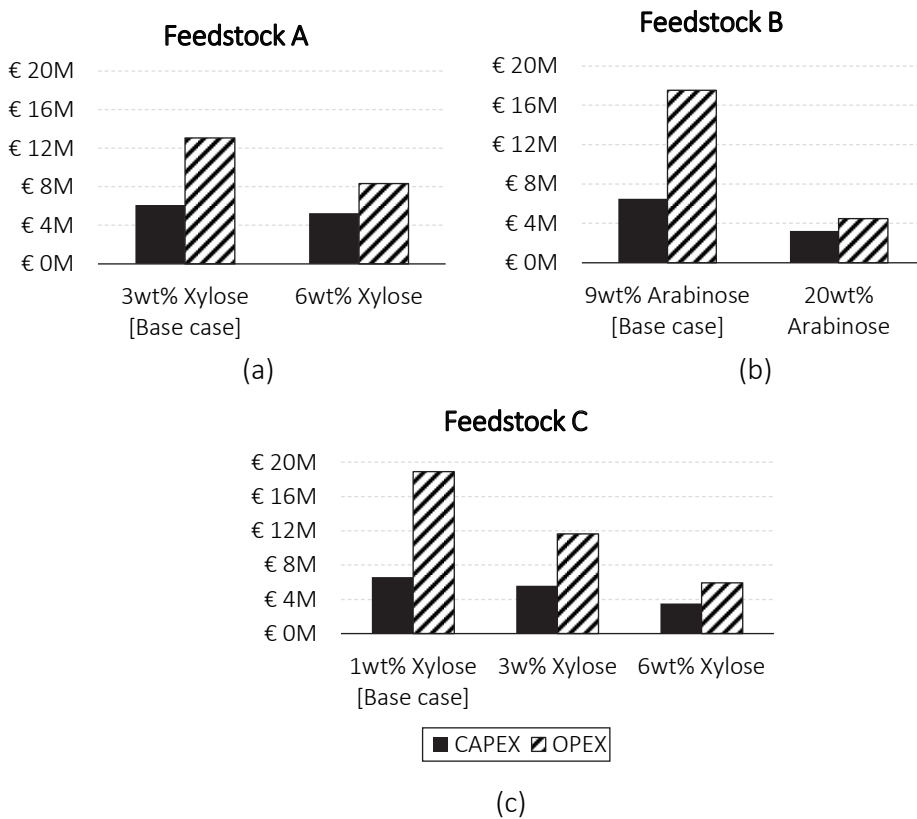


Figure 5.8. CAPEX and OPEX for concentrated feedstocks A (a), feedstock B (b) and feedstock C (c)

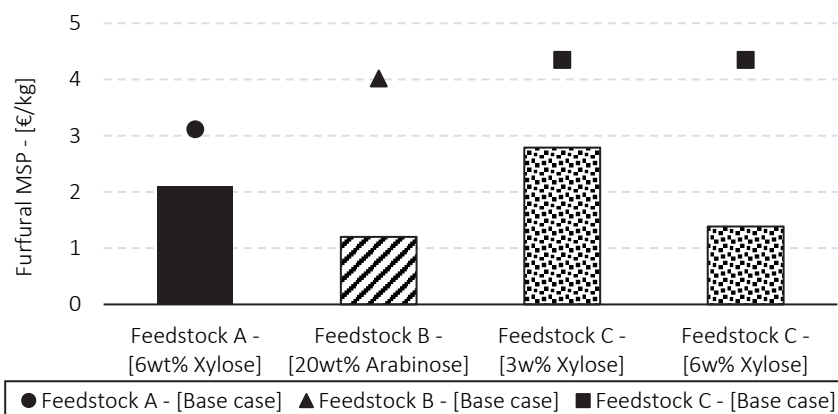


Figure 5.9. Furfural MSP with varying C5 sugar concentration in the feedstock

Finally, the savings in CAPEX (i.e., reduction the reaction volume and other equipment sizes) and in OPEX (reduction of the utilities) are reflected in the final furfural MSP (Figure 5.9.). The most promising feedstock in terms of MSP is feedstock B (lowest furfural MSP). However, this conclusion has a higher degree of uncertainty because of the lack of experimental data at high arabinose concentrations ($C_{ar}^0 > 10\text{wt}\%$). When comparing feedstocks A (i.e., pure xylose) and C (i.e., biomass hydrolysate), both at 6wt% initial xylose concentration, it appears that furfural MSP is within the range of the current market price for feedstock C (6wt%xylose) but not yet for feedstock A - $C_{xy}^0 = 6\text{wt}\%$. This is to a large extent due to the more expensive feedstock, and the slightly larger reactor volumes required for feed A compared to feedstock C in order to obtain the same process performance with the respective base cases (Case study 2). This, it is concluded that feedstock C with 6wt% initial xylose concentration is very good candidate in terms of process feasibility and financial viability.

5.3.4. Heat integration opportunities

Another key aspect to reduce the process utility requirements (and hence, OPEX) is the heat integration of the process. It has been already identified in the section *Case study 2: Feedstock composition* that more dilute systems result in large energy demands. It should be noted that the opportunities of energy savings in this work are based on the energy available in the process streams without altering process operating conditions. Among all utilities, medium pressure (MP) and high pressure (HP) steam consumption is the main contributor to the operating costs, and it ultimately defines furfural MSP. Hence, the possibilities for heat integration are investigated for feedstocks A, C and D in this section. These three feedstock types have shown the highest potential in terms of process performance and economics.

Several heat integration projects are defined for each case and summarized in Appendix D.8. along with the utility requirements after the implementation.

As summarized in Table 5.11, two main heat integration strategies are introduced for the three feedstocks. Firstly, the total demand of fresh MP steam originally intended to pre-heat the organic solvent can be decreased by passing a fraction of the organic solvent stream through the condensers of the two distillation columns. The exact fraction of organic solvent that can be used for this purpose depends on the requirements of the distillation columns. Further temperature increase to reaction temperature (200°C) is performed by using HP fresh steam in the existing heat exchangers. This strategy reduces simultaneously the overall cooling demands, which would otherwise be needed in the condensers of the distillation columns. The second strategy summarized in Table 5.10. contemplates the use of the heat released during MP steam condensation to pre-heat the feed stream up to ca. 90°C. Then, an additional heat exchanger is added to warm up the feedstock until the target temperature with MP steam. This strategy represents a reduction of the MP steam and cooling water consumption, but also the addition of an extra heat exchanger. A detailed description of the heat integration opportunities is presented in Appendix D.10. In general, the heat integration projects lead to a significant decrease in OPEX (ca. 20-25% for all feedstocks), and a small increase in CAPEX by the addition of new heat exchangers (Appendix D.11.). However, the impact of the latter is insignificant, leading to a net improvement process economics.

Table 5.11. Concepts for heat integration for the cases of feedstocks A, C and D

#	Energy Source	Energy Sink	Conclusion
1	Cooling top streams exiting distillation columns	Heating solvent inlet stream	Savings in cooling water and MP steam from pre-heated solvent inlet stream at the condensers of distillation columns
2	Condensation of MP steam from (1) reboiler of first distillation column, and (2) pre-heating of catalyst stream	Heating fresh feedstock	Savings in MP steam used for feedstock pre-heating and addition of new heat exchanger installation

Finally, Figure 5.10. shows the impact of implementing the integration projects on the final furfural MSP for all process scenarios. An average 8.8% reduction in furfural MSP is achieved

for all cases, with greater improvements for the processes with more dilute feeds (i.e., largest process and utilities streams). Even though the heat integration of the process shows potential of improving process economics, the impact of C5 sugar in the feedstock seems to have higher impact furfural MSP as shown in Figure 5.9. Additional heat integration opportunities could become available if the synthesis of furfural would be combined with other biorefinery processes (e.g., biomass fractionation and/or downstream furfural valorization) in the same site (i.e., in proximity to several process streams). Besides, this level of integration would minimize cooling and re-heating of intermediates (e.g., hydrolysates), which is an energy consuming practice but nevertheless required if such streams need to be efficiently stored, transported, and eventually converted at a different location. Finally, selling leftover HP steam condensate to a power generation facility may also improve process economics.

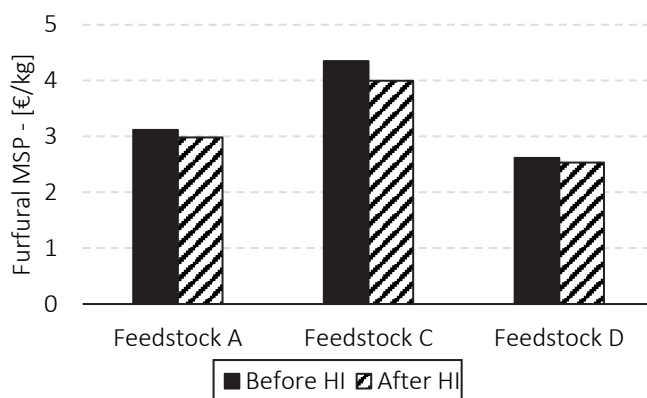


Figure 5.10. Furfural MSP before and after heat integration for feedstocks A, C and D

5.3.5. Environmental considerations

This section discusses main environmental aspects of the proposed designs. All designs discussed in this chapter meet the main principles of circular economy, because all examined feedstocks are side or waste streams of existing industrial processes, providing an additional valorization route in these industries. Then, the carbon footprint of the process is assessed by comparing CO₂ emissions. There are no direct CO₂ emissions from the process, but CO₂ emissions are allocated to steam generation. These emissions are calculated from ASPEN Plus® Software based on EU-2007/589/EC, assuming natural gas as fuel for steam generation.

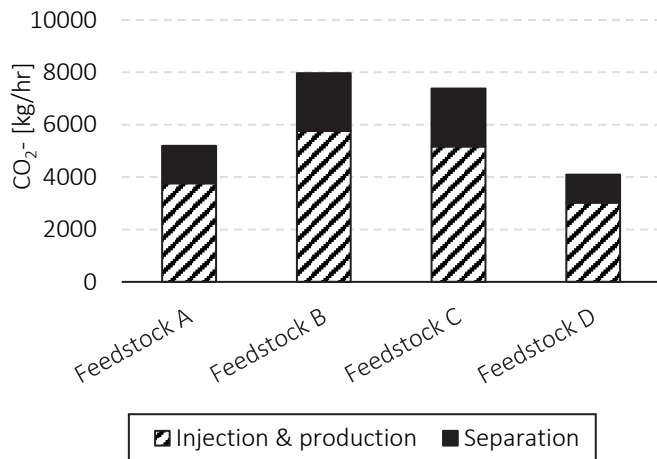


Figure 5.11. Carbon footprint of biphasic furfural production for Case study 2

As depicted in Figure 5.11., the majority of the emissions are detected in the Injection & Production Section due to the heating requirements of inlet streams and reactors in some cases (feedstocks C, D). Feedstock D has the lowest emissions, following its lowest heating requirements. In Table 5.12., the impact reduction of steam usage on carbon footprint is presented for *Case study 3*. It is remarkable that the reduction of steam usage decreases furfural MSP (as explained in *Case study 3: Feedstock Concentration*), but also significantly improves the carbon footprint of the process, reaching a reduction up to 71-86%. To further comply with sustainability principles, it would be preferred that the fuel source for steam generation was CO₂ neutral (e.g., green H₂ or biogenic gas), so potential CO₂ tax credit could further improve the process economics.

Table 5.12. Carbon Footprint of biphasic furfural production for Case study 3

Feedstock	Injection & Production [kg/hr]	Separation [kg/hr]	Total CO ₂ Reduction [%]*
Feedstock A [6wt% xylose]	1841	713	51%
Feedstock B [20wt% arabinose]	794	359	86%
Feedstock C [3wt% xylose]	2645	1142	49%
Feedstock C [6wt% xylose]	1486	666	71%

* Comparison against the CO₂ emissions from feedstocks base cases as depicted in Figure 5.10.

Regarding the waste generation, it is considered that most of the chemicals are recycled and reused, without creating considerable amounts of liquid wastewater streams during the normal operation. The use of highly corrosive catalyst requires careful operation, very frequent maintenance of the equipment and cleaning. The equipment with direct contact with the catalyst should be checked frequently to avoid leakages and water contamination.

5.4. Conclusions

The biphasic continuous process of furfural synthesis using stirred tank reactors is proposed as an alternative approach for furfural production. First, two organic water-immiscible solvents (i.e., MIBK and 2-sec-butylphenol) are examined as candidates to perform furfural in-situ extraction in the biphasic reactive system. The simulation results show that 2-sec-butylphenol is a more suitable solvent when compared against MIBK, with a higher boiling point that results in a less capital intensive and energy demanding downstream purification process (i.e., lower CAPEX and OPEX). Next, the study is extended with an evaluation of various hemicellulosic feedstocks as potential raw materials for furfural production using 2-sec-butylphenol. The processes based on highly dilute (<3wt%) xylose feeds (i.e., the reference case with pure xylose and the hemicellulosic herbaceous hydrolysate, hereby referred as feedstocks A and C, respectively), produce furfural with high selectivity (>91%). In addition, the impact of C6 sugars (derivatives) and other impurities present in the herbaceous hydrolysate stream did not seem to affect negatively the overall process performance when compared to the reference case, at least in the concentration level considered in this study. Even more, the presence of formic acid in the reactor outlet seemed to facilitate the production of 100% pure furfural streams. Next, the study considered a hemicellulosic softwood hydrolysate (i.e., hereby feedstock D), containing xylose as main C5 sugar but in greater concentrations than the herbaceous counterpart. Mostly attributed to the greater concentrations, this feedstock was deemed the most attractive based on furfural MSP. On the other hand, the process design based on pure arabinose from an industrial waste stream (i.e., here referred as feedstock B) was the least attractive due to the fact that arabinose kinetics dictate optimum performance at greater temperatures than those considered in this work. Following the initial feedstock evaluation, the sugar concentration is identified as a key parameter that determines economic viability. Thus, the work continues with an insight on the effect of feedstock concentration on process performance, using as basis the least attractive feedstocks (i.e., herbaceous hydrolysate and arabinose-rich industrial waste stream) as well as the reference case (i.e., pure xylose). The results predict great savings potential, both in CAPEX (e.g., 55% reduction by decreasing up to 70% the size of reactor and other process equipment) and OPEX (e.g., 70% reduction by decreasing utilities and energy requirements) upon increasing sugar concentration (e.g., from 9 to 20% in the arabinose-rich stream, or from 1 to 6 wt% in the herbaceous hydrolysate). Therefore,

the furfural MSP can be decreased close to the market price. From all the above, both herbaceous and softwood hydrolysates with sufficient (6 wt%) xylose concentration are deemed attractive feeds for this process. Therefore, these two feeds, along with the reference (pure xylose) case are further considered for the energy integration study. This final study identifies the main opportunities for savings in utilities, leading to greater cost reductions (i.e., up to 9% reduction of furfural MSP) as well as carbon footprint reduction (i.e., avoiding the CO₂ emissions by 75%).

CHAPTER 6

Conclusions & Outlook

6.1. Conclusions

The valorization of lignocellulosic biomass is of high importance considering the increasing need of alternative resources for the production of chemicals and fuels. Among the wide range of possible valorization routes of lignocellulose, the synthesis of furfural, an important platform chemical, provides many opportunities for the production of biobased chemicals and polymers. However, the synthesis of furfural suffers from selectivity loss due to undesired parallel degradation reactions that lead to humins formation, making the transition to continuous process challenging. The recently discovered biphasic furfural production process holds the promise to abate furfural degradation by coupling the synthesis of furfural with its in-situ rapid removal from the reaction medium. Although the recent reports on the biphasic synthesis of furfural show promising results, the available literature also reveals a limited fundamental understanding on its operating principles and its optimization potential. This thesis focuses on this novel process concept and its prospects to enable the transition towards continuous production. To that end, the work combines experiments and modelling tools to elucidate on the role of the reactor technology on balancing the interplay between reaction kinetics and mass transfer in this process. Further, the study dives into the effects of feedstocks from the perspective of reaction kinetics, reactor performance and process design. The main conclusions from this work are summarized below.

Biphasic synthesis of furfural in a continuous reactor

First, we conclude in Chapter 2 that furfural can be successfully produced in a biphasic continuous reactor using dilute H_2SO_4 as catalyst and toluene as extraction medium. The current work uses a millireactor operated under the Taylor flow regime in order to achieve optimum control of experimental conditions (e.g., residence times, temperature, and mass transfer properties) with minimal use of chemicals, which was key to gain a thorough understanding on the influence of process parameters on final performance. The work concluded that the enhanced mass transfer properties of this reactor configuration were instrumental to achieve high furfural selectivity (ca. 70%) at nearly full xylose conversion and short residence time. Even more important, these conditions were also important to achieve negligible (<2% at 190°C) formation of humins, which is key to guarantee stable continuous operation. Thus, although the millireactor was chosen as an ideal lab-scale reactor for research purposes, it also served as example of intensified reactor technology, identified as key to the success of this process concept. An in-depth assessment of mass transfer performance of furfural in-situ extraction demonstrated that the mass transfer coefficient of the biphasic reactor and the solvent of choice (specifically the furfural partition coefficient in the solvent/water system) are the main parameters affecting furfural yield.

Kinetic modelling of C5 sugars dehydration to furfural

The kinetic study on the sulfuric acid-catalysed dehydration of xylose to furfural presented in Chapter 3 supports the participation of reaction intermediates during furfural degradation reactions. Unlike for xylose, the reaction of arabinose dehydration to furfural can be model accurately as a one-step dehydration with a parallel arabinose degradation scheme. For both C5 sugars, the kinetic models (and the set of fitted parameters) described the experimental trends adequately. Thus, the developed kinetic models can be used for process and reactor optimization purposes. The assessment of reaction conditions for the biphasic synthesis of furfural using the developed kinetic models showed that high reaction temperatures (ca. 200°C-220°C) and short residence time (ca. 7-8 min) render the highest furfural yield (70-80%) for a C5-rich hemicellulosic feedstock.

Effects of feedstock type and composition

Chapter 4 concludes that the feedstock composition affects furfural yield when using dilute H₂SO₄ as catalyst and toluene as extraction medium. The experimental study using model feeds demonstrated that increasing initial xylose concentration does not affect the rate of sugar conversion, but it has a negative impact on the final furfural selectivity for more concentrated feeds (>6wt% xylose). Arabinose is less reactive than xylose upon dehydration under the same reaction conditions, thus requiring greater reaction temperatures to achieve significant yields. Moreover, the experiments with glucose and/or fructose in the xylose feed (as a simulated mixture of hemicellulosic hydrolysates) suggest that there is no significant interaction among the C5 and C6 dehydration routes, encouraging the prospects of using of hemicellulosic hydrolysates for the continuous synthesis of furfural using biphasic medium. Nevertheless, more severe humins formation occurs when HMF is present (or formed from C6 sugars, and more selectively from fructose) in the stream, jeopardizing the stability of the continuous operation. When feeding real feedstocks (i.e., a wheat straw hydrolysate and an arabinose-rich food side stream) to the furfural synthesis process, the experimental trends are well predicted by the previously developed kinetic model using model feeds. This supports the validity of the kinetic model and also demonstrate the lack of significant interactions of the stream impurities in the main C5 dehydration pathway.

Process design considerations

The techno-economic evaluation of the continuous biphasic furfural production presented in Chapter 5 concluded that, for this application, 2-sec-butylphenol is a better solvent than MIBK in terms of furfural selectivity and process economics. This is partly because the furfural partition coefficient in 2-sec-butylphenol is remarkably higher compared to MIBK, although it decreases significantly with temperature in both cases. The higher boiling point of 2-sec-butylphenol also leads to lower energy demands. The economic evaluation of the various

feedstocks concluded that the cost of the reactors and the use of steam for heat supply are the main contributors to the CAPEX and OPEX, respectively, resulting in furfural minimum selling price (MSP) higher than the market price. Thus, more concentrated feedstock streams are preferred, since they require smaller reactor volume and have lower energy demands. Finally, greater cost reductions can be obtained after heat integration.

6.2. Recommendations

The current work has yielded important views regarding the biphasic production of furfural in continuous systems. Further considerations are likely to enhance and further optimize the proposed process. The suggested recommendations, which would serve as areas of further research, are presented below.

Category 1 - Process of biphasic furfural production in the millireactor

In this research work, two water-immiscible organic solvents (i.e., MIBK and toluene) were tested in the millireactor for the biphasic furfural synthesis for a mixture of C5/C6 sugars. Our process simulations show that 2-sec-butylphenol is a good alternative for in-situ furfural extraction. Future experimental work in this direction is recommended to validate that assumption, as well as to evaluate possible side effects that were not accounted for in our model (e.g., effects on the reaction kinetics). Furthermore, in Chapter 3, we explored the mechanisms and the kinetics of xylose and arabinose dehydration in a temperature range up to 190°C. According to the predictions of the developed kinetic models, even higher reaction temperatures (>190°C) favour the selective furfural formation and offer an interesting window for process intensification when such high temperatures are coupled with very fast in situ extraction (e.g., in a biphasic millireactor) in a very short residence time. However, the investigation of the reaction kinetics beyond 190°C is necessary to validate these predictions. Moreover, Chapter 4 showed that the increase of xylose concentration above 6wt% has a negative impact on furfural yield which was not accurately captured by the proposed kinetic model. On the other hand, Chapter 5 reveals that, as it is expected, processing greater feed concentrations potentially offers important advantages in terms of energy efficiency and eventually economics. Hence, it is of high relevance to further explore the effect of concentration on the kinetics of sugar dehydration in a wider concentration range. Additionally, both the experimental and process modelling work reveal arabinose may also be an interesting substrate for dehydration into furfural. Nevertheless, our study was rather limited to dilute conditions (i.e., 1wt%), so it is recommended to perform a similar study on the effect of arabinose concentration on furfural selectivity. Finally, the techno-economic evaluation performed in Chapter 5 showed the potential of several hemicellulosic feedstocks as raw materials for the biphasic furfural production such as softwood-based hydrolysates.

In this regards, it is recommended to extend and validate the study with more C5-rich hemicellulosic feedstocks.

Category 2 – Optimization of process design for biphasic furfural production

In the present work, a techno-economic evaluation (TEE) of the continuous biphasic production was performed aiming at identifying suitable hemicellulosic feedstocks for furfural synthesis and their financial potential. While C5-rich side streams from pulp and paper industry also show very good potential for furfural production, their composition strongly depends on the process of pulp production (e.g., Kraft, sulphite pulping or hot water extraction prior to wood cooking) and on the wood type (e.g., hardwood or softwood or mixture), and it can also vary per region. A brief analysis on the proposed process concept based on this feed type is shown in the supporting material, using as a reference non-detailed information of the composition reported in literature. In this respect, an in-depth investigation of the availability and composition of hemicellulosic side streams from pulp and paper industry is strongly recommended. Moreover, two concepts of heat integration within the proposed process design are discussed in Chapter 5. It is recommended to consider the furfural production process within an integrated biorefinery scheme and expand the heat integration study using methodologies like pinch analysis. The integration within the biorefinery will provide more opportunities for energy integration, further improving the feasibility of the process. Finally, the analysis of the TEE showed that more concentrated feedstocks significantly improve process economics by reducing the CAPEX and OPEX. The implementation of a robust kinetic model for a wide range of xylose concentration in this analysis will demonstrate to which extent concentrated feedstocks promote the selective and feasible furfural production.

Category 3 - Sustainability of continuous biphasic furfural production

The sustainability of the biphasic furfural production is briefly discussed in Chapter 5. As discussed in this work, there are no direct CO₂ emissions from the process, but CO₂ emissions are allocated to the utilities usage. A detailed investigation of the opportunities for decreasing the carbon footprint according to EU regulations is recommended in order to enhance the process sustainability, and potentially improve process economics by reducing the imposed taxation. Moreover, even though the water-immiscible organic solvent used for in-situ furfural extraction is fully recycled, it is strongly recommended to investigate “greener” options for furfural extraction in order to improve process sustainability. A promising alternative for furfural extraction is the use of deep eutectic solvents (DES) to extract furfural from the reaction medium. However, there are still several issues around the nature and the performance of DES that need to be addressed to properly assess their applicability in the concept of reactive extraction. Their stability under relevant reaction

conditions (e.g., around 160-190°C and acidic medium) as well as their potential interactions with furfural, water or other reaction intermediates remain relevant topics of research. Finally, the feedstock sustainability is addressed in the present work by studying feedstocks that are side streams of existing industries or biomass pre-treatment processes. To that extent, it is recommended to ensure that suitable feedstocks for furfural production comply with the principles of sustainability including valorization of waste from existing processes, forestry, or other lignocellulosic residues.

Appendices

Appendix A

Appendix A.1.

MATLAB® Model Equations

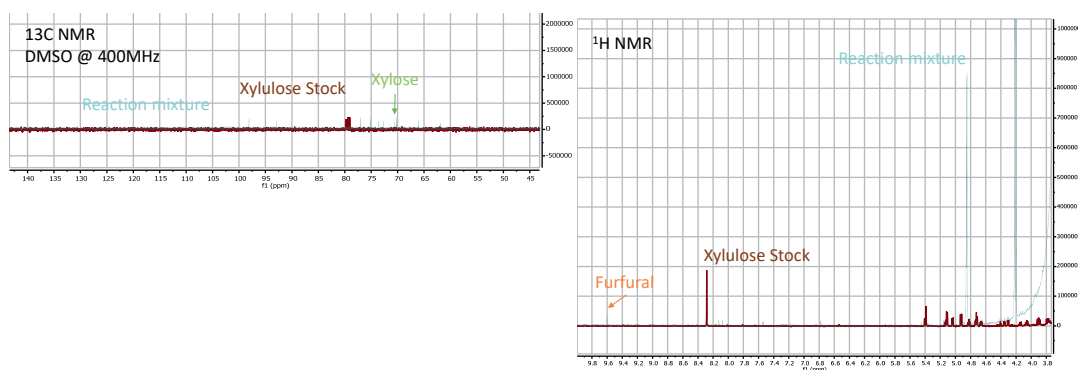
$$\frac{dC_x}{dt} = -k_1 * C_x - k_2 * C_x * C_F^{inorg}$$

$$\frac{dC_F^{inorg}}{dt} = k_1 * C_x - k_2 * C_x * C_F^{inorg} - k_3 * C_F^{inorg} - k_L a * (m * C_F^{inorg} - C_F^{org}) * \frac{1}{\epsilon_{inorg}}$$

$$\frac{dC_F^{org}}{dt} = k_L a * (m * C_F^{inorg} - C_F^{org}) * \frac{1}{\epsilon_{org}}$$

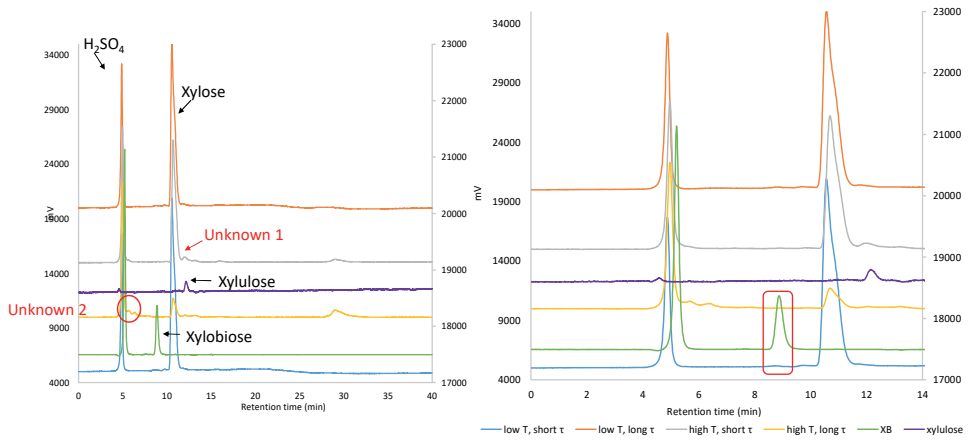
Appendix A.2.

NMR Spectra for Xylulose



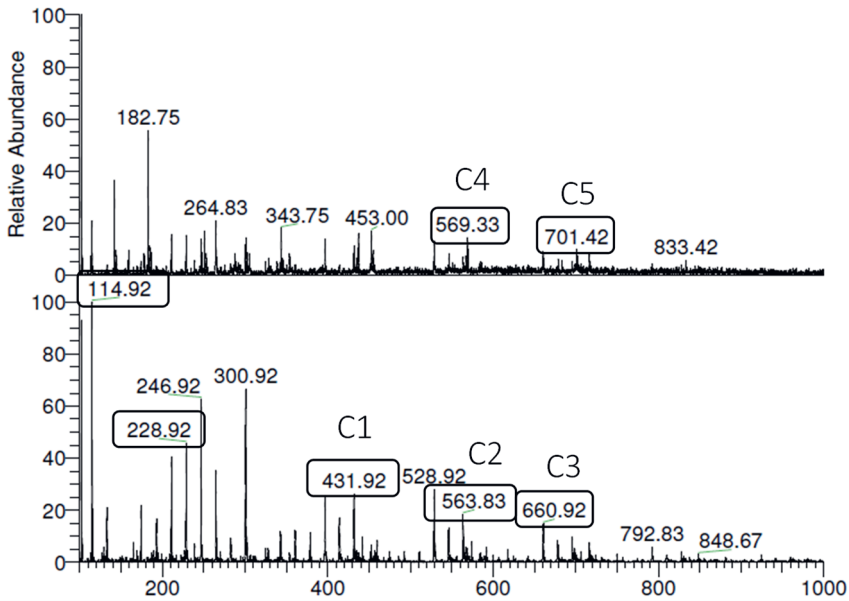
HPLC Chromatogram of aqueous phase

Unknown 1 has similar retention time with xylulose. But the MS of individual peaks reveals that at this retention time, a mixture of compounds with high molecular weight (up to MW=980) is separated. Group of unknown peak 2 is present in significant amount only at extreme conditions (i.e., high temperature and long residence time)

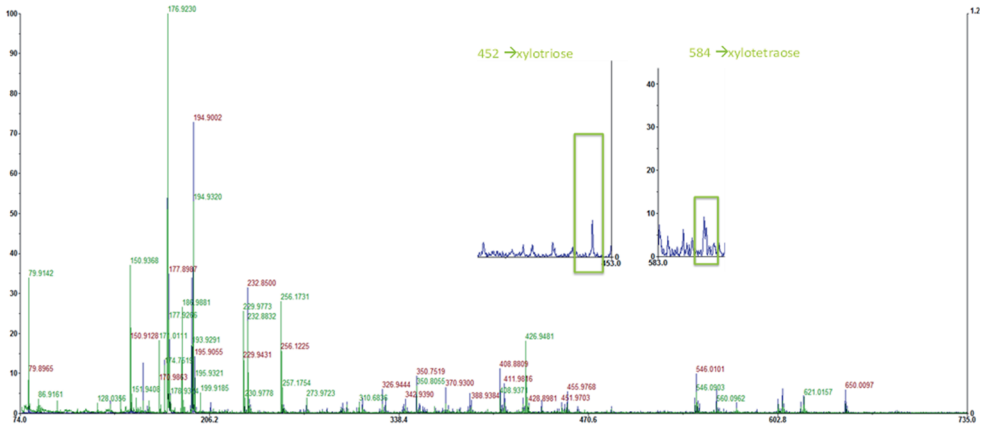


Appendix A.3.

LC MS (T=170°C and residence time=141 s)

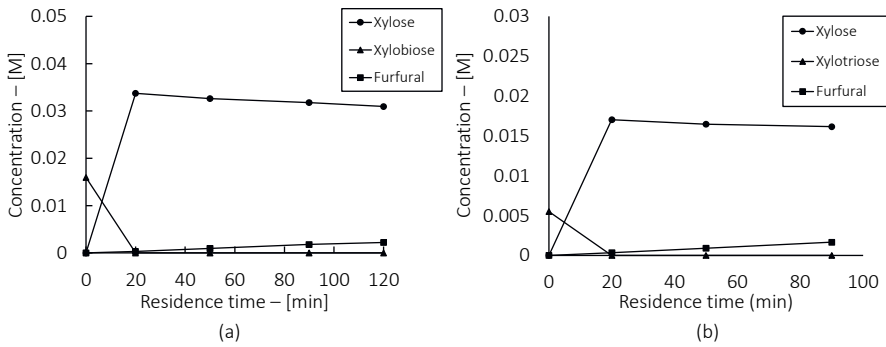


MALDI TOF for stock solution (blue) and reaction solution (green):



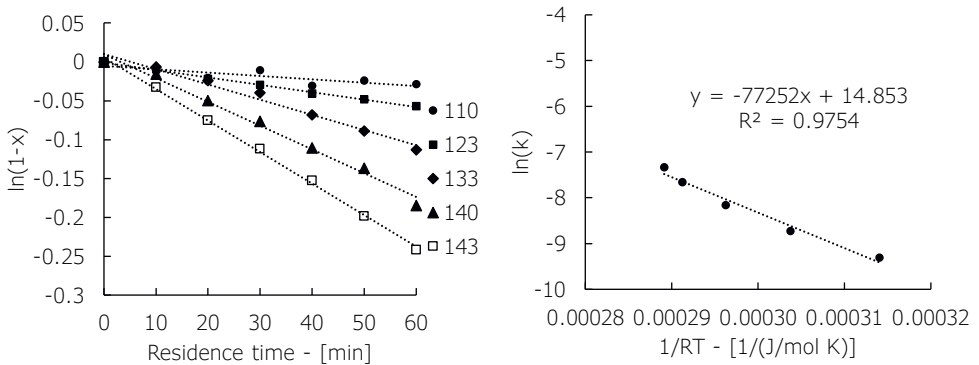
Appendix A.4.

Xylose oligomers Reaction at 130°C in monophasic batch system



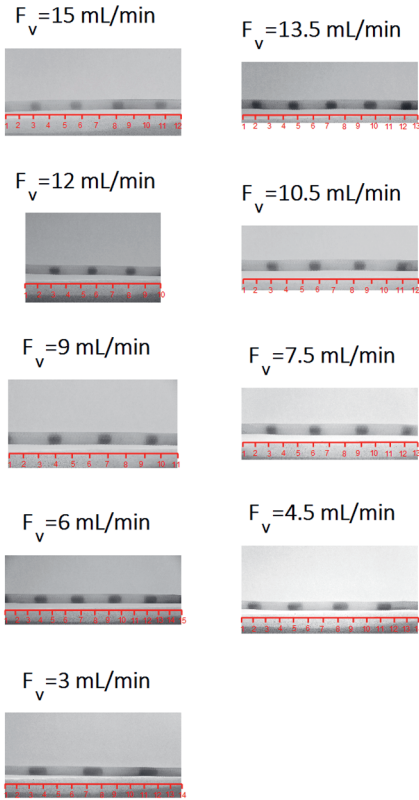
Appendix A.5.

Furfural Degradation Kinetics



Appendix A.6.

Taylor flow development in the biphasic millireactor - slugs for $F_{v,org}/F_{v,inorg}=2:1$ mL_{org} (mL_{inorg})⁻¹:



Appendix A.7.

Estimation of Mass transfer Coefficient

The film thickness (δ) is calculated based in Bretherson law. The equations used for these calculations are presented in equations A.1. and A.2. Additionally, the interfacial area is calculated for both mechanisms. Along with the time calculation, they indicate the dominant mechanism of furfural mass transfer. The equations A.3. and A.4. were used for the interfacial area estimation.

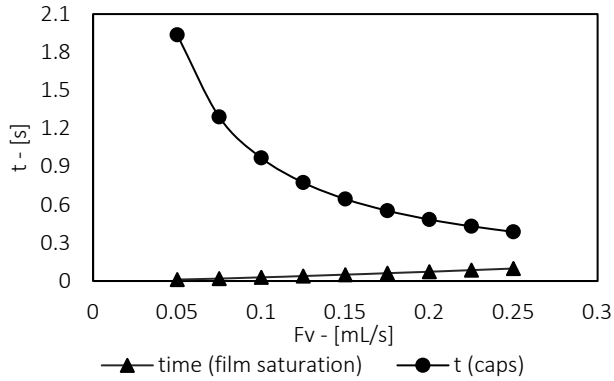
$$t_f = \frac{\delta^2}{\nu_{sl}} \quad (A.1)$$

$$t_c = \frac{L_{sl}}{D_f} \quad (A.2)$$

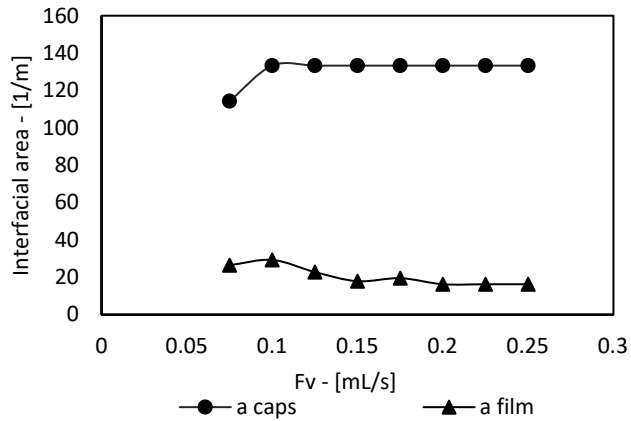
$$a_f = \frac{4 * L_f}{ID * L_{uc}} \quad (A.3)$$

$$a_c = \frac{4}{L_{uc}} \quad (A.4)$$

Time required for mass transfer through the caps and for film saturation for $F_v^{org}/F_v^{inorg}=2:1$ $m_{L,org} (m_{L,inorg})^{-1}$:



Interfacial area for two mechanism of mass transfer in Taylor flow:



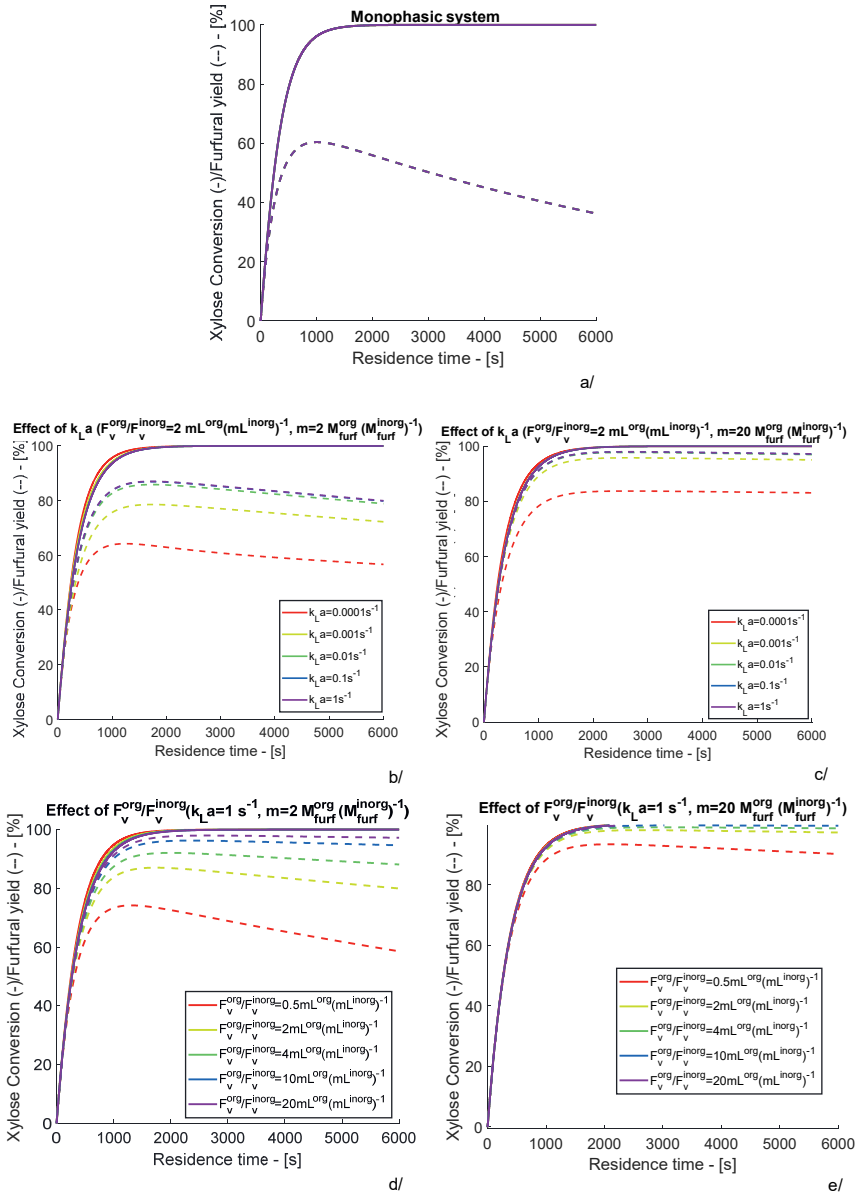
The mass transfer coefficient from Figure 2.4. of the examined system is calculated based on the following equations as reported in literature [206]:

$$k_{L,cap} a_{cap} = \left[\frac{2\sqrt{2}}{\pi} \sqrt{\frac{D v_{sl}}{ID}} \right] \left[\frac{4}{L_{uc}} \right] \quad (A.5)$$

$$k_{L,film} a_{film} = \left[3.41 \frac{D}{\delta} \right] \left[\frac{4 * L_f}{ID * L_{uc}} \right] \quad (A.6)$$

$$k_{L,cap} a_{cap} = k_{L,cap} a_{cap} + k_{L,film} a_{film} \quad (A.7)$$

Appendix A.8.



Xylose conversion and furfural yield vs residence time at 190°C. (a) Monophasic reaction; (b) effect of $k_L a$ with $O/I=2 \text{ mL}^{org}(\text{mL}^{inorg})^{-1}$ and $m=2 \text{ M}_{furf}^{org}(\text{M}_{furf}^{inorg})^{-1}$; (c) effect of $k_L a$ with $F_v^{org}/F_v^{inorg}=2:1 \text{ mL}^{org}(\text{mL}^{inorg})^{-1}$ and $m=20 \text{ M}_{furf}^{org}(\text{M}_{furf}^{inorg})^{-1}$; (d) effect of O/I with $k_L a=1 \text{ s}^{-1}$ and $m=2 \text{ M}_{furf}^{org}(\text{M}_{furf}^{inorg})^{-1}$; (e) effect of O/I with $k_L a=1 \text{ s}^{-1}$, $m=20 \text{ M}_{furf}^{org}(\text{M}_{furf}^{inorg})^{-1}$

Appendix B

Appendix B.1.

Table B.1.1: Equations of mole balances used in MATLAB® for C5 sugars dehydration

Mechanism	Equations
Xylose	
Literature	$\frac{dC_X}{dt} = -k_X * C_X$ $\frac{dC_I}{dt} = k_X * C_X - k_I * C_I - k_{IF} * C_I * C_F^{inorg}$ $\frac{dC_F^{inorg}}{dt} = k_I * C_I - k_{IF} * C_I * C_F^{inorg} - k_F * C_F^{inorg} - k_L a * (m * C_F^{inorg} - C_F^{org}) * \frac{1}{\epsilon_{inorg}}$ $\frac{dC_F^{org}}{dt} = k_L a * (m * C_F^{inorg} - C_F^{org}) * \frac{1}{\epsilon_{org}}$ $\frac{dC_{DP1}}{dt} = k_{IF} * C_I * C_F^{inorg}$ $\frac{dC_{RP}}{dt} = k_F * C_F^{inorg}$
Arabinose	
A	$\frac{dC_A}{dt} = -k_A * C_A - k_{ADP} * C_A$ $\frac{dC_F^{inorg}}{dt} = k_A * C_A - k_{fd} * C_F^{inorg} - k_L a * (m * C_F^{inorg} - C_F^{org}) * \frac{1}{\epsilon_{inorg}}$ $\frac{dC_F^{org}}{dt} = k_L a * (m * C_F^{inorg} - C_F^{org}) * \frac{1}{\epsilon_{org}}$ $\frac{dC_{DP1}}{dt} = k_{ADP} * C_A$ $\frac{dC_{RP}}{dt} = k_{fp} * C_F^{inorg}$

$$\frac{dC_A}{dt} = -k_{IA} * C_A$$

$$\frac{dC_I}{dt} = k_{IA} * C_A - k_{AF} * C_I - k_{FIA} * C_I - C_I * C_F^{inorg}$$

$$\frac{dC_F^{inorg}}{dt} = k_{AF} * C_I - k_{FIA} * C_I * C_F^{inorg} - k_{fd} * C_F^{inorg} - k_L a * (m * C_F^{inorg} - C_F^{org}) * \frac{1}{\epsilon_{inorg}}$$

B

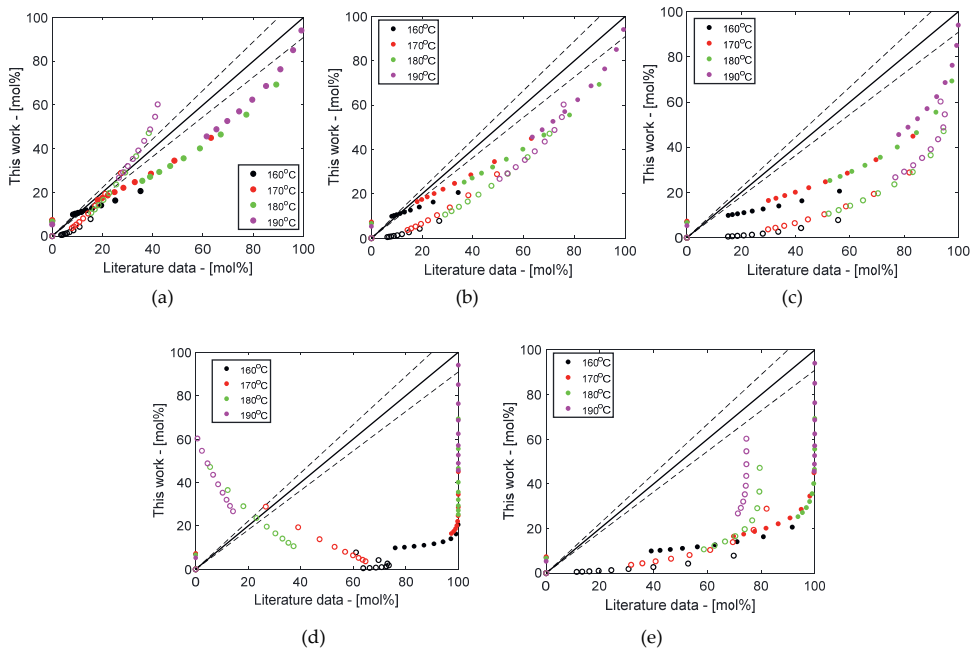
$$\frac{dC_F^{org}}{dt} = k_L a * (m * C_F^{inorg} - C_F^{org}) * \frac{1}{\epsilon_{org}}$$

$$\frac{dC_{DP1}}{dt} = k_{FIA} * C_I * C_F^{inorg}$$

$$\frac{dC_{RP}}{dt} = k_{fp} * C_F^{inorg}$$

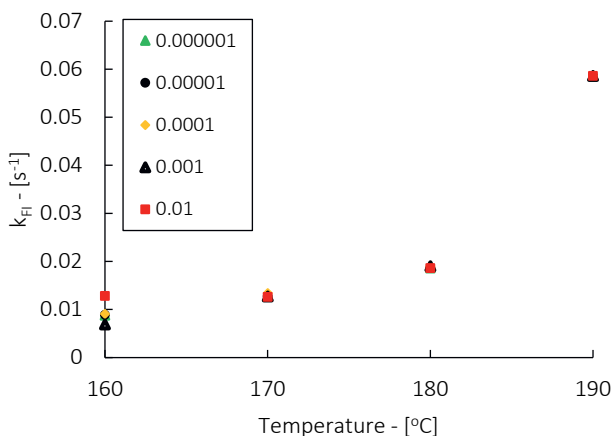
Appendix B.2.

Experimental data evaluation with literature kinetics by Marcotullio et. al (a), Hommes et. al (b), Weingarten et. al (c), Lamminpää et. al (d) and Dussan et. al (e); xylose conversion (closed symbols) and furfural yield (open symbols) for conditions: extraction medium: toluene, $F_V^{org}/F_V^{inorg}=2:1$, $[H_2SO_4]=0.1M$ and $C_{xyI}^0=4wt\%$



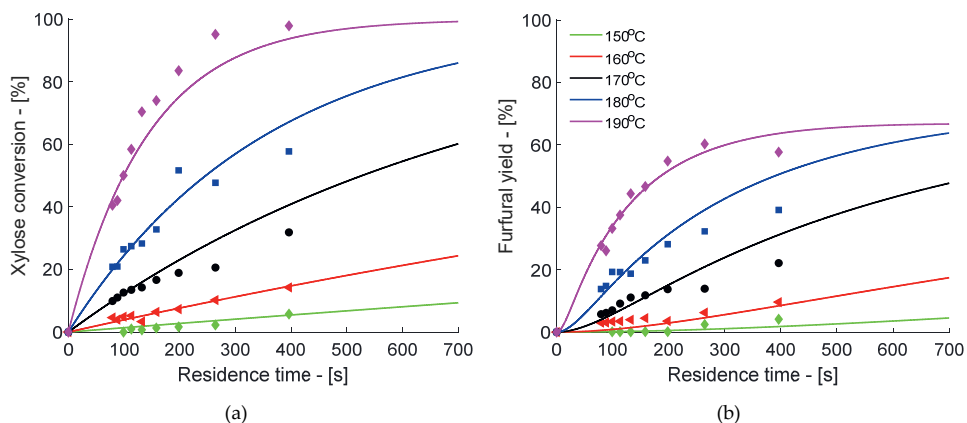
Appendix B.3.

Effect of initial value on reaction rate constants of furfural formation from xylose



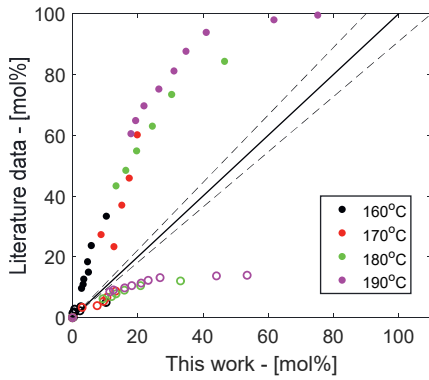
Appendix B.4.

Xylose conversion and furfural yield for calculated set of kinetic data, extraction medium: toluene, $F_{v,org}/F_{v,inorg}=2:1$, $[H_2SO_4]=0.1M$

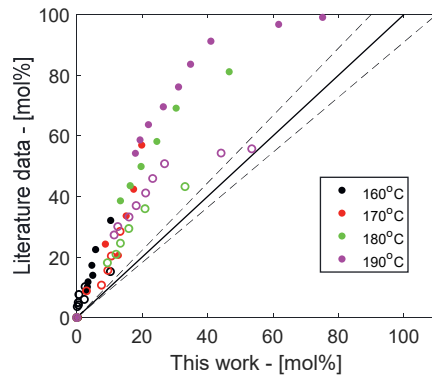


Appendix B.5.

Experimental data evaluation with literature kinetics reported by Dussan et. al (a) and Yasuda et. al (b); arabinose conversion (closed symbols) and furfural yield (open symbols) for conditions: extraction medium: toluene, $F_v^{org}/F_v^{inorg}=2:1$, $[H_2SO_4]=0.1M$ and $C_{arab}^0=1wt\%$



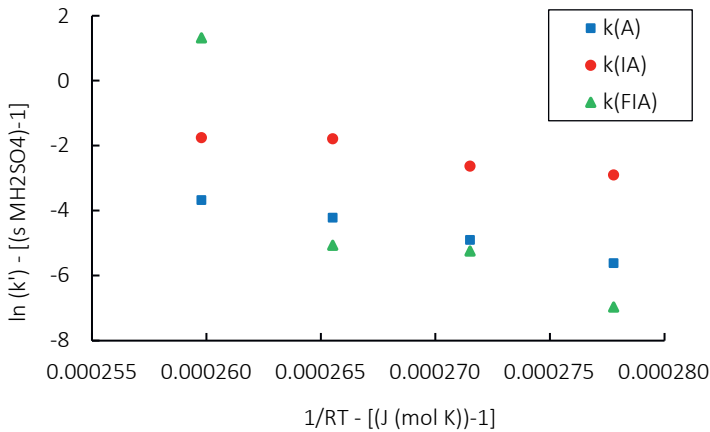
(a)



(b)

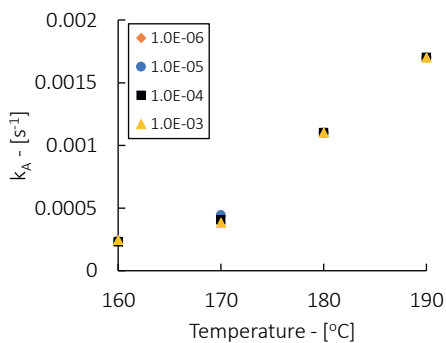
Appendix B.6.

Arrhenius plot for arabinose dehydration for Mechanism B

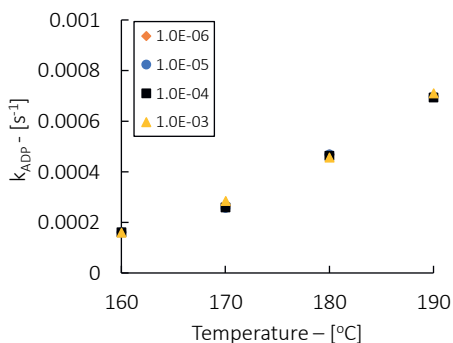


Appendix B.7.

Effect of initial value on reaction rate constants of furfural formation from arabinose (Mechanism A)



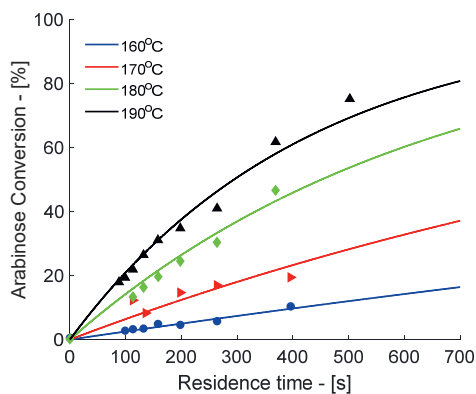
(a)



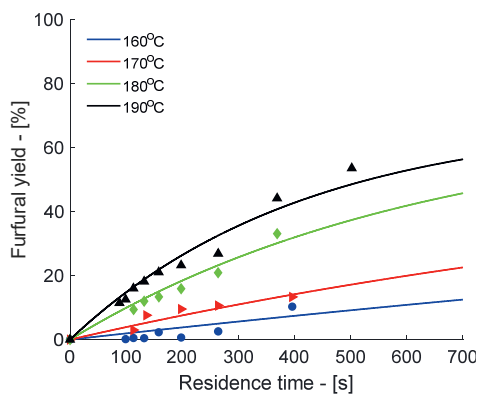
(b)

Appendix B.8.

Arabinose conversion (a) and furfural yield (b) using calculated set of kinetic data



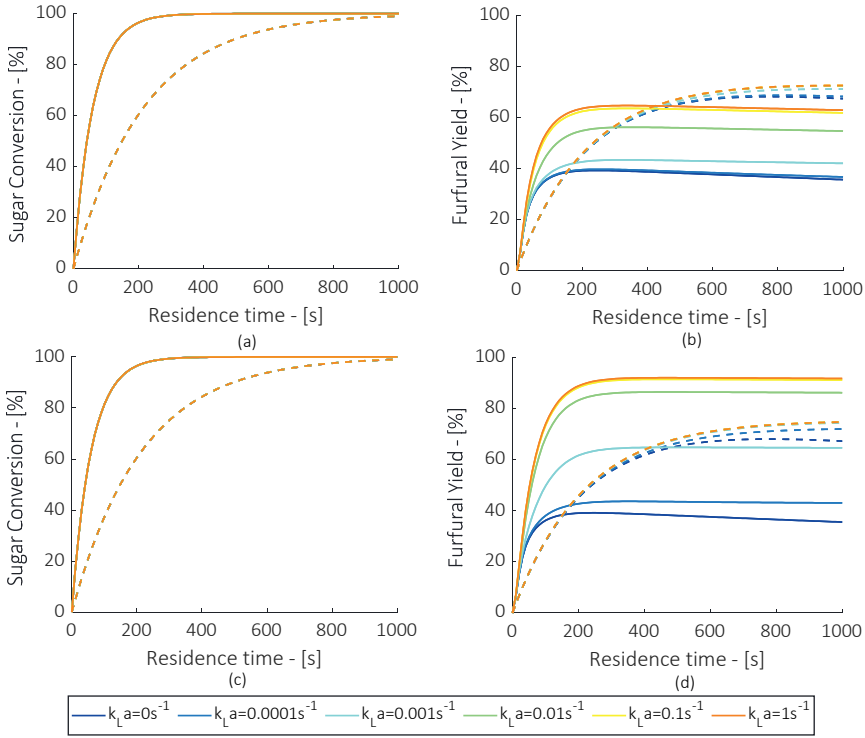
(a)



(b)

Appendix B.9.

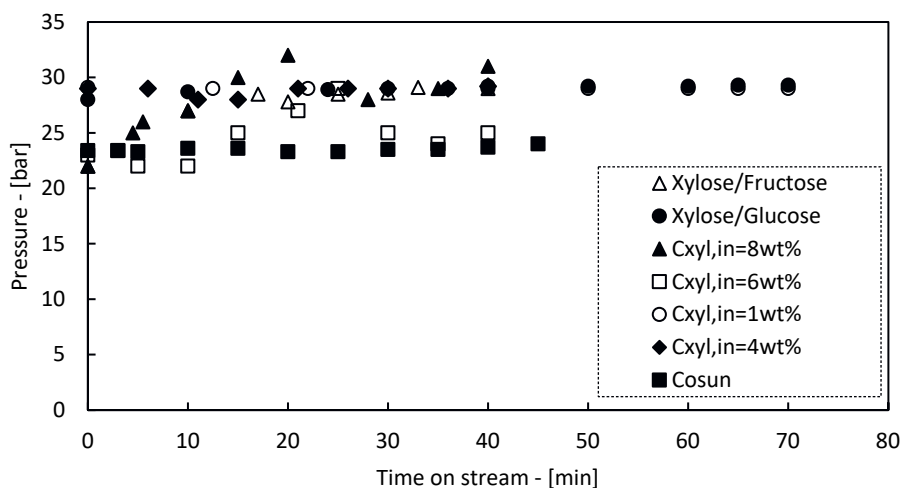
Sensitivity analysis of $k_L a$ and its effect on C5 sugars conversion (left column) and furfural yield (right column) at 200°C for $m = 1 M_{\text{furf}}^{\text{org}}(M_{\text{furf}}^{\text{inorg}})^{-1}$ (top row) and $m = 10 M_{\text{furf}}^{\text{org}}(M_{\text{furf}}^{\text{inorg}})^{-1}$ (bottom row), $F_v^{\text{org}}/F_v^{\text{inorg}} = 2$, $[\text{H}_2\text{SO}_4] = 0.1\text{M}$, $C_{\text{xy}}^0 = 4\text{wt}\%$, $C_{\text{arab}}^0 = 1\text{wt}\%$



Appendix C

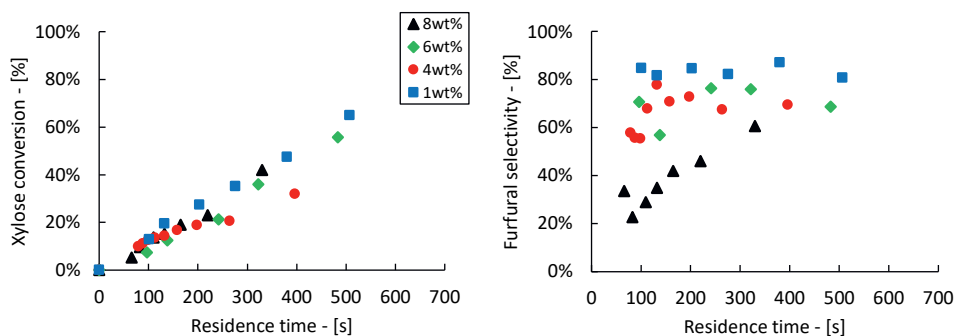
Appendix C.1.

Pressure Profiles



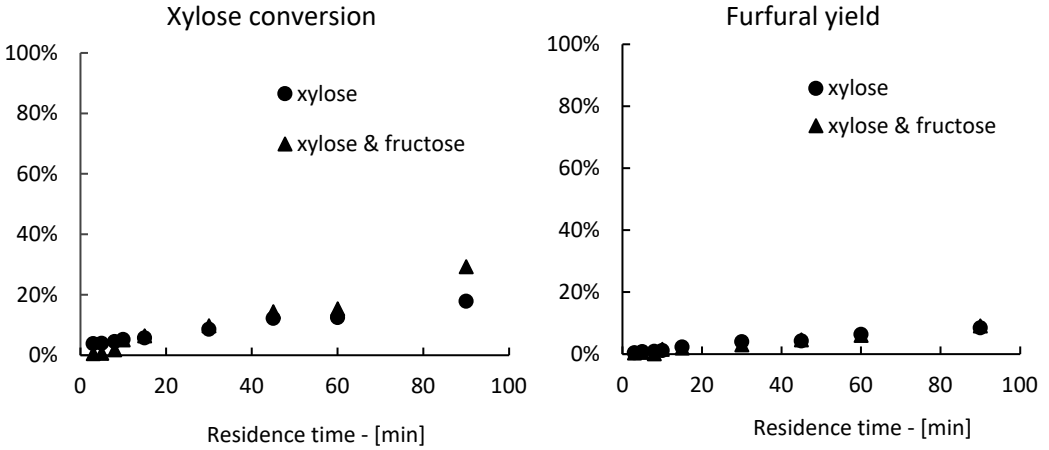
Appendix C.2.

Effect of initial xylose concentration on xylose conversion (left) and furfural selectivity (right) at 170°C, toluene, $F_v^{org}/F_v^{inorg}=2:1$, $[H_2SO_4]=0.1M$

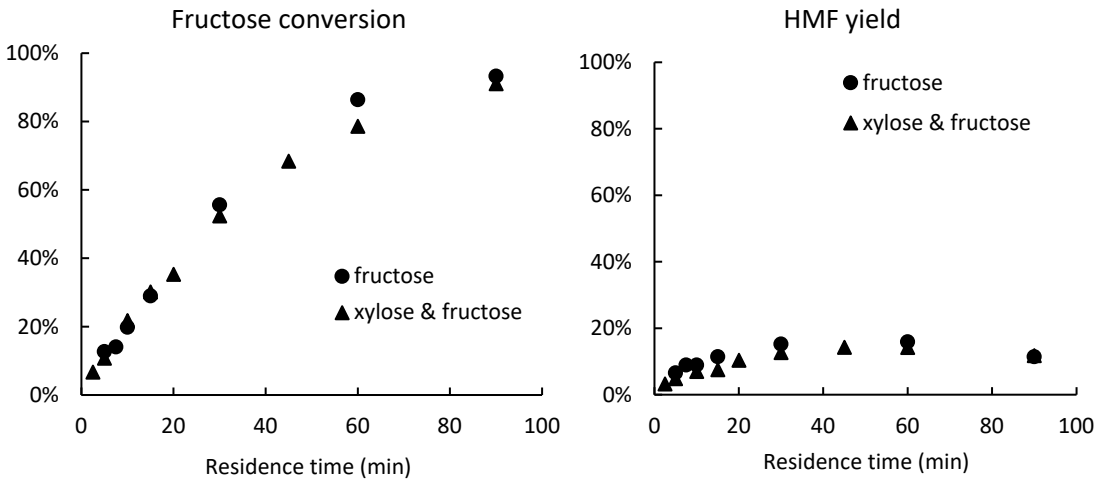


Appendix C.3.

Monophasic batch experiment of xylose conversion at 130°C for substrates: $C_{\text{xy}}^0=1\text{wt}\%$ and $C_{\text{xy}}^0=1\text{wt}\%-C_{\text{fruc}}^0=1\text{wt}\%$ and 0.1M H_2SO_4

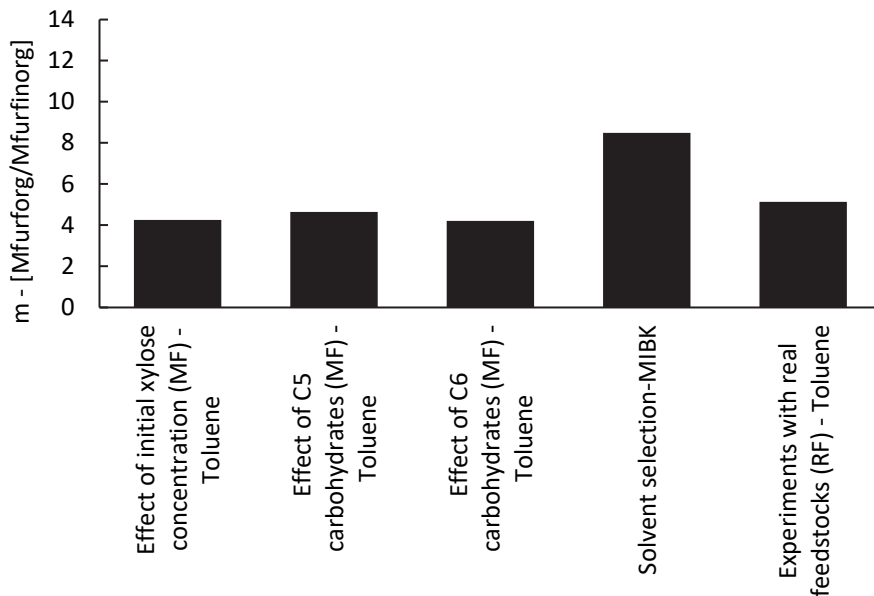


Monophasic batch experiment of fructose conversion at 130°C for substrates: $C_{\text{xy}}^0=1\text{wt}\%$ and $C_{\text{xy}}^0=1\text{wt}\%-C_{\text{fruc}}^0=1\text{wt}\%$ and 0.1M H_2SO_4



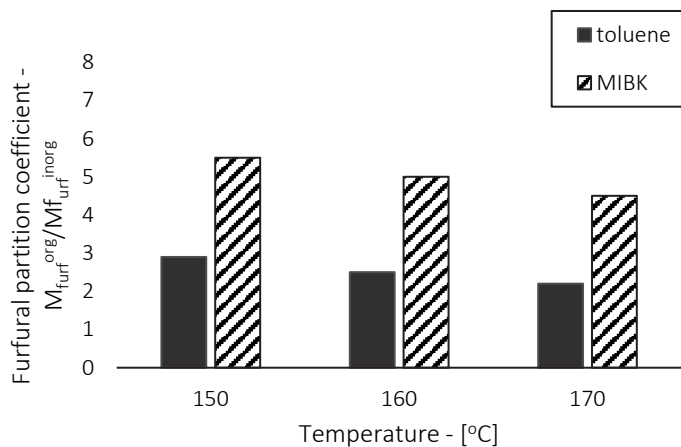
Appendix C.4.

Average furfural distribution between organic and inorganic phase for each tested feedstock type at room temperature



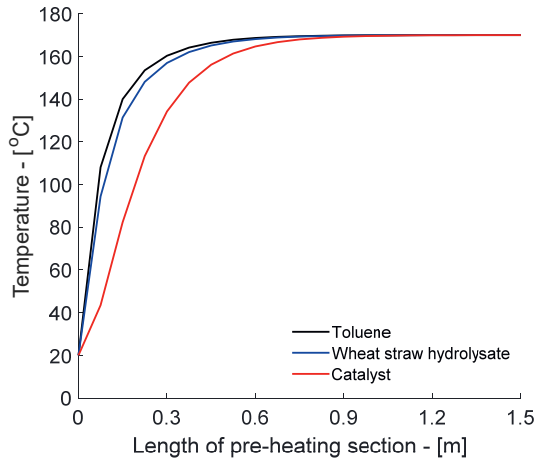
Appendix C.5.

Furfural Partition Coefficient with temperature: Uniquac was used as thermodynamic model for the prediction of furfural partition coefficient in MIBK and toluene using ASPEN Plus® Software

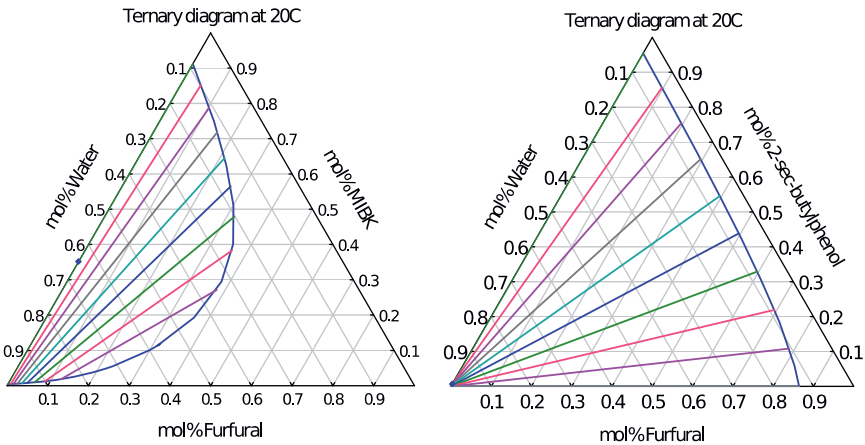


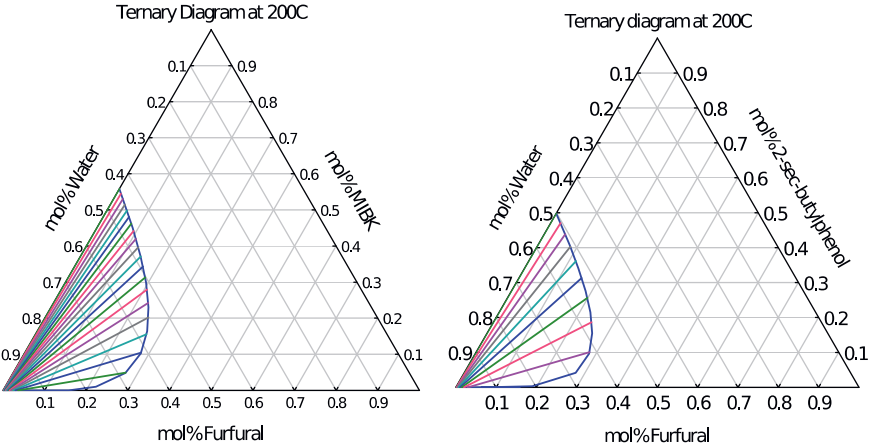
Appendix C.6.

Temperature profile for pre-heating section for wheat straw hydrolysate biphasic dehydration with pre-heating section length for 10 min at 170°C, Solvent: Toluene, $F_V^{org}/F_V^{inorg}=2:1$, $[H_2SO_4]=0.1M$

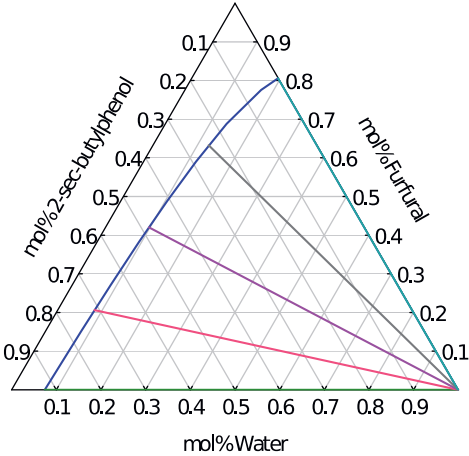


Appendix D Appendix D.1.



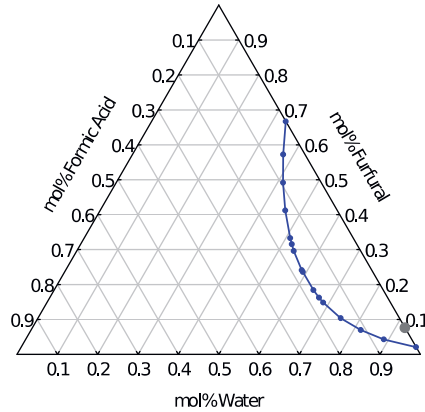


Ternary diagram for the system: water, furfural and 2-sec-butylphenol. The red point indicates the composition and the biphasic nature of the top stream from the solvent recovery column distillation column for feedstock A.



Appendix D.2.

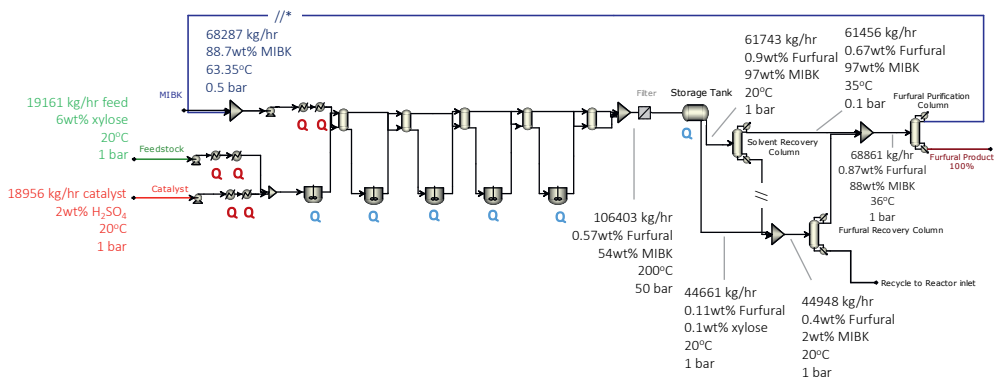
Ternary diagram for the system: water, furfural and formic acid for liquid-liquid separation.



Appendix D.3.

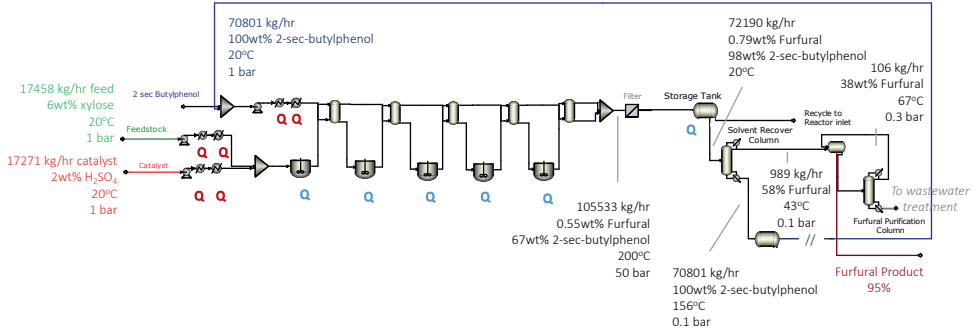
In flowcharts, **Q** is for heating utility and **Q** is for cooling utility. Degradation products are calculated for the total of degradation products formed during xylose and arabinose dehydration to furfural and furfural resinification products.

ASPEN Plus® model flowchart for MIBK

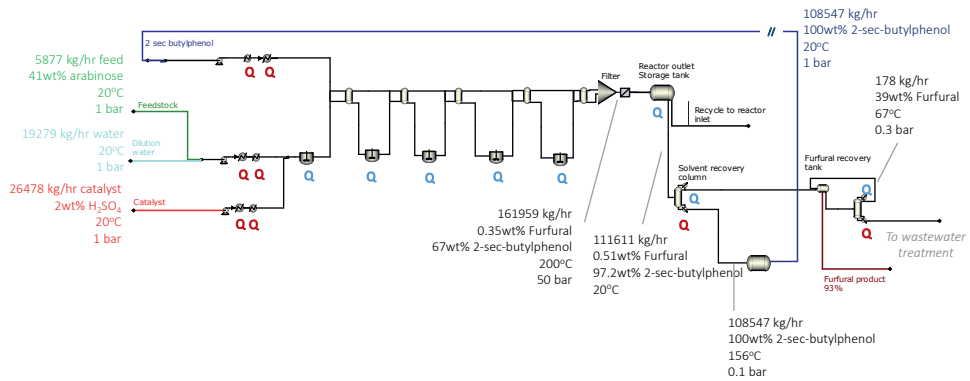


* This symbol indicates semi-continuous operation of the process

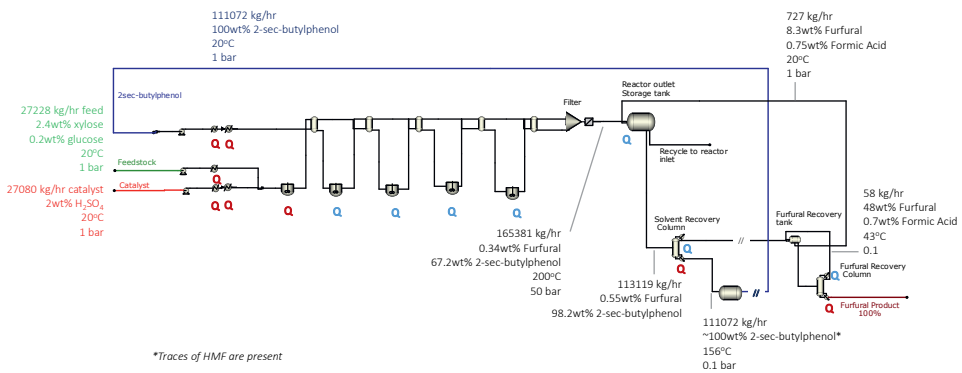
ASPEN Plus® model flowchart for 2-sec-butylphenol [Feedstock A]



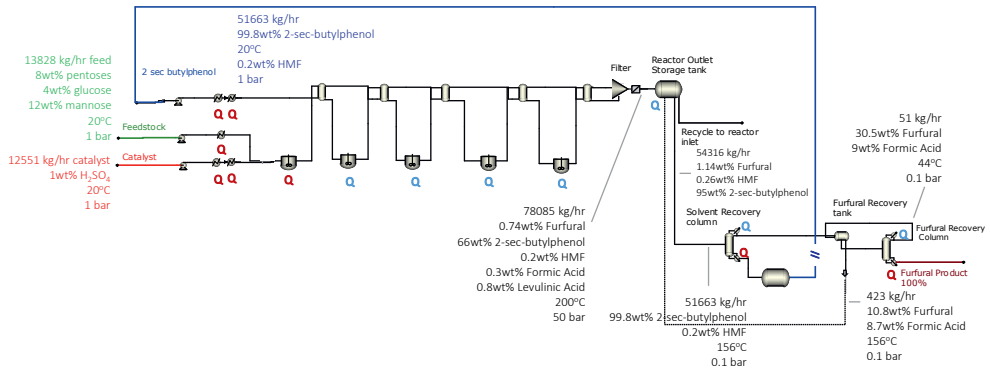
ASPEN Plus® model flowchart for feedstock B



ASPEN Plus® model flowchart for feedstock C



ASPEN Plus® model flowchart for feedstock D

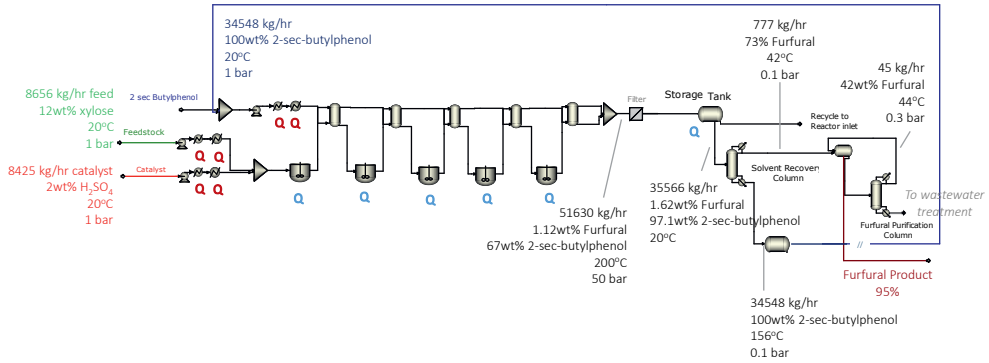


Appendix D.5.
Table D.5.1: CAPEX and OPEX for Case studies 1 and 2

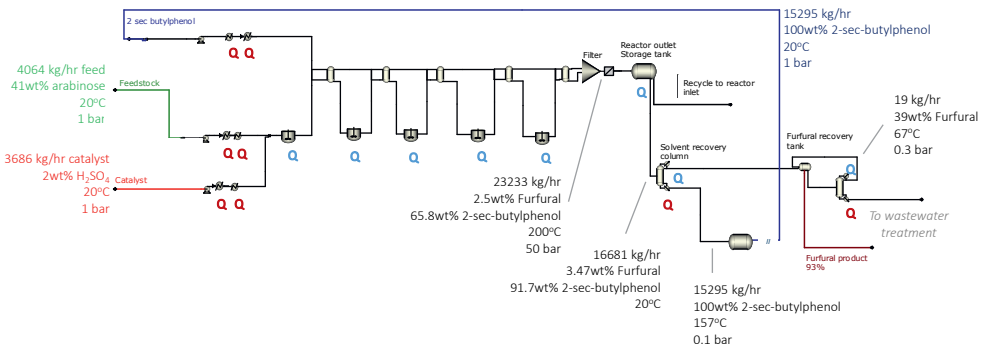
CAPEX					
Equipment Type	MIBK	2-sec-butylphenol	B	C	D
Storage tanks	€ 0.70M	€ 0.53M	€ 0.77M	€ 0.95M	€ 0.52M
Pumps	€ 0.08M	€ 0.09M	€ 0.10M	€ 0.09M	€ 0.06M
HEs	€ 0.23M	€ 0.19M	€ 0.31M	€ 0.24M	€ 0.16M
Reactors	€ 5.12M	€ 5.12M	€ 5.12M	€ 5.12M	€ 5.12M
Distillation Columns	€ 1.09M	€ 0.17M	€ 0.21M	€ 0.20M	€ 0.20M
TOTAL CAPEX	€ 7.22M	€ 6.10M	€ 6.51M	€ 6.60M	€ 6.08M
OPEX					
Raw materials	€ 0.42M	€ 0.36M	€ 0.00M	€ 0.00M	€ 0.00M
Utility-Water	€ 4.56M	€ 0.93M	€ 1.55M	€ 1.37M	€ 0.68M
Utility-Electricity	€ 0.21M	€ 0.18M	€ 0.26M	€ 0.26M	€ 0.14M
Utility-Stream	€ 19.99M	€ 7.00M	€ 10.68M	€ 12.16M	€ 4.90M
Operating Labor	€ 1.24M	€ 0.99M	€ 1.09M	€ 1.10M	€ 1.02M
Maintenance	€ 0.46M	€ 0.35M	€ 0.39M	€ 0.40M	€ 0.37M
Laboratory	€ 0.01M	€ 0.01M	€ 0.01M	€ 0.01M	€ 0.01M
Fixed Charges	€ 3.81M	€ 2.95M	€ 3.26M	€ 3.31M	€ 3.05M
Plant Overhead	€ 0.34M	€ 0.28M	€ 0.30M	€ 0.30M	€ 0.28M
TOTAL OPEX	€ 31.03M	€ 13.07M	€ 17.54M	€ 18.92M	€ 10.46M

Appendix D.6.

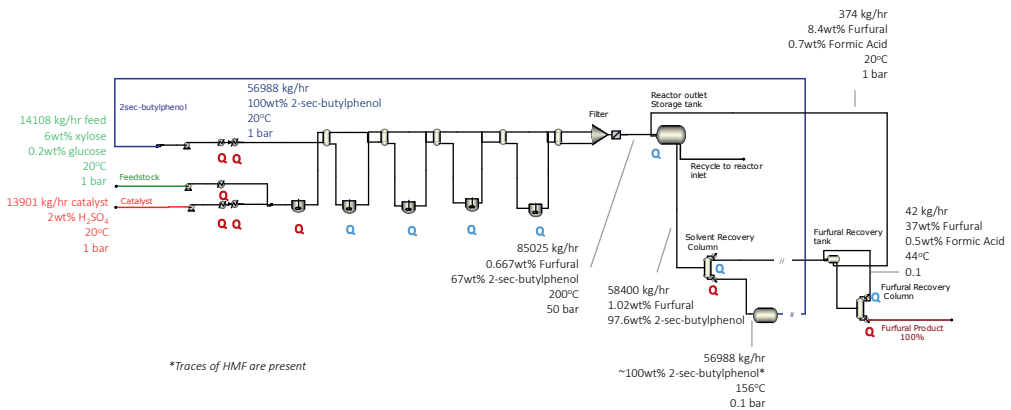
ASPEN Plus® model flowchart for feedstock A – [6wt% xylose]



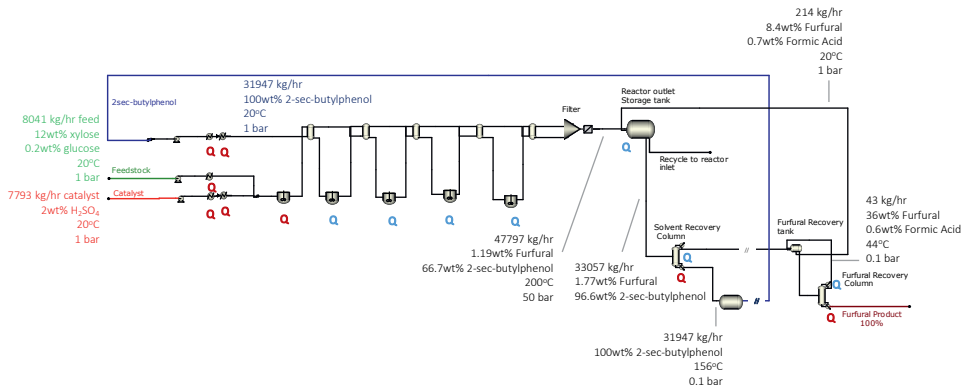
ASPEN Plus® model flowchart for feedstock B [20wt% arabinose]



ASPEN Plus® model flowchart for feedstock C [3wt% xylose]



ASPEN Plus® model flowchart for feedstock C [6wt%xylose]



Appendix D.7.

Estimation of steam/energy demands for water vaporization from Feedstock C

In this calculation, 3wt% xylose is the target concentration and low pressure is assumed.

Table D.7.1: Calculations of energy required for water removal from feedstock C

	Parameter	Value
For feedstock stream	$M_{\text{water to be removed}}$ [kg/hr]	12988
	$\Delta H_{\text{vaporization of water}}$ [kJ/kg]	2.26
	$Q_{\text{required for water vaporization}}$ [kJ/hr]	29353
For steam	ΔT of steam [K]	60
	$Q_{\text{required for water vaporization}}$ [kJ/hr]	29353
	$C_{p,\text{steam}}$ [kJ/kg/K]	4.2
	$M_{\text{steam required for water vaporization}}$ [kg/h]	116.5

Table D.7.2: Calculations of OPEX and MSP for water removal from feedstock C

Parameter	Case study 2 – before evaporation	After evaporation
OPEX	€ 11.63M	€ 11.64M
Furfural MSP	€ 2.79	€ 2.80

Appendix D.8.

Table D.8.1: CAPEX and OPEX for Case study 3

Equipment type	Feedstock A 6wt%xylose	Feedstock B 20wt% arabinose	Feedstock C 3wt% xylose	Feedstock C 6wt%xylose
CAPEX				
Tanks	€ 0.19M	€ 0.19M	€ 0.49M	€ 0.34M
Reactors	€ 4.80M	€ 2.76M	€ 4.75M	€ 2.84M
HEs	€ 0.17M	€ 0.15M	€ 0.17M	€ 0.15M
Pumps	€ 0.00M	€ 0.04M	€ 0.06M	€ 0.04M
Distillation Columns	€ 0.09M	€ 0.12M	€ 0.12M	€ 0.13M
Total CAPEX	€ 5.25M	€ 3.24M	€ 5.59M	€ 3.50M
OPEX				
Raw materials	€ 0.36M	€ 0.00M	€ 0.00M	€ 0.00M
Utility-Water	€ 0.52M	€ 0.28M	€ 0.74M	€ 0.45M
Utility-Electricity	€ 0.11M	€ 0.06M	€ 0.15M	€ 0.10M
Utility-Steam	€ 3.36M	€ 1.50M	€ 6.51M	€ 3.62M
Operating Labor	€ 0.87M	€ 0.61M	€ 0.92M	€ 0.42M
Maintenance	€ 0.31M	€ 0.20M	€ 0.33M	€ 0.13M
Laboratory	€ 0.01M	€ 0.01M	€ 0.01M	€ 0.01M
Fixed Charges	€ 2.55M	€ 1.66M	€ 2.71M	€ 1.07M
Plant Overhead	€ 0.25M	€ 0.18M	€ 0.26M	€ 0.14M
TOTAL OPEX	€ 8.33M	€ 4.50M	€ 11.63M	€ 5.94M

Appendix D.9.

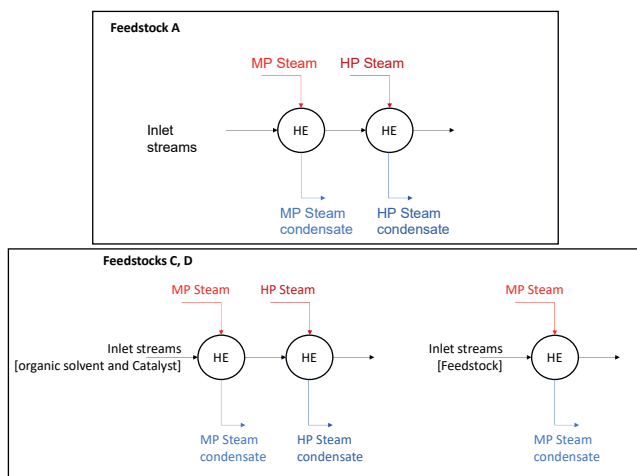
Table D.9.1: Final utilities requirements for each feedstock type after implementing the two concepts of heat integration.

Utility type [kg/hr]	Feedstock A	Feedstock C	Feedstock D
Water	458505	693636	343614
<i>Reduction from base case</i>	6.2%	4.2%	6.2%
Medium pressure steam	26868	38621	17937
<i>Reduction from base case</i>	15.2%	16.4%	17.9%

Appendix D.10.

Description of heat integration concepts

In Scheme 5.8.1, the energy demands of the inlet streams are depicted for feedstocks A, C and D. It is observed that all inlet streams require heat exchangers to bring the temperature stream to 200°C. Both MP and HP steam are needed to reach the required temperature. In the case of the feedstocks C and D, the feed inlet streams require only one heat exchanger, because the inlet temperature to the reactor is set at 120°C. Additionally, the condensers and the reboilers of both distillation columns require cooling water and MP steam for cover their energy demands.



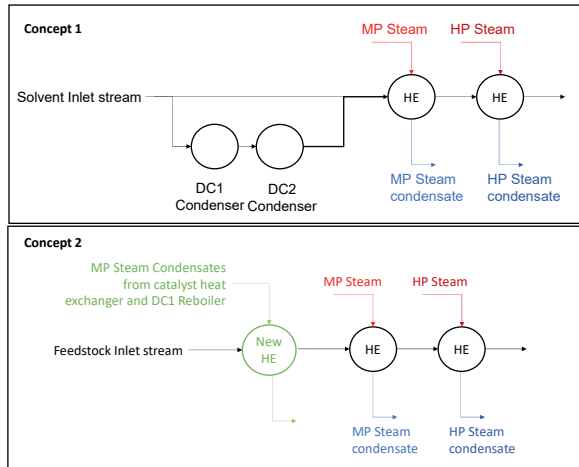
Scheme D.10.1. Energy requirements for base cases of feedstocks A, C and D [Case study 2]

The first concept of heat integration suggests that part of the organic solvent inlet stream passes through the condensers of the two distillation columns. By applying this, the MP steam demand in the inlet stream and the cooling water demands in the condensers are reduced.

Table D.10.1: Percentage of the stream passing through the condensers and the final temperature of the combined stream of the organic solvent are shown.

Feedstock	% Organic solvent passing through condensers	Final stream temperature
A	79%	52 °C
C	68%	49 °C
D	86%	57 °C

The second concept proposes that the MP steam condensates from the reboiler of the first distillation column and the catalyst heat exchanger are used as heating medium in a new heat exchanger added in the process. In the scheme above, the new heat exchanger is shown in the feedstock inlet stream in order to display the purpose of the addition. The function of this heat exchanger is to increase the feedstock of the inlet temperature and reduce the MP steam demands in the subsequent heat exchanger.



Scheme D.10.2. Two concepts of heat integration

Table D.10.2: Feedstock stream temperature after the new heat exchanger

Feedstock	Stream temperature after new heat exchanger
A	80 °C
C	92 °C
D	92°C

Appendix D.11.

Table D.11.1: CAPEX and OPEX after heat integration

Equipment Type	Feedstock A	Feedstock C	Feedstock D
CAPEX			
Storage tanks	€ 0.53M	€ 0.95M	€ 0.52M
Pumps	€ 0.09M	€ 0.09M	€ 0.06M
HEs	€ 0.21M	€ 0.26M	€ 0.18M
Reactors	€ 5.12M	€ 5.12M	€ 5.12M
Distillation Columns	€ 0.18M	€ 0.27M	€ 0.20M
TOTAL CAPEX	€ 6.13M	€ 6.68M	€ 6.1M

OPEX			
Raw materials	€ 0.36M	€ 0.00M	€ 0.00M
Utility-Water	€ 0.88M	€ 1.37M	€ 0.66M
Utility-Electricity	€ 0.273M	€ 0.39M	€ 0.22M
Utility-Steam	€ 7.00M	€ 9.06M	€4.51M
Operating Labor	€ 1.00M	€ 1.08M	€ 1.03M
Maintenance	€ 0.36M	€ 0.40M	€ 0.37M
Laboratory	€ 0.01M	€ 0.01M	€ 0.01M
Fixed Charges	€ 2.96M	€ 2.55M	€ 3.06M
Plant Overhead	€ 0.28M	€ 0.31M	€ 0.28M
TOTAL OPEX	€ 12.41M	€ 17.174M	€ 9.85M

Appendix D.12.

Analysis of hemicellulosic side stream from pulp & paper industry

Pulping is a well-established and optimized process of wood/biomass refining that targets the cellulose fibers as main products and render hemicellulose and lignin mixtures as side streams. Aiming to valorize most of the raw material and reduce the amount of side streams generated, integrated schemes of pulp and paper plants are of high interest. Some concepts propose isolation of the hemicellulose stream prior to the main pulping process via hot water extraction [211,291]. Here, we focus on the hemicellulosic fraction of hot water extract using prehydrolysate composition found in literature [291]. It is observed that no furfural or HMF are reported in this pre-hydrolysate and it can be speculated that the pre-hydrolysis conditions are mild. Other types of pre-hydrolysates from pulp and paper industry report the presence of furfural and HMF [211]. In the model, no cross-condensation reactions between soluble lignin, sugar and furfural are considered. The presence of acetic acid is not expected to significantly decrease the pH because it is present in very low concentration (<1wt%).

Table D.11.1: Final chemical composition of hemicellulosic stream from pulp & paper industry

Chemical composition	wt%
Xylose (from pre-hydrolysate and after xylo-oligomers hydrolysis)	9.49
Arabinose	0.17
Glucose	0.15
Acetic acid	0.31

In literature, kinetic studies of xylose oligomers hydrolysis have been reported starting from xylo-tetraose at the same reaction conditions (i.e., 200°C, 0.1M H₂SO₄) [292]. The xylose concentration has been corrected using reported to identify the increase of xylose

concentration from the hydrolysis of xylose oligomers under the reaction conditions. The final stream composition is shown Table D.11.1. As shown in Table D.11.2, almost complete C5 conversion is achieved, and high furfural selectivity is reached in line with the model results of the other feedstock types. The analysis of process economics (Table D.11.3) shows that CAPEX and OPEX strongly depends on the reactor and steam usage respectively. The furfural MSP is calculated at 3.1€/kg.

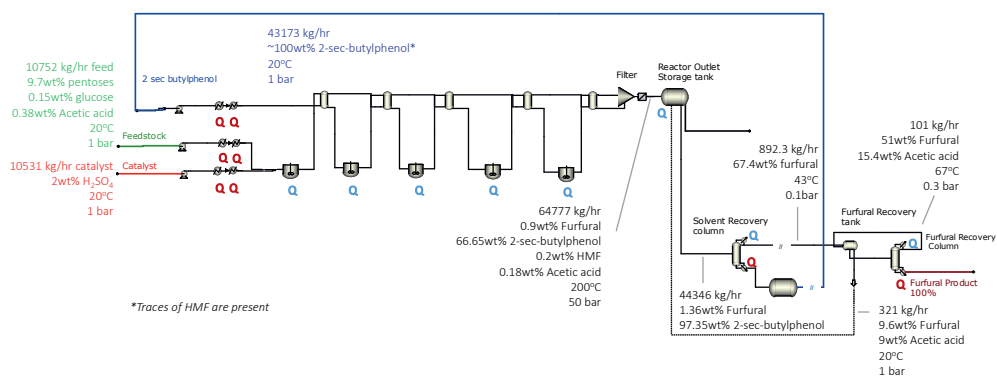
Table D.11.2: Process performance KPIs of hemicellulosic stream from pulp & paper industry

KPI	Value
Feedstock per product flows [kton feedstock / kton furfural]	18.85
C5 Sugar per product flows	1.79 kton xylose / kton furfural 0.032 kton arabinose / kton furfural
C5 Sugar concentration [wt%]	4.8% (Xylose), 0.09% (Arabinose)
Residence time	3'
Xylose Conversion	96%
Arabinose Conversion	86%
Furfural Selectivity	89%
Furfural purity (Furfural/Water)	100%
# Distillation columns	2
Solvent recovery	100%
Solvent purity	100%
Energy requirements (kW)	
Heating duties	13476
Cooling duties	10207
Power	226

Table D.11.3: Economical performance KPIs of hemicellulosic stream from pulp & paper industry

Equipment Type	CAPEX
Storage tanks	€ 0.52M
Pumps	€ 0.07M
HEs	€ 0.17M
Reactors	€ 5.12M
Distillation Columns	€ 0.21M
TOTAL CAPEX	€ 6.09M
Expense type	OPEX
Raw materials	€ 0.00M
Utility-Water	€ 0.60M
Utility-Electricity	€ 0.17M
Utility-Steam	€ 7.29M
Operating Labor	€ 1.03M
Maintenance	€ 0.37M
Laboratory	€ 0.01M
Fixed Charges	€ 3.06M
Plant Overhead	€ 1.85M
TOTAL OPEX	€ 12.82M

ASPEN Plus® model flowchart for hemicellulosic side stream from pulp & paper industry



References

- [1] C.W. Lewis, Biomass through the ages, *Biomass*. 1 (1981) 5–15. [https://doi.org/10.1016/0144-4565\(81\)90011-1](https://doi.org/10.1016/0144-4565(81)90011-1).
- [2] K. Rypdal, P. Newton, S. Eggleston, J. Goodwin, W. Irving, J. Penman, and M.W. (UK), 2006 IPCC Guidelines for National Greenhouse Gas Inventories, in: 2006: pp. 215–218. https://www.eia.gov/totalenergy/data/monthly/pdf/sec11_n.pdf.
- [3] Zobelein H., *Dictionary of Renewable Resources*, John Wiley & Sons, Inc., Weinheim, Germany, 2001.
- [4] A. M. Watkins, *Biomass Research and Development Act, 2000*. <https://doi.org/2019-12022> Filed.
- [5] T.J. McNerney, *Developing and Promoting Biobased Products and Bioenergy*, 1999.
- [6] R.A. Lee, J.-M. Lavoie, From first- to third-generation biofuels: Challenges of producing a commodity from a biomass of increasing complexity, *Anim. Front.* 3 (2013) 6–11. <https://doi.org/10.2527/af.2013-0010>.
- [7] M.B. Charles, R. Ryan, N. Ryan, R. Oloruntoba, Public policy and biofuels: The way forward?, *Energy Policy*. 35 (2007) 5737–5746. <https://doi.org/10.1016/j.enpol.2007.06.008>.
- [8] L. Brennan, P. Owende, Biofuels from microalgae-A review of technologies for production, processing, and extractions of biofuels and co-products, *Renew. Sustain. Energy Rev.* 14 (2010) 557–577. <https://doi.org/10.1016/j.rser.2009.10.009>.
- [9] V. Alfonsín, R. Maceiras, C. Gutiérrez, Bioethanol production from industrial algae waste, *Waste Manag.* 87 (2019) 791–797. <https://doi.org/10.1016/j.wasman.2019.03.019>.
- [10] G. Seon, H.S. Kim, J.M. Cho, M. Kim, W.K. Park, Y.K. Chang, Effect of post-treatment process of microalgal hydrolysate on bioethanol production, *Sci. Rep.* 10 (2020) 1–12. <https://doi.org/10.1038/s41598-020-73816-4>.
- [11] European Commission, *European Green Deal*, (2021). https://ec.europa.eu/info/strategy/priorities-2019-2024/european-green-deal_en.
- [12] B. Allen, D. Baldock, S. Nanni, C. Bowyer, *Sustainability criteria for biofuels made from land and non-land based feedstocks*, Institute for European Environmental Policy (IEEP), London, 2016.
- [13] Directives 98/70/EC relating to the quality of petrol and diesel fuels and 2009/28/EC on the promotion of the use of energy from renewable sources, *Official Journal of The European Union*, The European Parliament and the Council of the European Union, 2015.
- [14] S.S. Hassan, G.A. Williams, A.K. Jaiswal, Moving towards the second generation of lignocellulosic biorefineries in the EU: Drivers, challenges, and opportunities, *Renew. Sustain. Energy Rev.* 101 (2019) 590–599. <https://doi.org/10.1016/j.rser.2018.11.041>.
- [15] H. Kawaguchi, T. Hasunuma, C. Ogino, A. Kondo, Bioprocessing of bio-based chemicals produced from lignocellulosic feedstocks, *Curr. Opin. Biotechnol.* 42 (2016) 30–39. <https://doi.org/10.1016/j.copbio.2016.02.031>.
- [16] M.J. Bidy, C.J. Scarlata, C.M. Kinchin, *Chemicals from biomass: A market assessment of bioproducts with near-term potential*, NREL Rep. (2016).

- <https://doi.org/10.2172/1244312>.
- [17] P. Mäki-Arvela, T. Salmi, B. Holmbom, S. Willför, D.Y. Murzin, Synthesis of sugars by hydrolysis of hemicelluloses- A review, *Chem. Rev.* 111 (2011) 5638–5666. <https://doi.org/10.1021/cr2000042>.
- [18] P. Havlík, U.A. Schneider, E. Schmid, H. Böttcher, S. Fritz, R. Skalský, K. Aoki, S. De Cara, G. Kindermann, F. Kraxner, S. Leduc, I. McCallum, A. Mosnier, T. Sauer, M. Obersteiner, Global land-use implications of first and second generation biofuel targets, *Energy Policy.* 39 (2011) 5690–5702. <https://doi.org/10.1016/j.enpol.2010.03.030>.
- [19] F. Dalena, A. Senatore, M. Basile, D. Marino, A. Basile, From sugars to ethanol— from agricultural wastes to algal sources: An overview, in: *Second Third Gener. Feed.*, Elsevier Inc., Amsterdam, Netherlands, 2019: pp. 3–34. <https://doi.org/10.1016/b978-0-12-815162-4.00001-x>.
- [20] B. Kamm, P.R. Gruber, M. Kamm, *Biorefineries-Industrial Processes and Products. Status Quo and Future Directions*, Wiley, Weinheim, Germany, 2006.
- [21] C. Panoutsou, Overview report on the current status of biomass for bioenergy, biofuels and biomaterials in EU, Western Balkans, Ukraine, Turkey and Moldova, London, United Kingdom, 2016.
- [22] L. Rytter, K. Andreassen, J. Bergh, P.-M. Ekö, A. Kilpeläinen, D. Lazdina, P. Muiste, T. Nord-Larsen, Land areas and biomass production for current and future use in the Nordic and Baltic countries, Denmark, 2014.
- [23] C.S. Nunes, A. Kunamneni, Laccases-properties and applications, in: J.A. Truesdell (Ed.), *Enzym. Hum. Anim. Nutr. Princ. Perspect.*, Elsevier Inc., London, United Kingdom, 2018: pp. 133–161. <https://doi.org/10.1016/B978-0-12-805419-2.00007-1>.
- [24] F. Deswarte, *Introduction to Chemicals from Biomass*, Wiley, Cornwall, 2011.
- [25] G.T. Marangwanda, D.M. Madyira, T.O. Babarinde, Combustion models for biomass: A review, *Energy Reports.* 6 (2020) 664–672. <https://doi.org/10.1016/j.egy.2019.11.135>.
- [26] K. Veijonen, P. Vainikka, T. Järvinen, L. Eija, Biomass co-firing: an efficient way to reduce greenhouse gas emissions, n.d.
- [27] D.A. Tillman, Biomass cofiring: The technology, the experience, the combustion consequences, *Biomass and Bioenergy.* 19 (2000) 365–384. [https://doi.org/10.1016/S0961-9534\(00\)00049-0](https://doi.org/10.1016/S0961-9534(00)00049-0).
- [28] P. Kumar, D.M. Barrett, M.J. Delwiche, P. Stroeve, Methods for pretreatment of lignocellulosic biomass for efficient hydrolysis and biofuel production, *Ind. Eng. Chem. Res.* 48 (2009) 3713–3729. <https://doi.org/10.1021/ie801542g>.
- [29] A. Kumar, D.D. Jones, M.A. Hanna, Thermochemical biomass gasification: A review of the current status of the technology, *Energies.* 2 (2009) 556–581. <https://doi.org/10.3390/en20300556>.
- [30] A. Molino, S. Chianese, D. Musmarra, Biomass gasification technology: The state of the art overview, *J. Energy Chem.* 25 (2016) 10–25. <https://doi.org/10.1016/j.jechem.2015.11.005>.
- [31] J.S. Kim, G.G. Choi, A. V. Bridgwater, N. Abdoulmoumine, S. Adhikari, A. Kulkarni, S.

- Chattanathan, A. Kumar, D.D. Jones, M.A. Hanna, Review of fast pyrolysis of biomass and product upgrading, *Appl. Energy*. 2 (2018) 556–581. <https://doi.org/10.1016/j.biombioe.2011.01.048>.
- [32] X. Hu, M. Gholizadeh, Biomass pyrolysis: A review of the process development and challenges from initial researches up to the commercialisation stage, *J. Energy Chem.* 39 (2019) 109–143. <https://doi.org/10.1016/j.jechem.2019.01.024>.
- [33] BTG Bioliquids, BTG Pyrolysis plant, Hengelo, The Netherlands, (n.d.). <https://www.btg-bioliquids.com/plant/empyro-hengelo/>.
- [34] S. Mandal, R. Bandyopadhyay, A.K. Das, Thermo-catalytic process for conversion of lignocellulosic biomass to fuels and chemicals: a review, *Int. J. Petrochemical Sci. Eng.* 3 (2018) 77–89. <https://doi.org/10.15406/ipcse.2018.03.00077>.
- [35] G.W. Huber, S. Iborra, A. Corma, Synthesis of transportation fuels from biomass: Chemistry, catalysts, and engineering, *Chem. Rev.* 106 (2006) 4044–4098. <https://doi.org/10.1021/cr068360d>.
- [36] S.I. Mussatto, G.M. Dragone, Biomass Pretreatment, Biorefineries, and Potential Products for a Bioeconomy Development, in: *Biomass Fractionation Technol. a Lignocellul. Feed. Based Biorefinery*, Elsevier Inc., 2016: pp. 1–22. <https://doi.org/10.1016/B978-0-12-802323-5.00001-3>.
- [37] L. Mesa, Y. Albornas, M. Morales, G. Corsano, E. González, Integration of Organosolv Process for Biomass Pretreatment in a Biorefinery, *Biomass Fractionation Technol. a Lignocellul. Feed. Based Biorefinery*. (2016) 229–254. <https://doi.org/10.1016/B978-0-12-802323-5.00011-6>.
- [38] H. Chen, *Lignocellulose biorefinery feedstock engineering*, 2015. <https://doi.org/10.1016/b978-0-08-100135-6.00003-x>.
- [39] W. Stelte, Steam explosion for biomass pre-treatment, *Danish Technol. Inst.* (2013) 1–15.
- [40] S. Brethauer, M.H. Studer, Biochemical conversion processes of lignocellulosic biomass to fuels and chemicals - A review, *Chimia (Aarau)*. 69 (2015) 572–581. <https://doi.org/10.2533/chimia.2015.572>.
- [41] K. Vasić, Ž. Knez, M. Leitgeb, Bioethanol production by enzymatic hydrolysis from different lignocellulosic sources, *Molecules*. 26 (2021). <https://doi.org/10.3390/molecules26030753>.
- [42] S.Y. Li, Z.P. Wang, L.N. Wang, J.X. Peng, Y.N. Wang, Y.T. Han, S.F. Zhao, Combined enzymatic hydrolysis and selective fermentation for green production of alginate oligosaccharides from *Laminaria japonica*, *Bioresour. Technol.* 281 (2019) 84–89. <https://doi.org/10.1016/j.biortech.2019.02.056>.
- [43] M. Idrees, A. Adnan, S.A. Bokhari, F.A. Qureshi, Production of fermentable sugars by combined chemo-enzymatic hydrolysis of cellulosic material for bioethanol production, *Brazilian J. Chem. Eng.* 31 (2014) 355–363. <https://doi.org/10.1590/0104-6632.20140312s00002415>.
- [44] A. V. Bridgwater, Review of fast pyrolysis of biomass and product upgrading, *Biomass and Bioenergy*. 38 (2012) 68–94. <https://doi.org/10.1016/j.biombioe.2011.01.048>.
- [45] J.S. Kim, G.G. Choi, Pyrolysis of lignocellulosic biomass for biochemical production,

- in: *Waste Biorefinery Potential Perspect.*, Elsevier B.V., Amsterdam, Netherlands, 2018: pp. 323–348. <https://doi.org/10.1016/B978-0-444-63992-9.00011-2>.
- [46] J.K. Neathery, *Biomass Gasification*, RSC Energy Environ. Ser. 2010 (2010) 67–94. <https://doi.org/10.1016/b978-1-78242-269-3.50018-8>.
- [47] N. Abdoulmoumine, S. Adhikari, A. Kulkarni, S. Chattanathan, A review on biomass gasification syngas cleanup, *Appl. Energy*. 155 (2015) 294–307. <https://doi.org/10.1016/j.apenergy.2015.05.095>.
- [48] A.R.K. Gollakota, N. Kishore, S. Gu, A review on hydrothermal liquefaction of biomass, *Renew. Sustain. Energy Rev.* 81 (2018) 1378–1392. <https://doi.org/10.1016/j.rser.2017.05.178>.
- [49] L. Singh, V.C. Kalia, *Liquefaction of Biomass for Bio-oil Products*, *Waste Biomass Manag. - A Holist. Approach.* (2017) 1–392. <https://doi.org/10.1007/978-3-319-49595-8>.
- [50] M. Balat, Production of bioethanol from lignocellulosic materials via the biochemical pathway: A review, *Energy Convers. Manag.* 52 (2011) 858–875. <https://doi.org/10.1016/j.enconman.2010.08.013>.
- [51] R.P. John, K.M. Nampoothiri, A. Pandey, Fermentative production of lactic acid from biomass: An overview on process developments and future perspectives, *Appl. Microbiol. Biotechnol.* 74 (2007) 524–534. <https://doi.org/10.1007/s00253-006-0779-6>.
- [52] J.K. Ko, T. Enkh-Amgalan, G. Gong, Y. Um, S.M. Lee, Improved bioconversion of lignocellulosic biomass by *Saccharomyces cerevisiae* engineered for tolerance to acetic acid, *GCB Bioenergy*. 12 (2020) 90–100. <https://doi.org/10.1111/gcbb.12656>.
- [53] R. Bedoić, L. Čuček, B. Čosić, D. Krajnc, G. Smoljanić, Z. Kravanja, D. Ljubas, T. Pukšec, N. Duić, Green biomass to biogas – A study on anaerobic digestion of residue grass, *J. Clean. Prod.* 213 (2019) 700–709. <https://doi.org/10.1016/j.jclepro.2018.12.224>.
- [54] P. Weiland, Biogas production: Current state and perspectives, *Appl. Microbiol. Biotechnol.* 85 (2010) 849–860. <https://doi.org/10.1007/s00253-009-2246-7>.
- [55] A.A. Modenbach, S.E. Nokes, Enzymatic hydrolysis of biomass at high-solids loadings - A review, *Biomass and Bioenergy*. 56 (2013) 526–544. <https://doi.org/10.1016/j.biombioe.2013.05.031>.
- [56] S. Sun, R. Yang, X. Wang, S. Yan, Hydrogenation and hydrodeoxygenation of biomass-derived oxygenates to liquid alkanes for transportation fuels, *Data Br.* 17 (2018) 638–646. <https://doi.org/10.1016/j.dib.2018.01.069>.
- [57] R. Fang, H. Liu, R. Luque, Y. Li, Efficient and selective hydrogenation of biomass-derived furfural to cyclopentanone using Ru catalysts, *Green Chem.* 17 (2015) 4183–4188. <https://doi.org/10.1039/c5gc01462j>.
- [58] M.J. Gilkey, B. Xu, Heterogeneous Catalytic Transfer Hydrogenation as an Effective Pathway in Biomass Upgrading, *ACS Catal.* 6 (2016) 1420–1436. <https://doi.org/10.1021/acscatal.5b02171>.
- [59] S.R. Collinson, W. Thielemans, The catalytic oxidation of biomass to new materials focusing on starch, cellulose and lignin, *Coord. Chem. Rev.* 254 (2010) 1854–1870. <https://doi.org/10.1016/j.ccr.2010.04.007>.

- [60] Y. Hou, M. Niu, W. Wu, Catalytic Oxidation of Biomass to Formic Acid Using O₂ as an Oxidant, *Ind. Eng. Chem. Res.* 59 (2020) 16899–16910. <https://doi.org/10.1021/acs.iecr.0c01088>.
- [61] D.Y.C. Leung, X. Wu, M.K.H. Leung, A review on biodiesel production using catalyzed transesterification, *Appl. Energy.* 87 (2010) 1083–1095. <https://doi.org/10.1016/j.apenergy.2009.10.006>.
- [62] J. Vakros, Biochars and their use as transesterification catalysts for biodiesel production: A short review, *Catalysts.* 8 (2018) 562. <https://doi.org/10.3390/catal8110562>.
- [63] K. Kohli, R. Prajapati, B.K. Sharma, Bio-based chemicals from renewable biomass for integrated biorefineries, *Energies.* 12 (2019) 233. <https://doi.org/10.3390/en12020233>.
- [64] P. Harmsen, W. Huijgen, L. Bermudez, R. Bakker, Literature review of physical and chemical pretreatment processes for lignocellulosic biomass, Wageningen, The Netherlands, 2010.
- [65] A. Hommes, H.J. Heeres, J. Yue, Catalytic Transformation of Biomass Derivatives to Value-Added Chemicals and Fuels in Continuous Flow Microreactors, *ChemCatChem.* 11 (2019) 4671–4708. <https://doi.org/10.1002/cctc.201900807>.
- [66] R. Alén, Manufacturing Cellulosic Fibres for Making Paper: A Historical Perspective, Springer International Publishing, 2018. https://doi.org/10.1007/978-3-319-94962-8_2.
- [67] D. Zhang, M.J. Dumont, Advances in polymer precursors and bio-based polymers synthesized from 5-hydroxymethylfurfural, *J. Polym. Sci. Part A Polym. Chem.* 55 (2017) 1478–1492. <https://doi.org/10.1002/pola.28527>.
- [68] J.F. Harris, A.J. Baker, A.H. Conner, T.W. Jeffries, J.L. Minor, R.C. Pettersen, R.W. Scott, E.L. Springer, T.H. Wegner, J.I. Zerbe, Two-stage, dilute sulfuric acid hydrolysis of wood : an investigation of fundamentals, *Gen. Tech. Rep. FPL-45.* Madison, WI U.S. Dep. Agric. For. Serv. For. Prod. Lab. 1985. 73 P. 45 (1985) 1–73. <https://doi.org/10.2737/FPL-GTR-45>.
- [69] X. Huang, T.I. Korányi, M.D. Boot, E.J.M. Hensen, Catalytic depolymerization of lignin in supercritical ethanol, *ChemSusChem.* 7 (2014) 2276–2288. <https://doi.org/10.1002/cssc.201402094>.
- [70] F. Lu, J. Ralph, Lignin, in: *Cereal Straw as a Resour. Sustain. Biomater. Biofuels*, 1st ed., Elsevier, Madison, WI, USA, 2010: pp. 169–207. <https://doi.org/10.1016/B978-0-444-53234-3.00006-7>.
- [71] P.D. Kouris, X. Huang, M.D. Boot, E.J.M. Hensen, Scaling-Up Catalytic Depolymerisation of Lignin: Performance Criteria for Industrial Operation, *Top. Catal.* 61 (2018) 1901–1911. <https://doi.org/10.1007/s11244-018-1048-5>.
- [72] V.F. Wendisch, Y. Kim, J.H. Lee, Chemicals from lignin: Recent depolymerization techniques and upgrading extended pathways, *Curr. Opin. Green Sustain. Chem.* 14 (2018) 33–39. <https://doi.org/10.1016/j.cogsc.2018.05.006>.
- [73] T. Yoshikawa, T. Yagi, S. Shinohara, T. Fukunaga, Y. Nakasaka, T. Tago, T. Masuda, Production of phenols from lignin via depolymerization and catalytic cracking, *Fuel Process. Technol.* 108 (2013) 69–75. <https://doi.org/10.1016/j.fuproc.2012.05.003>.

- [74] C. Liu, S. Wu, H. Zhang, R. Xiao, Catalytic oxidation of lignin to valuable biomass-based platform chemicals: A review, *Fuel Process. Technol.* 191 (2019) 181–201. <https://doi.org/10.1016/j.fuproc.2019.04.007>.
- [75] L. Zhang, G. Hu, S. Hu, J. Xiang, X. Hu, Y. Wang, D. Geng, Hydrogenation of fourteen biomass-derived phenolics in water and in methanol: Their distinct reaction behaviours, *Sustain. Energy Fuels*. 2 (2018) 751–758. <https://doi.org/10.1039/c8se00006a>.
- [76] B. Abdullah, S.A.F.A.S. Muhammad, N.A.N. Mahmood, Production of Biofuel via Hydrogenation of Lignin from Biomass, in: *New Adv. Hydrog. Process. Appl.*, 2017: p. 13.
- [77] A.J.J.E. Eerhart, M.K. Patel, A.P.C. Faaij, Fuels and plastics from lignocellulosic biomass via the furan pathway: An economic analysis, *Biofuels, Bioprod. Biorefining*. 9 (2015) 307–325. <https://doi.org/10.1002/bbb.1537>.
- [78] M. Kabbour, R. Luque, Furfural as a platform chemical: From production to applications, in: *Biomass, Biofuels, Biochem. Recent Adv. Dev. Platf. Chem.*, Elsevier B.V., Amsterdam, Netherlands, 2019: pp. 283–297. <https://doi.org/10.1016/B978-0-444-64307-0.00010-X>.
- [79] P. Dongre, M. Driscoll, T. Amidon, B. Bujanovic, Lignin-furfural based adhesives, *Energies*. 8 (2015) 7897–7914. <https://doi.org/10.3390/en8087897>.
- [80] M. Dashtban, A. Gilbert, P. Fatehi, Production of furfural: Overview and challenges, *J-For*. 2 (2012) 44–53. <https://doi.org/DOI> <https://doi.org/10.1039/C3RA45396K>.
- [81] J.P. Lange, E. Van Der Heide, J. Van Buijtenen, R. Price, Furfural-A promising platform for lignocellulosic biofuels, *ChemSusChem*. 5 (2012) 150–166. <https://doi.org/10.1002/cssc.201100648>.
- [82] L.C. Kemp, Jr., G.B. Hamilton, H.H. Gross, Furfural as a Selective Solvent in Petroleum Refining., *Ind. Eng. Chem.* 40 (1948) 220–227. <https://doi.org/10.1021/ie50458a009>.
- [83] D. Crighton, Risk Assessment, *Appl. Psychol. to Forensic Pract.* (2008) 64–81. <https://doi.org/10.1002/9780470693971.ch4>.
- [84] K.J. Zeitsch, *The Chemistry and Technology of Furfural and its Many By-products*, Elsevier B.V., Amsterdam, The Netherlands, 2001.
- [85] R. Kroes, Safety evaluation of certain food additives: Furfural (WHO Food Additives Series 42), (1999) 1–14.
- [86] F. Kerkel, M. Markiewicz, S. Stolte, E. Müller, W. Kunz, The green platform molecule gamma-valerolactone - ecotoxicity, biodegradability, solvent properties, and potential applications, *Green Chem.* 23 (2021) 2962–2976. <https://doi.org/10.1039/d0gc04353b>.
- [87] T. Raj, K. Chandrasekhar, R. Banu, J.J. Yoon, G. Kumar, S.H. Kim, Synthesis of γ -valerolactone (GVL) and their applications for lignocellulosic deconstruction for sustainable green biorefineries, *Fuel*. 303 (2021) 121333. <https://doi.org/10.1016/j.fuel.2021.121333>.
- [88] M.A. Ershov, E. V. Grigoreva, A.I. Guseva, N.Y. Vinogradova, P.A. Nikul'shin, V.S. Dorokhov, Prospects for the Use of Furfural Derivatives in Gasoline, *Chem. Technol. Fuels Oils*. 53 (2018) 830–834. <https://doi.org/10.1007/s10553-018-0868-0>.

- [89] I. V. Bessonov, M.N. Kopitsyna, A. V. Polezhaev, V.A. Nelyub, A mechanistic study of the reaction between furfural-acetone resins and polyamines, *Polym. Sci. - Ser. D.* 9 (2016) 17–21. <https://doi.org/10.1134/S1995421216010044>.
- [90] J. Zhang, H. Chen, A. Pizzi, Y. Li, Q. Gao, J. Li, Characterization and application of urea-formaldehyde- furfural co-condensed resins as wood adhesives, *BioResources.* 9 (2014) 6267–6276. <https://doi.org/10.15376/biores.9.4.6267-6276>.
- [91] X. Lun-gang, Z. Hong-bo, X. Xiang, Z. Jin-lü, Y. Jian, Pyrolysis of furfural-acetone resin as matrix precursor for new carbon materials, *J. Cent. South Univ. Technol.* 15 (2008) 753–756. <https://doi.org/10.1007/s11771-008-0139-z>.
- [92] J. Liu, J. Wang, Y. Fu, J. Chang, Synthesis and characterization of phenol-furfural resins using lignin modified by a low transition temperature mixture, *RSC Adv.* 6 (2016) 94588–94594. <https://doi.org/10.1039/c6ra17877d>.
- [93] L.H. Brown, Resin Forming Reactions of Furfural and Phenol, *Ind. Eng. Chem.* 44 (1952) 2673–2675. <https://doi.org/10.1021/ie50515a051>.
- [94] A.T. Adeleye, H. Louis, O.U. Akakuru, I. Joseph, O.C. Enudi, D.P. Michael, A Review on the conversion of levulinic acid and its esters to various useful chemicals, *AIMS Energy.* 7 (2019) 165–185. <https://doi.org/10.3934/ENERGY.2019.2.165>.
- [95] V. Ghorpade, M. Hanna, Industrial Applications for Levulinic Acid, *Cereals.* (1997) 49–55. https://doi.org/10.1007/978-1-4757-2675-6_7.
- [96] K. Huang, Z.J. Brentzel, K.J. Barnett, J.A. Dumesic, G.W. Huber, C.T. Maravelias, Conversion of Furfural to 1,5-Pentanediol: Process Synthesis and Analysis, *ACS Sustain. Chem. Eng.* 5 (2017) 4699–4706. <https://doi.org/10.1021/acssuschemeng.7b00059>.
- [97] S. Mailaram, P. Kumar, A. Kunamalla, P. Saklecha, S.K. Maity, Biomass, biorefinery, and biofuels, INC, 2021. <https://doi.org/10.1016/b978-0-12-822989-7.00003-2>.
- [98] M.N. Gebresillase, R.Q. Raguindin, J.G. Seo, Application of 2-methylfuran and 5-methylfurfural for the synthesis of C16 fuel precursor over fibrous silica-supported heteropoly acid-functionalized ionic liquid, *Korean J. Chem. Eng.* 38 (2021) 1170–1178. <https://doi.org/10.1007/s11814-021-0768-6>.
- [99] D. Heggie, William, J. Bandarra, Process for the preparation of mometasone furoate, EP1074558 B1, 2002.
- [100] A.K. Mathew, A. Abraham, K.K. Mallapureddy, R.K. Sukumaran, Lignocellulosic biorefinery wastes, or resources?, in: *Waste Biorefinery Potential Perspect.*, Elsevier B.V., Amsterdam, Netherlands, 2018: pp. 267–297. <https://doi.org/10.1016/B978-0-444-63992-9.00009-4>.
- [101] A. Yousuf, D. Pirozzi, F. Sannino, Fundamentals of lignocellulosic biomass, INC, 2019. <https://doi.org/10.1016/B978-0-12-815936-1.00001-0>.
- [102] N. Ahmad, M.R. Zakaria, Oligosaccharide from hemicellulose, *Lignocellul. Futur. Bioeconomy.* (2019) 135–152. <https://doi.org/10.1016/B978-0-12-816354-2.00008-6>.
- [103] H. Kobayashi, A. Fukuoka, Current Catalytic Processes for Biomass Conversion, in: *New Futur. Dev. Catal. Catal. Biomass Convers.*, Elsevier B.V., Amsterdam, Netherlands, 2013: pp. 29–52. <https://doi.org/10.1016/B978-0-444-53878-9.00002-3>.

- [104] C. Delattre, T.A. Fenoradosoa, P. Michaud, Galactans: An overview of their most important sourcing and applications as natural polysaccharides, *Brazilian Arch. Biol. Technol.* 54 (2011) 1075–1092. <https://doi.org/10.1590/S1516-89132011000600002>.
- [105] C.J. Biermann, Hydrolysis and other cleavage of glycosidic linkages, *Anal. Carbohydrates by GLC MS.* 46 (1989) 27–41.
- [106] C.L. Stylianopoulos, Carbohydrates | Chemistry and Classification, *Encycl. Hum. Nutr.* (2005) 303–309. <https://doi.org/10.1016/B0-12-226694-3/00042-9>.
- [107] M.J. Antal, T. Leesomboon, W.S. Mok, G.N. Richards, Mechanism of formation of 2-furaldehyde from d-xylose, *Carbohydr. Res.* 217 (1991) 71–85. [https://doi.org/10.1016/0008-6215\(91\)84118-X](https://doi.org/10.1016/0008-6215(91)84118-X).
- [108] R. Weingarten, J. Cho, W.C. Conner, Jr., G.W. Huber, Kinetics of furfural production by dehydration of xylose in a biphasic reactor with microwave heating, *Green Chem.* 12 (2010) 1423. <http://xlink.rsc.org/?DOI=c003459b>.
- [109] B. Danon, G. Marcotullio, W. de Jong, Mechanistic and kinetic aspects of pentose dehydration towards furfural in aqueous media employing homogeneous catalysis, *Green Chem.* 16 (2014) 39–54. <https://doi.org/10.1039/c3gc41351a>.
- [110] M. Papaioannou, R.J.T. Kleijwegt, J. van der Schaaf, M.F. Neira d'Angelo, Furfural Production by Continuous Reactive Extraction in a Millireactor under the Taylor Flow Regime, *Ind. Eng. Chem. Res.* (2019) 16106–16115. <https://doi.org/10.1021/acs.iecr.9b00604>.
- [111] Z. Chen, W. Zhang, J. Xu, P. Li, Kinetics of xylose dehydration into furfural in acetic acid, *Chinese J. Chem. Eng.* 23 (2015) 659–666. <https://doi.org/10.1016/j.cjche.2013.08.003>.
- [112] K. Dussan, B. Girisuta, M. Lopes, J.J. Leahy, M.H.B. Hayes, Conversion of hemicellulose sugars catalyzed by formic acid: Kinetics of the dehydration of D -xylose, L -arabinose, and D -glucose, *ChemSusChem.* 8 (2015) 1411–1428. <https://doi.org/10.1002/cssc.201403328>.
- [113] C. D. Hurd, L. L. Isenhour., Pentoses Reactions. I. Furfural Formation, *J. Am. Chem. Soc.* 1255 (1932) 1927–1929. <https://doi.org/10.1021/ja01340a048>.
- [114] W.A. Bonner, M.R. Roth, M.R. Roth, The Conversion of D-Xylose-l-C14 into 2-Furaldehyde-a-C14, 81 (1958) 5454–5456. <https://doi.org/10.1021/ja01529a051>.
- [115] M.R. Nimlos, X. Qian, M. Davis, M.E. Himmel, D.K. Johnson, Energetics of xylose decomposition as determined using quantum mechanics modeling, *J. Phys. Chem. A.* 110 (2006) 11824–11838. <https://doi.org/10.1021/jp0626770>.
- [116] X. Qian, D.K. Johnson, M.E. Himmel, M.R. Nimlos, The role of hydrogen-bonding interactions in acidic sugar reaction pathways, *Carbohydr. Res.* 345 (2010) 1945–1951. <https://doi.org/10.1016/j.carres.2010.07.008>.
- [117] E.R. Garrett, B.H. Dvorchik, Kinetics and mechanisms of the acid degradation of the aldopentoses to furfural, *J. Pharm. Sci.* 58 (1969) 813–820. <https://doi.org/10.1002/jps.2600580703>.
- [118] V. Choudhary, S.I. Sandler, D.G. Vlachos, Conversion of xylose to furfural using Lewis and Bronsted acid catalysts in aqueous media, *ACS Catal.* 2 (2012) 2022–2028. <https://doi.org/10.1021/cs300265d>.

- [119] J.E. Romo, N. V. Bollar, C.J. Zimmermann, S.G. Wettstein, Conversion of Sugars and Biomass to Furans Using Heterogeneous Catalysts in Biphasic Solvent Systems, *ChemCatChem*. 10 (2018) 4819–4830. <https://doi.org/10.1002/cctc.201800926>.
- [120] C. Moreau, R. Durand, D. Peyron, J. Duhamet, P. Rivalier, Selective preparation of furfural from xylose over microporous solid acid catalysts, *Ind. Crops Prod.* 7 (1998) 95–99. [https://doi.org/10.1016/S0926-6690\(97\)00037-X](https://doi.org/10.1016/S0926-6690(97)00037-X).
- [121] I. Agirrezabal-Telleria, A. Larreategui, J. Requies, M.B. Güemez, P.L. Arias, Furfural production from xylose using sulfonic ion-exchange resins (Amberlyst) and simultaneous stripping with nitrogen, *Bioresour. Technol.* 102 (2011) 7478–7485. <http://dx.doi.org/10.1016/j.biortech.2011.05.015>.
- [122] B. Danon, L. Van Der Aa, W. De Jong, Furfural degradation in a dilute acidic and saline solution in the presence of glucose, *Carbohydr. Res.* 375 (2013) 145–152. <http://dx.doi.org/10.1016/j.carres.2013.04.030>.
- [123] V. Krzelj, J. Ferreira Liberal, M. Papaioannou, J. Van Der Schaaf, M.F. Neira D'Angelo, Kinetic Model of Xylose Dehydration for a Wide Range of Sulfuric Acid Concentrations, *Ind. Eng. Chem. Res.* 59 (2020) 11991–12003. <https://doi.org/10.1021/acs.iecr.0c01197>.
- [124] Dunlop A.P., Furfural formation and behaviour, *Ind. Eng. Chem.* 40 (1948) 204–209. <https://doi.org/10.1021/ie50458a006>.
- [125] G. Marcotullio, *The Chemistry and technology of furfural production in modern lignocellulose-feedstock biorefineries*, Delft University, 2011.
- [126] D. Yasuda, *Modeling the conversion of arabinose to furfural*, Oregon State University, 1989.
- [127] A.M.J. Kootstra, N.S. Mosier, E.L. Scott, H.H. Beeftink, J.P.M. Sanders, Differential effects of mineral and organic acids on the kinetics of arabinose degradation under lignocellulose pretreatment conditions, *Biochem. Eng. J.* 43 (2009) 92–97. <https://doi.org/10.1016/j.bej.2008.09.004>.
- [128] F.M. Size, F.M. Size, T. Analysis, R. By, Report Coverage & Deliverables End-use Insights, (2021) 1–6.
- [129] IFC, Central Romana Corporation, (2021) 2021.
- [130] G. Newswire, T. Furfural, R. Material, S. Bagasse, Global Furfural Market 2019-2024 - Emerging Demand for Furfural Derivatives (Apart From Furfuryl Alcohol) in Various Applications, 2019 (2019).
- [131] J.F.L. Silva, M.A. Selicani, T.L. Junqueira, B.C. Klein, S. Vaz, A. Bonomi, Integrated furfural and first generation bioethanol production: Process simulation and technoeconomic analysis, *Brazilian J. Chem. Eng.* 34 (2017) 623–634. <https://doi.org/10.1590/0104-6632.20170343s20150643>.
- [132] J.G. Segovia-Hernández, E. Sánchez-Ramírez, C. Ramírez-Márquez, G. Contreras-Zarazúa, Furfural, in: *Improv. Bio-Based Build. Blocks Prod. Through Process Intensif. Sustain. Concepts*, 2022. <https://doi.org/10.1016/B978-0-323-89870-6.00008-1>.
- [133] W. De Jong, G. Marcotullio, Overview of biorefineries based on co-production of furfural, existing concepts and novel developments, *Int. J. Chem. React. Eng.* 8 (2010). <https://doi.org/10.2202/1542-6580.2174>.

- [134] J. Gravitis, N. Vedernikov, J. Zandersons, A. Kokorevics, K. Mochidzuki, A. Sakoda, M. Suzuki, *Chemicals and biofuels from hardwoods, fuel crops and agricultural wastes*, (2000) 1–5.
- [135] X. Pan, N. Gilkes, J. Kadla, K. Pye, S. Saka, D. Gregg, K. Ehara, D. Xie, D. Lam, J. Saddler, *Bioconversion of hybrid poplar to ethanol and co-products using an organosolv fractionation process: Optimization of process yields*, *Biotechnol. Bioeng.* 94 (2006) 851–861. <https://doi.org/10.1002/bit.20905>.
- [136] W. Guo, *Development of Catalytic Strategies and Microreactor Technology for the Synthesis of Bio-based Furanics from Lignocellulose- derived Carbohydrates*, 2021.
- [137] Lenzing AG, *The origin of solutions: LENZING™*, (2022). <https://www.lenzing.com/de/produkte/lenzingtm>.
- [138] J.A. Haire, G.M. Lobel, *Responsible Production Initiatives, Keys to Prod. Off.* (2022) 165–179. <https://doi.org/10.4324/9781003252825-8>.
- [139] W. Guo, H.C. Bruining, H.J. Heeres, J. Yue, *Efficient synthesis of furfural from xylose over HCl catalyst in slug flow microreactors promoted by NaCl addition*, *AIChE J.* 68 (2022) 1–17. <https://doi.org/10.1002/aic.17606>.
- [140] S. Peleteiro, J.C. Parajó, S. Rivas, J.L. Alonso, V. Santos, *Furfural production using ionic liquids: A review*, *Bioresour. Technol.* 202 (2015) 181–191. <http://dx.doi.org/10.1016/j.biortech.2015.12.017>.
- [141] T. Huang, K. Yuan, X.L. Nie, J. Chen, H.X. Zhang, J.Z. Chen, W.M. Xiong, *Preparation of Furfural From Xylose Catalyzed by Diimidazole Hexafluorophosphate in Microwave*, *Front. Chem.* 9 (2021) 1–9. <https://doi.org/10.3389/fchem.2021.727382>.
- [142] C. Sener, A.H. Motagamwala, D.M. Alonso, J.A. Dumesic, *Enhanced Furfural Yields from Xylose Dehydration in the Γ -Valerolactone/Water Solvent System at Elevated Temperatures*, *ChemSusChem.* 11 (2018) 2321–2331. <https://doi.org/10.1002/cssc.201800730>.
- [143] Y. Luo, Z. Li, Y. Zuo, Z. Su, C. Hu, *A Simple Two-Step Method for the Selective Conversion of Hemicellulose in Pubescens to Furfural*, *ACS Sustain. Chem. Eng.* 5 (2017) 8137–8147. <https://doi.org/10.1021/acssuschemeng.7b01766>.
- [144] K. Xin, Y. Song, F. Dai, Y. Yu, Q. Li, *Liquid–liquid equilibria for the extraction of furfural from aqueous solution using different solvents*, *Fluid Phase Equilib.* 425 (2016) 393–401. <http://dx.doi.org/10.1016/j.fluid.2016.06.040>.
- [145] G. Gómez Millán, R.P. Bangalore Ashok, P. Oinas, J. Llorca, H. Sixta, *Furfural production from xylose and birch hydrolysate liquor in a biphasic system and techno-economic analysis*, *Biomass Convers. Biorefinery.* (2020). <https://doi.org/10.1007/s13399-020-00702-4>.
- [146] T. Brouwer, M. Blahusiak, K. Babic, B. Schuur, *Reactive extraction and recovery of levulinic acid, formic acid and furfural from aqueous solutions containing sulphuric acid*, *Sep. Purif. Technol.* 185 (2017) 186–195. <http://dx.doi.org/10.1016/j.seppur.2017.05.036>.
- [147] D.J.G.P. Van Osch, C.H.J.T. Dietz, S.E.E. Warrag, M.C. Kroon, *The Curious Case of Hydrophobic Deep Eutectic Solvents: A Story on the Discovery, Design, and Applications*, *ACS Sustain. Chem. Eng.* 8 (2020) 10591–10612.

- <https://doi.org/10.1021/acssuschemeng.0c00559>.
- [148] C.H.J.T. Dietz, M.C. Kroon, M. Di Stefano, M. Van Sint Annaland, F. Gallucci, Selective separation of furfural and hydroxymethylfurfural from an aqueous solution using a supported hydrophobic deep eutectic solvent liquid membrane, *Faraday Discuss.* 206 (2018) 77–92. <https://doi.org/10.1039/c7fd00152e>.
- [149] H. Ramshaw, Colin, *Process Intensification: Engineering for efficiency, sustainability and flexibility*, Elsevier B.V., Oxford, 2008.
- [150] F.J. Keil, *Process intensification*, *Rev. Chem. Eng.* 34 (2018) 135–200. <https://doi.org/10.1515/revce-2017-0085>.
- [151] A. I. Stankiewicz, J. A. Moulijn, *Process Intensification: Transforming Chemical Engineering*, *Chem. Eng. Prog.* 96 (2000) 22–34.
- [152] D. Reay, C. Ramshaw, A. Harvey, *Process Intensification - An Overview*, in: *Process Intensif. Eng. Effic. Sustain. Flex.*, 2008.
- [153] D. Reay, C. Ramshaw, A. Harvey, *The Mechanisms Involved in Process Intensification*, *Process Intensif.* (2013) 57–90. <https://doi.org/10.1016/b978-0-08-098304-2.00003-1>.
- [154] M. Meeuwse, J. van der Schaaf, J.C. Schouten, *Multistage Rotor-Stator Spinning Disc Reactor*, *AIChE J.* 58 (2012) 247–255. <https://doi.org/DOI.10.1002/aic>.
- [155] J. Yue, *Green process intensification using microreactor technology for the synthesis of biobased chemicals and fuels*, *Chem. Eng. Process. - Process Intensif.* 177 (2022) 109002. <https://doi.org/10.1016/j.cep.2022.109002>.
- [156] M. Meeuwse, S. Lempers, J. van der Schaaf, J.C. Schouten, *Liquid-Solid Mass Transfer and Reaction in a Rotor-Stator Spinning Disc Reactor*, *Ind. Eng. Chem. Res.* 49 (2010) 10751–10757.
- [157] S.K. Dhiman, V. Verma, D.P. Rao, M.S. Rao, *Process intensification in a trickle-bed reactor: Experimental studies*, *AIChE J.* 51 (2005) 3186–3192. <https://doi.org/10.1002/aic.10560>.
- [158] N. Mameda, H.J. Park, K.H. Choo, *Membrane electro-oxidizer: A new hybrid membrane system with electrochemical oxidation for enhanced organics and fouling control*, *Water Res.* 126 (2017) 40–49. <https://doi.org/10.1016/j.watres.2017.09.009>.
- [159] D.L. Grzenia, D.J. Schell, S. Ranil Wickramasinghe, *Detoxification of biomass hydrolysates by reactive membrane extraction*, *J. Memb. Sci.* 348 (2010) 6–12. <https://doi.org/10.1016/j.memsci.2009.10.035>.
- [160] V. Krzelj, J. Van Kampen, J. van der Schaaf, M.F. Neira D'Angelo, *Furfural Production by Reactive Stripping: Process Optimization by a Combined Modeling and Experimental Approach*, *Ind. Eng. Chem. Res.* 58 (2019) 16126–16137. <https://doi.org/10.1021/acs.iecr.9b00445>.
- [161] S. Kumar, S. Pandey, K.L. Wasewar, N. Ak, H. Uslu, *Reactive Extraction as an Intensifying Approach for the Recovery of Organic Acids from Aqueous Solution: A Comprehensive Review on Experimental and Theoretical Studies*, *J. Chem. Eng. Data.* 66 (2021) 1557–1573. <https://doi.org/10.1021/acs.jced.0c00405>.
- [162] X. Wang, Y. Wang, F. Li, L. Li, X. Ge, S. Zhang, T. Qiu, *Scale-up of microreactor: Effects of hydrodynamic diameter on liquid–liquid flow and mass transfer*, *Chem.*

- Eng. Sci. 226 (2020) 115838. <https://doi.org/10.1016/j.ces.2020.115838>.
- [163] J. Jovanovic, Liquid-liquid microreactors for phase transfer catalysis, 2017. <https://doi.org/10.6100/IR719772>.
- [164] E. Dłuska, S. Wroński, T. Ryszczuk, Interfacial area in gas-liquid Couette-Taylor flow reactor, *Exp. Therm. Fluid Sci.* 28 (2004) 467–472. <https://doi.org/10.1016/j.expthermflusci.2003.06.003>.
- [165] M. Oyevaar, A. Zijl, R. Westerterp, Interfacial areas and gas hold-ups at elevated pressures in a mechanically agitated gas-liquid reactor, *Chem. Eng. Technol.* 11 (1988) 1–10. <https://doi.org/10.1002/ceat.270110102>.
- [166] A.A. Yawalkar, A.B.M. Heesink, G.F. Versteeg, V.G. Pangarkar, Gas-liquid mass transfer coefficient in stirred tank reactors, *Can. J. Chem. Eng.* 80 (2002) 840–848. <https://doi.org/10.1002/cjce.5450800507>.
- [167] A. Kapic, T.J. Heindel, Correlating gas-liquid mass transfer in a stirred-tank reactor, *Chem. Eng. Res. Des.* 84 (2006) 239–245. <https://doi.org/10.1205/cherd.05117>.
- [168] F. Scargiali, A. Busciglio, F. Grisafi, A. Brucato, Influence of viscosity on mass transfer performance of unbaffled stirred vessels, *Chem. Eng. Trans.* 32 (2013) 1483–1488. <https://doi.org/10.33032/CET1332248>.
- [169] P. Angeli, A. Gavriilidis, Taylor Flow in Microchannels BT - Encyclopedia of Microfluidics and Nanofluidics, in: D. Li (Ed.), Springer US, Boston, MA, 2008: pp. 1971–1976. https://doi.org/10.1007/978-0-387-48998-8_1526.
- [170] P. Angeli, A. Gavriilidis, Hydrodynamics of Taylor flow in small channels: A review, *Proc. Inst. Mech. Eng. Part C J. Mech. Eng. Sci.* 222 (2008) 737–751. <https://doi.org/10.1243/09544062JMES776>.
- [171] A. Etminan, Y.S. Muzychka, K. Pope, A review on the hydrodynamics of Taylor flow in microchannels: Experimental and computational studies, *Processes*. 9 (2021). <https://doi.org/10.3390/pr9050870>.
- [172] S.S.Y. Leung, Y. Liu, D.F. Fletcher, B.S. Haynes, Heat transfer in well-characterised Taylor flow, *Chem. Eng. Sci.* 65 (2010) 6379–6388. <https://doi.org/10.1016/j.ces.2010.09.014>.
- [173] A. Abdollahi, S.E. Norris, R.N. Sharma, Fluid flow and heat transfer of liquid-liquid Taylor flow in square microchannels, *Appl. Therm. Eng.* 172 (2020) 115123. <https://doi.org/10.1016/j.applthermaleng.2020.115123>.
- [174] Y. Muranaka, K. Matsubara, T. Maki, S. Asano, H. Nakagawa, K. Mae, 5-Hydroxymethylfurfural Synthesis from Monosaccharides by a Biphasic Reaction-Extraction System Using a Microreactor and Extractor, *ACS Omega*. 5 (2020) 9384–9390. <https://doi.org/10.1021/acsomega.0c00399>.
- [175] J. Yue, Multiphase flow processing in microreactors combined with heterogeneous catalysis for efficient and sustainable chemical synthesis, *Catal. Today*. 308 (2018) 3–19. <https://doi.org/10.1016/j.cattod.2017.09.041>.
- [176] C. Aellig, D. Scholz, P.Y. Dapsens, C. Mondelli, J. Pérez-Ramírez, When catalyst meets reactor: Continuous biphasic processing of xylan to furfural over GaUSY/Amberlyst-36, *Catal. Sci. Technol.* 5 (2015) 142–149. <https://doi.org/10.1039/c4cy00973h>.
- [177] G.Y. Jeong, A.K. Singh, S. Sharma, K.W. Gyak, R.A. Maurya, D.P. Kim, One-flow

- syntheses of diverse heterocyclic furan chemicals directly from fructose via tandem transformation platform, *NPG Asia Mater.* 7 (2015) 3–10.
<https://doi.org/10.1038/am.2015.21>.
- [178] Z. Dong, Z. Wen, F. Zhao, S. Kuhn, T. Noël, Scale-up of micro- and milli-reactors: An overview of strategies, design principles and applications, *Chem. Eng. Sci.* X. 10 (2021) 100097. <https://doi.org/10.1016/j.cesx.2021.100097>.
- [179] D.T. Win, Furfural – Gold from Garbage, *Assumpt. Univ. J. Technol.* 8 (2005) 185–190.
- [180] X. Chen, L. Zhang, B. Zhang, X. Guo, X. Mu, Highly selective hydrogenation of furfural to furfuryl alcohol over Pt nanoparticles supported on g-C₃N₄ nanosheets catalysts in water, *Sci. Rep.* 6 (2016) 1–13. <https://doi.org/10.1038/srep28558>.
- [181] X. Wang, Y. Weng, X. Zhao, X. Xue, S. Meng, Z. Wang, W. Zhang, P. Duan, Q. Sun, Y. Zhang, Selective Hydrogenolysis and Hydrogenation of Furfuryl Alcohol in the Aqueous Phase Using Ru-Mn-Based Catalysts, *Ind. Eng. Chem. Res.* 59 (2020) 17210–17217. <https://doi.org/10.1021/acs.iecr.0c01023>.
- [182] J.N. Chheda, J.P. Lange, P.R. Weider, R.L. Blackburn, Process for preparing furfural from biomass, WO2016025678A1, 2016.
- [183] K. Stefan, A. Kindler, Production of furfural from xylose, WO2015087248A1, 2015.
- [184] T.Z. Evert van der Heide, METHOD FOR PRODUCING FURFURAL FROM LIGNOCELLULOSIC BIOMASS MATERIAL, n.d.
- [185] A. Mittal, S.K. Black, T.B. Vinzant, M. O'Brien, M.P. Tucker, D.K. Johnson, Production of Furfural from Process-Relevant Biomass-Derived Pentoses in a Biphasic Reaction System, *ACS Sustain. Chem. Eng.* 5 (2017) 5694–5701.
<https://doi.org/10.1021/acssuschemeng.7b00215>.
- [186] N. Sweygers, J. Harrer, R. Dewil, L. Appels, A microwave-assisted process for the in-situ production of 5-hydroxymethylfurfural and furfural from lignocellulosic polysaccharides in a biphasic reaction system, *J. Clean. Prod.* 187 (2018) 1014–1024. <https://doi.org/10.1016/j.jclepro.2018.03.204>.
- [187] Y. Zhu, W. Li, Y. Lu, T. Zhang, H. Jameel, H.M. Chang, L. Ma, Production of furfural from xylose and corn stover catalyzed by a novel porous carbon solid acid in γ -valerolactone, *RSC Adv.* 7 (2017) 29916–29924.
<https://doi.org/10.1039/c7ra03995f>.
- [188] Q. Lin, H. Li, X. Wang, L. Jian, J. Ren, C. Liu, R. Sun, SO₄²⁻/Sn-MMT solid acid catalyst for xylose and xylan conversion into furfural in the biphasic system, *Catalysts.* 7 (2017) 1–14. <https://doi.org/10.3390/catal7040118>.
- [189] B. Pholjaroen, N. Li, Z. Wang, A. Wang, T. Zhang, Dehydration of xylose to furfural over niobium phosphate catalyst in biphasic solvent system, *J. Energy Chem.* 22 (2013) 826–832. [https://doi.org/10.1016/S2095-4956\(14\)60260-6](https://doi.org/10.1016/S2095-4956(14)60260-6).
- [190] V. Krzelj, D.P. Ferrandez, M.F. Neira D'Angelo, Sulfonated foam catalysts for the continuous dehydration of xylose to furfural in biphasic media, *Catal. Today.* 365 (2021) 274–281. <https://doi.org/10.1016/j.cattod.2020.12.009>.
- [191] A. Demibras, Biomass Feedstocks, in: *Biofuels*, 2009: pp. 45–85.
http://link.springer.com/10.1007/978-1-84882-011-1_2.
- [192] B. Kamm, P.R. Gruber, M. Kamm, *Biorefineries – Industrial Processes and Products*,

- 1st editio, Wiley, Weinheim, 2006.
- [193] W.B. and T. Services, *Furfural Chemicals and Biofuels from Agriculture*, Sydney, Australia, 2006.
- [194] Q. Jing, X. Lu, Kinetics of Non-catalyzed Decomposition of D-xylose in High Temperature Liquid Water, *Chinese J. Chem. Eng.* 15 (2007) 666–669. [https://doi.org/10.1016/S1004-9541\(07\)60143-8](https://doi.org/10.1016/S1004-9541(07)60143-8).
- [195] K. Lamminpää, J. Ahola, J. Tanskanen, Kinetics of furfural destruction in a formic acid medium, *RSC Adv.* 4 (2014) 60243–60248. <http://xlink.rsc.org/?DOI=C4RA09276G>.
- [196] O. Ershova, J. Kanervo, S. Hellsten, H. Sixta, The role of xylulose as an intermediate in xylose conversion to furfural: insights via experiments and kinetic modelling, *RSC Adv.* 5 (2015) 66727–66737. <https://doi.org/10.1039/C5RA10855A>.
- [197] P.J. Oefner, A.H. Lanziner, G. Bonn, O. Bobleter, Quantitative studies on furfural and organic acid formation during hydrothermal, acidic and alkaline degradation of D-xylose, *Monatshefte Fur Chemie.* 123 (2004) 547–556. <https://doi.org/10.1007/BF00816848>.
- [198] J. Lessard, J.F. Morin, J.F. Wehrung, D. Magnin, E. Chornet, High yield conversion of residual pentoses into furfural via zeolite catalysis and catalytic hydrogenation of furfural to 2-methylfuran, *Top. Catal.* 53 (2010) 1231–1234. <https://doi.org/10.1007/s11244-010-9568-7>.
- [199] A.R.C. Morais, R. Bogel-Lukasik, Highly efficient and selective CO₂-adjunctive dehydration of xylose to furfural in aqueous media with THF, *Green Chem.* (2016) 2331–2334. <https://doi.org/10.1039/c5gc02863a>.
- [200] S. Peleteiro, A.M. Da Costa Lopes, G. Garrote, J.C. Parajó, R. Bogel-Lukasik, Simple and efficient furfural production from xylose in media containing 1-butyl-3-methylimidazolium hydrogen sulfate, *Ind. Eng. Chem. Res.* (2015) 8368–8373. <https://doi.org/10.1021/acs.iecr.5b01771>.
- [201] I. Agirrezabal-Telleria, I. Gandarias, P.L. Arias, Production of furfural from pentosan-rich biomass: Analysis of process parameters during simultaneous furfural stripping, *Bioresour. Technol.* 143 (2013) 258–264.
- [202] M. Meeuwse, Rotor-Stator Spinning Disc Reactor, Eindhoven University of Technology, 2011. <https://doi.org/10.6100/IR702643>.
- [203] L. Lin, S. Ma, P. Li, T. Zhu, H. Chang, Mutual Solubilities for the Water-2-sec-Butylphenol System and Partition Coefficients for Furfural and Formic Acid in the Water-2- sec -Butylphenol System, *J. Chem. Eng. Data.* 60 (2015) 1926–1933. <https://doi.org/10.1021/acs.jced.5b00170>.
- [204] L. Negahdar, I. Delidovich, R. Palkovits, Aqueous-phase hydrolysis of cellulose and hemicelluloses over molecular acidic catalysts: Insights into the kinetics and reaction mechanism, *Appl. Catal. B Environ.* 184 (2016) 285–298. <https://doi.org/10.1016/j.apcatb.2015.11.039>.
- [205] I.C. Rose, N. Epstein, A.P. Watkinson, Acid-Catalyzed 2-Furaldehyde (Furfural) Decomposition Kinetics, *Ind. Eng. Chem. Res.* 39 (2000) 843–845. <https://doi.org/10.1021/ie990550>.
- [206] D. Tsaoulidis, P. Angeli, Effect of channel size on mass transfer during liquid – liquid

- plug flow in small scale extractors, *Chem. Eng. J.* 262 (2015) 785–793. <http://dx.doi.org/10.1016/j.cej.2014.10.012>.
- [207] S.J.C. Meeuwse M., van der Schaaf J., Multistage Rotor-Stator Spinning Disc Reactor, *AIChE J.* 58 (2012) 247–255. <https://doi.org/10.1002/aic.12586>.
- [208] R. Cox, K. Salonitis, E. Rebrov, S.A. Impey, Revisiting the Effect of U-Bends, Flow Parameters, and Feasibility for Scale-Up on Residence Time Distribution Curves for a Continuous Bioprocessing Oscillatory Baffled Flow Reactor, *Ind. Eng. Chem. Res.* 61 (2022) 11181–11196. <https://doi.org/10.1021/acs.iecr.2c00822>.
- [209] D. Reay, C. Ramshaw, A. Harvey, *Reactors*, 2013. <https://doi.org/10.1016/b978-0-08-098304-2.00005-5>.
- [210] B.H. Um, G.P. Van Walsum, Acid hydrolysis of hemicellulose in green liquor pre-pulping extract of mixed northern hardwoods, *Appl. Biochem. Biotechnol.* 153 (2009) 127–138. <https://doi.org/10.1007/s12010-009-8561-8> Acid.
- [211] R. Xing, W. Qi, G.W. Huber, Production of furfural and carboxylic acids from waste aqueous hemicellulose solutions from the pulp and paper and cellulosic ethanol industries, *Energy Environ. Sci.* 4 (2011) 2193–2205. <https://doi.org/10.1039/c1ee01022k>.
- [212] A. Esteghlalian, A.G. Hashimoto, J.J. Fenske, M.H. Penner, Modeling and optimization of the dilute-sulfuric-acid pretreatment of corn stover, poplar and switchgrass, *Bioresour. Technol.* 59 (1997) 129–136. [https://doi.org/10.1016/S0960-8524\(97\)81606-9](https://doi.org/10.1016/S0960-8524(97)81606-9).
- [213] F.H. Isikgor, C.R. Becer, Lignocellulosic biomass: a sustainable platform for the production of bio-based chemicals and polymers, *Polym. Chem.* 6 (2015) 4497–4559. <https://doi.org/10.1039/C5PY00263J>.
- [214] H.E. Hoydonckx, W.M. Van Rhijn, W.M. Van Rhijn, D.E. De Vos, P.A. Jacobs, Furfural and Derivatives, *Ullmann's Encycl. Ind. Chem.* d (2007) 285–313. https://doi.org/10.1002/14356007.a12_119.pub2.
- [215] S.H. Shinde, A. Hengne, C. V. Rode, Lignocellulose-derived platform molecules: An introduction, in: *Biomass, Biofuels, Biochem. Recent Adv. Dev. Platf. Chem.*, Elsevier B.V., 2019: pp. 1–31. <https://doi.org/10.1016/B978-0-444-64307-0.00001-9>.
- [216] R. Pulicharla, L. Lonappan, S.K. Brar, M. Verma, Production of Renewable C5 Platform Chemicals and Potential Applications, in: *Platf. Chem. Biorefinery*, Elsevier Inc., 2016: pp. 201–216. <https://doi.org/10.1016/b978-0-12-802980-0.00011-0>.
- [217] J.M.R. Gallo, D.M. Alonso, M.A. Mellmer, J.H. Yeap, H.C. Wong, J.A. Dumesic, Production of furfural from lignocellulosic biomass using beta zeolite and biomass-derived solvent, *Top. Catal.* 56 (2013) 1775–1781. <https://doi.org/10.1007/s11244-013-0113-3>.
- [218] W.A. Bonner, M.R. Roth, The Conversion of D-Xylose-l-C14 into 2-Furaldehyde-a-C14, 81 (1958) 5454–5456. <https://doi.org/10.1021/ja01529a051>.
- [219] T. Ahmad, L. Kenne, K. Olsson, O. Theander, The formation of 2-furaldehyde and formic acid from pentoses in slightly acidic deuterium oxide studied by 1H NMR spectroscopy, *Carbohydr. Res.* 276 (1995) 309–320. [https://doi.org/10.1016/0008-6215\(95\)00176-T](https://doi.org/10.1016/0008-6215(95)00176-T).
- [220] K. Dussan, B. Girisuta, M. Lopes, J.J. Leahy, M.H.B. Hayes, Conversion of

- Hemicellulose Sugars Catalyzed by Formic Acid: Kinetics of the Dehydration of D-Xylose, L-Arabinose, and D-Glucose, *ChemSusChem*. 8 (2015) 1411–1428. <https://doi.org/10.1002/cssc.201403328>.
- [221] X. Hu, R.J.M. Westerhof, D. Dong, L. Wu, C. Li, Acid-Catalyzed Conversion of Xylose in 20 Solvents: Insight into Interactions of the Solvents with Xylose, Furfural, and the Acid Catalyst, *ACS Sustain. Chem. Eng.* (2014).
- [222] J. Ahola, J. Tanskanen, K. Lamminpää, Kinetics of xylose dehydration into furfural in formic acid, *Ind. Eng. Chem. Res.* 51 (2012) 6297–6303. <https://doi.org/10.1021/ie2018367>.
- [223] E. van der Heide, T. Zhang, Method for producing furfural from lignocellulosic biomass material, 2014. [https://patents.google.com/patent/US20110144359A1/en?q=US2011144359+\(A1\)+](https://patents.google.com/patent/US20110144359A1/en?q=US2011144359+(A1)+).
- [224] R. Weingarten, W.C. Conner, G.W. Huber, Production of levulinic acid from cellulose by hydrothermal decomposition combined with aqueous phase dehydration with a solid acid catalyst, *Energy Environ. Sci.* 5 (2012) 7559–7574. <https://doi.org/10.1039/c2ee21593d>.
- [225] D. Nabarlatz, X. Farriol, D. Montané, Kinetic modeling of the autohydrolysis of lignocellulosic biomass for the production of hemicellulose-derived oligosaccharides, *Ind. Eng. Chem. Res.* 43 (2004) 4124–4131. <https://doi.org/10.1021/ie034238i>.
- [226] B.P. Lavarack, G.J. Griffin, D. Rodman, The acid hydrolysis of sugarcane bagasse hemicellulose to produce xylose, arabinose, glucose and other products, *Biomass and Bioenergy*. 23 (2002) 367–380. [https://doi.org/10.1016/S0961-9534\(02\)00066-1](https://doi.org/10.1016/S0961-9534(02)00066-1).
- [227] E.I. Gürbüz, S.G. Wettstein, J.A. Dumesic, Conversion of hemicellulose to furfural and levulinic acid using biphasic reactors with alkylphenol solvents, *ChemSusChem*. 5 (2012) 383–387. <https://doi.org/10.1002/cssc.201100608>.
- [228] C.H.J.T. Dietz, M. Verra, S. Verberkt, F. Gallucci, M.C. Kroon, M.F. Neira D'Angelo, M. Papaioannou, M. Van Sint Annaland, Sequential and in Situ Extraction of Furfural from Reaction Mixture and Effect of Extracting Agents on Furfural Degradation, *Ind. Eng. Chem. Res.* 58 (2019) 16116–16125. <https://doi.org/10.1021/acs.iecr.9b00694>.
- [229] D.J.G.P. Van Osch, L.F. Zubeir, A. Van Den Bruinhorst, M.A.A. Rocha, M.C. Kroon, Hydrophobic deep eutectic solvents as water-immiscible extractants, *Green Chem.* 17 (2015) 4518–4521. <https://doi.org/10.1039/c5gc01451d>.
- [230] Y. Lee, E.E. Kwon, J. Lee, Polymers derived from hemicellulosic parts of lignocellulosic biomass, *Rev. Environ. Sci. Biotechnol.* 18 (2019) 317–334. <https://doi.org/10.1007/s11157-019-09495-z>.
- [231] A.A. Rosatella, S.P. Simeonov, R.F.M. Frade, C.A.M. Afonso, 5-Hydroxymethylfurfural (HMF) as a building block platform: Biological properties, synthesis and synthetic applications, *Green Chem.* 13 (2011) 754–793. <https://doi.org/10.1039/c0gc00401d>.
- [232] J.N. Chheda, Y. Román-Leshkov, J.A. Dumesic, Production of 5-

- hydroxymethylfurfural and furfural by dehydration of biomass-derived mono- and poly-saccharides, *Green Chem.* 9 (2007) 342–350.
<https://doi.org/10.1039/b611568c> Furan.
- [233] R. Weingarten, J. Cho, R. Xing, W.C. Conner, G.W. Huber, Kinetics and reaction engineering of levulinic acid production from aqueous glucose solutions, *ChemSusChem.* 5 (2012) 1280–1290. <https://doi.org/10.1002/cssc.201100717>.
- [234] I. Van Zandvoort, Y. Wang, C.B. Rasrendra, E.R.H. Van Eck, P.C.A. Bruijninx, H.J. Heeres, B.M. Weckhuysen, Formation, molecular structure, and morphology of humins in biomass conversion: Influence of feedstock and processing conditions, *ChemSusChem.* 6 (2013) 1745–1758. <https://doi.org/10.1002/cssc.201300332>.
- [235] X. Liu, N. Ai, H. Zhang, M. Lu, D. Ji, F. Yu, J. Ji, Quantification of glucose, xylose, arabinose, furfural, and HMF in corncob hydrolysate by HPLC-PDA-ELSD, *Carbohydr. Res.* 353 (2012) 111–114. <http://dx.doi.org/10.1016/j.carres.2012.03.029>.
- [236] B.C. Saha, Hemicellulose bioconversion, *J. Ind. Microbiol. Biotechnol.* 30 (2003) 279–291. <https://doi.org/10.1007/s10295-003-0049-x>.
- [237] A. Fehér, Combined Approaches to Xylose Production from Corn Stover by Dilute Acid Hydrolysis, *Chem. Biochem. Eng. Q.* 31 (2017) 77–87.
<https://doi.org/10.15255/CABEQ.2016.913>.
- [238] X. Ji, H. Ma, Z. Tian, G. Lyu, G. Fang, J. Chen, H.A.M. Saeed, Production of xylose from diluted sulfuric acid hydrolysis of wheat straw, *BioResources.* 12 (2017) 7084–7095. <https://doi.org/10.15376/biores.12.4.7084-7095>.
- [239] N. Sun, H. Liu, N. Sathitsuksanoh, V. Stavila, M. Sawant, A. Bonito, K. Tran, A. George, K.L. Sale, S. Singh, B.A. Simmons, B.M. Holmes, Production and extraction of sugars from switchgrass hydrolyzed in ionic liquids, *Biotechnol. Biofuels.* 6 (2013). <https://doi.org/10.1186/1754-6834-6-39>.
- [240] B. Godin, N. Nagle, S. Sattler, R. Agneessens, J. Delcarte, E. Wolfrum, Improved sugar yields from biomass sorghum feedstocks: Comparing low-lignin mutants and pretreatment chemistries, *Biotechnol. Biofuels.* 9 (2016) 1–11.
- [241] R.J. van Putten, J.C. van der Waal, E. de Jong, C.B. Rasrendra, H.J. Heeres, J.G. de Vries, Hydroxymethylfurfural, A Versatile Platform Chemical Made from Renewable Resources, *Chem. Rev.* 113 (2013) 1499–1597.
- [242] J.N.M. Tan-Soetedjo, H.H. Van De Bovenkamp, R.M. Abdilla, C.B. Rasrendra, J. Van Ginkel, H.J. Heeres, Experimental and Kinetic Modeling Studies on the Conversion of Sucrose to Levulinic Acid and 5-Hydroxymethylfurfural Using Sulfuric Acid in Water, *Ind. Eng. Chem. Res.* 56 (2017) 13228–13239.
- [243] A. Smit, W. Huijgen, Effective fractionation of lignocellulose in herbaceous biomass and hardwood using a mild acetone organosolv process, *Green Chem.* 19 (2017) 5505–5514. <https://doi.org/10.1039/c7gc02379k>.
- [244] H.W.C. Raaijmakers, J.G.M. Van Nispen, J.P.M. Bink, Methods of enriching arabinose fractions and products obtainable thereby, WO 2017/058017 A1, 2013.
- [245] B. Girisuta, L.P.B.M. Janssen, H.J. Heeres, A kinetic study on the conversion of glucose to levulinic acid, *Chem. Eng. Res. Des.* (2006) 339–349.
<https://doi.org/10.1205/cherd05038>.
- [246] B. Danon, W. Hongsiri, L. van der Aa, W. de Jong, Kinetic study on homogeneously

- catalyzed xylose dehydration to furfural in the presence of arabinose and glucose, *Biomass and Bioenergy*. 66 (2014) 364–370. <https://doi.org/10.1016/j.biombioe.2014.04.007>.
- [247] R. Katz, Production of furfural, *Front. Chem.* 54 (2015) 309–315. <https://doi.org/10.1111/2047-8852.12112>.
- [248] E. Ramiro, Process for separating furfural from a liquid aqueous phase comprising furfural and one or more organic acids, WO 2U11/161141 A1, 2011.
- [249] G. Marcotullio, M. a. T. Cardoso, W. De Jong, A.H.M. Verkooijen, Bioenergy II: Furfural Destruction Kinetics during Sulphuric Acid-Catalyzed Production from Biomass, *Int. J. Chem. React. Eng.* 7 (2009).
- [250] H. Olcay, R. Malina, A.A. Upadhye, J.I. Hileman, G.W. Huber, S.R.H. Barrett, Techno-economic and environmental evaluation of producing chemicals and drop-in aviation biofuels via aqueous phase processing, *Energy Environ. Sci.* 11 (2018) 2085–2101. <https://doi.org/10.1039/c7ee03557h>.
- [251] R.P. Verma, M.M. Sharma, Mass transfer in packed liquid-liquid extraction columns, *Chem. Eng. Sci.* 30 (1975) 279–292. [https://doi.org/10.1016/0009-2509\(75\)80078-9](https://doi.org/10.1016/0009-2509(75)80078-9).
- [252] A.R. Kelishami, H. Bahmanyar, A.M. Mohamad, Prediction of mass transfer coefficients in regular packed columns, *Chem. Eng. Commun.* 198 (2011) 1041–1062. <https://doi.org/10.1080/00986445.2011.545305>.
- [253] F. Visscher, Liquid-liquid processes in spinning disc equipment door, Eindhoven University of Technology, 2013. <https://doi.org/10.6100/IR758245>.
- [254] L.C. Nhien, N.V.D. Long, S. Kim, M. Lee, Techno-economic assessment of hybrid extraction and distillation processes for furfural production from lignocellulosic biomass, *Biotechnol. Biofuels*. 10 (2017) 1–12. <https://doi.org/10.1186/s13068-017-0767-3>.
- [255] International Energy Agency (IEA), Electricity price, [www.iea.org](http://www.iea.org/about/mission). (2020). <https://www.iea.org/about/mission>.
- [256] P. Ning, G. Yang, L. Hu, J. Sun, L. Shi, Y. Zhou, Z. Wang, J. Yang, Recent advances in the valorization of plant biomass, *Biotechnol. Biofuels*. 14 (2021) 1–22. <https://doi.org/10.1186/s13068-021-01949-3>.
- [257] B. Song, R. Lin, C.H. Lam, H. Wu, T.H. Tsui, Y. Yu, Recent advances and challenges of inter-disciplinary biomass valorization by integrating hydrothermal and biological techniques, *Renew. Sustain. Energy Rev.* 135 (2021) 110370. <https://doi.org/10.1016/j.rser.2020.110370>.
- [258] European Commission (EC), Sustainable Biomass, (2012). https://ec.europa.eu/energy/topics/renewable-energy/biomass_en?redir=1#documents.
- [259] M. Banja, R. Sikkema, M. Jégard, V. Motola, J.F. Dallemand, Biomass for energy in the EU – The support framework, *Energy Policy*. 131 (2019) 215–228. <https://doi.org/10.1016/j.enpol.2019.04.038>.
- [260] M. Hronec, K. Fulajtarová, Selective transformation of furfural to cyclopentanone, *Catal. Commun.* 24 (2012) 100–104. <https://doi.org/10.1016/j.catcom.2012.03.020>.
- [261] M. Dashtban, A. Technologies, Production of Furfural : Overview and Challenges

- Production of Furfural : Overview and Challenges, J-FOR. (2012) 44–53.
- [262] J. Ebert, Furfural: future feedstock for fuels and chemicals, *Biomass Mag.* (n.d.). <http://biomassmagazine.com/articles/1950/furfural-future-feedstock-for-fuels-and-chemicals>.
- [263] D. Mackay, B. Cole, R. Fort, A. Mares, Potential Markets for Chemicals and Pharmaceuticals from Woody Biomass in Maine Potential Markets for Chemicals and Pharmaceuticals from Woody Biomass in Maine, 2021.
- [264] T. Dallas Swift, H. Nguyen, A. Anderko, V. Nikolakis, D.G. Vlachos, Tandem Lewis/Brønsted homogeneous acid catalysis: conversion of glucose to 5-hydroxymethylfurfural in an aqueous chromium(iii) chloride and hydrochloric acid solution, *Green Chem.* 17 (2015) 4725–4735. <https://doi.org/10.1039/c5gc01257k>.
- [265] A. Woitalka, S. Kuhn, K.F. Jensen, Scalability of mass transfer in liquid-liquid flow, *Chem. Eng. Sci.* 116 (2014) 1–8. <https://doi.org/10.1016/j.ces.2014.04.036>.
- [266] M. Schrimpf, J. Esteban, T. Rösler, A.J. Vorholt, W. Leitner, Intensified reactors for gas-liquid-liquid multiphase catalysis: From chemistry to engineering, *Chem. Eng. J.* 372 (2019) 917–939. <https://doi.org/10.1016/j.cej.2019.03.133>.
- [267] S.C. Pereira, L. Maehara, C.M.M. Machado, C.S. Farinas, 2G ethanol from the whole sugarcane lignocellulosic biomass, *Biotechnol. Biofuels.* 8 (2015) 1–16. <https://doi.org/10.1186/s13068-015-0224-0>.
- [268] S. McIntosh, Z. Zhang, J. Palmer, H.H. Wong, W.O.S. Doherty, T. Vancov, Pilot-scale cellulosic ethanol production using eucalyptus biomass pre-treated by dilute acid and steam explosion, *Biotechnol. Biofuels.* 10 (2016) 346–358. <https://doi.org/10.1002/bbb.1651>.
- [269] *Physical Property Methods and Models*, (2021).
- [270] L.D. Schmidt, *Engineering of Chemical Reactions*, *Eng. Chem. React.* (2005) 601–605.
- [271] S. Moran, K.-D. Henkel, Reactor Types and Their Industrial Applications, *Ullmann's Encycl. Ind. Chem.* (2016) 1–49. https://doi.org/10.1002/14356007.b04_087.pub2.
- [272] W. De Jong, G. Marcotullio, Process for the production of furfural from pentoses, US 2012/0108829 A1, 2012.
- [273] Mohamed Nageeb Rashed, Adsorption Technique for the Removal of Organic Pollutants from Water and Wastewater, in: *Org. Pollut. - Monit. Risk Treat.*, 2013. <https://www.intechopen.com/books/advanced-biometric-technologies/liveness-detection-in-biometrics>.
- [274] J. Esteban, A.J. Vorholt, W. Leitner, An overview of the biphasic dehydration of sugars to 5-hydroxymethylfurfural and furfural: A rational selection of solvents using COSMO-RS and selection guides, *Green Chem.* 22 (2020) 2097–2128. <https://doi.org/10.1039/c9gc04208c>.
- [275] N. Frederick, N. Zhang, X. Ge, J. Xu, M. Pelkki, E. Martin, D.J. Carrier, Poplar (*Populus deltoides* L.): The effect of washing pretreated biomass on enzymatic hydrolysis and fermentation to ethanol, *ACS Sustain. Chem. Eng.* 2 (2014) 1835–1842. <https://doi.org/10.1021/sc500188s>.
- [276] N. Frederick, N. Zhang, A. Djiroleu, X. Ge, J. Xu, D.J. Carrier, The Effect of Washing Dilute Acid Pretreated Poplar Biomass on Ethanol Yields, in: *Sustain. Degrad.*

- Lignocellul. Biomass - Tech. Appl. Commer., 2013: p. 15.
<https://doi.org/10.5772/1490>.
- [277] A. Rusanen, K. Lappalainen, J. Kärkkäinen, T. Tuuttila, M. Mikola, U. Lassi, Selective hemicellulose hydrolysis of Scots pine sawdust, *Biomass Convers. Biorefinery*. 9 (2019) 283–291. <https://doi.org/10.1007/s13399-018-0357-z>.
- [278] S.S. Adav, S.K. Sze, *Trichoderma Secretome: An Overview*, Elsevier, 2014.
<https://doi.org/10.1016/B978-0-444-59576-8.00008-4>.
- [279] T.E. Timell, Recent progress in the chemistry of wood hemicelluloses, *Wood Sci. Technol.* 1 (1967) 45–70. <https://doi.org/10.1007/BF00592255>.
- [280] A. Jacobs, O. Dahlman, Characterization of the molar masses of hemicelluloses from wood and pulps employing size exclusion chromatography and matrix-assisted laser desorption ionization time-of-flight mass spectrometry, *Biomacromolecules*. 2 (2001) 894–905. <https://doi.org/10.1021/bm010050b>.
- [281] M. Peters, T. Klaus, *Plant Design and economics for chemical engineers*, 4th ed., McGraw-Hill Chemical Engineering Series Editorial, 1991.
- [282] alibaba.com, Furfural market price, (2021).
http://www.alibaba.com/trade/search?fsb=y&IndexArea=product_en&CatId=&SearchText=magnesite+oxide+price.
- [283] J.Q. Bond, A.A. Upadhye, H. Olcay, G.A. Tompsett, J. Jae, R. Xing, D.M. Alonso, D. Wang, T. Zhang, R. Kumar, A. Foster, S.M. Sen, C.T. Maravelias, R. Malina, S.R.H. Barrett, R. Lobo, C.E. Wyman, J.A. Dumesic, G.W. Huber, Production of renewable jet fuel range alkanes and commodity chemicals from integrated catalytic processing of biomass, *Energy Environ. Sci.* 7 (2014) 1500–1523.
<https://doi.org/10.1039/C3EE43846E>.
- [284] T. Shen, R. Hu, C. Zhu, M. Li, W. Zhuang, C. Tang, H. Ying, Production of cyclopentanone from furfural over Ru/C with Al₁₁.6PO₂₃.7 and application in the synthesis of diesel range alkanes, *RSC Adv.* 8 (2018) 37993–38001.
<https://doi.org/10.1039/c8ra08757a>.
- [285] L.C. Nhien, N.V.D. Long, M. Lee, Design and optimization of the levulinic acid recovery process from lignocellulosic biomass, *Chem. Eng. Res. Des.* 107 (2016) 126–136. <https://doi.org/10.1016/j.cherd.2015.09.013>.
- [286] T. Boonyakarn, P. Wataniyakul, P. Boonnoun, A.T. Quitain, T. Kida, M. Sasaki, N. Laosiripojana, B. Jongsomjit, A. Shotipruk, Enhanced Levulinic Acid Production from Cellulose by Combined Brønsted Hydrothermal Carbon and Lewis Acid Catalysts, *Ind. Eng. Chem. Res.* 58 (2019) 2697–2703.
<https://doi.org/10.1021/acs.iecr.8b05332>.
- [287] Z. Yu, F. Meng, Y. Wang, Z. Sun, Y. Liu, C. Shi, W. Wang, A. Wang, Catalytic Transfer Hydrogenation of Levulinic Acid to γ -Valerolactone over Ni₃P-CePO₄ Catalysts, *Ind. Eng. Chem. Res.* 59 (2020) 7416–7425. <https://doi.org/10.1021/acs.iecr.0c00257>.
- [288] X. Huang, K. Liu, W.L. Vrijburg, X. Ouyang, A. Iulian Dugulan, Y. Liu, M.W.G.M. Tiny Verhoeven, N.A. Kosinov, E.A. Pidko, E.J.M. Hensen, Hydrogenation of levulinic acid to γ -valerolactone over Fe-Re/TiO₂ catalysts, *Appl. Catal. B Environ.* 278 (2020) 119314. <https://doi.org/10.1016/j.apcatb.2020.119314>.
- [289] K. Dalvand, J. Rubin, S. Gunukula, M. Clayton Wheeler, G. Hunt, Economics of

- biofuels: Market potential of furfural and its derivatives, *Biomass and Bioenergy*. 115 (2018) 56–63. <https://doi.org/10.1016/j.biombioe.2018.04.005>.
- [290] M.S. Hossain, C. Theodoropoulos, A. Yousuf, Techno-economic evaluation of heat integrated second generation bioethanol and furfural coproduction, *Biochem. Eng. J.* 144 (2019) 89–103. <https://doi.org/10.1016/j.bej.2019.01.017>.
- [291] T. Shen, Y. Hu, R. Hu, W. Zhuang, M. Li, H. Niu, H. Xu, C. Zhu, H. Ying, Continuous production of furfural from pulp prehydrolysate in a vaporization reactor, *Ind. Crops Prod.* 153 (2020) 112565. <https://doi.org/10.1016/j.indcrop.2020.112565>.
- [292] C.-S. Lau, G.J. Thoma, E.C. Clausen, D.J. Carrier, Kinetic Modeling of Xylose Oligomer Degradation during Pretreatment in Dilute Acid or in Water, *Ind. Eng. Chem. Res.* 53 (2014) 2219–2228. <https://doi.org/10.1021/ie403722d>.

Research output

Journal articles

- [1] M. Papaioannou, R.J.T. Kleijwegt, J. van der Schaaf, M.F. Neira d'Angelo, Furfural Production by Continuous Reactive Extraction in a Millireactor under the Taylor Flow Regime, *Ind. Eng. Chem. Res.* (2019) 16106–16115.
- [2] C. Dietz, M. Verra, S. Verberkt, F. Gallucci, M. Kroon, M.F. Neira d'Angelo, M. Papaioannou, M. van Sint Annaland, Sequential and in situ extraction of furfural from reaction mixture and effect of extracting agents on furfural degradation *Ind. Eng. Chem. Res.* 2019, 58, 35, 16116–16125
- [3] V. Krzelj, J. Ferreira Liberal, M. Papaioannou, J. van Der Schaaf, M.F. Neira D'Angelo, Kinetic Model of Xylose Dehydration for a Wide Range of Sulfuric Acid Concentrations, *Ind. Eng. Chem. Res.* 59 (2020) 11991–12003. <https://doi.org/10.1021/acs.iecr.0c01197>.

Conference proceedings

- [1] M. Papaioannou, R.J.T. Kleijwegt, J. C. Schouten, J. van der Schaaf, Furfural production by continuous reactive extraction, Oral presentation at 16 AIChE Annual Meeting, San Francisco, USA, 2016
- [2] M. Papaioannou, J. C. Schouten, J. van der Schaaf, Furfural production by reactive extraction in biphasic system, Oral presentation at 1st Annual InSciTe Meeting, Geleen, The Netherlands, 2016
- [3] M. Papaioannou, M. F. Neira d'Angelo, J.C. Schouten, J. van der Schaaf, Furfural production by continuous reactive extraction, Poster presentation at 10th World Congress of Chemical Engineering, Barcelona, Spain, 2017
- [4] M. Papaioannou, M. F. Neira d'Angelo, J. C. Schouten, J. van der Schaaf, Optimization of Furfural Production: Evaluation of Intensified Multiphase Reactors, Oral presentation at 3rd Annual InSciTe Meeting, Geleen, The Netherlands, 2018

[5] M. Papaioannou, V. Krzelj, M.F. Neira d'Angelo, J.C. Schouten, J. van der Schaaf, Intensified biphasic reactors for furfural production, Poster presentation at 25th International Conference on Chemical Reaction Engineering, Florence, Italy, 2018

[6] M. Papaioannou, M.F. Neira d'Angelo, J. van der Schaaf, Process Intensification for bio-based platform chemicals - The furfural challenge, Oral presentation at 25th Netherlands Process Technology Symposium, Enschede, The Netherlands, 2018

Acknowledgements

«Να 'σαι ανήσυχος, αφχαρίστητος, απροσάρμοστος πάντα. Όταν μια συνήθεια καταντήσει βολική, να τη συντρίβεις.»
Νίκος Καζαντζάκης, *Ασκητική*, 1927

“Be always restless, unsatisfied, unconfirming. Whenever a habit becomes convenient, crush it.”

Nikos Kazantzakis, *Ascesis: The saviors of God*, 1927

With similar mindset as described by N. Kazantzakis, some years ago I decided to leave my comfort zone and move to the Netherlands to start a new chapter. This journey led me to the completion of one of the most important achievements of my life. The completion of this journey would not have been possible without the help of many.

First, I would like to thank my supervisors during my PhD years who helped me and mentored me throughout my research. John, thank you for pushing me to think more critically. I really admire your enthusiasm for science and innovation, and the discussions during our meetings really encouraged me to think out-of-the box. Your scientific approach to research has been an important asset for my current career as chemical engineer. I would like to thank you Fernanda for having me as one of your first PhD students. Your positive mentality, the time and passion you devoted to our meetings and research discussions kept me motivated. Thank you for all the meetings, suggestions, and insights, you provided me during my PhD time. Finally, a special thank you for the “remote” supervision and support in the past 3.5 years.

I would like to express my gratitude to the examination committee: prof.dr.ir. B. Schuur, prof.dr.ir. W. de Jong, prof. dr. E. Rebrov and prof.dr.ir. M. van Sint Annaland. Thank you for evaluating this thesis and attending my defense.

I would also like to express my deepest gratitude to all the members of the HORIZONTAL project and Chemelot InSciTe. Firstly, I would like to thank prof. dr. ir. Fausto Gallucci, the project leader, for the constructive meetings and efforts towards team formation and project completion. Henk Oevering, Peter Quaedflieg, Natascha Sereinig, Paul Alsters, thank you all for organizing and putting effort on this project. My special thanks go to the other PhD students of the HORIZONTAL Project. Geert and Christian, I enjoyed our discussions during the progress meetings and always enjoying the annual InSciTe meetings. I would also like to thank Carin Dietz for our close collaboration and discussions in TU/e. Finally, I would like to

thank Panos Kouris. Even though he was not part of the HORIZONTAL project, he was also involved in other Chemelot InSciTe projects. I really enjoyed meeting you again (after Patras) and having nice discussions during coffee breaks. I wish all the best for you and your family.

All the laboratory work would not have been possible without the great help from the supporting staff. A special thank you to Carlo for caring about our safety, for your help, and your incredible efficiency. Peter, thank you for taking care of all the analytics and helping with all different kinds of problems in the lab - especially with the pumps. Marlies, thank you for all the help with the GCs and HPLCs. I always enjoyed having any kind of conversation with you. Erik, thank you and I really appreciate your patience with me, your positive attitude and making an extra effort to make my set-ups actually work. A big thanks also to all the other support staff and faculty at the university.

I would also like to express my appreciation to Saskia and Denise, the secretaries of SPE. Denise, thank you for making everything seem easy and going smoothly. Saskia, thank you for being such a great help. I have bothered you a lot recently with my emails and questions and all the work for the PhD defense, I sincerely appreciate all your help.

During my PhD, I had the chance to work with a number of incredible students from whom I learned a lot. Floriane, thank you for being my first student ever and for helping each other. Special thanks to Roel Kleijwegt, my first master student, for his contribution to this research and helping me set the bases of the experiments. Steven, Kevin, Evangelia, Dirk, Thomas, and Romy, I thank you all for your motivation, contribution, and effort you put into this work.

Here is the list of people whose companionship in the office, lab, and breaks made this journey much more bearable. Firstly, Manjunath thank you for being together side-by-side at the beginning of this project and having fun inside and outside of TU/e. Many thanks to Leticia and Slavisa, the first SPE PhD students I met, who helped me to adapt and acclimate to the group. My special thank you goes to the people that I was closer during this journey. A special thank you goes to Vladan. It was such a pleasure working together on this project. Thank you for all the research discussions we had through these years, for helping me, believing that everything will be fine in the end. I really enjoyed having you as “partner in crime” and I wish all the best for you and your family. Alexei, I really enjoyed having you as my office mate. Your enthusiasm and your motivation for science and research kept us all going even during more difficult times. Thank you for the conversations during lunch and borrels and trying to introduce me (unsuccessfully) to the world of bitcoins. Finally, I would like to thank Katerina. Although we met in the last year of your PhD, *po poooo* I really enjoyed our discussions and the time we spent together on several occasions. I would also like to

mention a few more nice people I have had the pleasure to meet during my time at SPE: German, Vishnu, Arnab, Jasper, Pia, Leander, Ria, Stephan, Maurilio, Anke, Arturo, Amin, Alejo, Michiel, Paola and Shoreh, Lana, Lara, Teresa, Smitha and Samayita.

Also, there are people outside the Netherlands that I would like to thank for being close to me and support me one way or the other. I would like to thank Nikos Vrachatis, who convinced me to move to the Netherlands and introduced me to TU/e and Dutch habits like pepernoten. Iria, it was such a great pleasure to move together to the Netherlands after a long time since our undergraduate years in Patras. I really enjoyed our short time living together, cooking us brussels sprouts, and eating them by yourself. Finally, a big thank you to my dear friend Nancy. I really enjoyed my multiple visits to Zurich, our trips to Lisbon and Belgrade, and our discussions about our parallel paths in research. I am so grateful and happy that you are still one of my best friends after so many years in different countries. Let's keep it that way!

I would like to thank my best friends in the world, Vasia and Elpida. We had the chance and the fortune to meet at primary school in 1995 and being together since then. Many thanks for your support, numerous phone and video calls, and the unforgettable moments we had and keep having together. To many more! Ελπίζω το μέλλον να μας βρει μαζί, αγαπημένες και να συνεχίσουμε να μετράμε χρόνια.

A heartfelt special thank you goes to my husband Vassilis for his undivided comprehension and support throughout this journey. At the beginning, your thoughts were always with me, but you moving to the Netherlands was the biggest source of motivation to continue the hard work not only in research, but in life as well. Thank you for having faith in me and encouraging me to follow my dreams. Σ' ευχαριστώ για τη συνεχή υποστήριξη και που δεν σταμάτησες να πιστεύεις σ' εμένα.

Finally, I want to say a sincere thank you to my parents. There are no words to express how much I love you. Since I was a little girl, you have always encouraged me to do my best and you have supported me with your unconditional love in every decision that I have made. Σας ευχαριστώ που ήσασταν πάντα στο πλάι μου να με συμβουλευέτε, να με κατευθύνετε και να με εμπνέετε. Χωρίς την υποστήριξή σας, δεν θα ήμουν ο άνθρωπος που είμαι σήμερα.

I want to thank all my current colleagues at API Europe. I am incredibly lucky to be part of this team of dedicated and talented people.

To everyone who has made this journey possible – once again, thank you!

About the author

Myrto Papaioannou was born on 25th January 1990 in Athens, Greece. Upon completing her education at “Ecole des Ursulines” high school in Athens, she attended University of Patras (UP) in Patras, Greece, and obtained her Diploma degree in Chemical Engineering in 2013. Myrto carried out her research project in the Institute of Chemical Engineering Sciences (ICE-HT) at UP, studying “Patras organic atmospheric aerosols”. In 2013, she moved to the Netherlands to pursue a Professional Doctorate in Engineering (Process and Product Design) at Eindhoven University of Technology. She obtained her PDEng (EngD) degree in 2015 by working on “High pressure and temperature intensified biobased conversion processes, case selection and development” for her individual design project at Eindhoven University of Technology in Eindhoven, the Netherlands. From 2015, Myrto started a PhD project at University of Technology in Eindhoven, the Netherlands of which the results are presented in this dissertation. Both PDEng (EngD) individual project and the given research work was part of the HORIZONTAL Project supported by Chemelot InSciTe (Institute of Science and Technology). She has presented her research findings orally as well as with posters in several conferences. Since 2019, Myrto is employed at API Europe as chemical engineer. Her work mainly involves the development of process simulations for pulp and paper industry, and she is member of the research team performing experimental work on biomass processing for 2G bio-ethanol production.

